Summer 8-9-2018

Chemically Cross-Linked Polysaccharide-Based Hydrogels via Thiol-Norbornene Reaction as Sustainable Biomaterials

Nayereh Dadoo
University of Maine, nayereh.dadoo@maine.edu

CHEMICALLY CROSS-LINKED POLYSACCHARIDE-BASED HYDROGELS VIA THIOL-NORBORNENE REACTION AS SUSTAINABLE BIOMATERIALS

By

Nayereh Dadoo

B.A. Ferdowsi University of Mashhad-Iran, 2006

M.A. Chemistry and Chemical Engineering Research Center of Iran, Tehran-Iran, 2010

A DISSERTATION

Submitted in Partial Fulfillment of the

Requirements for the Degree of

Doctor of Philosophy

(in Chemistry)

The Graduate School

The University of Maine

August 2018

Advisory Committee:

William M. Gramlich, Assistant Professor of Chemistry, Advisor

Barbara J.W. Cole, Professor of Chemistry

Carl P. Tripp, Professor of Chemistry

Matthew Brichacek, Assistant Professor of Chemistry

Michael D. Mason, Associate Professor of Chemical Engineering

CHEMICALLY CROSS-LINKED POLYSACCHARIDE-BASED HYDROGELS VIA THIOL-NORBORNENE REACTION AS SUSTAINABLE BIOMATERIALS

By Nayereh Dadoo

Dissertation Advisor: Dr. William M. Gramlich

An Abstract of the Dissertation Presented
in Partial Fulfillment of the Requirements for the
Degree of Doctor of Philosophy
(in Chemistry)

August 2018

Hydrogels are 3D polymeric networks with high water content and are widely being investigated for biomedical applications such as tissue engineering. Polysaccharides have been used to fabricate hydrogels due to their natural abundance, biocompatibility, and immunogeniety. Additionally, polysaccharide-based hydrogels can provide mechanical and biological cues similar to those of the natural environments. In this work, thiol-norbornene chemistry was used to fabricate polysaccharide-based hydrogels including hyaluronic acid (HA), carboxymethyl cellulose (CMC), and cellulose nanofibrils (CNFs). Hydrogels with tunable physical and mechanical properties were achieved. The properties of these hydrogels were spatiotemporally modified by photopatterning. Also, high stem cell viability was achieved when cells were encapsulated in these hydrogels.

DEDICATION

Dedicated to

My Lovely Parents, Abdollah and Razieh,

And

My Amazing Brothers, Naser and Majid,

For All the Support, Encouragement, and Love They Have Always Provided

ACKNOWLEDGEMENTS

I would like to express my deepest appreciation to my advisor, Prof. William M. Gramlich for being a great mentor, always supportive, and for all the encouragements he always provided.

I would like to thank all my friends in “Gramlich Group” and department of chemistry, especially Anushka Vithanage and Hathaitep (Grape) Senkum, for always being so kind and supportive.

Special thanks to Samuel Landry and Jonathan Bomar for their incorporation in this work. I also would like to thank Jonathan Bomar and Phaneendra Chenampally for the gteat help with cell culture experiments. Many thanks to Dr. Scott Collins, Dr. Rosemary Smith, and Dr. Paul Millard for generously allowing me to use their cell culture lab, facilities, and fluorescent microscopes.

I would like to thank my advisory committee members, Prof. Barbara Cole, Prof. Carl Tripp, Prof. Matthew Brichacek and Prof. Michael Mason for their great help and advice during my Ph.D work. I would like to thank David Labrecque for NMR training and helping us all the time very kindly, and Diane Muir for her kind heart.

Many thanks to Dr. Brian Frederick for all the support he provided.

Special thanks to Akbar Mahdavi Shakib, Roghiyeh Ebrahimi Kalan, Behtash Shakeri, and Natalie Kelly for the great help and support on the first year of my life in the United State. It could not be so easy without their support.

Finally, I would like to thank my family. They are my number one fans and always cheering me up. Also, I would like to thank my best friends, Atefeh Rajaee, Azadeh Pahlevanzadeh, Grape Senkum, Jalal Tavana, Jonathan Bomar, Koorosh Kashkooli, Samuel Landry, and Zahra Naghizadeh Mahani for making my days very happy.

TABLE OF CONTENTS

LIST OF TABLES

LIST OF FIGURES

CHAPTER 1

INTRODUCTION

1.1. Hydrogels

Hydrogels are three-dimensional polymer networks that absorb large volumes of water and biological fluids, are widely used in biomedical applications. The water content of hydrogel varies upon the structure of polymer network and the environmental conditions such as pH, ionic strength and temperature (Figure 1.1).[1] Hydrogels can be created through physical or chemical crosslinking of polymer precursors.[2-4] Polymer entanglements and molecular self-assembly through hydrogen bonds and electrostatic interaction could form physically cross-linked gels or reversible hydrogels.[1] Cellulose nanofibrils (CNF), cellulose derivatives such as methyl cellulose (MC) and hydroxymethyl cellulose (HMC), gelatin, and collagen form physical gels. To fabricate chemically cross-linked hydrogels, covalent bonds (through chemical reagents or radiations) between polymer chains are needed.[5] In general, chemical hydrogels are more stable than physical gels against dilution, pH and temperature changes, and mechanical forces.

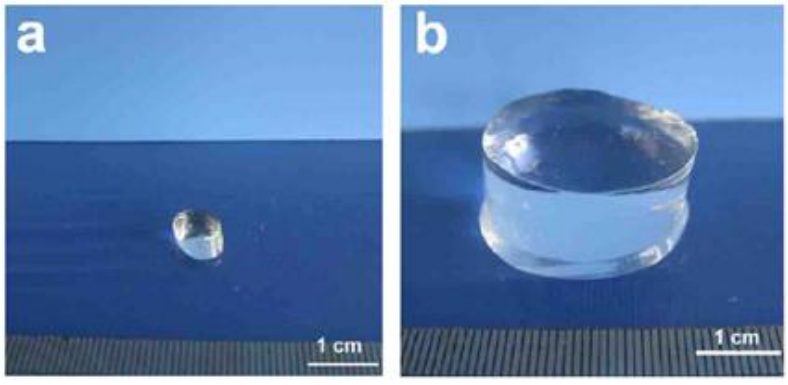

Figure 1.1. Swelling of a cellulose based hydrogel. A cellulose-based hydrogel in its (a) original size and (b) after swelling due to water uptake.[1]

1.2. Hydrogels as extracellular matrix (ECM) mimics

Because of their highly hydrated state and three dimensional structure, hydrogels closely mimic the physical properties of the extracellular matrix (ECM) and as a result they have been used for a wide range of biomedical applications. The ECM is the fibrillar hydrated gel-like structure that is produced by cells and fills the space between cells and tissues. This structure facilitates the fast diffusion of nutrients, biological molecules, and waste materials between cells and blood vessel. It has been proven that ECM not only provides the physical stability and mechanical strength for the cells, but also is involved in the regulation of the behavior of cells.

Hydrogels derived directly from the ECM benefit from having bioactive sites and biodegradability, but they are not inert when they are used in-vivo. Therefore, it is possible that the immune system reacts to it. In addition, the purification difficulties and the complexity of these materials can cause the lack of reproducibility and the difficulties in interpretation of the observations.[6]

To address these issues, hydrogels from synthetic biologically inert polymers with known chemistry have been investigated which can produce repeatable structure and provide the control over chemical and physical properties.[7] However, these synthetic hydrogels should be modified to provide the requirements for cell growth and survival. Also, synthetic polymers suffer from the lack of biodegradability that makes the surgery inevitable to remove it where it is used in vivo, or requires complex processes to release the tissue that have been regenerated inside the hydrogel scaffold. For example, Matrigel (an ECM-derived hydrogel) that is usually used in biological studies, includes components that are not fully defined. So, it is not reproducible.

Another approach is to modify polymers from natural resources or make natural-synthetic hybrid hydrogels that benefits from the advantages of both categories while reducing the downsides.

1.3. Polysaccharide-based hydrogels

Hydrogels and biomaterials from natural sources such as polysaccharides and proteins are promising alternatives to synthetic materials because of their potential biodegradability, low toxicity, low inflammatory response, and low tissue adhesion properties.[8-10] Additionally, their abundance, low cost, and ease of modification make natural-based biomaterials interesting targets for the future of regenerative medicine.

1.3.1. Hyaluronic acid (HA)

The alternating copolymer of D-glucuronic acid and N-acetyl-glucosamine monosaccharides is a naturally occurring anionic, unbranched polysaccharide called hyaluronic Acid (HA) or also hyaluronan. To form hyaluronic acid, D-glucuronic acid and N-acetyl-glucosamine are linked by β (1, 4) and β (1, 3) bonds (Figure 1.2).[11] The glycoside bonds are susceptible to hydrolysis in both acidic and alkaline conditions and the latter one is much faster.[12] Multiple different functional groups present in each repeat units of HA makes it possible to modify HA with desired reactive sites.[13-17] At physiological conditions, hyaluronic acid is found as its sodium salt. The negative charge gives the hydrophilic character to hyaluronic acid which causes the formation of swelled structure.

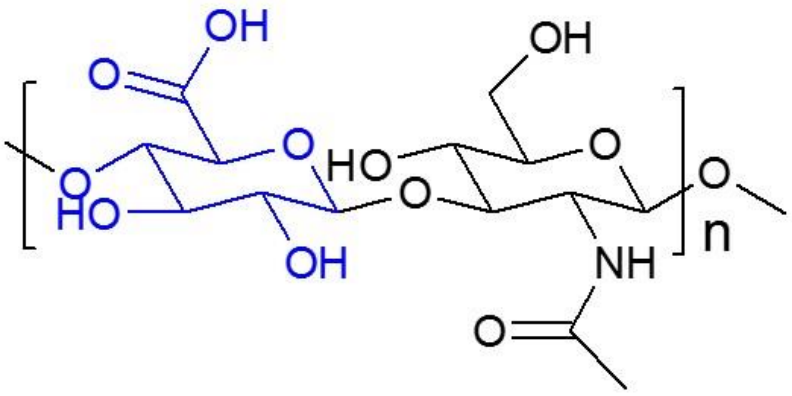

Figure 1.2. The chemical structure of hyaluronic acid repeat unit. HA repeat unit is a disaccharide unit consist of D-glucuronic acid (blue) and N-acetyl-glucosamine (black).

The major source for HA is extraction from rooster combs. Recombinant production using *Streptococcus bacterium* is another common resource for HA production. Hyaluronic acid constitutes the majority of extra cellular matrix (ECM) and is mostly found in skin, lung, intestine, and synovial liquid of vertebrates. Biological function of hyaluronic acid in the body covers a wide variety of activities such as cell migration, proliferation, adhesion, recognition, and tumor invasion. Its vital interference in morphogenesis and embryonic development shows its importance in the body and also its role in growth factor action, cartilage stability, and joint lubrication makes hyaluronan a much demanded target of study.[18]

HA has viscoelastic properties caused by its high molecular weight (102-104 kDa), electrostatic repulsion of carboxylate ions, and intra molecular hydrogen bond.[19] The pseudo-random coil configuration of HA is another reason for its viscoelastic properties. HA has high water affinity therefore it forms hydrogels when in contact with water. Due to its characteristics, HA is wildly used in cosmetic industry, dermal filler and anti-aging medicine, and wound healing.[20] The application of HA as tissue engineering scaffolds was limited by its fast degradability and lack of mechanical strength. These issues can be fixed by modification of HA, cross-linking HA, and HA hybrid networks. Several groups have reported HA-based hydrogels to be used as scaffolds for

tissue regeneration. For example, Gunci-Unal et al. has shown that hybrid hydrogel of methacrylated gelatin with methacrylated HA has enhanced mechanical properties compare to each component individually.[21] Additionally, it supports spreading of human umbilical cord vein endothelial cells and can be a candidate for vascular tissue regeneration. In another work done by Wu et al., human pluripotent stem cells were encapsulated in 3D methacrylated HA hydrogels.[22] Aside from high cell viability of HA hydrogel, formation of 3D spheroids and neural differentiation was also observed. There are much more examples of HA-based hydrogels that show the broad applications of HA not only for tissue engineering, but also for many other biomedical applications.

1.3.2. Cellulose

Cellulose derived from plants with its unique properties has shown the potential to be a popular material for many biomaterials and bioengineering applications. Its inherent biocompatibility and mechanical properties along with sustainable sources that are available in large volume are part of its advantages. Cellulose constitutes one third to one half of plant tissues and is known as the ECM of plant cells. Cellulose is the most abundant natural polymer and more 10 tons of cellulose are produced by the photosynthesis process annually. Additionally, the human body does not possess the enzymes to degrade cellulose. Therefore, cellulose can be a natural replacement for the inert synthetic polymers. This non-degradability in the human body causes some compatibility issues, but it can be advantageous for some applications when both biocompatibility and non-biodegradability are required.[23] For example, cellulose-based hydrogels were used to make artificial heart valves or menisci. Another advantage of non-degradability of cellulose in the human body is the orthogonal degradation of the cellulosic scaffold while the generated tissue remains intact.[24]

For the first time, in 1920, Staudinger suggested a polymeric structure for cellulose instead of small oligomers.[25] Cellulose polymer is generated from β-D-glucose units (1000-1500 units) which are linked by β (1→4) bonds (Figure 1.3.A).[5] These β (1→4) linkages are responsible for the linear structure of cellulose chains which cause cellulose to be highly crystalline and insoluble in water and most common solvents.[5] In fact, three hydroxyl groups on each glucose unit form intra- and inter-molecular hydrogen bonds which are responsible for the chain tendency to arrange in parallel order into crystalline structure (Figure 1.3.B).[25]

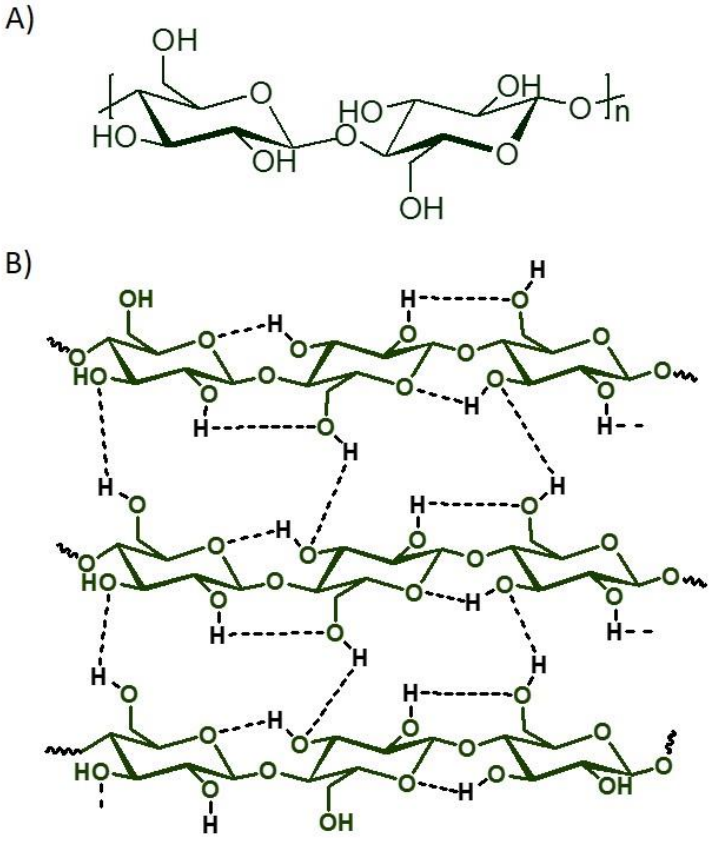

Figure 1.3. The chemical structure of cellulose repeat unit. A) The molecular structure of cellulose repeat units linked by β (1→4) linkages. B) An illustration of intra and inter molecular hydrogen bonds that hold cellulose chains together and are responsible for cellulose highly crystalline structure.

However, cellulose is not completely crystalized and there can be found some less ordered regions between highly ordered parts in which cellulose chains are arranged in a random fashion.[25] While solvents and chemical reagents cannot pass into crystalline region without disrupting it, the amorphous region enables penetration of chemicals to reactive sites due to lack of hydrogen bonds.[25] Figure 1.4 illustrates the ultrastructure of plant cellulose from fibers in cell wall to fibrils and crystal structure of cellulose chains.

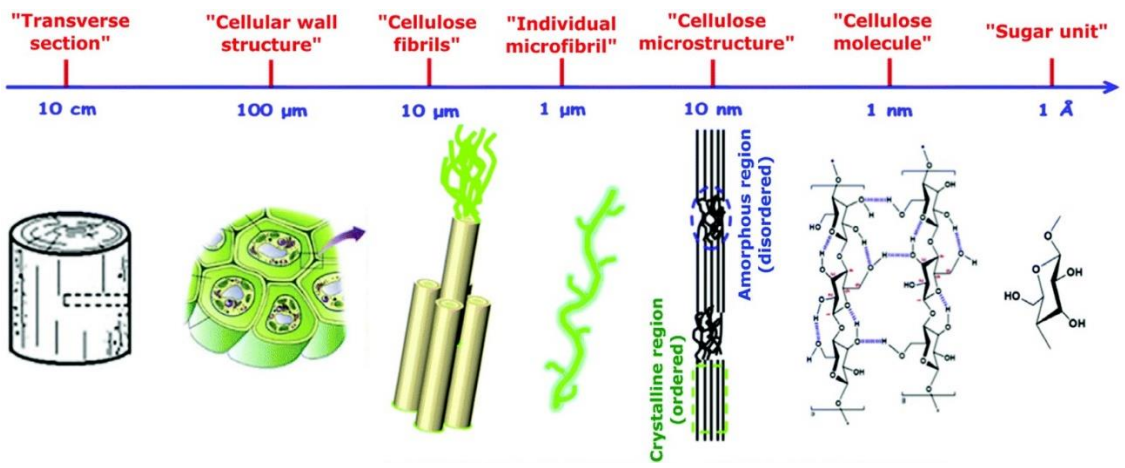

Figure 1.4. Picture of a wood cell wall. Cellulose exists as a system of fibrils.[155]

Three hydroxyl groups for each glucose unit make cellulose a chemically active molecule. The one primary hydroxyl group which is located at C-6 is the most reactive OH group of cellulose and undergoes esterification reaction with anhydrides or carboxylic acids. Two secondary OH groups are located at C-2 and C-3 and C-2 hydroxyl is more reactive than C-3 hydroxyl. In general, the reactivity of hydroxyl groups depends on their intrinsic reactivity, steric effects of reagents and steric effects resulting from the supramolecular structure of cellulose.[25]

Cellulose can be degraded through an enzymatic process by microorganisms (bacteria, fungi) present in air, water, and soil to the glucose units at the end of materials life.[5] Therefore, replacing synthetic materials by cellulose-based products could also be environmentally beneficial.

1.3.2.1. CMC-based hydrogels

The carboxymethyl group has been added to native cellulose to form a negatively charged, water soluble polymer that is commercially available in high purity and low cost.[26-28] Additionally, carboxymethyl cellulose (CMC) is not degradable by human enzymes nor it is part of typical human cell signaling cascades; therefore, it can be an alternative for synthetic, biologically resistant polymers like polyethylene glycol (PEG). CMC has an advantage over PEG as it has numerous reaction points along its backbone that can be used to introduce significantly more cross-linking points, reactive sites, and biological activity in one molecule.

Another valuable property of CMC biomaterials is that they can be orthogonally and selectively enzymatically degraded using cellulase, opening new routes in biotechnology. Since CMC is not part of the extracellular matrix (ECM) it can be post-cell culture degraded completely without any harm to the ECM produced by cultured cells. For example, Ko *et al.* reported a successful porcine aortic endothelia cell (PAEC) culture on a CMC-coated glass substrate with immobilized fibronectin followed by degradation by cellulase enzyme under physiological conditions.[29] Cell-cell connections were preserved in the PAEC sheet after treating with enzyme and the cell sheet was further transferred to a secondary cell culture dish. Sakai et al. reported similar results with L929 cell sheets on phenol-functionalized CMC hydrogels.[10] This cell detachment process can be cell-type dependent.[30] Though these studies showed the cytocompatibility of cellulase and the culture and release of cells in two dimensions, new chemistry and methods are needed so that these techniques can be used in 3D systems.

Covalently cross-linked CMC hydrogels have been synthesized and demonstrated to support chondrogenic differentiation of hMSCs and to promote surface cell adhesion.[31,32] These hydrogels were fabricated by cross-linking methacrylated CMC through the polymerization with UV light

irradiation or using a thermal radical initiator.[33] Other CMC hydrogels have been covalently cross-linked with an external cross-linker using methods such as thermal radical reactions and interpenetration network formation as well as sometimes requiring cytotoxic chemicals.[34-38] These chemically cross-linked CMC based materials have functioned as protein and drug carriers as well as physical bulking materials.[39-45] However, many of these CMC-based hydrogels suffer from long gelation times and toxic gelation conditions that prevent them from being viable materials for 3D ECM mimics.[46,47] New crosslinking methods are needed to create cytocompatible and robust CMC hydrogels where cells can be cultured within the 3D environment.

1.3.2.2. CNF-based hydrogels

Recently, cellulose nanofibrils (CNF) attracted much attention due to low cost and availability. CNF is a waste product of the wood pulp industry and can be used after mechanical grinding or chemical treatments.[48] CNF can be found as individual and aggregated cellulosic fibers that hold together with strong intra- and inter-molecular hydrogen bonds along with entanglement of these aligned fibers. As a result, fibrils with diameters of 10-100 nm and 1 μm length are achieved that are comparable with of collagen fibrils in ECM with diameters of 10-300 nm. Because of these hydrogen bonding and the entanglements of long fibrils, CNF dispersion exhibits a gel-like character in aqueous media even at concentrations as low as 0.1 wt%. CNF suspensions have been utilized as scaffolds for tissue engineering because their fibril structure mimics the fibrous components of the extracellular matrix (ECM). Lou et al. reported spheroid formation of human pluripotent stem cells (hPSC) in a 3D plant derived CNF physical hydrogel at low concentration (0.5 wt%).[49] In their work, CNF without any further treatment was used and no evidence of toxicity was observed. They showed that stem cells retain their pluripotency after 26 days of culture. Additionally, a 3D CNF hydrogel has been degraded using Cellulase enzyme and 3D hPSC spheroids

were recovered and used to direct differentiation to desired cell types. Bhattacharya et al. reported culture of HepaRG and HepG2 cells into 3D single component CNF hydrogels (0.1-1.2 wt %) and formation of spheroids was observed.[50] No toxicity was observed for these cell types. These hydrogels were also injectable due to shear-thinning character of CNF. Malinen et al. also reported the same result with HepaRG cells.[51] In another study, Mathew and coworkers introduced CNF as a replacement for ligament and tendons. It has been proven in this study that CNF supports cell adhesion and proliferation of both human ligament cells (HLC) and endothelial cells (HEC) and showed high cytocompatibility.[52]

To improve the stability and mechanical properties of these materials, further physical or chemical cross-linking is necessary. For chemical cross-linking reactions, the addition of proper functional groups to CNF surface is needed. The presence of three hydroxyl groups on each cellulose repeat units provides a reactive surface on CNF that can be chemically modified and functionalized with diverse functional groups to adopt desired chemistry. Several surface modifications have been done on CNF, such as functionalization with carboxyl, azide, carboxymethyl, trimetylammonium, and aldehyde groups. These modifications usually take place in organic solvents and include toxic and harmful reagents. Moreover, they need a post-oxidation fibrillation step to produce modified fibrils. CNF itself is known as a biocompatible material, but it has been shown that surface modification can change the cytotoxicity of CNF.[53] Although it has been proven that modified CNF exhibits less cytocompatibility compare to untreated CNF, in many cases this decrement is not remarkable. For example, carboxymethylated CNF has shown promising properties to replace nucleus pulposus.[54] A physical gel of CNF and polyurethane has been used by Cherian and coworkers to fabricate blood vessel that has been implanted in a 26-year old patient.[55] There are examples of CNF-based materials with variety of applications such as drug delivery and wound healing.

1.4. Thiol-ene reaction to make hydrogels

Synthetic methods used in biomaterials should be operable in mild physiological conditions and produce no or easily removable by-products. These factors are among the characteristics of click reactions. Because of these characteristics, click reactions are extremely used to fabricate and modify biomaterials. As introduced by Sharpless et al. in 2001, click reactions benefit from high yield, rapid reaction rate, chemo-selectivity, and insensitivity to ambient oxygen and moisture.[56] A click reaction does not affect or is not affected by other chemical reactions in the system and function in bulk, solventless conditions, or in complex aqueous media. Furthermore, there should be a variety of compounds available that can react via a click reaction. There exist examples of reactions that have all or most of these criteria including copper-catalyzed azide-alkyne reaction, strain-promoted azide-alkyne cycloaddition, Diels-Alder reaction between tetrazine and norbornene, nucleophilic ring opening, and thiol-ene reaction.[57]

Copper-catalyzed azide-alkyne reaction was one of the most investigated click reactions. But because of the cytotoxicity of copper, other approaches attracted more attention in biomedical fields in recent years. Due to the enormous variety of thiol molecules such as cysteine-bearing proteins and peptides in biological systems, along with its almost quantitative conversion and fast (within few seconds) reaction rate under physiological pH and temperature, thiol-ene reaction is of interest in biomaterials synthesis.

The thiol-ene reaction is a known chemistry and has been studied since 1900. It is simply a reaction between thiol molecules and reactive carbon-carbon double bonds (Figure 1.5). Thiol-ene chemistry is not limited to alkyl thiols and examples of thiophenols, thiopropionates, and thiol glycolates have been reported to be reactive for thiol-ene reaction. Almost any terminal carbon-carbon double bond (ene) that is not sterically hindered undergoes thiol-ene click reactions. If

thiols and enes are sterically hindered, thiol-ene reaction still may work, but it does not meet the criteria of a click reaction.[58] When multifunctional thiols or enes are used, thiol-ene reaction produces a cross-linked polymeric network with high conversion. This technique has been utilized to form hydrogel networks for many biomedical applications such as cell encapsulation.

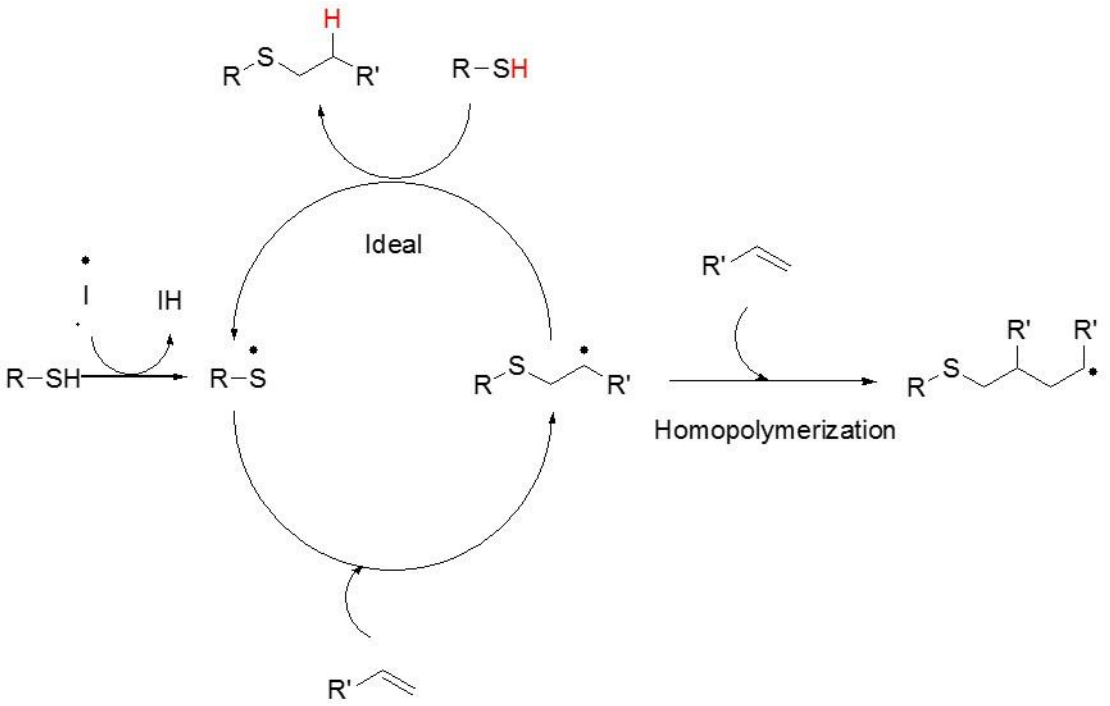

Figure 1.5. The mechanism of free radical thiol addition to carbon-carbon double bond. A thioyl radical forms by the reaction of thiol and radical initiator. Thioyl radical then reacts with ene and the radical transfers to carbon (thioether radical). The thioether radical either completely forms the thioether molecule (product) or partially undergoes homopolymerization (by-product).

Thiol-ene reaction can be through a free radical addition (when an electron rich carbon and an electron poor carbon are forming ene) or a catalyzed thiol Michael addition (when both carbons of ene are electron deficient). Both these approaches have the characteristics of click reactions. But in the radical-based reaction, when the ene moiety is electron rich (vinyl ether) or it is part of a strained ring (norbornene), the reaction is much faster than when an electron poor ene is involved.[58]

Figure 1.5 is a schematic illustration of the mechanism of free radical addition of thiol to ene. The first step is radical generation which can be promoted by light, heat, or chemicals. The radical will be transferred to the carbon after addition of thiol to ene. In an ideal thiol-ene reaction, a radical hydrogen will be added to the carbon and form the thiol-ene product and a thioyl radical which promotes more thiol-ene addition (step-growth of chain).[58] Thiol addition to vinyl ether and norbornene are examples of an ideal thiol-ene. In some cases, for example when (meth)acrylates are used, the carbon radical undergoes uncontrolled homopolymerization and so, a heterogeneous mixture of products would be obtained (chain-growth). The homogeneity of the network influences the properties of a polymeric network. For example, Mũnoz et al. functionalized gelatin with norbornene (GelNB) and cross-linked it with dithiothreitol (DTT) using a visible-light initiator (lithium phenyl-2,4,6-trimethylbenzoyl phosphinate (LAP)) to encapsulate human mesenchymal stem cells (hMSCs).[59] They observed that cell spreading in GelNB hydrogels is faster and more than in GelMA (methacrylated gelatin) hydrogels that are made through a chain-growth polymerization process. This proves that the uniform structure of the matrix improves cell-matrix interactions.

Other examples of cell encapsulation in hydrogel formed via thiol-norbornene (thiol-NB) chemistry could be found in literature proving that it is a biologically benign reaction. McKinnon et al. has reported the successful encapsulation of embryonic stem cell-derived motor neurons (ESMNs) in poly(ethyleneglycol) (PEG) hydrogels using thiol-NB chemistry.[60] They used a dithiol peptide sequence to cross-link 4-arm PEG by the irradiation of visible-light (Figure 1.6.A). ESMNs survived in the hydrogel after a week and extended axons were also observed. hMSC encapsulation and survival in PEG cross-linked resilin (an insect protein) has been reported by McGann et al (Figure 1.6.B).[61] In their work, resilin was functionalized with norbornene and 4-arm PEG with a thiol at each terminus was used as cross-linker. Here LAP was used as the initiator.

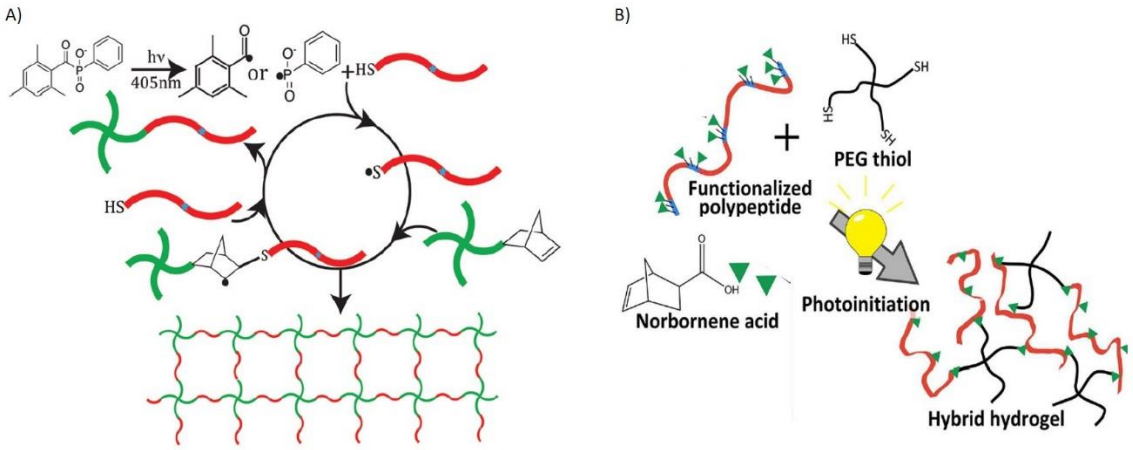

Figure 1.6. Two examples of the hydrogel formation via thiol-ene reaction. A) between 4-arm norbornene functionalized PEG and a dithiol peptide sequence[60], and B) between 4-arm thiol functionalized PEG with a norbornene functionalized peptide.[61]

As mentioned before, there are different ways to generate thioyl radical, but photo-initiated thiol-ene reaction is of more interest. Photo-initiated processes benefit from the ability to be activated in a controlled fashion at the desired time and position. By adding this high control to the advantages of click-reaction, light-induced thiol-ene chemistry would be a powerful tool in applications such as modification of the substrate surfaces, functionalization of polymers, photolithography, fabrication of nanostructured networks, and light-induced cross-linking of functional polymers. For example, orthogonal patterning of HA hydrogels with different dyes using UV light (photpatterning) has been studied by Gramlich and coworkers.[62] Norbornene functionalized hyaluronic acid (NorHA) was gelled via a UV-light initiated thiol-NB reaction using DTT as cross-linker. These hydrogels then were photopatterned by three different thiolated dyes in different patterns (Figure 1.7). Photomasks with different patterns have been used that allowed UV exposure in some regions and blocking UV in other regions. This photo-initiated thiol-NB reaction led to a method to spatiotemporally pattern hydrogels after they have been made.

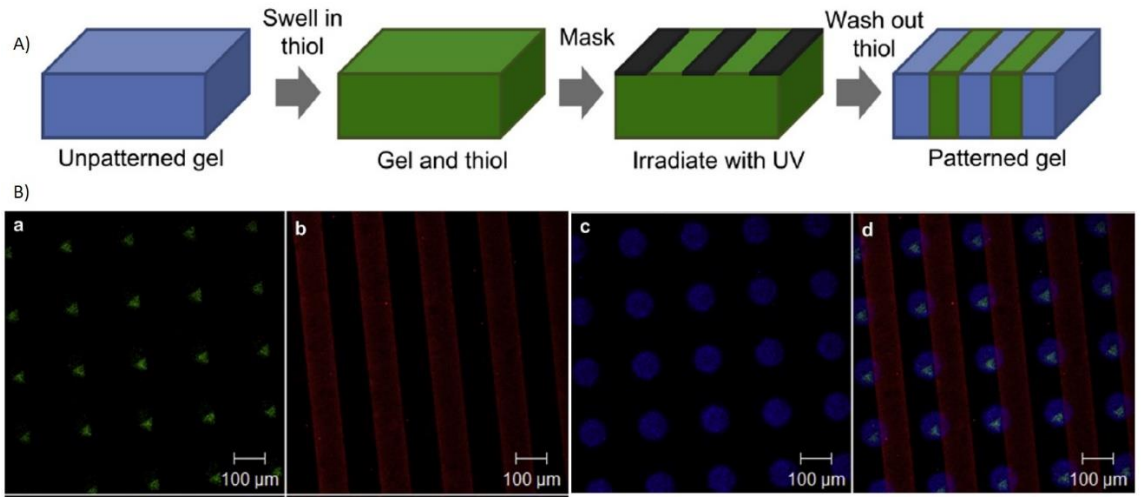

Figure 1.7. Light-induced thiol-NB reaction enables spatiotemporal modification of already prepared hydrogels. A) Photopatterning strategy of NorHA hydrogels using photomask patterned with compounds that block light. The thiol-ene reaction will be activated only at UV exposed regions. B) Images NorHA hydrogels patterned with different dyes using photomasks with different shapes of UV-exposed regions.

The advantages of click chemistry, the potentials of photo-initiated reaction, and the biologically benign nature made the thiol-NB reaction the perfect candidate for the work presented in this dissertation.

1.5. Spatiotemporal modifications

The focus of current work is to make hydrogels more adaptable and tunable to multiple applications - much like the natural systems that they mimic. Of particular interest is the spatiotemporal control of the physical and chemical properties to simulate the dynamic behavior of natural tissues. Spatiotemporal control requires robust and highly specific orthogonal chemistries such that “click” reactions have become the preferred method to impart these properties through an additive process.[60,61,63-65]

Light initiated modifications to hydrogels are an ideal method to spatiotemporally control properties. Through light sensitive thiol-ene chemistry and photopatterning, removal of crosslinks

and molecules of interest have controlled physical and chemical properties as well as the subsequent direction of cell behavior.[66-72] However, such subtractive processes are not designed to increase the modulus of the hydrogels that is needed for some applications. To spatiotemporally add in functionality, photopatterned thiol-ene reactions are attractive methods as these light induced click chemistries are highly specific and cytocompatible.[72-75] Both allylic ethers and norbornene functionalities have been reacted with dithiol terminated crosslinkers to yield spatiotemporally modifiable natural and artificial hydrogel matrices.[76]

1.6. Stimuli-responsiveness

Spatiotemporal modifiable systems are just one aspect towards creating hydrogels with biologically relevant properties as the materials must also respond to stimuli. Such stimuli include enzymatic, temperature, and pH changes that are observed in the body due to a variety processes. Numerous biomaterials have used these stimuli to impart temporal changes to the material and chemical properties; however, significantly fewer examples exist of spatiotemporal changes to the extent that the material responds to such stimuli.[2-4,77,78] Previous examples of spatiotemporal changes to stimuli response have typically removed the stimuli response.[79] For example, such spatiotemporal changes have been achieved by arresting the enzymatic degradation of materials by adding a non-enzymatically degradable crosslinker.[80] These current methods limit spatiotemporal changes to stimuli to only reducing the effect. To increase the available designs of biomaterials, methods are needed to add in stimuli response spatiotemporally after hydrogel formation.

Hydrogels that respond to thermal stimuli have been utilized in a myriad of applications such as temperature induced drug delivery and injectable hydrogels.[81-84] Many materials have used poly(*N*-isopropylacrylamide) (PNIPAM) (Figure 1.8.A) as the thermally responsive polymer in their

formulation as it has a lower critical solution temperature (LCST) around body temperature (32 °C).[85-87] Below its LCST, polymer is soluble in water. But when the polymer is heated up to temperatures above the LCST, a phase transition from soluble to insoluble (hydrophilic to hydrophobic) would occur. In this state, the intra molecular interactions are stronger than hydrogen bonds with water molecules. Because of these intra molecular interactions, polymer chains collapse which leads to a volume change in hydrogels and decrease in mass due to the repulsion of water.

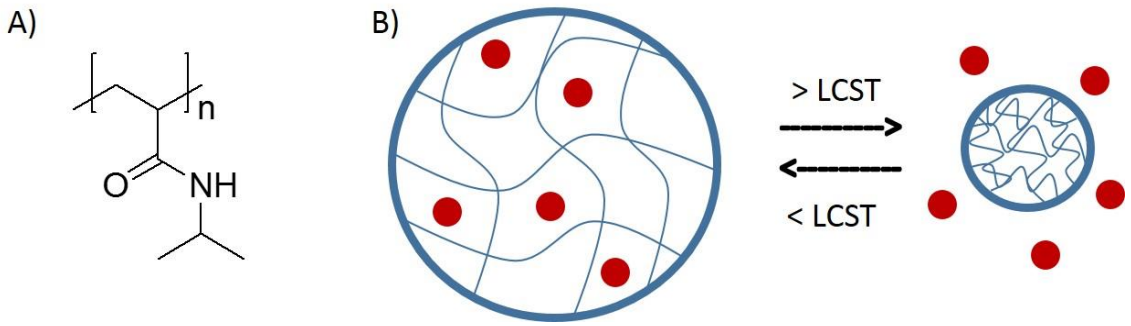

Figure 1.8. PNIPAM and thermo-responsiveness. A) Chemical structure of PNIPAM. PNIPAM has a LCST in water around physiological temperature. B) A diagram to illustrate the reversible response of thermo-responsive hydrogel to changes in temperature.

Applications of thermally responsive PNIPAM-based hydrogels vary from temperature-responsive cell culture dishes to microlenses and bioactuators.[88-92] Some PNIPAM-based materials have thermally induced the release of proteins and several therapeutics such as heparin, ovalbumin, doxorubicin, mesalamine, and other model compounds.[93-97] Self-propelling microjets made of 2D PNIPAM hydrogels have been studied to mimic the movement of biological swimmers triggered by changing temperature.[91] Furthermore, patterned and functionalized PNIPAM 2D hydrogels have been used to fabricate cell culture dishes with dual cell adhesion properties. However, these hydrogels have typically been made from a majority of synthetic polymers.

Hydrogels that are a majority of biological polymers while retaining the thermo-responsive nature could open the door to new biomaterial applications.

1.7. Mechanical properties of hydrogels

The mechanical properties and moduli of hydrogels are just as important for biomaterial applications as the stimuli responsiveness. For example, stem cell fate is directed not only by chemical cues, but also by the stiffness of its environment. Many cellular activities such as stem cell spreading, proliferation, and differentiation are influenced by the mechanical properties of the extracellular matrix or substrate.[98-105] As an example, human mesenchymal stem cells (hMSCs) cultured within a polyethylene glycol (PEG)-Silica 3D hydrogel, differentiated into neurons at lower modulus (7 kPa), while at higher modulus (25 kPa) underwent myogenic differentiation.[106] Additionally, living tissues have different moduli, due to their different functions, that vary from 0.5-1.5 kPa for fat or bone marrow to several thousand kPa for cartilage and bone (Figure 1.9).[102] Tissue stiffness is dynamic and can change during biological processes such as embryonic development and diseases like cancer.[101-103] New biomaterials should be tunable to this range of material properties to be biologically relevant.

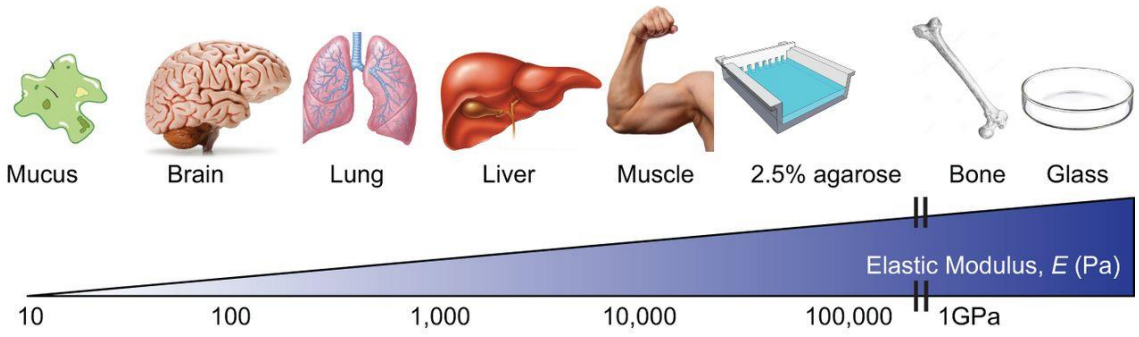

Figure 1.9. The elasticity of tissues. The diagram shows the wide range of elastic modulus of tissues that is necessary for its function. The stiffness of a hydrogel as scaffold for tissue engineering should be in the range of the stiffness of the tissue to be generated.[107]

1.8. The goal of this project

Current thermo-responsive PNIPAM-based hydrogels can suffer from poor mechanical properties, they are not biodegradable, and in some cases they are cytotoxic limiting the applications of PNIPAM-hydrogels in biological aspects.[108] To overcome these limitations, combining thermo-responsive PNIPAM with natural biodegradable polysaccharides and proteins and/or using peptide crosslinkers have attracted attention.[109,110] These hydrogels are typically either robust synthetic materials with high modulus for the drug delivery systems or soft, physically crosslinked thermo-gelling materials that incorporate a biopolymer as a backbone material.[111,112] A currently missing hydrogel from this field is a robust and tunable, thermally responsive hydrogel that consists of a majority of natural polymers. Such a material could be used for degradable drug delivery, shape memory physical bulking, and cell scaffolding applications.

The work presented here in chapter two addresses the above limitations by using a dithiol-functionalized PNIPAM, synthesized through reversible addition-fragmentation chain transfer (RAFT) polymerization and subsequent aminolysis, to crosslink norbornene functionalized hyaluronic acid (NorHA) through a thiol-norbornene reaction. Through selection of the crosslinker and gelation conditions a range of thermo-response and mechanical properties could be controlled. This crosslinking reaction was used not only to form hydrogels, but also to spatiotemporally change the stimuli response of the materials after the initial gelation as well as change the surface topology of hydrogels. Such materials demonstrate new methods to create spatiotemporally controlled stimuli response in hydrogels made from a majority of natural materials and serve as a platform for a variety of biomedical uses in future applications.

To address the limitations of current CMC hydrogels towards creating spatiotemporally modifiable biomaterials, norbornene-functionalized CMC (NorCMC) was synthesized and used to

create hydrogels using several dithiol cross-linkers through the photoinitiated thiol-norbornene reaction. Thiol-NB reaction was previously applied, but CMC was functionalized with thiols and NB functionalized cross-linker was used to make hydrogels.[47] One limitation of that system was unwanted cross-linking due to formation of disulfide bonds when the material is stored. Such a problem would not be an issue in NorCMC polymers because norbornene has no tendency to react with another norbornene group. Additionally, a larger selection of thiol cross-linkers including peptides are available.

Chapter three focuses on development of CMC-based hydrogels. Several experiments have been designed to validate the capability of NorCMC to be applied in different aspects of biomaterials. Different hydrogel moduli were obtained by varying parameters such as the UV irradiation time, thiol to norbornene molar ratio (T/NB), polymer weight percent (wt%), and length of the cross-linker. The behavior of thermoresponsive NorCMC/PNIPAM hydrogels was explored as well as the spatiotemporal modification of NorCMC hydrogels. In addition, NorCMC was demonstrated to be cytocompatible and could be modified so that cells could adhere and spread in two and three-dimensions. These following results demonstrate that NorCMC is a robust and capable material that can be a natural alternative for next generation biomaterials. However, separate studies should be done in the future to investigate NorCMC hydrogels for specific applications.

In chapter four, functionalization and chemical gelation of CNF will be discussed. Several cross-linking strategies have been applied to form CNF hydrogels such as azide-alkyne click reaction, aldehyde-amine reactions, hydrogen bonding of carboxylates, and cationic metal interactions with carboxylate.[113-116] Many of current cross-linking strategies suffer from long gelation time, using toxic compounds, and do not allow spatiotemporal modification.[50,51] In this study, we

introduce a straightforward reaction to functionalize CNF with norbornene groups in aqueous media and room temperature. Norbornene functionalized CNF (nCNF) then can be chemically cross-linked using light induced thiol-ene click chemistry. This could benefit from the wide range of biocompatible thiolated cross-linkers including peptides and polymers.

Methods to characterize functionality on CNF are limited to acid-base titration for anionic functional groups, $AgNO_3$ titration for cationic functional groups, and, recently, quantitative solid state ^{13}C-NMR spectroscopy.[117] To our knowledge, however, ^{1}H-NMR spectroscopy has never been done to characterize CNF because CNF and its derivatives are insoluble in common ^{1}H-NMR solvents. Here for the first time we obtained the quantitative degree of functionality using ^{1}H-NMR spectroscopy. To do this, CNF was degraded into smaller soluble segments by cellulase enzyme and the resulting sugar units were dissolved in D_2O for ^{1}H-NMR spectroscopy. The extent of degradation along with the degree of functionalization were calculated. This straightforward and effective strategy opens the door to complete characterization of modified CNF.

In this work, the CNF surface was modified with norbornene functional groups in a straightforward aqueous reaction and quantitatively characterized by ^{1}H-NMR spectroscopy after enzymatic hydrolysis. Thiol-norbornene chemistry was applied to fabricate nCNF hydrogels varying cross-linkers type and amount. To investigate the mechanical properties of nCNF and its hydrogels, dynamic mechanical analysis and rheology were conducted. Human mesenchymal stem cell (hMSC) viability in these hydrogels was briefly studied.

In order to apply our materials in real biological studies, methods of gelation and pre-gelation solution preparation should be developed. Any researcher with limited chemistry knowledge and skills should be able to use these materials. Therefore, the pre-gelation solution was prepared in a fashion that solutions could be stored for long time while retaining its reactivity. The gelation

protocol was as simple as mixing two solutions followed by either incubation at physiological conditions or UV light exposure.

CHAPTER 2

THERMO-RESPONSIVE HYALURONIC ACID-POLY(N-ISOPROPYLACRYLAMIDE) HYDROGELS

2.1. Introduction

Current methods to spatiotemporally modify stimuli response in hydrogels are typically subtractive and lead to a decrease in response. To increase the breadth of hydrogel applications and biomedical systems, new formulations are needed that can introduce and increase stimuli response spatiotemporally in hydrogels. In this work, the light induced thiol-norbornene click chemistry reaction was used to modify the stimuli response of robust hyaluronic acid hydrogels through an additive process in spatiotemporal fashion, overcoming this limitation. These stimuli responsive hydrogels were made from norbornene functionalized hyaluronic acid (NorHA) cross-linked with thermo-responsive dithiol-terminated poly(N-isopropylacrylamide) (DTPN). Varying cross-linker molecular weight and gelation conditions led to a range of compression modulus (5 to 54 kPa) and mass loss (9 to 33%) upon heating to 37 °C while retaining a majority NorHA in the hydrogel. The thermo-response of these hydrogels could not only be controlled by the cross-link density, but also by heating to 55 °C to increase the dewatering of the hydrogels. The stimuli response of the hydrogels were temporally increased by introducing additional DTPN and UV-initiator to an original hydrogel with subsequent irradiation. This modification was extended to spatiotemporally changing the stimuli response by photopatterning DTPN into a NorHA hydrogel, yielding a hydrogel that changed shape and topology through heating. Furthermore, human mesenchymal stem cells could adhere and proliferate on the DTPN patterned surface, demonstrating that the materials could be used for studies where cells are present.

2.2. Experimental

2.2.1. Materials

Chemicals were purchased from either Sigma-Aldrich or Fisher scientific and used without further purification unless otherwise noted. N-isopropyl acrylamide (NIPAm) was purified by recrystallization in hexanes prior to use. Alpha-omega hydroxyl-terminated ethylene glycol polyethylene oxide (EGPEO, M_n = 1700 g/mol) was purchased from Polymer Source Inc. Norbornene-functionalized hyaluronic acid (NorHA) was synthesized following a previously reported procedure at reference 62. All cell culture materials and assays were purchased from Life Technologies.

2.2.2. Synthesis of di-functionalized RAFT CTA (DiCTA)

The RAFT chain transfer agent S-1-dodecyl-S-(α,α'-dimethyl-α''-acetic acid)trithiocarbonate (mono-RAFT CTA) was synthesized following a modified literature procedure.[118] In a representative synthesis, the mono-RAFT CTA (4.00 g, 10 mmol) was placed in a multi-necked round bottom flask connected to a bubbler. The flask was purged with nitrogen and then 4 mL anhydrous dichloromethane was added as solvent. A 10-fold molar excess (100 mmol) of oxalyl chloride was added by a syringe to the solution while stirring until gas generation stopped to synthesize the CTA acyl chloride. The unreacted oxalyl chloride and solvent were removed by pulling vacuum. In another round bottom flask under nitrogen atmosphere, triethylamine (1.03 mL, 7.40 mmol) and 1,4-butanediol (0.32 mL, 3.70 mmol) were dissolved in 10 mL of dichloromethane and the mixture was cooled in ice bath. The CTA acyl chloride reaction was transferred into this flask by syringe and the mixture was stirred overnight at room temperature. The product was diluted with dichloromethane and washed once with DI water and once with brine solution. The organic phase was purified through a silica gel column using a 90:10 mixture

of hexane and ethyl acetate as the mobile phase. Solvent was removed by rotary evaporator to yield the final product. The DiCTA synthesis was confirmed by proton NMR (^{1}H NMR) spectroscopy (Overall reaction 61% yield compare to mono-RAFT CTA).^{1}H NMR spectroscopy of mono-RAFT CTA ($CDCl_3$, 400 MHz) **δ** 0.88 (t, *J*=8 Hz, -CH_3 end group, 3H), 1.24-1.4 and 1.60-1.67 (m,-$C_{10}H_{20}$ alkyl chain, 20H), 1.68 (s, germinal –CH_3s, 6H), 3.26 (t, *J*=4 Hz, -SCH_2, 2H).

^{1}H NMR spectroscopy of DiCTA ($CDCl_3$, 400 MHz) **δ** 0.87 (t, *J*=8 Hz, -CH_3 end group, 6H), 1.25-1.45 and 1.60-1.7 (m, -$C_{10}H_{20}$ and –CH_2CH_2 butanediol, 44H), 1.68 (s, geminal CH_3s, 12H), 3.26 (t, *J*=8 Hz, -SCH_2, 4H), 4.08 (t, *J*=4 Hz, -OCH_2, 4H).

2.2.3. Synthesis of DiCTA terminated poly(*N*-isopropyl acrylamide) (DCTAPN)

DiCTA PNIPAM polymers with varying molecular weights were synthesized by RAFT polymerization by varying the NIPAm to DiCTA ratio. In a representative polymerization, NIPAm (3.00g, 26.5 mmol), DiCTA (0.46 gr, 0.59 mmol), and α,α'-azobisisobutyronitrile (AIBN) (0.4g, 0.24 mmol) were dissolved in 5 ml of 1,4-dioxane and then transferred to a reaction vessel. The mixture were degassed by three cycles of freeze-pump-thaw method, the vessel was sealed, and the mixture was heated at 70 °C for 18 h while stirring. The solution was precipitated in diethyl ether from dioxane, reprecipitated from THF into diethylether, and vacuum dried for 48 hours. The product was analyzed by size exclusion chromatography (SEC) and ^{1}H NMR spectroscopy. SEC was conducted using an Agilent 1260 infinity SEC system consisting of a series of three Phenogel columns with different pore sizes (Phenomenex Organic columns, 50A, 10E3A, 10E6A), an interferometric refractometer under the following conditions: DMF as eluent; injection volume of 50 µL; flow rate of 1 mL/min; and oven temperature of 50 °C. All measurements were conducted based on calibration against polystyrene standards.

^{1}H NMR spectroscopy of DCTAPN ($CDCl_3$, 400 MHz) **δ** 0.86 (t, *J*=4 HZ, -CH_3 end group, 6H), 1.12 (s, germinal CH_3s of repeat unit, 12H), 1.24-2.3 (m, -$C_{10}H_{20}$, –CH_2CH_2 butanediol, geminal CH_3s of CTA, and PNIPAM backbone, 3.32 (t, *J*=8 Hz, -SCH_2, 4H), 3.98 (br, -NCH and –OCH_2, 5H), 4.56 (very small, -SCH backbone, 2H), 6-6.7 (br, -NH, 2H).

2.2.4. Synthesis of monoCTA terminated PNIPAM (MCTAPN)

In a typical synthesis of a MCTAPN, mono-RAFT CTA (0.032 g, 0.088 mmol), NIPAm (0.5 g, 4 mmol), and AIBN (150 µl, 0.009 mmol) were dissolved in 1 mL of 1,4-dioxane and solution was transferred to an ampule. The sample was degassed through three freeze-pump-thaw cycles before sealing the ampule. The solution was heated at 70 °C for 18 h, cooled, and the product was precipitated into diethyl ether followed by re-precipitation from THF into diethyl ether. Solvent was removed by purging nitrogen and pulling vacuum after filtration. The sample was characterized by ^{1}H NMR spectroscopy and SEC. ^{1}H NMR spectroscopy of MCTAPN ($CDCl_3$, 400 MHz) **δ** 0.85 (t, *J*=8 HZ, -CH_3 end group, 3H), 1.11 (s, germinal CH_3s of repeat unit, 6H), 1.12-2.49 (m, -$C_{10}H_{20}$, geminal CH_3s of CTA, and PNIPAM backbone (29H), 3.31 (t, *J*=8 Hz, -SCH_2, 2H), 3.97 (br, -NCH, 1H), 5.7-7 (br, -NH, 2H).

2.2.5. Synthesis of thiol-terminated PNIPAM

The dithiol-terminated PNIPAM (DTPN) cross-linkers and mono-thiol terminated PNIPAM (MTPN) were synthesized by aminolysis of the CTA-terminated PNIPAMs following a modified literature experiment.[119] In a representative synthesis, DCTAPN (1 g, 0.13 mmol), 1-butylamine (0.088 g, 1.20 mmol) at a 10-fold excess of the trithiocarbonate moieties, and small amount of reducing agent tris(2-carboxyethyl)phosphine hydrochloride (TCEP) (0.14 g, 0.40 mmol) were dissolved in 10 ml THF and stirred for 1 h at room temperature under nitrogen atmosphere. The product was precipitated into diethyl ether twice and dried on vacuum overnight. The yield of

aminolysis reaction was 65%. ^{1}H NMR and UV-vis spectroscopy (PerkinElmer UV-Vis spectrometer, 0.33 gml^{-1} solution of samples in THF, 250-600 nm wavelength range) were used to confirm removal of the trithiocarbonate group and the generation of the thiol. The products were stored in a fridge at 4 °C prior to use. Two DTPN were synthesized with M_n of 4 and 8 kg/mol (^{1}H NMR calculated), labeled DTPN4 and DTPN8, respectively. A MTPN with a M_n of 8 kg/mol (MTPN8) was also synthesized by this method. Also the products were analyzed by SEC applying the same condition mentioned previously in this paper. Molecular weights of polymers were calculated via end group analysis using peak integrals. ^{1}H NMR spectroscopy of DTPN ($CDCl_3$, 400 MHz) **δ** 1.13 (s, germinal CH_3s of repeat unit, 12H), 1.2-2.7 (m, $–CH_2CH_2$ butanediol, geminal CH_3s of CTA, and PNIPAM backbone (19H), 3.98 (br, -NCH, 1H), 6-7 (br, -NH, 2H).

^{1}H NMR spectroscopy of MTPN ($CDCl_3$, 400 MHz) **δ** 1.12 (s, germinal CH_3s of repeat unit, 6H), 1.2-3 (m, geminal CH_3s of CTA, and PNIPAM backbone, 3.98 (br, -NCH, 1H), 6-7 (br, -NH, 1H).

2.2.6. Measurement of the LCST of DTPNs

The LCST of the DTPNs was measured by dynamic light scattering (DLS) with a Malvern Nanoseries Zetasizer Zen 3600 instrument. Solutions of 0.01 wt % DTPN8 and 0.1 wt % DTPN4 were prepared in HPLC grade submicron filtered water. Data were collected at 1 °C intervals using a temperature range of 10 to 65 °C. To ensure that the sample viscosity was equilibrated, a 5-minute delay time was applied at each temperature before recording data. The mean count rate (kcps) and Z-average diameter (nm) were measured versus temperature (°C).

2.2.7. Synthesis of dithiol-terminated polyethylene glycol (DTPEO)

DiCTA-terminated polyethylene glycol was synthesized following a procedure similar to that used to make the DTPNs. In a multi-neck round bottom flask connected to a bubbler, RAFT CTA (2

g, 5 mmol) was purged with nitrogen and followed by sequential addition of anhydrous dichloromethane (5 ml) and 10-fold molar excess of oxalyl chloride (4.7 ml, 50 mmol) to synthesize the RAFT CTA acyl chloride. After two hours, at the end of the reaction, solvent and unreacted oxalyl chloride were removed by vacuum. In a separate round bottom flask and under a nitrogen atmosphere, EGPEO (1.6 g, 0.917 mmol), triethylamine (0.250 ml, 2.5 mmol), and dichloromethane (6 ml) were added. This mixture was cooled in an ice bath and the RAFT CTA acyl chloride was added to it and allow to react for 18 h at room temperature. The product was precipitated into 10-fold excess hexane and dried under vacuum. ^{1}H NMR spectroscopy confirmed formation of diCTA-functionalized PEO (DCTAPEO) (Figure S5). ^{1}H NMR spectroscopy of DCTAPEO ($CDCl_3$, 400 MHz) **δ** 0.82 (t, *J*=4 HZ, -CH_3 end group, 6H), 1.19-1.31 (m, -$C_{10}H_{20}$, (40H), 1.68 (s, geminal CH_3s, 12H), 3.20 (t, *J*=8 Hz, -SCH_2, 4H), 3.4-3.8 (m, -CH_2 PEO backbone, 4H), 4.19 (t, *J*=4 Hz, -$COOCH_2$, 4H).

The DCTAPEO was transformed into DTPEO through subsequent aminolysis. In a typical reaction, DCTAPEO (0.6g, 0.280 mmol), 1-butylamine (1.11 ml, 11.2 mmol, 20 molar excess of amine to trithiocarbonate moiety), and TCEP (0.19g) were dissolved in 10 ml THF, following the procedure used to make DTPN. The product was precipitated into 10-fold excess hexanes. Greyish precipitant was then dissolved in THF, filtered through filter paper, and precipitated into 10-fold excess hexanes. The white precipitant was collected and dried under vacuum for 48 hours. ^{1}H NMR spectroscopy and SEC measurements were conducted to calculate M_n and Đ for the product. SEC analysis used THF as eluent and oven temperature was 35 °C. All measurements were conducted based on calibration against polystyrene standards. ^{1}H NMR spectroscopy of DTPEO ($CDCl_3$, 400 MHz) **δ** 1.53 (s, germinal CH_3s, 12H), 2.85 (br, -SH (2H), 3.4-3.7 (m, -CH_2, PEO backbone, 4H), 4.22 (t, *J*=4 Hz, -$COOCH_2$, 4H).

2.2.8. Preparation of NorHA hydrogels

NorHA hydrogels were prepared with various polymer concentrations, molar ratios of thiol to norbornene ($X_{T/N}$), and cross-linkers. To prepare pre-hydrogel solutions, NorHA, cross-linker, and the radical initiator 2-hydroxy-4'-(2-hydroxyethoxy)-2-methylpropiophenone (I2959) (0.05 wt %) were dissolved in PBS by vortexing for 1 h. Air bubbles were removed by centrifuging for 10 minutes at a speed of 6000 min^{-1}. To synthesize hydrogels, 50 µl portions of solution were transferred to 1 mL syringes with the top cut off. The solution was covered with coverslip (0.22 mm thickness) and irradiated with 365 nm light (Omnicure S1000 UV lamp filtered for 320-390 nm) at 10 mW/cm^2 power for various times (t_{ir}). The hydrogels were stored in 1 mL PBS for 24 hours at 4 °C prior to subsequent testing.

2.2.9. Measuring hydrogel thermal response

The mass loss (ML) of hydrogels were measured as a function of temperature to characterize their thermal response. Hydrogels were synthesized as described above and incubated in PBS at 4 °C for 24 h as an initial condition. Subsequently, hydrogels (n≥4) were incubated in PBS at either 4, 37, or 55 °C for 24 h cycles. After each temperature cycle, the hydrogels were blotted with a Kimwipe to remove excess water and massed. Measurements were carried out in a cycle between 4 and either 37 or 55 °C. The mass loss percentage (ML %) defined as:

$$ML = \frac{W_{initial} - W_{measured}}{W_{initial}} \times 100 \qquad \text{(Equation 2.1)}$$

Where $W_{initial}$ is the mass of hydrogel after first 24 hours at 4 °C in PBS and $W_{measured}$ is the mass of hydrogel at each temperature after 24 hours in PBS.

The initial mass increase of the hydrogel after fabrication upon swelling in PBS at 4 °C (MI_i) is defined as:

$$MI_i = \frac{W_{measured} - W_{am}}{W_{am}} \times 100 \qquad \text{(Equation 2.2)}$$

Where $W_{measured}$ is the mass of the hydrogel after incubating for 24 h at 4 °C and W_{am} is the mass of the hydrogel immediately after gelation.

Experiments were conducted to find that 24 h of incubation was sufficient for hydrogels to reach to their equilibrium mass prior to measurements. In such an experiment, hydrogels were incubated in 4 °C and weighed in one hour intervals for 8 hours and then weighed after 24 and 72 hours of incubation. Plotting the initial mass increase (MI) due to water uptake versus time (Figure 2.1.a) showed the mass change plateau at 24 hours. A similar experiment was done at 37 °C to find the time to reach equilibrium during heating. In this case, mass loss was plotted versus time and 24 hours was found to be sufficient to reach to equilibrium mass (Figure 2.1.b).

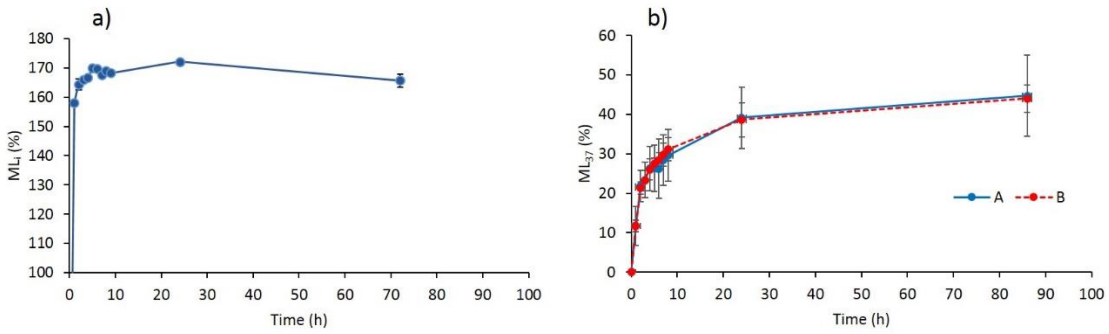

Figure 2.1. Equilibrium swelling of NorHA hydrogels. a) Initial swelling of PNIPAM cross-linked NorHA hydrogel at 4 °C. Hydrogels (n=2) were massed for 8 hours with 1 hour intervals and after 24 and 72 hours to find the equilibrium time. b) Swelling behavior of PNIPAM cross-linked NorHA hydrogels were studied at 37 °C to find the best time interval between mass measurements. After 24 hours it seems that hydrogels reached to the equilibrium mass (A: 6 wt%, $X_{T/N}$=0.5, 45 s; B: 6 wt%, $X_{T/N}$=0.3, 45 s).

2.2.10. Measure of compression modulus

Prior to testing, hydrogels were incubated at 4 °C for 24 h. The compression moduli of the hydrogels were measured using a dynamic mechanical analyzer (DMA) (Q8000 Thermal Analysis)

with a compression fixture. The hydrogels (n≥3) were subjected to a constant compression strain rate experiment at 10% strain/min up to 30% total strain. Compression modulus was defined as the slope of strain-stress curve in the limit of 10 to 20% compressive strain.

2.2.11. Additional cross-linking of NorHA/PNIPAM hydrogels

NorHA hydrogels (n=4) were synthesized using the DTPN8 cross-linker, 6 wt % polymer in solution, a $X_{T/N}$ of 0.3, and a t_{ir} of 45 s following the procedure mentioned above. These hydrogels were incubated in a solution of PNIPAM (0.015 gml^{-1} concentration) and I2959 (0.05 wt %) in PBS right after gelation for 24 hours at 4 °C. These hydrogels were irradiated with 365 nm light at 10 mW/cm^2 for 5 minutes. Thermal and mechanical tests were conducted on these samples following the above procedures.

2.2.12. Spatiotemporal modification of the stimuli response of NorHA hydrogels

DTPEO was used to cross-link NorHA following the procedure described above (6 wt %, $X_{T/N}$= 0.3, and t_{ir}= 60 s) to form initially non-responsive hydrogels. These hydrogels were incubated in a solution of 20 mg/mL DTPN8 and 50 mg/mL I2959 in PBS for 24 hours at 4 °C. The hydrogels were removed from the solution and were irradiated with 365 nm light at 10 mW/cm^2 for 5 minutes while were covered with a photomask of 200 µm solid stripes alternating with 200 µm blank stripes. Control hydrogels of DTPEO cross-linked NorHA were covered with the mask and irradiated as described above. Patterned hydrogels were placed in PBS and incubated at 4, 37, and 55 °C for 24 hours before imaging. Images were taken utilizing an inverted optical microscope (ZEISS.AXIO Observer.Z1) at 5x magnification immediately after removing the hydrogels from the incubator. Photopatterned dimensions as a function of temperature were measured using ImageJ software.

2.2.13. Cell adhesion on NorHA hydrogels

The behavior of human mesenchymal stem cells (hMSC) on the wrinkled surface of NorHA/DTPEO/DTPN hydrogels was studied. NorHA/DTPEO hydrogels were made following abovementioned procedure (6 wt %, $X_{T/N}$= 0.3, and t_{ir}= 60 s). The NorHA/DTPEO hydrogels were incubated in a solution of PNIPAM (0.02 gmL^{-1}), RGD peptide (with the sequence GCGYGRGDSPG) (2 µM), RhodamineB-peptide with the sequence GCDDD-Rhodamine B ($4.3x10^{-5}$ $g.mL^{-1}$), and I2959 (0.05 wt %) in sterile PBS (DPBS) for 24 hours at 4 °C. The RGD-peptide sequence GCGYGRGDSPG has been used previously in another study.[62] In general, any RGD-peptide sequence with cysteine that has a thiol functional group can be used in this method. RhodamineB-peptide was synthesized previously in reference 62. As control experiments, NorHA/DTPEO hydrogels also were incubated in the following solutions: only DPBS without RGD-peptide and PNIPAM, a solution of 2 µM RGD-peptide and 0.05 wt% I2959 in DPBS without PNIPAM, and a solution of 0.02 gmL^{-1} PNIPAM, 0.05 wt% I2959, and $4.3x10^{-5}$ $g.mL^{-1}$ RhodamineB-peptide in DPBS without RGD-peptide. After incubating for 24 hours, all hydrogels were irradiated with 365 nm light for 5 minutes while covered with a striped photomask (200 µm solid stripes alternating with 200 µm blank stripes) to make four different hydrogels: NorHA/DTPEO hydrogels, RGD patterned NorHA/DTPEO hydrogels, PNIPAM and RhodamineB patterned NorHA/DTPEO hydrogels, and PNIPAM, RGD, and RhodamineB patterned NorHA/DTPEO hydrogels. All hydrogels were incubated at 37 °C and 5% CO_2 incubator in cell culture media for 24 hours in a 24-well plate.

One petri dish of passage 5 hMSCs were suspended in DPBS and added to each well (25000 cell cm^{-2}). Hydrogels were incubated for 24 hours at 37 °C and 5% CO_2 prior to fluorescence imaging using a ZEISS.AXIO Observer.Z1 microscope. For imaging, cells were first fixed using a 4 wt% paraformaldehyde solution. To make 10 mL of a 4 wt % paraformaldehyde solution, 1 mL

deionized water and 10 µL NaOH 1N were added to 0.4 g of paraformaldehyde in a vial and heated at 80 °C water bath for around 10 minutes. Then, 9 mL DPBS and 2 µL HCL 6N were added and mixed with the solution. This paraformaldehyde solution (1 mL) was added to each well and incubated for 15 minutes at room temperature. Afterward, hydrogels were washed with DPBS two times. The fixed hydrogels and cells were kept in 1 mL of 0.5 wt % solution of triton X-100 at room temperature for 20 minutes to permeabilize the cells. The hydrogels were washed with DPBS as least twice before staining the cells with DAPI and phalloidin. A solution of DAPI (300 nM) and phalloidin (2.5 v/v %) in DPBS was prepared in which hydrogels were incubated for 20 minutes at room temperature. Hydrogels were washed two times with DPBS prior to imaging.

After imaging, the number of cells in each region (PNIPAM cross-linked and no-PNIPAM cross-linked stripes) were counted using ImageJ software. Nuclei (blue dots) accompanied by ECM (green medium) were counted to find the number of cells and the ratio of numbers (number of cells in PNIPAM cross-linked stripe to the number of cells in no-PNIPAM cross-linked stripe) were calculated. Stripes were distinguishable by the red color of rhodamine B-peptide patterned along with PNIPAM. Technical replicates of each hydrogel formulation were evaluated by imaging three hydrogels of each condition that were fabricated from the same hydrogel stock solution and cell culture plate. An image was taken of each hydrogel and the number of cell nuclei in two PNIPAM-containing stripes and two no-PNIPAM-containing stripes were counted for each replicate, yielding a total of 6 stripes for patterned and unpatterned regions per formulation. These regions were used to calculate average number of cells and standard deviation.

2.2.14. Estimation of cross-link density

Measured values for the modulus and degree of swelling were used to calculate theoretical effective cross-links at 4, 37, and 55 °C. The experimentally measured elastic modulus from the

uniaxial compression of a hydrogel sample (E) was related to the cross-link density of the hydrogel through Equation 2.3,[120]

$$E = 3\nu_e \phi_e^{\frac{1}{3}} RT \qquad \text{(Equation 2.3)}$$

where ν_e is the effective cross-links per volume (i.e. cross-link density), $\phi_e$is the equilibrium volume fraction of polymer, R is the gas constant, and T is the temperature in degrees Kelvin. Given the modulus and volume fraction from DMA experimental data this equation can be rearranged to solve for the cross-link density (ν_e) at 4 °C as given in Equation 2.4.

$$\nu_e = \frac{E}{3\phi_e^{\frac{1}{3}} RT} \qquad \text{(Equation 2.4)}$$

Flory-Rehner theory also was applied to these systems to estimate the effective cross-links at different temperatures due to the collapse of the PNIPAM in the hydrogels.[121] Using Equation 2.5,

$$\ln(1-\phi_e) + \phi_e + \chi{\phi_e}^2 = \nu_e \frac{\hat{V}_1}{N_{Av}} \left(\frac{\phi_e}{2} - {\phi_e}^{1/3} \right) \qquad \text{(Equation 2.5)}$$

where χ is the Flory-Huggins interaction parameter, $\hat{V}_1$ is the molar volume of the solvent, and N_{Av} is Avogadro's number. Using the expansion $\ln(1-\phi_e) \approx -\phi_e - {\phi_e}^2/2$ and assuming that ${\phi_e}^{1/3} \gg \phi_e/2$ Equation S5 can be simplified to Equation 2.6,

$$\phi_e^{5/3} = \nu_e \frac{\hat{V}_1}{N_{Av}} (0.5 - \chi)^{-1} \quad \text{(Equation 2.6)}$$

Or simply,

$$\phi_e^{5/3} = C\nu_e \quad \text{(Equation 2.7)}$$

assuming that $C = \frac{\hat{V}_1}{N_{Av}} (0.5 - \chi)^{-1}$ is constant. For each sample, C was calculated using the ν_e calculated from modulus data at 4 °C. In turn, the C value was used to calculate ν_e values at 37 and 55 °C based off the measured ϕ_e as modulus data were not measured at the elevated temperatures. The primary limitation of the C value is that its calculation assumes that χ varies little with temperature over the ranges tested. Additionally the C value includes the non-idealities of the system that arise from the fact that the examined hydrogel system is a ternary (polymer-polymer-solvent) mixture and not the binary mixture that this version of the Flory-Rehner theory depicts. Nevertheless, such assumptions result in ν_e values that can qualitatively describe the nature of cross-linking in the hydrogels.

2.3. Results and Discussion

2.3.1. Synthesis of cross-linkers

PNIPAM cross-linkers were synthesized via RAFT polymerization with subsequent aminolysis of the CTA to introduce thiols at both termini of the polymer chain as described in Section 2.2.2 in detail (Figure 2.2). The cross-linkers were synthesized by first generating a di-trithiocarbonate functionalized CTA (DiCTA) that was subsequently used to polymerize NIPAM, yielding a di-trithiocarbonate-terminated PNIPAM (DCTAPN) (Figure 2.3). To generate DCTAPNs with different lengths, two different molar ratios of DiCTA to NIPAm were used in the synthesis, yielding polymers with chain lengths of 64 and 30 repeat units as measured by ^{1}H NMR spectroscopic end group analysis (Table 2.1). SEC elution data for these CTA terminated polymers indicated a narrow dispersity (Đ) of 1.06 and 1.09 for the DCTAPNs of 8 and 4 kg/mol, respectively (Figure 2.4).

Table 2.1. Dispersity and number average M_n of cross-linkers. Number average molecular weight (M_n) calculated by ^{1}H NMR spectroscopic end group analysis of DCTAPN before aminolysis and dispersity (Đ) calculated by SEC after aminolysis of thiol functionalized polymers used.

Thiol Code	M_n (g/mol)	Đ
DTPN8	8000	1.06
DTPN4	4000	1.14
DTPEO	1700	2.1
DTT	154	---
MTPN8	8000	1.08

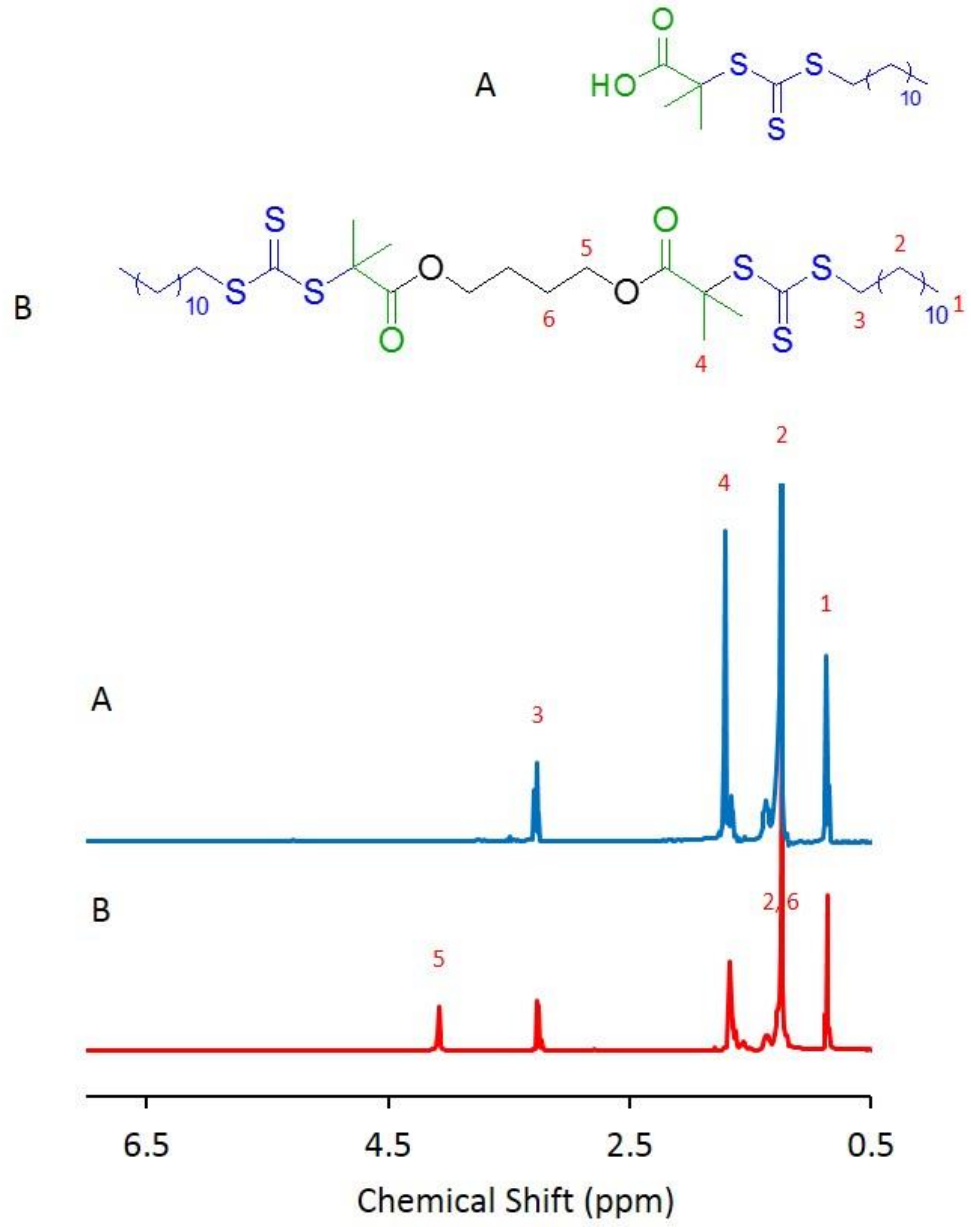

Figure 2.2. ^{1}H-NMR spectra of RAFT agent and DiCTA. NMR spectra of synthesized RAFT agent (top, A) and DiCTA (bottom, B). Appearance of a new peak at 4.08 ppm confirms formation of ester bond.

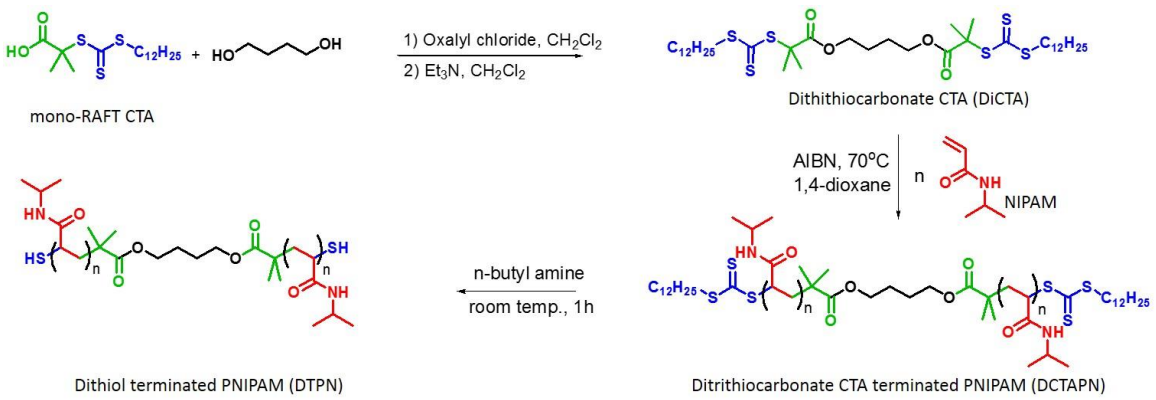

Figure 2.3. Synthesis of DTPN. Synthesis of di-thiol-terminated PNIPAM (DTPN) was accomplished by the RAFT polymerization of NIPAM with a di-trithiocarbonate CTA (DiCTA) to yield a DiCTA terminated PNIPAM (DCTAPN). Aminolysis of the DCTAPN generated di-thiol-terminated PNIPAM (DTPN).

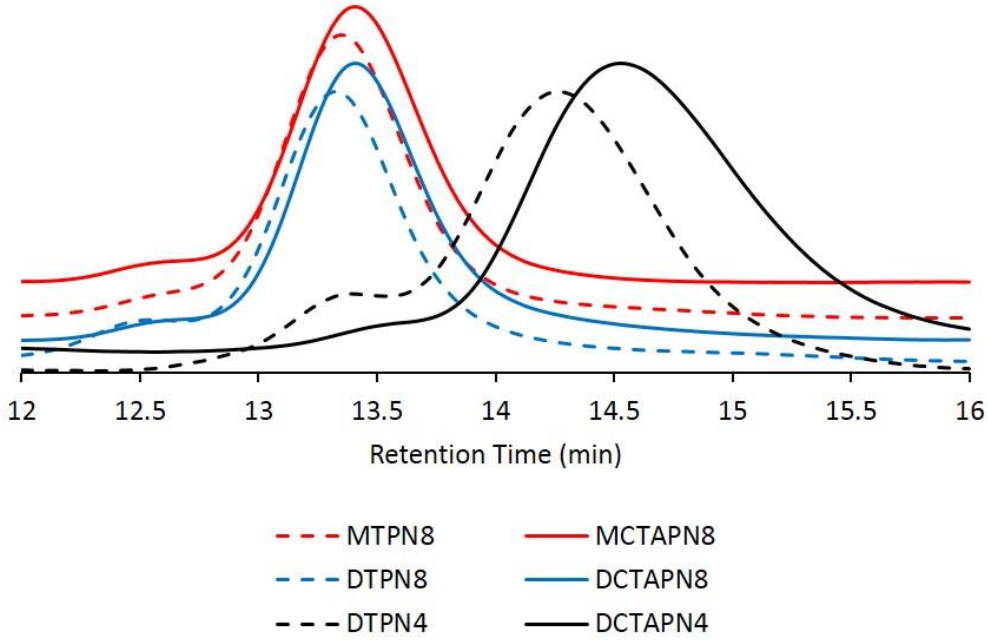

Figure 2.4. SEC elution curves of synthesized PNIPAMs before and after aminolysis. Polymers listed in Table 2.1. Dashed lines represent polymers after aminolysis.

Subsequent aminolysis of the DCTAPN polymers yielded dithiol-terminated PNIPAM (DTPN) cross-linkers (Figure 2.3) as indicated by a visible disappearance of the yellow color indicative of the trithiocarbonate CTA. Complete removal of the CTA was confirmed by UV-vis spectroscopy (Figure 2.5) as the absorbance peak due to the CTA was no longer present in the product. Additionally, ^{1}H NMR spectra of the DTPNs (Figure 2.6) confirm removal of the CTA as peaks associated with it are no longer present. The SEC elution curves of DTPN had a slight increase in dispersity (Đ) (Table 2.1) as compared to the DCTAPN that suggests some disulfide bonds formed (Figure 2.4), but this disulfide bond formation did not adversely affect the reactivity of the cross-linkers to synthesize hydrogels such that all terminal thiols were assumed to be free for subsequent hydrogel synthesis.

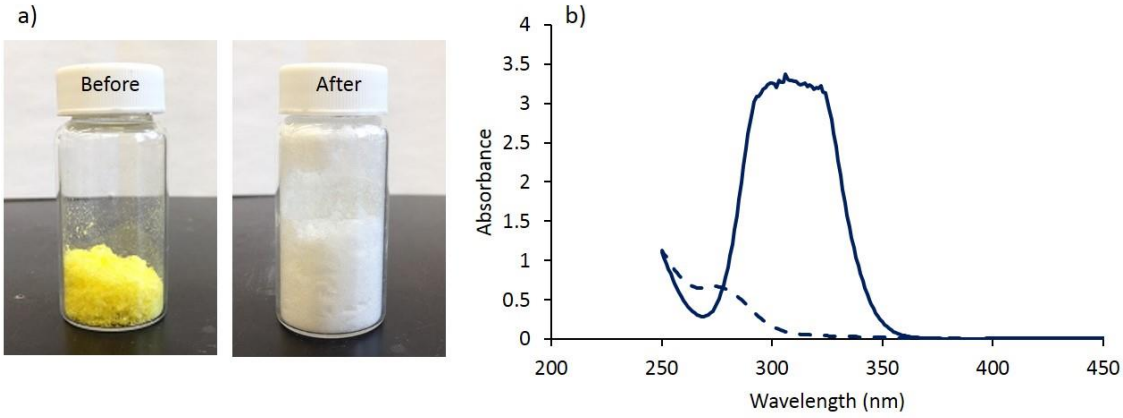

Figure 2.5. UV-Vis specta of DCTAPN and DTPN. a) Visual demonstration of successful removal of trithiocarbonate group (RAFT moiety) from DCTAPN through aminolysis. b) UV-Vis spectra of DCTAPN before (solid line) and after aminolysis (dashed line). The absorption peak at 300-340 nm belongs to trithiocarbonate group which disappeared after the aminolysis reaction.

In addition to the DTPN, a mono-thiol-terminated PNIPAM (MTPN) with a number average molecular weight (M_n) of 8 kg/mol was synthesized following the DTPN synthesis procedure (Figure 2.7) to give a thiol-terminated PNIPAM that could be incorporated into the hydrogels without cross-linking. A non-thermo-responsive cross-linker was synthesized by coupling di-

hydroxy-functionalized polyethylene oxide (PEO) with the CTA followed by aminolysis to yield a dithiol-terminated PEO (DTPEO) (Figures 2.8 and 2.9). A PEO with a M_n of 2 kg/mol was selected for the DTPEO to have nearly the same number of bonds along the polymer backbone as compared to DTPN8. With these control cross-linkers and DTPN, hydrogels were made to study how the cross-linker type affects properties.

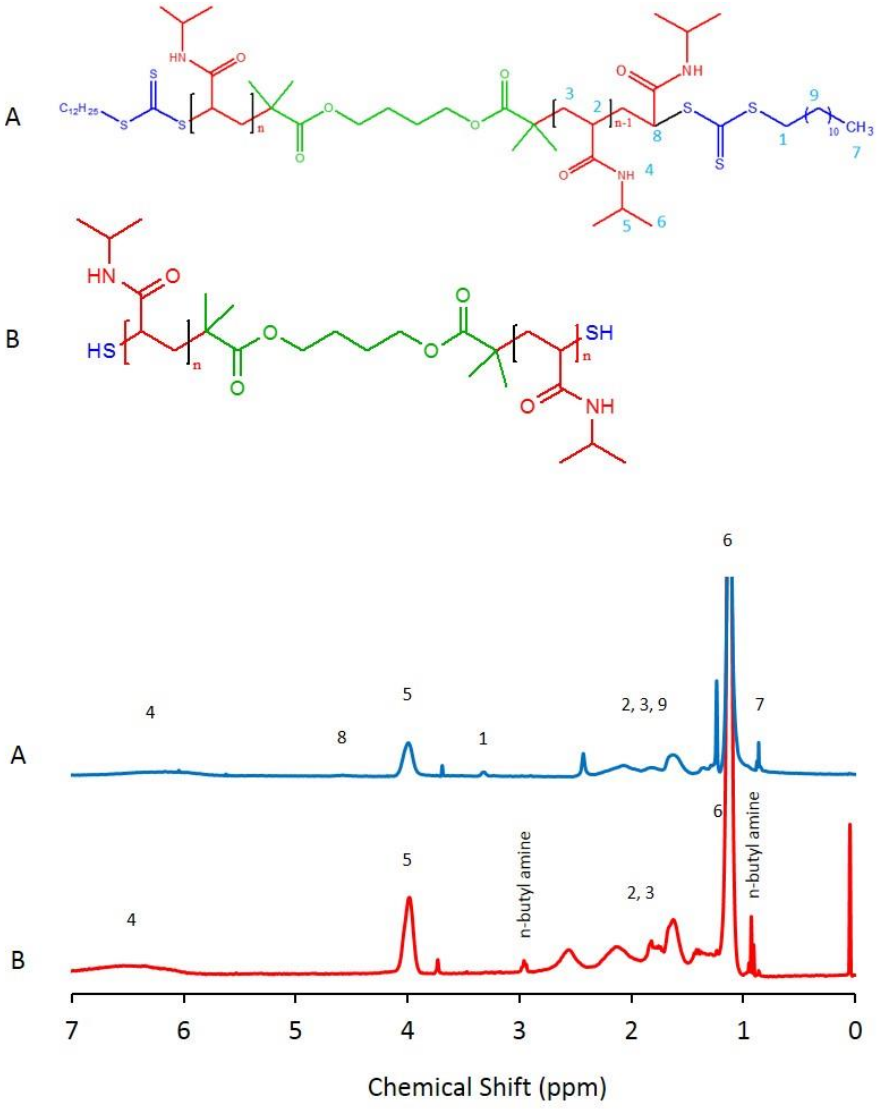

Figure 2.6. NMR spectra of DCTAPN (A) and DTPN (B). Peak labeled 1 at 3.27 ppm, which belongs to the alkyl chain of RAFT moiety, is removed in spectrum B and confirms formation of DTPN.

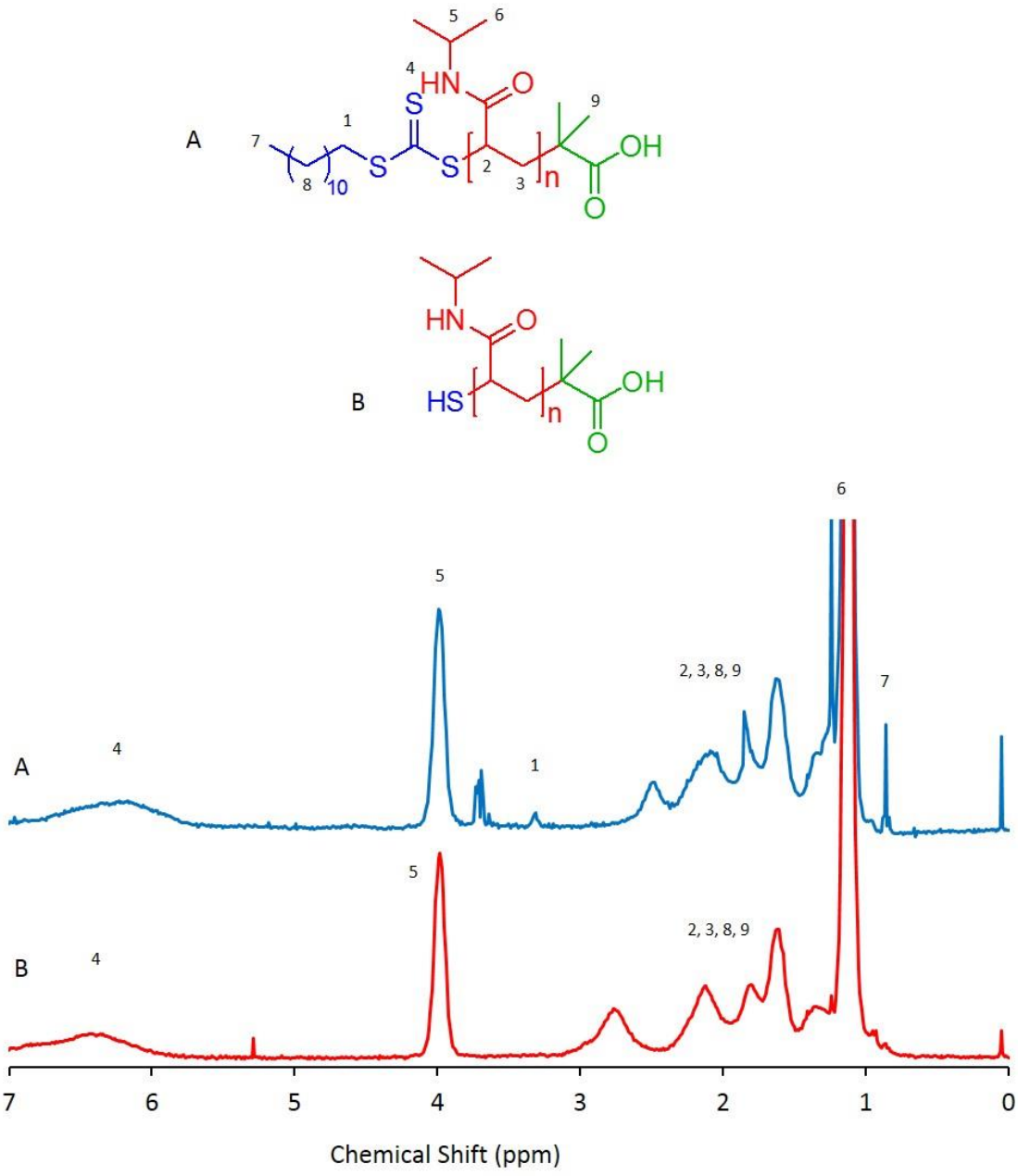

Figure 2.7. ^{1}H NMR spectra of MCTAPN (A) and MTPN (B). The peak at 3.31 ppm which belongs to RAFT moiety is no longer present in the MTPN spectra, indicating CTA removal.

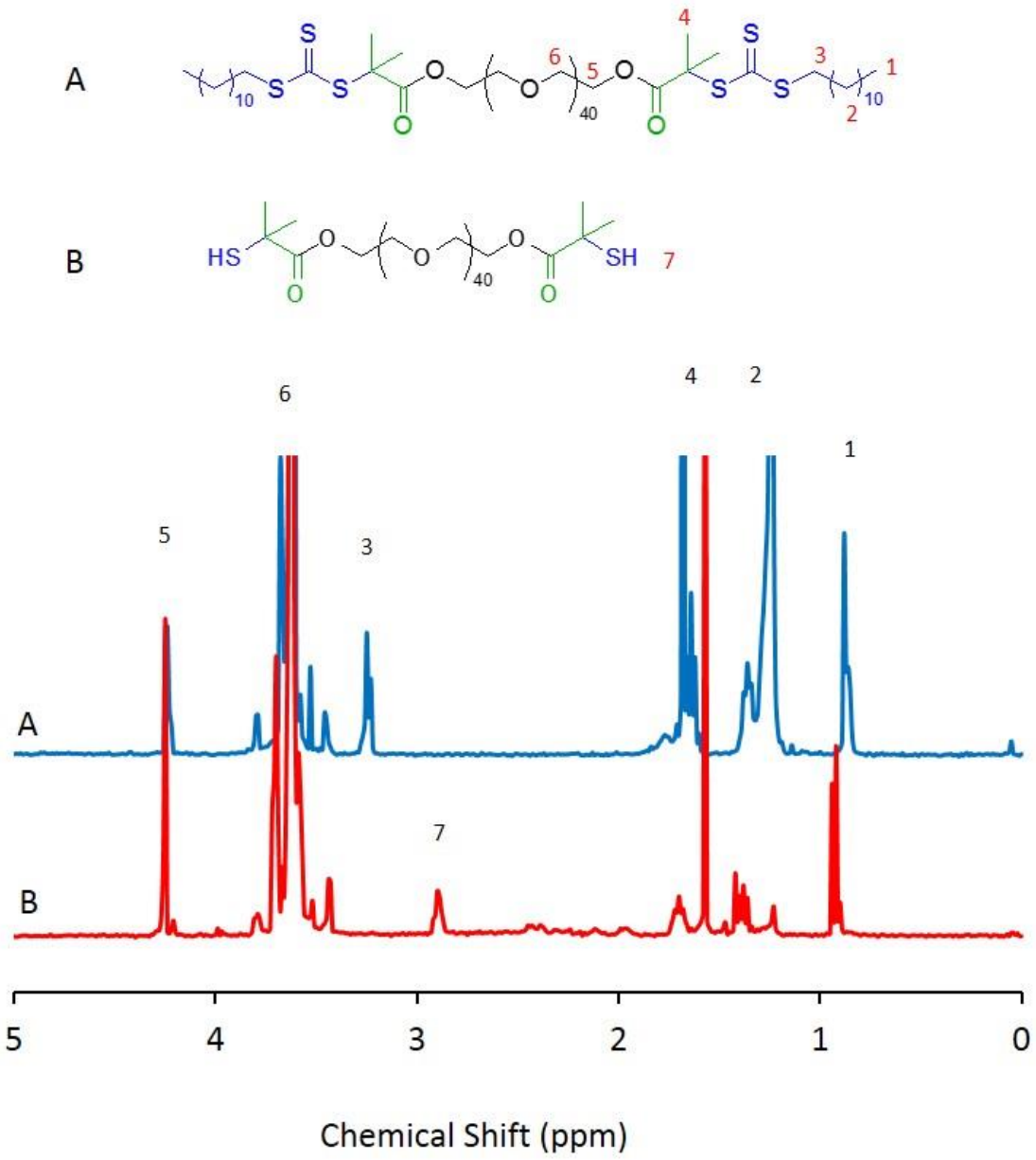

Figure 2.8. ^{1}H NMR spectra of DCTAPEO (A) and DTPEO (B). The removal of methylene (marked as 3) peak at 3.2 ppm and appearance of thiol proton peak at 2.85 ppm at spectrum B confirm successful alkyl end group removal.

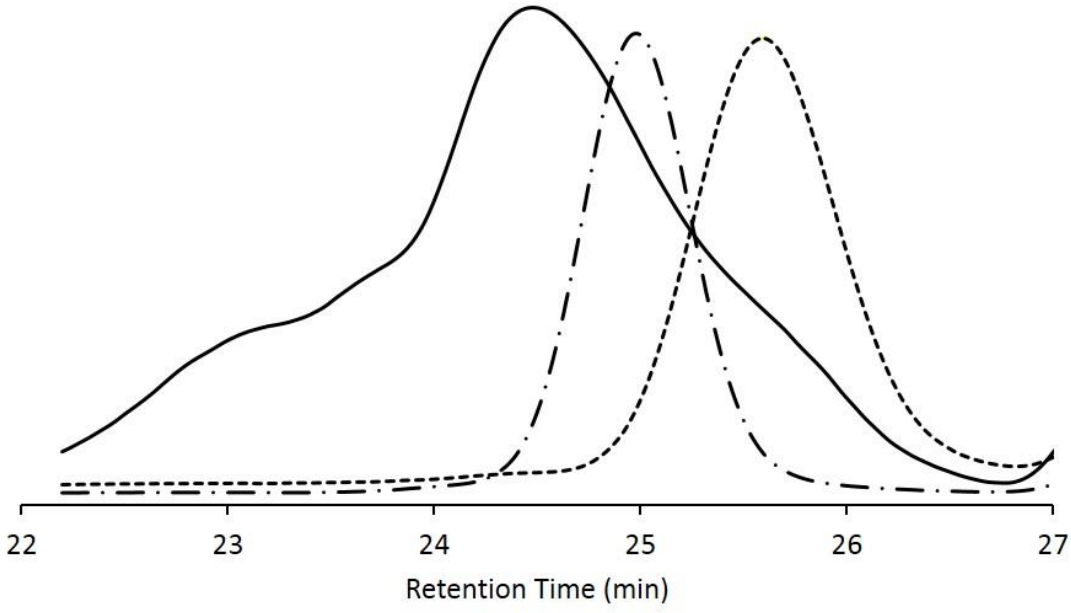

Figure 2.9. SEC elution curves of EGPEO (dash, Đ = 1.9), DCTAPEO (dash dot, Đ = 1.9), and DTPEO (solid, Đ = 2.1).

2.3.2. Fabrication of thermo-responsive hydrogels

To create thermo-responsive hydrogels and control their response to temperature, NorHA and thiol-terminated cross-linkers were mixed at various ratios in phosphate buffered saline (PBS) with 2-hydroxy-4'-(2-hydroxyethoxy)-2-methylpropiophenone (I2959) as the UV-light sensitive radical initiator. UV-light was applied (365 nm, 10 mW/cm^2) to generate radicals and initiate the thiol-norbornene reaction (Figure 2.10.a). This wavelength and initiator pair was chosen as it is cytocompatible and has been used previously to fabricate hydrogels and to encapsulate cells within 3D networks.[62,64-66]

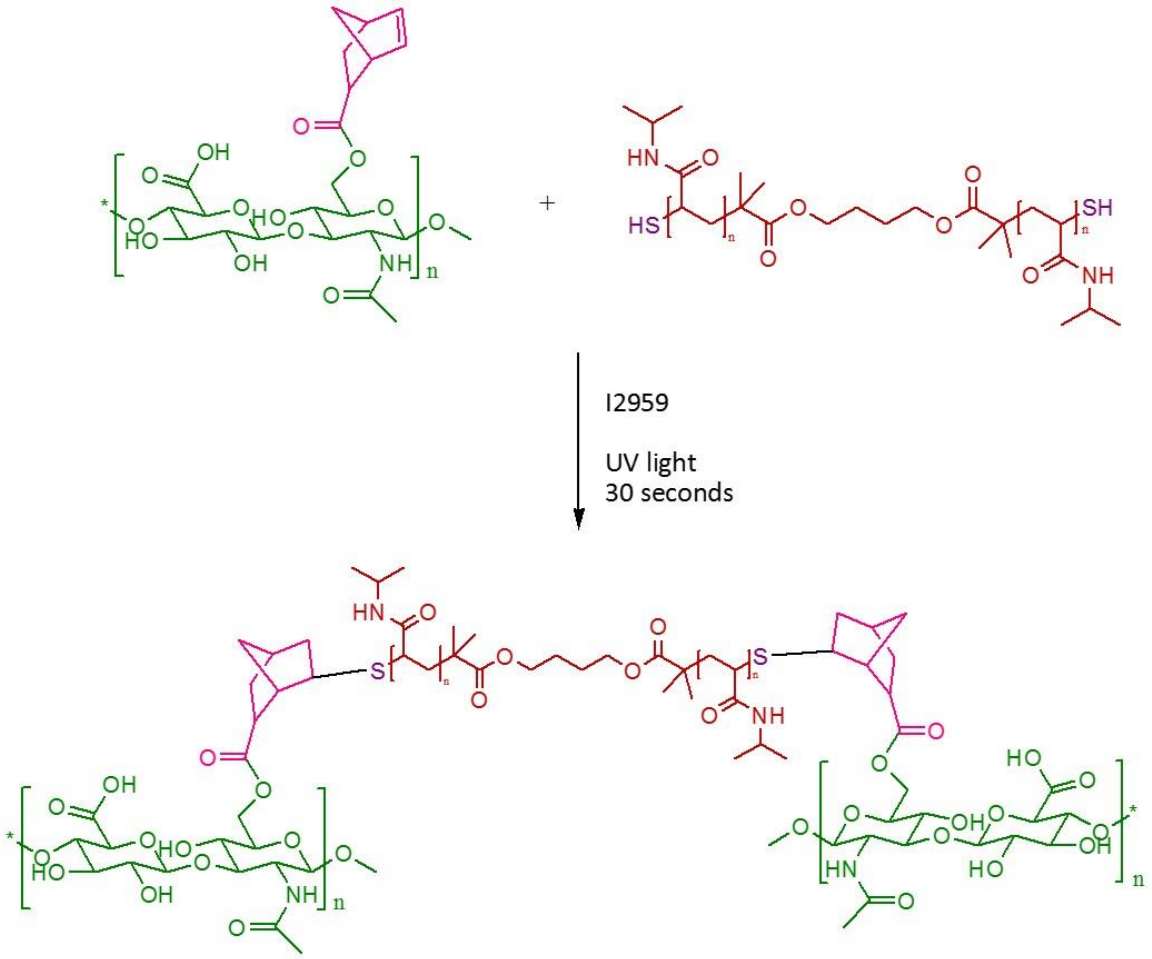

Figure 2.10. Thermo-responsive hydrogel synthesis scheme. a) DTPN and norbornene-functionalized hyaluronic acid (NorHA) were combined with the UV-sensitive radical initiator I2959 in PBS and irradiated with 365 nm light to generate hydrogels. b

The cross-linking density and thermo-response were controlled by varying the molar ratio of thiol to norbornenes ($X_{T/N}$), the chain length of cross-linker, and the irradiation time (t_{ir}) (Table 2.2). By changing these parameters, the modulus at 4 °C (E) and the percent mass loss upon heating above 4 °C (ML) changed between formulations (Table 2.2).

Table 2.2 NorHA hydrogel formation under different conditions. NorHA hydrogel formulations, thermal properties, and physical properties at 6 wt % total polymer

Formulation	$X_{T/N}$ [a]	t_{ir} [b] (s)	Cross-linker	$M_{P/HA}$ [c]	E [d] (kPa)	MI_i [e] (%)	ML_{37} [f] (%)
0.3DTPN8-45	0.3	45	DTPN8	0.6	5.3±1.4	212.0±30.2	24.4±5.6
0.3DTPN8-90	0.3	90	DTPN8	0.6	14.5±3.3	153.6±1.8	18.7±1.0
M,D-TPN8-90	0.3*	90	DTPN8+ MTPN8	0.9	8.5±2.0	166.2±2.8	21.1±1.6
0.5DTPN8-45	0.5	45	DTPN8	0.9	11.8±6.0	130.1±7.0	28.1±3.1
0.5DTPN8-90	0.5	90	DTPN8	0.9	25.9±1.4	92.2±2.7	19.4±0.9
0.5DTPN8-180	0.5	180	DTPN8	0.9	25.7±4.2	86.8±4.3	19.6±0.7
0.5DTPN4-90	0.5	90	DTPN4	0.4	54.4±2.3	75.3±4.1	9.4±1.0
0.7DTPN8-45	0.7	45	DTPN8	1.3	9.3±0.6	101.6±19.9	33.2±8.9
0.7DTPN8-90	0.7	90	DTPN8	1.3	18.3±6.6	69.1±7.8	30.5±5.2
0.5DTPEO-60	0.5	60	DTPEO	0.2	2.8±0.1	220.5±6.7	5.0±1.3
0.5DTT-45	0.5	45	DTT	---	81.8±19.0	23.4±0.8	1.8±0.6

[a] $X_{T/N}$ = thiol to norbornene ratio, [b] t_{ir} = irradiation time, [c] $M_{P/HA}$ = ratio of the mass of cross-linker to mass of NorHA, [d] compression modulus, [e] MI_i = percent mass increase due to initial swelling at 4 °C, [f] ML_{37} = mass loss percentage of gels at 37 °C, * $X_{T/N}$ = 0.3 for DTPN8 (cross-linker) with MTPN8 added to reach $M_{P/HA}$=0.9.

ML was measured at elevated temperatures (37 and 55 °C) to track the thermo-response of these materials. Although thermo-response could be measured using compression or dynamic elastic modulus measurements, ML was preferred as it is an accepted method to measure stimuli response and it can be measured in a straightforward manner.[78,122,123] In addition to the DTPN cross-linked hydrogels, NorHA was also cross-linked with the non-thermally responsive cross-

linkers dithiothreitol (DTT) and DTPEO. The properties of these two control hydrogels were measured at the same conditions as the NorHA/DTPN hydrogels to serve as representative non-thermo-responsive hydrogels.

2.3.3. Reversibility of thermo-response

NorHA/DTPN8 and control NorHA/DTT hydrogels were synthesized and subjected to thermal cycling between 4 °C and either 37 or 55 °C (Figure 2.11 and 2.12) while incubating in excess PBS. Incubating the 0.5DTPN8-45 hydrogel at 37 °C lead to a significant ML which was recovered upon cooling to 4 °C. The mass loss was due to PBS expulsion from the hydrogel at temperatures above the LCST. Incubating the hydrogels in PBS for 24 hours at temperatures below the LCST (for example 4 °C), the hydrogels recover the mass lost due to PBS re-uptake. As expected, the DTT hydrogel did not have a significant change in ML due to heating. Interestingly, repeated heating and cooling cycles for the DTT hydrogel yielded an increased uptake of water (Figure 2.12), which suggests degradation of the cross-links occur upon heating. Successive heating/cooling cycles for the DTPN8 cross-linked hydrogel did not demonstrate the same behavior (Figure 2.11), suggesting that the DTPN8 cross-links are more stable towards degradation. The lack of ML hysteresis for the DTPN cross-linked hydrogels upon heating/cooling cycles suggest that these materials could be used as thermal shape memory materials.

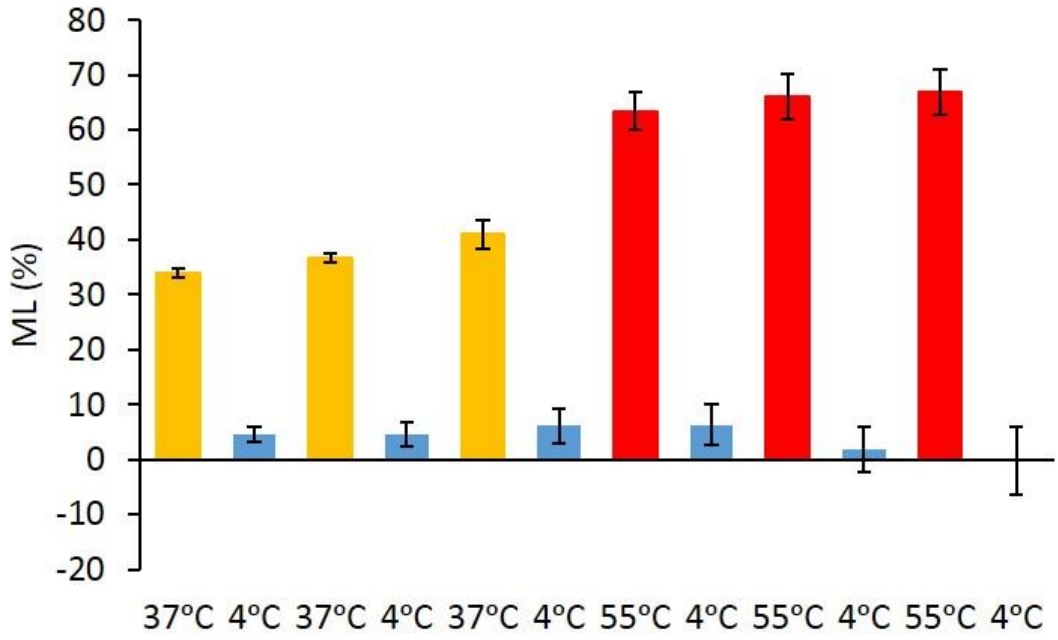

Figure 2.11. Mass loss (ML) percentages of 0.5DTPN8-45 hydrogels cycling between 4 °C and either 37 or 55 °C cycles (n=4).

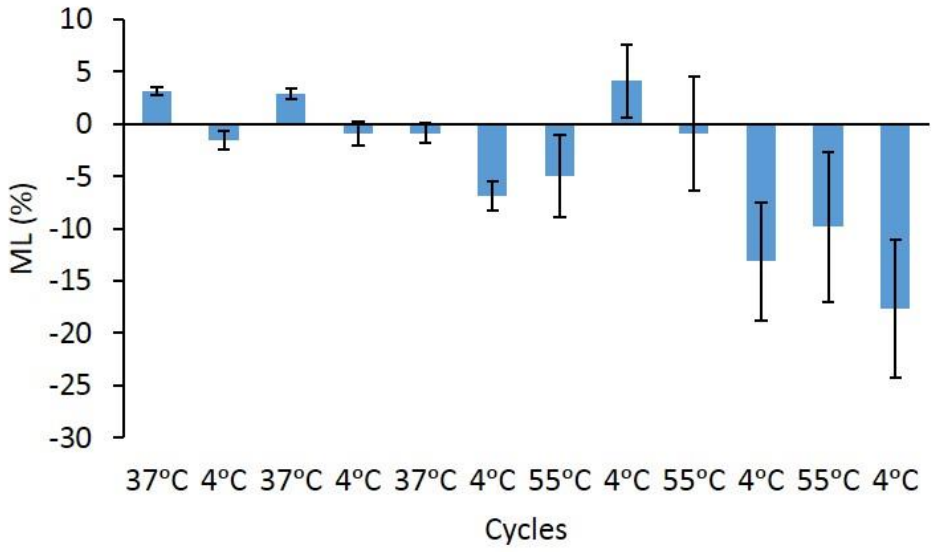

Figure 2.12. Mass loss (ML) percentages of DTT cross-linked NorHA hydrogels cycling between 4 °C and either 37 or 55 °C cycles (n=4). The results indicate that the NorHA/DTT hydrogel is not thermo-responsive. The negative ML values means that the mass of hydrogels increases after sequential heating which indicates that the hydogels were degrade.

2.3.4. Controlling thermo-responsive properties

Several parameters were investigated as methods to control the thermo-response of hydrogels cross-linked with DTPN. Hydrogels with different total weight percent of polymer used (2, 4, and 6 wt %) were synthesized with the DTPN8 cross-linker ($X_{T/N}$ = 0.5, t_{ir} = 45 s) and found to have ML_{37} values (Table 2.3) around 30%. Though the ML_{37} values for these samples were relatively similar, the relative initial mass increase (MI_i) upon swelling the 50 µL hydrogel in PBS at 4 °C was significantly different for all samples (Figure 2.13). The MI_i increased with increasing total weight percent of polymer as the higher concentrations of hydrophilic polymer (NorHA) intensified hydration. Such results indicate that the total weight percent of polymer can be used to control fluid uptake, while the DTPN cross-linker could be used to cycle between release and uptake of this fluid upon heating and cooling (Appendix A, Figure A.1- A.2).

Table 2.3. Thermal response and compression modulus of NorHA/DTPN8 hydrogels at different polymer concentrations.

Formulation	wt[a] (%)	$X_{T/N}$[b]	t_{ir}[c] (s)	Cross-linker	$M_{P/HA}$[d]	E[e] (kPa)	MI_i[f] (%)	ML_{37}[g] (%)
2DTPN8-45	2	0.5	45	DTPN8	0.9	3.1±0.8	49.3±13.0	30.1±1.5
4DTPN8-45	4	0.5	45	DTPN8	0.9	6.1±1.7	92.6±4.4	27.4±0.9
0.5DTPN8-45	6	0.5	45	DTPN8	0.9	11.8±6.0	130.1±7.0	28.1±3.1

[a] **wt (%)** polymer concentration as weight percent, [b] **$X_{T/N}$** = thiol to norbornene ratio, [c] **t_{ir} (s) =** radiation time, [d] **$M_{P/HA}$** = ratio of the mass of cross-linker to mass of polymer, [e] **E=** compression modulus, [f] **MI_i =** mass increased due to initial swelling at 4 °C, [g] **ML_{37}** = mass loss percentage of hydrogels at 37 °C.

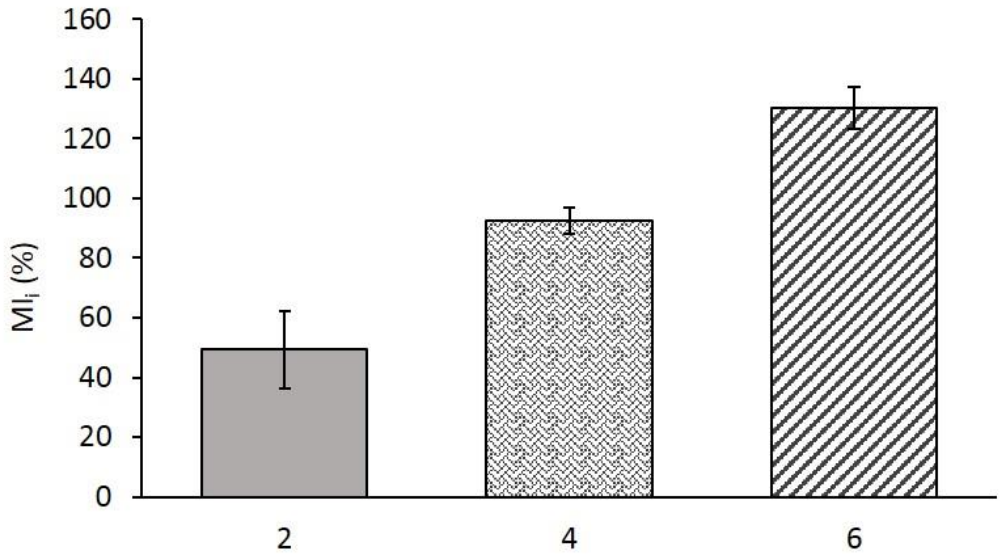

Figure 2.13. Initial water uptake (MI_i) for NorHA/DTPN8 hydrogels with 2 (solid), 4 (weaved), and 6 (striped) wt % polymer concentration.

Both the modulus (E) and ML could be controlled varying only the irradiation time ($X_{T/N}$ = 0.5, wt % =6, DTPN8) as both properties were significantly increased when irradiation time was increased from 45 to 90 s (Table 2.2, Figure 2.14.a). Further increasing the irradiation time from 90 to 180 s does not yield an observable difference in the modulus and ML_{37}, suggesting that the degree of cross-linking plateaus before 90 s.

Using Flory-Rehner theory,[121] an estimated effective cross-link density was calculated (Table 2.4) which confirmed that the cross-link density did not change by increasing the irradiation time from 90 to 180 s (Figure 2.15). The higher modulus and lower MI_i values observed with an increased irradiation time are consistent with a more cross-linked network (Table 2.2, Table 2.4). Additionally, more DTPN cross-linkers should be incorporated into the hydrogel with longer irradiation provided that unreacted DTPN remain. With more DTPN incorporated into the hydrogel, the ML_{37} could be expected to increase due to the greater PNIPAM content, but the opposite was observed. The hydrogels with a longer irradiation time have a greater cross-link

density (Table 2.4) so they absorb less water in the initial swelling. As a result, the hydrogels expel less water relative to their mass as compared to a loosely cross-linked hydrogel. Such results suggest that balancing cross-link density and desired thermal response is required to target a specific hydrogel behavior.

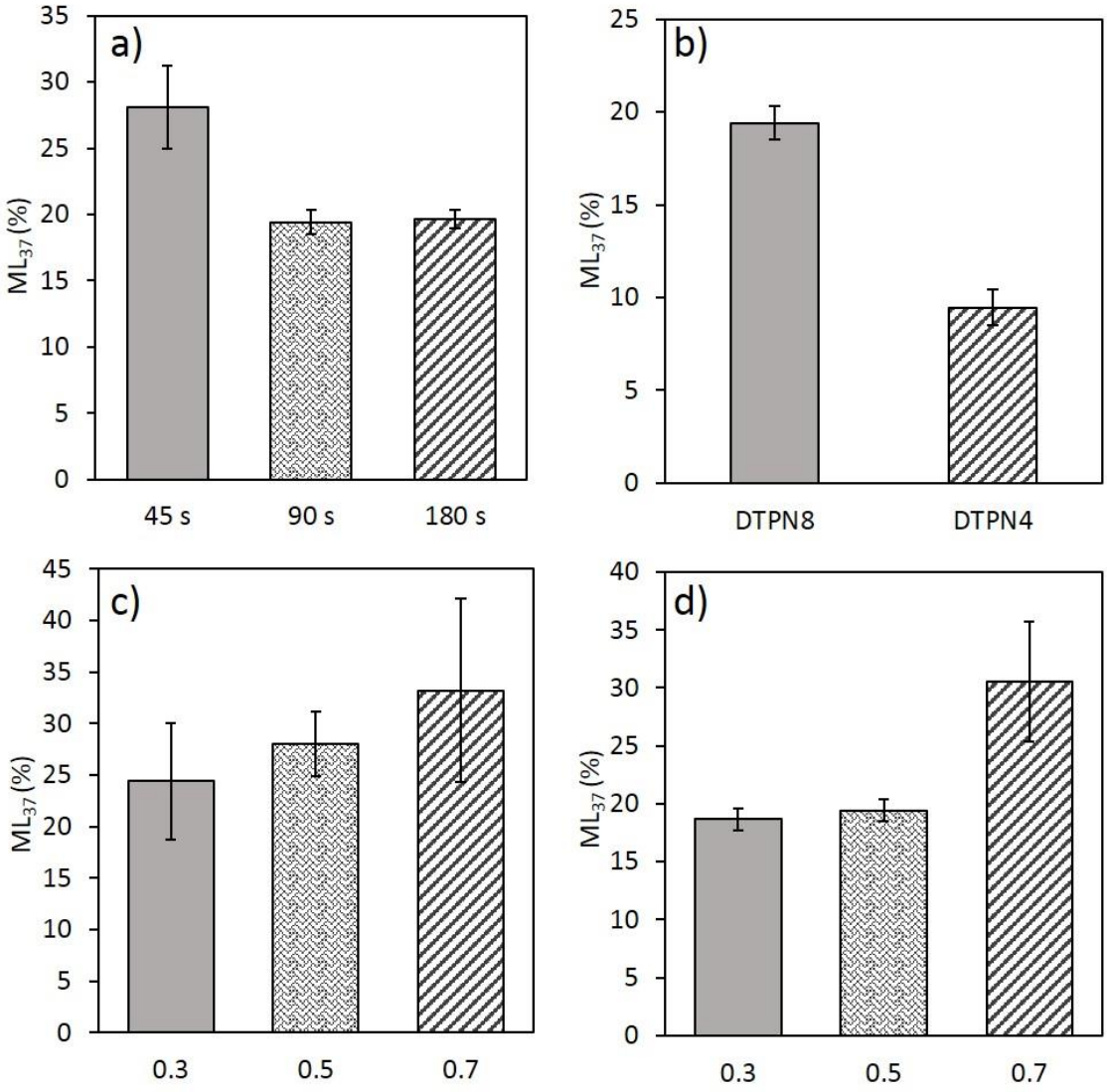

Figure 2.14. Controlling thermao-response of NorHA hydrogels. Control over the ML_{37} for NorHA/DTPN hydrogels by varying the a) irradiation time (t_{ir}), b) cross-linker chain length, c) $X_{T/N}$ at t_{ir} = 45 s, d) $X_{T/N}$ at t_{ir} = 90 s . Error bars indicate one standard deviation (n ≥ 4).

Table 2.4. The estimated equilibrium effective cross-linking density (ν_e) of various NorHA/PNIPAM hydrogels at 4 °C (ν_{e4}), 37 °C (ν_{e37}), and 55 °C (ν_{e55}).

Formulation	$\boldsymbol{\nu_{e4}}$ **(x 10^{-6} mol/mL)**	$\boldsymbol{\nu_{e37}}$ **(x 10^{-6} mol/mL)**	$\boldsymbol{\nu_{e55}}$ **(x 10^{-6} mol/mL)**
0.3DTPN8-45	3.1 ± 0.8	5 ± 2	10 ± 5
0.3DTPN8-90	8 ± 2	11 ± 3	18 ± 5
0.5DTPN8-45	6 ± 3	11 ± 2	20 ± 10
0.5DTPN8-90	13 ± 1	18 ± 1	35 ± 4
0.5DTPN8-180	13 ± 2	18 ± 3	31 ± 7
0.5DTPN4-90	27 ± 1	31 ± 2	33 ± 2
0.7DTPN8-45	4.6 ± 0.3	9 ± 2	18 ± 5
0.7DTPN8-90	9 ± 3	16 ± 7	30 ± 10
2DTPN8-45	2.0 ± 0.5	4 ± 1	11 ± 4
4DTPN8-45	3 ± 1	6 ± 2	19 ± 7

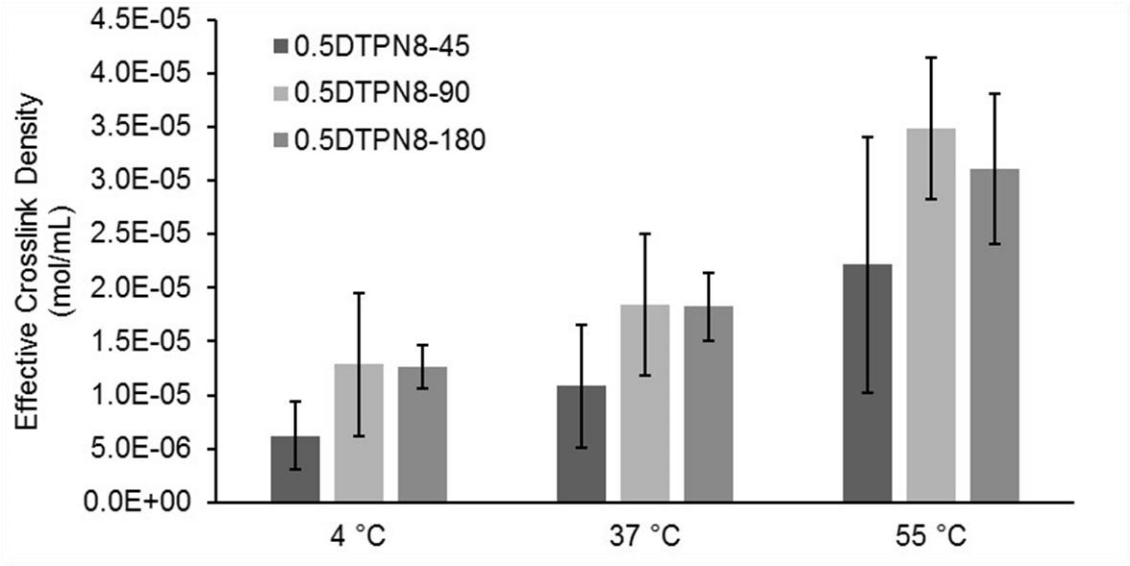

Figure 2.15. Effective cross-link density (ν_e) at various temperatures for the 0.5DTPN8 hydrogel formulations with different irradiation times. Error bars are from the standard deviations of the measurements propagated through the calculations.

Aside from the irradiation time, another variable that had a significant effect on the thermal properties of the hydrogels was the cross-linker chain length. With all variables held constant ($X_{T/N}$ = 0.5, t_{ir} = 90 s, wt % = 6), a shorter cross-linker (DTPN4) halved the ML_{37} of the NorHA hydrogel (Figure 2.14.b). Using the DTPN4 cross-linker in place of DTPN8 also doubled the modulus of the material (54 versus 26 kPa). Such a result could be expected as the modulus is inversely proportional to the molecular weight between cross-links and using DTPN4 instead of DTPN8 would halve this value. The calculated estimated effective cross-link density confirms this result as the value for DTPN4 cross-linked hydrogels is double that of the DTPN8 hydrogels (Table 2.4, Figure 2.16). Additionally, the tighter network has a lower MI_i as the DTPN4 cross-linker cannot stretch to the same extent as DTPN8 when the hydrogel reaches an equilibrium initial swelling due to the increased cross-link density (Table 2.4). The ML results suggest that upon heating the DTPN4 comes out of solution and collapses (Figure 2.17) pulling the NorHA half the distance that DTPN8 would, which is consistent with the lengths of the two cross-linkers.

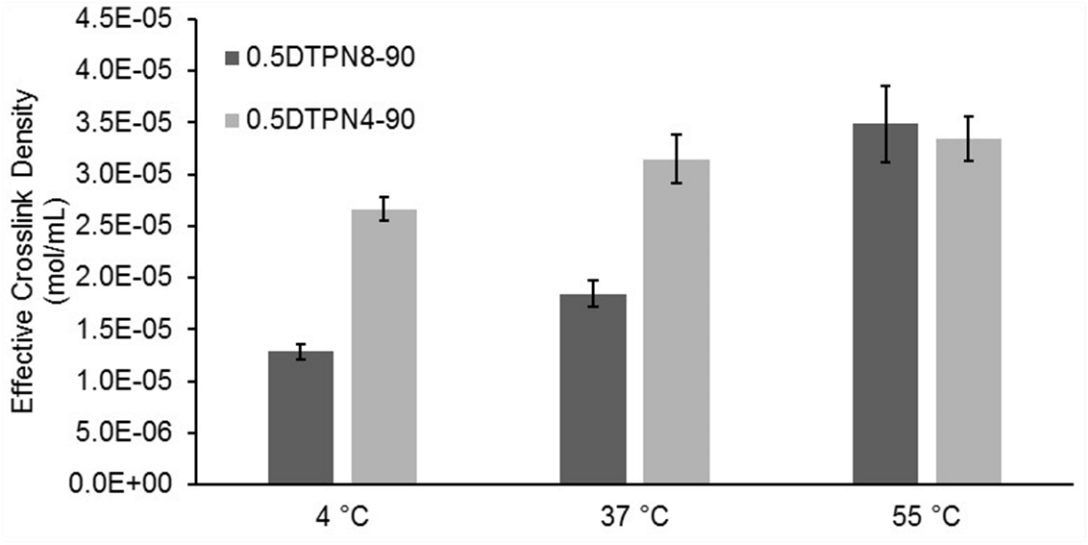

Figure 2.16. Effective cross-link density (ν_e) at various temperatures for the 0.5DTPN-45 hydrogel formulations with different length cross-linkers. Error bars are from the standard deviations of the measurements propagated through the calculations.

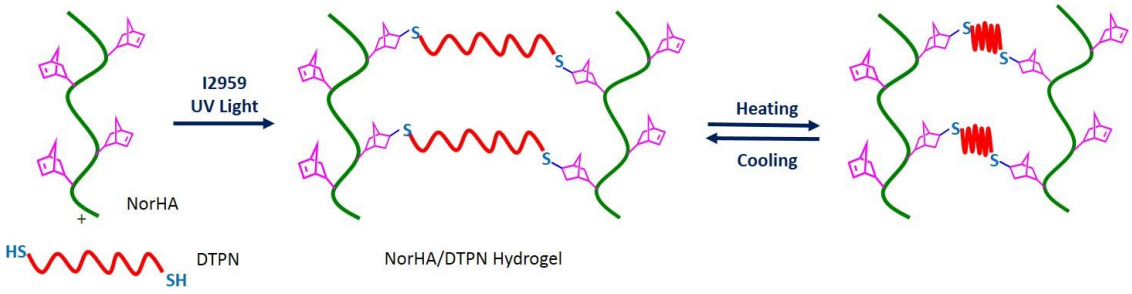

2.17. Schematic of NorHA/DTPN hydrogel thermo-response. Heating the NorHA/DTPN hydrogels causes a reversible collapse of the DTPN due to passing the lower critical solution temperature (LCST), resulting in the expulsion of water, a decrease in hydrogel volume, and mass loss.

Another parameter in this hydrogel system that can be used to control physical properties is the ratio of thiols to norbornenes ($X_{T/N}$). The ML_{37} increased when we increased the $X_{T/N}$ values at irradiation times of 45 (Figure 2.14.c) and 90 s (Figure 2.14.d). Higher $X_{T/N}$ values are expected to increase both cross-linking and the mass ratio of PNIPAM cross-linker to NorHA in the hydrogels ($M_{P/HA}$) as more reactants are available to form cross-links. As observed with increasing the irradiation time, the MI_i decreased while increasing $X_{T/N}$ (Table 2.2). However, unlike the results

for varying the irradiation time, the effective cross-link density when $X_{T/N}$ is varied does not significantly change (Table 2.4, Figure 2.18) with all hydrogels having statistically the same cross-link density. When the $X_{T/N}$ was increased, the ML_{37} values also increased (Figure 2.14.c and 2.14.d). This behavior is expected as the higher $X_{T/N}$ values result in a greater PNIPAM fraction in the hydrogel relative to NorHA. Since PNIPAM dewaters upon heating, more of it present in the hydrogel will lead to a higher mass of water lost relative to total mass. These results suggest that controlling the $M_{P/HA}$ of the hydrogel through varying $X_{T/N}$ can be used as another variable to target a desired ML.

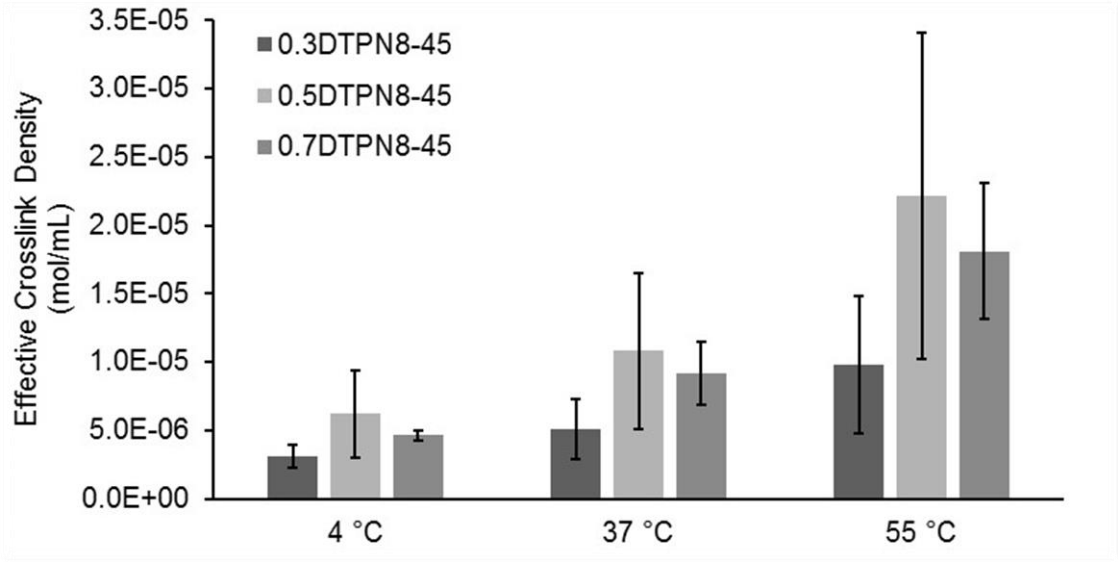

Figure 2.18. Effective cross-link density (ν_e) at various temperatures for the DTPN8-45 hydrogel formulations with different $X_{T/N}$. Error bars are from the standard deviations of the measurements propagated through the calculations.

To further explore how the degree of cross-linking and $M_{P/HA}$ affected the physical properties of the hydrogels, a mono-thiol functionalized PNIPAM (MTPN8) was synthesized and used along with the di-thiol functionalized DTPN8 in hydrogel fabrication. Since MTPN8 had one terminal thiol, it could covalently attach to the NorHA hydrogel network as a pendant group via the thio-ene reaction, but not cross-link. Thus, MTPN8 should still be incorporated into the hydrogel to

change the $M_{P/HA}$ value, but not change the degree of cross-linking. A hydrogel was synthesized (M,D-TPN8-90) with a $X_{T/N}$ value of 0.3 using the DTPN8 cross-linker and MTPN8 was added to yield a $M_{P/HA}$ similar that to a hydrogel with a $X_{T/N}$ of 0.5 ($M_{P/HA}$ = 0.9). At an irradiation time of 90 s, the degree of cross-linking of M,D-TPN8-90 appeared to be similar to its DTNP8 only counterpart (0.3DTPN8-90) as both the MI_i and modulus values were similar (Table 2.2). The ML_{37} values of M,D-TPN8-90 and 0.3DTPN8-90 as well as 0.5DTPN8-90 (the hydrogel with $M_{P/HA}$ equivalent to M,D-TPN8-90) are similar, suggesting that the MTPN8 did not appreciably affect the thermal behavior. Such results suggest that PNIPAM needs to be incorporated into the cross-links of these hydrogels to affect thermo-response.

The ML_{55} was also measured to observe the thermo-response of the hydrogels above the literature reported LCST for PNIPAM (32 °C). For all hydrogels, a higher ML was observed at 55 °C as compared to 37 °C (Table 2.5 and Appendix Figures A.2.1-A.2.2). As the NorHA hydrogels with the non-thermo-responsive cross-linkers did not demonstrate this response to temperature, the variable thermo-response as a function of temperature appeared to be due to the nature of the DTPN cross-linkers. Dynamic light scattering (DLS) analysis of the DTPNs (Figure 2.19) suggested a broad LCST transition as opposed to the typically sharp transition around 32 °C for typical PNIPAMs. As the Đ for the DTPN were narrow, suggesting a rather homogeneous molecular structure, a clear cause for the broad LCST in these DTPN is not apparent. Possibly the di-thiol-termination and CTA residue in the middle of the polymer affect the thermodynamics that drive the LCST in these molecules, but more a more in depth analysis at a later date is needed to ascertain the direct cause. Since the thermo-responsiveness of the NorHA/DTPN hydrogel system is a function of temperature, the amount of water expulsion from a particular formulation could also be controlled by changing temperature.

Table 2.5. Mass loss percentage of DTPN cross-linked NorHA hydrogels at 55 °C.

Formulation	ML_{55} (%)	Formulation	ML_{55} (%)
0.3DTPN8-45	48.5±6.2	0.5DTPN4-90	12.6±0.9
0.3DTPN8-90	38.5±3.3	0.7DTPN8-45	55.0±7.9
M,D-TPN8-90	40.2±3.9	0.7DTPN8-90	49.6±2.6
0.5DTPN8-45	52.9±3.1	2DTPN8-45	63.3±1.4
0.5DTPN8-90	44.7±2.2	4DTPN8-45	63.5±1.9
0.5DTPN8-180	41.2±3.7		

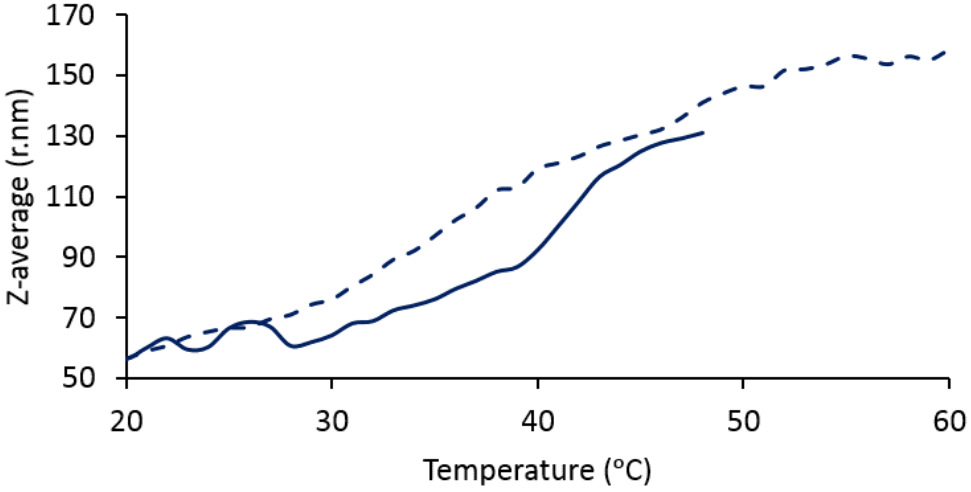

Figure 2.19. DLS digram of DTPN4 and DTPN8. Temperature trend diagram obtained by DLS for DTPN4 (dashed line) and DTPN8 (solid line). In both cases, a range of transition temperature is observed which means that different thermo-responsiveness is observed at different temperatures. Z.average represents the average size of a particle size distribution. The particle size increases upon heating due to the aggregation of insoluble particles.

This temperature dependence of ML could be used to thermally trigger drug delivery or use these materials for shape-memory applications in the future.[89,93,94] For example, different thermo-responsiveness at higher temperatures than the LCST can be useful in photothermal drug release in the body to treat inflammation and cancer. External triggers such as near-infrared light passing through tissue to induce surface plasmon resonance on gold nano-particles could simultaneously release drugs and photothermally treat cancer. Examples in literature exist of sustained release of methylene blue, ovalbumin, and bovine serum albumin from PNIPAM-based hydrogels at 50 °C and using carbon nanotubes and gold nano-particles to heat with near-infrared light.[96,124-129] Future studies could utilize these biopolymer based NorHA/DTPN hydrogels for similar applications where a bioactive scaffold could be necessary such as wound repair after the photothermal treatment.

2.3.5. Control of hydrogel modulus

The stiffness or modulus of hydrogels is controlled by the cross-link density of the network. Typically, cross-link density for thiol-ene hydrogels is controlled by the ratio of a fixed length cross-linker to the reactive group of the matrix polymer or otherwise the $X_{T/N}$. With the DTNP cross-linkers, the length of the cross-linker is an additional parameter that can be used to control the modulus of the hydrogel. The effective cross-link density was calculated for all hydrogels and an increased cross-link density mirrored the observed increase in modulus (Table 2.4). Using $X_{T/N}$, irradiation time, and the cross-linker length the modulus could be controlled from ca. 5 to 50 kPa (Table 2.2), which covers the modulus of most soft tissues. For example, the elastic moduli of kidney tissue (5-10 kPa), cardiac tissue (10-15 kPa), and intestine tissue (20-40 kPa) are within the range of modulus of the NorHA/DTPN hydrogels.[108] Such results suggest that modulus of these hydrogels could be targeted for any desired biomaterial application.

2.3.6. Temporal modification of hydrogel stimuli response

The light induced thiol-norbornene cross-linking process enables the modification of hydrogel properties with additional cross-linking. Figure 2.20 demonstrates methods for additional cross-linking and photopatterning where the hydrogel is initially cross-linked with the desired molecule and as long as norbornenes remain, additional cross-linking is possible. If the second cross-linker is stimuli responsive, the stimuli response should be modified.

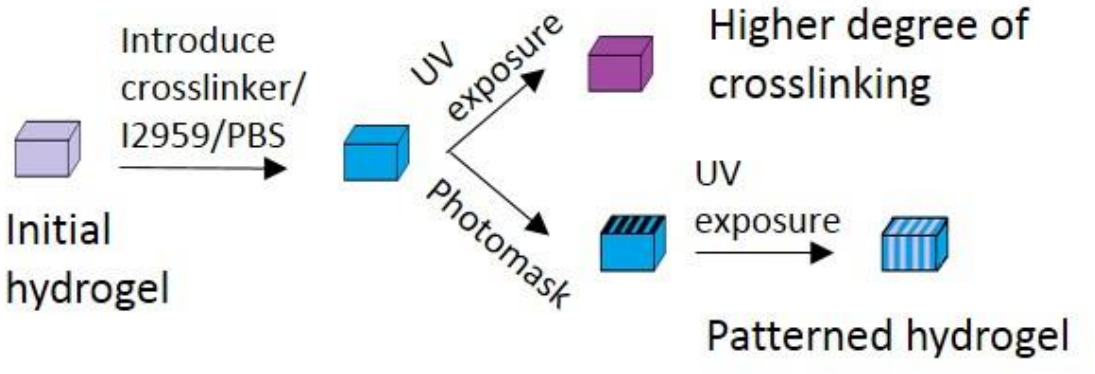

Figure 2.20. a) Schematic to modify NorHA hydrogels after gelation by introducing the hydrogel to a solution of cross-linker and UV-initiator with subsequent UV exposure.

To confirm this behavior, NorHA/DTNP8 hydrogels were synthesized ($X_{T/N}$ = 0.3, t_{ir} = 45 s, wt % = 6) and incubated at 4 °C. At this formulation, if all the thiols reacted with the norbornenes, 70% of the norbornene groups would remain, providing synthetic handles for subsequent reaction. Thermal analysis of this initial hydrogel gave ML values of 20.4 and 46.2% at 37 and 55 °C, respectively (Figure 2.21). These initial hydrogels were incubated in a solution of DTPN8 (0.015 g/mL) and I2959 (0.05 wt %) at 4 °C for 24 h prior to irradiating with UV light for 5 min. The temporally modified hydrogels ML significantly increased to 40.0% at 37 °C and 67.4% at 55 °C (Figure 2.21) which follows the trend observed for the hydrogels that underwent initial cross-linking. The observed bulk temporal modification demonstrates that a DTPN cross-linker can be

used to change the stimuli response when needed. Such a result has not been reported for physically cross-linked PNIPAM-grafted HA hydrogels.[111,112] The thermal cross-linking of PNIPAM-grafted HA requires that the materials are heated to body temperature and gelation does not occur at temperatures below the LCST. The light induced covalent thiol-ene cross-linking overcomes this limitation to fabricate stable hydrogels at ambient temperature as well as provides further modification of hydrogels properties as shown here.

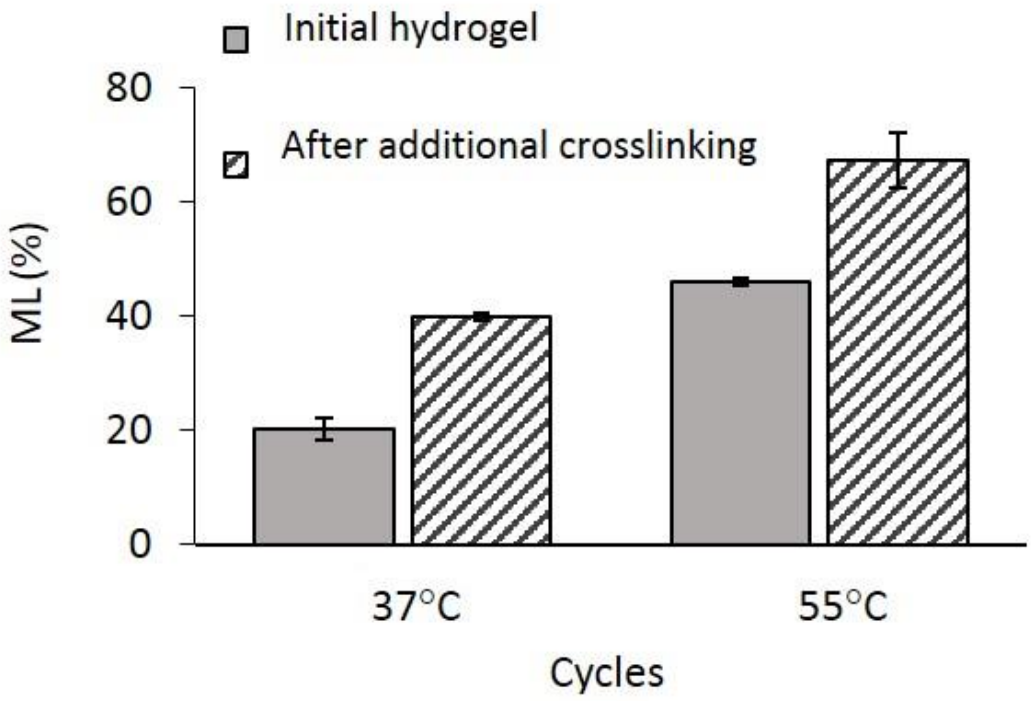

Figure 2.21. Mass loss percentage of hydrogel after additional cross-linking. ML at 37 and 55 °C of NorHA/DTPN8 hydrogels initially cross-linked at $X_{T/N}$ = 0.3 (solid bars, t_{ir} = 45 s, wt % = 6) and after incubating the hydrogels in a DTPN8 (15 mg/mL) and I2959 (0.05 wt %) solution for 24 h and irradiating for 5 min (striped bars). Error bars represent one standard deviation (n = 4).

2.3.7. Spatiotemporal modification of stimuli response

To investigate spatiotemporal modification of stimuli response, initial NorHA hydrogels were made using the non-thermo-responsive cross-linker DTPEO to give a non-stimuli responsive initial NorHA/DTPEO hydrogel. Light microscopy at 4 °C indicated a smooth hydrogel surface (Figure 2.22.a). The DTPEO hydrogel was incubated in a solution of DTPN8 (0.015 g/mL) and I2959 (0.05 wt %) in PBS for 24 h at 4 °C. Afterwards, a striped photo mask (200 µm alternating stripes) was used to cover hydrogels during a 5 minute UV light exposure (Figure 2.20). Regions exposed to UV-light had DTPN8 cross-link NorHA further, introducing thermo-responsiveness in particular regions as well as increasing the cross-link density. No cross-linking occurred in the regions blocked by the mask and thus these regions were composed of the initial NorHA/DTPEO hydrogel. The photopatterning of DTPN8 is visible at 4 °C (Figure 2.22.b) as the less-cross-linked NorHA/DTPEO only regions swell more than the NorHA/DTPEO/DTPN regions. These stripes are visible even with naked eye due to the different texture as a result of higher degree of cross-linking.

Control DTPEO cross-linked NorHA hydrogels were also synthesized as a control experiment by irradiating the NorHA/DTPEO hydrogels with UV-light for 5 minutes while covered by the same photomask without additional cross-linker. The ML values of the DTPN patterned bulk hydrogels as compared to the control hydrogels confirm that thermo-response was added through the photopatterning process (Figure 2.23.a). The substantial increase in mass loss percentage after introducing PNIPAM to the hydrogels suggests that thermal properties of NorHA/DTPEO/DTPN hydrogels are a result of PNIPAM cross-linker. PEO has no significant response to changing temperature.

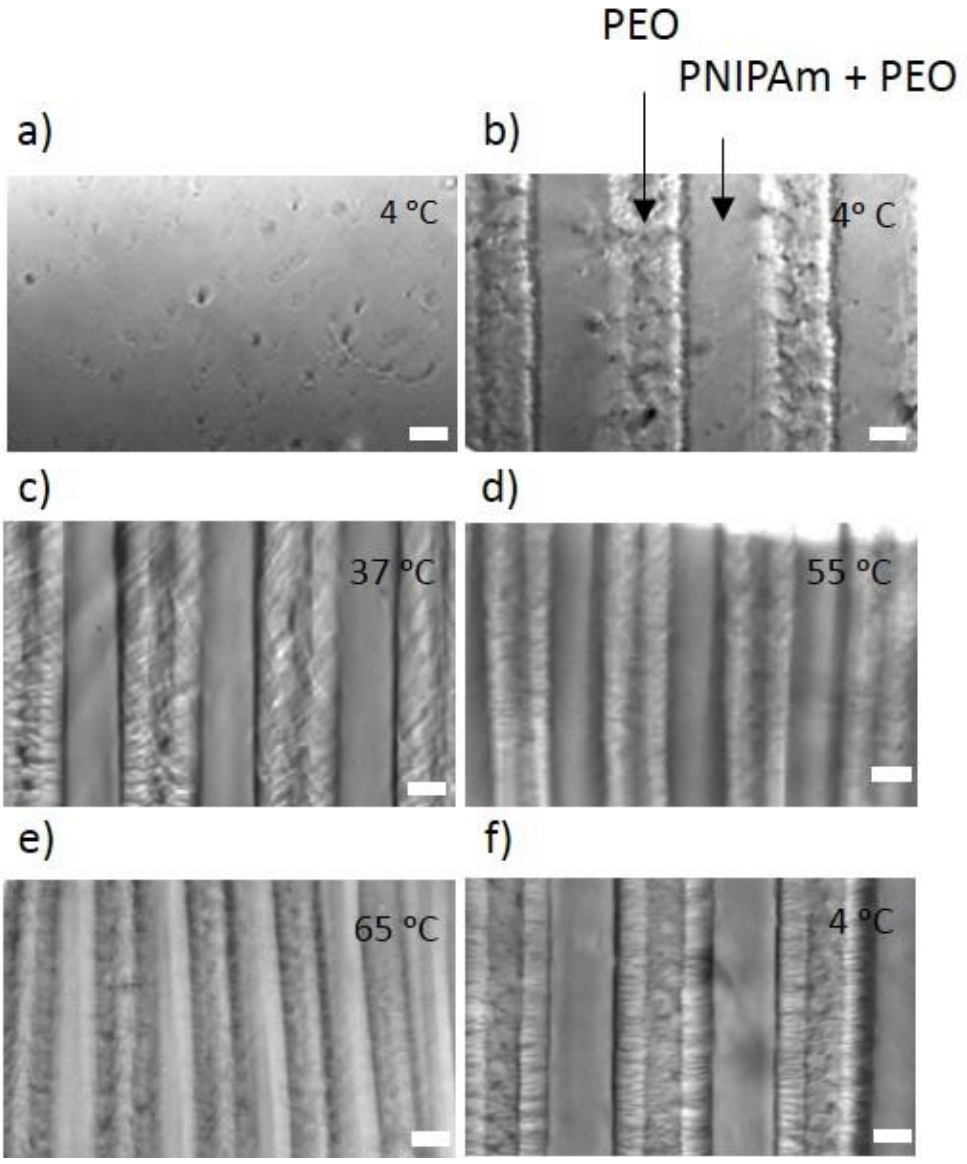

Figure 2.22. Bright field optical images (5x magnification) of hydrogels. Images of an a) unpatterned NorHA/DTPEO and images of the hydrogel surface patterned with DTPN8 cross-linker at b) 4 °C and sequentially incubated for 24 h at c) 37 °C, d) 55 °C, e) 65 °C, and f) 4 °C. Scale bars are 100 µm.

The spatiotemporal stimuli response to temperature changes was observed by imaging the surface of the hydrogels with optical microscopy (5x magnification) after incubating for 24 h in PBS in cycles at 4, 37, 55, 65 and 4 °C. The width of each stripe was measured using ImageJ software and result is shown in Figure 2.23.b. Initially at 4 °C, the line widths of the two compositions are similar with the more cross-linked NorHA/DTPEO/DTPN regions being slightly

narrower due to the reduced swelling from the higher degree of cross-linking. Heating the hydrogels to 37, 55, and 65 °C sequentially caused the widths of both regions to decrease with the DTPN cross-linked regions decreasing to a greater extent as evidenced by their thermo-response. The reduction in line width of the DTPEO regions upon heating is likely due to the stress applied to those regions from the dewatering of the adjacent DTPN cross-linked regions as the DTPEO cross-linked hydrogels alone should not be thermo-responsive. Cooling the hydrogels back to 4 °C increases the width of both regions (Figure 2.23.b), but some hysteresis is present as the DTPN hydrogels do not return to their original size. Qualitatively, the boundary between the DTPN/DTPEO and DTPEO only cross-linked region looks different and is suggestive of hydrogel damage due to the stress experienced (Figure 2.22.f). Such results suggest that when patterned, the reversibility of heating and cooling may be limited due to the internal stresses placed on the hydrogel. Nevertheless, these results demonstrate that spatiotemporal modification of stimuli response are possible with this hydrogel system.

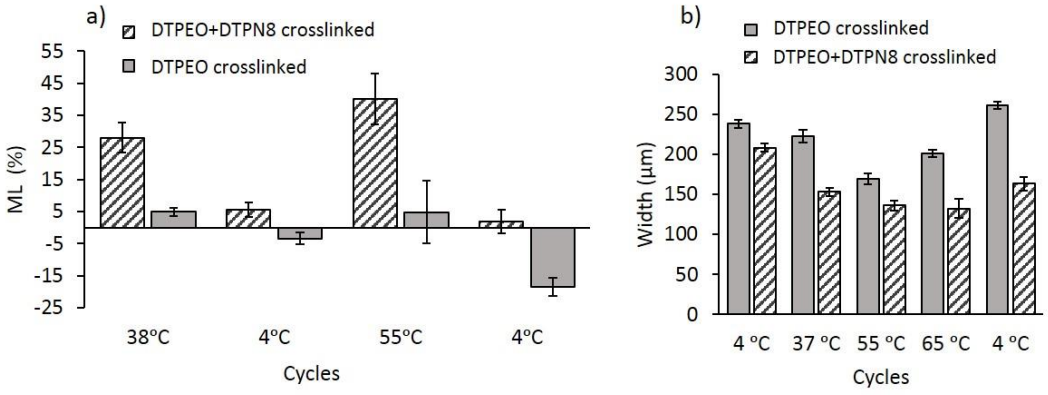

Figure 2.23. Thermo-responsivity of NorHA hydrogels with DTPN and DTPEO cross-linkers. a) Solid bars show mass loss percentages of DTPEO cross-linked NorHA hydrogels. Striped bars show mass loss percentages of the same PEO cross-linked NorHA hydrogels after being patterned with DTPN cross-linker. b) Domain widths were measured with ImageJ to calculate their average width as a function of cycle. Solid bars represent width of only PEO cross-linked regions and striped bars belong to regions cross-linked by DTPEO and DTPN8. Error bars are the standard deviation of 5 measurements.

2.3.8. Cell culture on NorHA/DTPN hydrogels

Human mesenchymal stem cells (hMSCs) were seeded on top of NorHA hydrogels to confirm that these hydrogels could be used as biomaterials and possibly to control cell behavior with wrinkled surface patterns.[104,130] As demonstrated in Figure 5, the surface of a DTPN8 patterned hydrogel has wrinkles due to shrinkage of PNIPAM cross-linker at 37 °C. To investigate the cell-surface interactions, a NorHA/DTPEO hydrogel was synthesized and patterned with DTPN8. A cysteine functionalized cell adhesion peptide (RGD) to promote hMSC adhesion and a cysteine-functionalized rhodamine B to visualize the pattern were included during patterning, following a previously reported method.[62] Fluorescence microscopy imaging on day 1 (24 h after seeding) demonstrated that hMSCs attached to both the wrinkled surface of DTPN8/RGD patterned NorHA/DTPEO hydrogels and to the NorHA/DTPEO hydrogel with RGD peptide present (Figure 2.24.A). No cell adhesion was observed when the RGD peptide was not patterned with the DTPN8, confirming that the RGD peptide was patterned and affected cell adhesion (Figure 2.24.B). For the NorHA/DTPEO/DTPN8 hydrogels, cell nuclei were counted to see whether they were on the RGD patterned stripes or the RGD free regions. Technical replicates were done by counting cell nuclei on a total of six stripes for each PNIPAM and no-PNIPAm regions from three individual hydrogels made from the same solution and cells from the same culture plate. The cell nuclei were 1.7±0.3 times more likely to be found on the RGD/DTPN8 patterned regions than the non-patterned regions, suggesting that hMSCs still preferred to adhere to the RGD patterned regions when DTPN8 was present. Moreover, imaging at day 7 shows that hMSCs proliferated and covered the hydrogel surface (Figure 2.24.C), confirming that cells can be grown on these materials and that the system can be used in future biomedical studies.

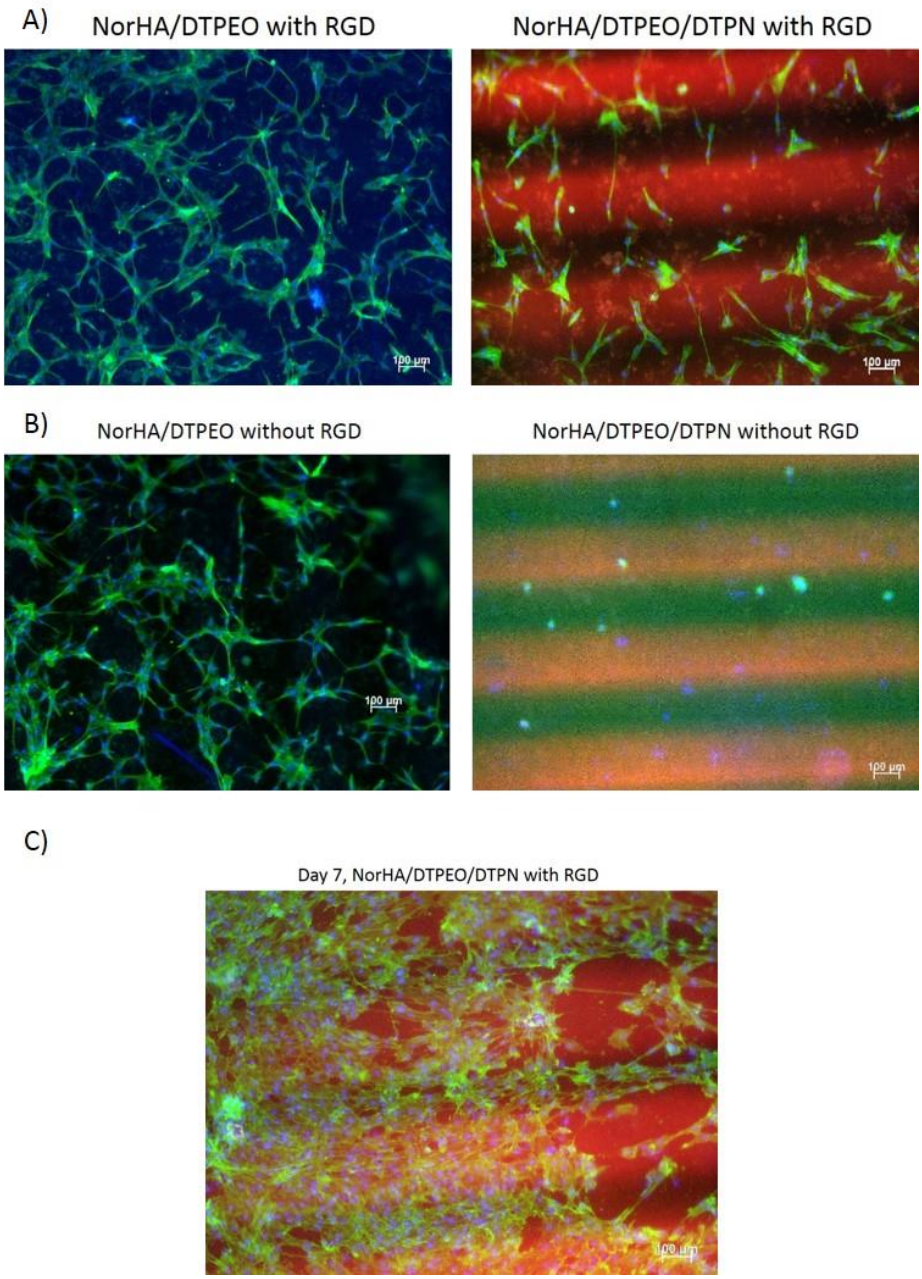

Figure 2.24. Fluorescence microscopy images (ZEISS.AXIO OBSERVER.Z1, 5x magnification) of hMSCs seeded on the surface of hydrogels: A) the surface of NorHA/DTPEO/RGD and DTPN/RGD patterned NorHA/DTPEO hydrogels, B) the surface of NorHA/DTPEO and PNIPAM patterned NorHA/DTPEO hydrogels without RGD protein, and C) the surface of RGD and PNIPAM patterned NorHA/DTPEO hydrogels at day 7 of seeding. hMSCs proliferated and covered the surface which is an indicative of hydrogel cytocompatibility. Nuclei of the cells were stained by DAPI shown in blue. Phalloidin (green) stained actin. DTPN patterned regions are indicated by the red color of cysteine-functionalized RhodamineB,

2.4. Conclusions

The spatiotemporal modification of thermal properties of thermo-responsive NorHA hydrogels was achieved using the UV-light initiated thiol-ene cross-linking reaction with DTPN cross-linkers. The ML of the hydrogels upon heating could be controlled by varying the cross-link density of the hydrogels and the amount of DTPN cross-linking the hydrogel. This ML also could be changed as a function of temperature, indicating that additional stimuli response is observed above 37 °C. Additionally, using one NorHA and DTPN the modulus of the material could be controlled over an order of magnitude. Spatiotemporal modification of the stimuli response was achieved by photopatterning of hydrogels with DTPN such that this hydrogel system can be used for spatiotemporal modification of topology and shape memory behavior. Since the hydrogel system was suitable for cell culture and the stimuli response can be spatiotemporally modified, these results demonstrate that it could be used in future work to elucidate cell behavior. Furthermore, this study demonstrates that significant stimuli control can be imparted through stimuli responsive cross-links while retaining a majority of natural component such that future studies can explore other stimuli responsive cross-linkers in similar thiol-ene hydrogels.

CHAPTER 3

SYNTHESIS AND SPATIOTEMPORAL MODIFICATION OF BIOCOMPATIBLE AND STIMULI RESPONSIVE CARBOXYMETHYL CELLULOSE HYDROGELS USING THIOL-NORBORNENE CHEMISTRY

3.1. Introduction

Carboxymethyl cellulose (CMC) was functionalized with norbornene groups to undergo thiol-norbornene cross-linking reactions. Hydrogels synthesized from a single norbornene modified carboxymethyl cellulose (NorCMC) via a light initiated thiol-ene cross-linking reaction with a variety of dithiol cross-linkers yielded hydrogels with a tunable compression modulus ranging from 1.7 to 103 kPa. Additionally, thermoresponsiveness was spatiotemporally imparted to NorCMC hydrogels by photopatterning a dithiol-terminated poly(N-isopropyl acrylamide) (PNIPAM) cross-linker, enabling swelling and topological control of the hydrogels as a function of incubation temperature. NorCMC hydrogels were cytocompatible as the viability of encapsulated human mesenchymal stem cells (hMSCs) was greater than 85% after 21 days while using a variety of cross-linkers. Moreover, hMSCs could remodel, adhere, and spread in the NorCMC matrix cross-linked with a matrix metalloproteinase (MMP) degradable peptide, further demonstrating the utility of these materials as a tunable biomaterial.

3.2. Experimental

3.2.1. Materials

Chemicals were purchased from either Sigma-Aldrich or Fisher Scientific and used without further purification unless otherwise noted. All cell culture materials were purchased from Life Technologies. Human mesenchymal stem cells were purchased from Lonza (1 mL vial containing ≥750,000 cells). Ethanolamine and 5-norbornene-2-methylamine were purchased from Alfa Aesar and TCI America, respectively. Peptides were purchased from Genscript and used without further purification.

3.2.2. Synthesis of norbornene functionalized carboxymethyl cellulose (NorCMC)

In a representative functionalization reaction, 0.25 g (1.2 mmol of repeat units) of sodium CMC (NaCMC, 90 kg/mol) was dissolved in 25 mL deionized water to make a 1 wt% NaCMC solution. To this solution, 0.148 g (0.77 mmol) of 1-ethyl-3-(3-dimethylaminopropyl)carbodiimide hydrochloride (EDC HCl), 0.089 g (0.77 mmol) of N-hydroxysuccinamide (NHS), and 0.1 mL (0.8 mmol) of 5-norbornene-2-ethylamine (NA) were added sequentially. After adding the NA, the solution became cloudy and was left to stir for 18 h at room temperature. Sodium chloride (0.75 g) was added to the mixture prior to precipitation in 250 mL ice-cold acetone. The solution was added to acetone dropwise, stirred for an hour, and then acetone was decanted to yield a white precipitant. The precipitant was dissolved in 22 mL of deionized water and dialyzed for three days prior to removing water by lyophilization and obtaining pure norbornene functionalized CMC (NorCMC). NorCMC was characterized by ^{1}H-NMR spectroscopy to confirm functionalization and determine the degree of functionalization. Different degrees of functionalization could be achieved by varying the molar ratios of reagents to NaCMC. To calculate the degree of functionalization, the integrations of the peak at 3-4.5 ppm and 5.8-6.07 ppm were normalized to

the number of corresponding hydrogen atoms (8.4 and 2 hydrogen atoms for backbone hydrogen and norbornene double bond hydrogen atoms respectively). The value 8.4 was obtained regarding 70% carboxymethyl functionalization on the CMC and represents the average number of hydrogen atoms per repeat unit. The percentage of the ratio of normalized values of norbornene double bond to backbone hydrogen atoms were reported as degrees of functionalization.

^{1}H-NMR spectroscopy of NorCMC (D_2O, 400 MHz): δ (ppm) = 0.35-3 (m, CHs and CH_2s of endo/exo norbornene amine, 9 H), 3-4.5 (m, Hs of CMC backbone), 5.8-6.07 (m, alkene CHs of endo/exo norbornene amine, 2 H).

Size exclusive chromatography (SEC) was conducted before and after the functionalization reaction, using an Agilent 1260 infinity SEC system consisting of a Phenomenex PolySep-GFC guard column, two analytical columns (Phenomenex PolySep-GFC P3000 and P5000) in series, and aqueous solution of 0.1 M sodium nitrate and 5 mM (in HPLC grade H_2O) as eluent. Polymer relative retention time and dispersity of CMC and NorCMC (Đ=3.22 and Đ=3.33, respectively) showed no significant change as compared to polyethylene oxide calibration standards (RI detector), suggesting that the functionalization reaction was not destructive to the CMC polymer chains.

3.2.3. Fabrication of 3D NorCMC hydrogels

NorCMC hydrogels were prepared by UV irradiation of a pre-polymer solution containing NorCMC, dithiol cross-linker, and the radical initiator 2-hydroxy-4'-(2-hydroxyethoxy)-2-methylpropiophenone (I2959) (0.05 wt%) dissolved in PBS. The solution was vortexed for an hour and air bubbles were removed by centrifugation. To form hydrogels, 50 µL portions of solution were transferred to a 1 mL syringe with the top cut off, sealed with a coverslip (0.22 mm thickness), and exposed to 365 nm UV light at 10 mW/cm^2 power (Omnicure S1000 UV lamp

filtered for 320-390 nm) for various times. The resulting hydrogels were stored in 1 mL of PBS in a 24-well plate at 4 °C for 24 hours prior to subsequent testing. Several formulations of hydrogels were prepared varying polymer weight percent (wt%), molar ratios of thiol to norbornene (T/NB), irradiation time, and type of cross-linker molecule.

3.2.4. Fabrication of 2D NorCMC hydrogels

Thin hydrogels (approximately 200 μm thick) were synthesized adhered to coverslips for cell culture and photopatterning experiments. Glass coverslips (No. 2, 22 x 22 mm) were plasma cleaned by a Tesla coil (Electro-Technic Products, BD-50E heavy duty generator, 115V) that was applied for 30 to 45 s on each coverslip. The cleaned coverslips were placed on an aluminum tray, covered with (3-mercaptopropyl)trimethoxy silane, and heated for 1 h at 100 °C. Heating was continued for additional 10 minutes at 110 °C to yield thiolated coverslips that were removed from heat and cooled. Prior to use, coverslips were washed with acetone, methanol, and dried by blowing nitrogen. Activated coverslips were stored under nitrogen atmosphere and used in less than 24 h after activation.

A solution of NorCMC, dithiothreitol (DTT) (4 wt% total polymer, T/NB=0.5), and 0.05 wt% I2959 was prepared in PBS and placed on a coverslip (glass No.1, 45 x 55 mm) while four coverslips (glass No. 2, 22 x 22 mm, 200 μm) were used at the edges to support the solution. Then, the solution was covered with an activated coverslip with the thiolated side down on the solution. The solution was irradiated 90 s with UV light (365 nm, 10 mW/cm^2) from the thiolated coverslip side. The coverslip adhered to the 200 μm thick 2D hydrogel was removed from the bottom coverslip and then stored in a 6-well plate with 3 mL of PBS at 37 °C prior to cell culture or photopatterning.

3.2.5. Measuring the compression modulus of 3D hydrogels

Compression experiments were conducted on 3D hydrogels at 10%/min strain rate up to 30% total strain using a dynamic mechanical analyzer (DMA) (Q8000 Thermal Analysis, TA Instruments) with a compression fixture at room temperature. The slope of strain-stress curve in the 10 to 20% compressive strain limit was defined as the compression modulus (Appendix B, Figure B.1-B.4). Hydrogels ($n \geq 9$ for each condition) were incubated in PBS at 4 °C for 24 h prior to testing to reach to equilibrium. This condition was applied for all hydrogels to keep the results consistent with PNIPAM experiment which underwent volume change at room temperature. Hydrogels were kept cool until testing.

3.2.6. Measuring the thermoresponse of NorCMC/PNIPAM hydrogels

Three-dimensional hydrogels of NorCMC were made using a dithiol-terminated PNIPAM (DTPN) cross-linker that was synthesized following a previously reported procedure (Chapter 2, Section2.2.9) The hydrogel formulation consisted of 6 wt% polymer, 60 s UV irradiation, a variable T/NB, and 0.05 wt% I2959 in PBS. Hydrogels (n=5) were incubated in PBS at 4 °C for 24 h and then were massed ($W_{initial}$). Subsequently, hydrogels were incubated at either 4, 37, or 55 °C in PBS for 24 h and massed after each temperature cycle ($W_{measured}$) as described in Chapter 2 Section 2.2.9. The relative mass loss (ML) was calculated as defined in Equation 3.1.

$$ML = \frac{W_{initial} - W_{measured}}{W_{initial}} \times 100 \qquad \text{(Equation 3.1)}$$

3.2.7. Photopatterning of NorCMC hydrogels

3.2.7.1. 2D hydrogels

The fabricated 2D hydrogels were incubated at 37 °C for 24 h in a solution of 0.05 wt% I2959 and 1 mg/mL of rhodamine B peptide (with the sequence GCDDD-rhodamine B) in PBS,

synthesized following a previously reported procedure.[62] Hydrogels were exposed to UV light (365 nm, 10 mW/cm^2) for 90 s while covered with a photomask with 200 µm dark stripes alternating with 200 µm blank stripes. The unreacted dye was removed from the patterned hydrogels by incubating them in PBS for 24 h at 37 °C prior to fluorescence imaging with a Zeiss.Axio Observer.Z1 microscope.

3.2.7.2. 3D hydrogels

NorCMC hydrogels cross-linked with dithiol-terminated poly(ethylene glycol) (DTPEG) were fabricated from a 4 wt% polymer solution with a T/NB of 0.3, 0.05 wt% I2959, and 60 s irradiation time. The hydrogels were incubated in a solution of PNIPAM (4000 g/mol, 8.5 mg/mL) and I2959 (0.05 wt%) in PBS for 24 h at 4 °C. Hydrogels (n=3) were stored in only PBS and I2959 (0.05 wt%) as control experiment. After incubation, the hydrogels were exposed to UV light (320-390 nm, 10 mW/cm^2) for 5 minutes while covered with a photomask with 200 µm masked stripes alternating with 200 µm blank stripes. Hydrogels were placed in 1 mL of PBS for one hour prior to imaging by optical microscopy (Zeiss.Axio Observer.Z1).

3.2.8. Cell encapsulation and viability

3.2.8.1. Preparation of pre-gelation solution

NorCMC, cross-linker, and equipment were sterilized by germicidal/sterilization UV light (254 nm) for 5 minutes and I2959 stock solution was sterile filtered (Santa Cruz Biotechnology, PVDF membrane, pore size 0.22 µm) prior to use. Pre-gelation solutions were prepared containing NorCMC, dithiol cross-linker (4 wt% polymer, T/NB=0.5), and 0.05 wt% I2959. Hydrogels were created either with a DTT cross-linker or a peptide cross-linker with the highly MMP-sensitive sequence GCRDGPQGIWGQDRCG (MMP-deg).[131] To prevent aggregation of the MMP-deg in solution, it was buffered with 0.02 v/v% ethanolamine to a pH of 8-8.5. For each cross-linker,

hydrogels were prepared with and without the cell adhesion peptide GCGYGRGDSPG (RGD) at a 2 mM concentration.

3.2.8.2. Cell culture

Passage five human mesenchymal stem cells (hMSCs) from Lonza were cultured in 90% low glucose Dulbecco's modified eagle serum (DMEM) with GlutaMAX and sodium pyruvate containing 9% fetal bovine serum (FBS), 1% antibiotic-antimycotic (100x), and 5 µL fibroblast growth factor until 90% confluency (day 6). Cells then washed with DPBS and trypsinized prior to encapsulation as follows. Warm (37 °C) 0.05% trypsin/EDTA (3 mL) was added to the 100 mm petri dish and swirled around until all cells were covered. The dishes were incubated at 37 °C and 5% CO_2 for 5-8 minutes. Warm media (37 °C, 7 mL) was added to the dish and this suspension was transferred into a conical tube. Cells were spun down, the media was removed, and cells were suspended in 1 mL of media, and spun down again.

3.2.8.3. 3D Cell encapsulation

After removing this media, hMSCs were suspended in sterile pre-gelation solution (4 wt% total polymer, T/NB=0.5) at a density of 1.6×10^5 cell per 400 µL of pre-gelation solution. The suspension (50 µL) was transferred to a syringe tip, sealed with a sterile coverslip, and exposed to 60 s UV irradiation (320-390 nm) at 10 mW/cm^2. Hydrogels were placed in a 24-well plate with 1 mL of cell culture media and incubated at 37 °C and 5% CO_2 for various periods of time.

3.2.8.4. 2D cell encapsulation

2D hydrogels with and without RGD peptide (sequence GCGYGRGDSPG) were made as described in the main manuscript (4 wt% total polymer, T/NB=0.4, 0.05% I2959, 90 s UV irradiation) and placed in a 6-well plate. Passage five hMSCs were suspended in sterile PBS (DPBS)

and 3 mL of suspension was added to each well (100,000 cell cm^{-2}). Hydrogels were incubated for 24 hours at 37 °C and 5% CO_2 prior to fluorescence imaging using a ZEISS.AXIO Observer.Z1 microscope. Before imaging, cells were fixed using a 4 wt% paraformaldehyde solution that was prepared by adding 1 mL deionized water and 10 µL NaOH (1N) to 0.4 g of paraformaldehyde in a vial, heating it at 80 °C in water bath for 10 minutes, and then adding 9 mL DPBS and 2 µL HCL (6N) to the solution (for each 10 mL of 4 wt% paraformaldehyde solution). This paraformaldehyde solution (3 mL) was added to each well and incubated for 15 minutes at room temperature. Afterward, hydrogels were washed with DPBS twice. The fixed hydrogels and cells were kept in 3 mL of 0.5 wt% solution of triton X-100 at room temperature for 20 minutes to permeabilize the cells. The hydrogels were washed with DPBS at least twice before staining the cells with DAPI and phalloidin. A solution of DAPI (300 nM) and phalloidin (2.5 v/v %) in DPBS was prepared in which hydrogels were incubated for 20 minutes at room temperature. Hydrogels were washed twice with DPBS prior to imaging.

3.2.8.5. Cell imaging

Florescence microscopy was conducted for hydrogels at days 3, 7, 10, 17, and 21 using a ZEISS.AXIO Observer.Z1 microscope. Hydrogels (n=4 for each formula at each day) were stained for 40 minutes with a LIVE/DEAD viability assay (Life Technologies) (0.25 µl of calcein and 1 µL of Ethidium homodimer-1 in 1 mL of sterile PBS for each hydrogel) prior to imaging. Live (green) and dead (red) cells were counted using ImageJ software and the ratio of live cells to total cells was defined as cell viability. The aspect ratio of the cells was calculated to study cell spreading and growth in 3D hydrogels over 21 days. ImageJ was use to take straight-line measurements along the longest axis of cells and the axis perpendicular to it. The aspect ratio was defined as ratio of the long axis to short axis.

3.3. Results and Discussion

3.3.1. Norbornene functionalization of CMC (NorCMC)

Norbornene-functionalized CMC (NorCMC) was synthesized using an EDC coupling reaction between CMC and norbornene amine (Figure 3.1). Through precipitation in acetone, dialysis, and lyophilization, the product was obtained at a 70% overall yield. The norbornene functional group provides reactive sites on the CMC backbone that can undergo the thiol-norbornene click reaction to form cross-linked hydrogels.

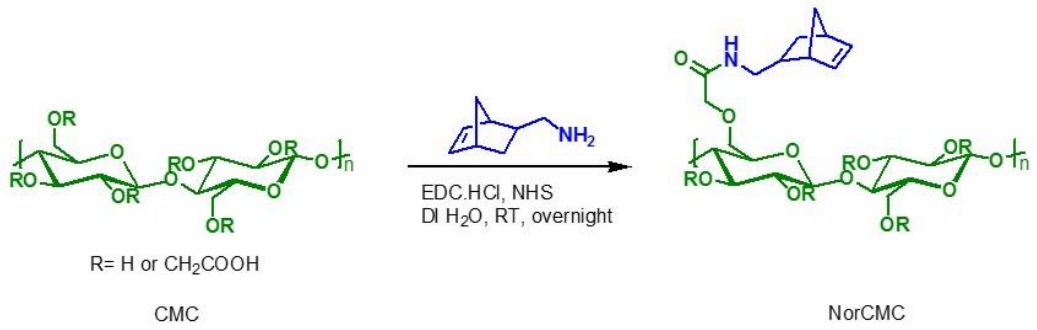

Figure 3.1. Functionalization of CMC with norbornene groups via EDC coupling reaction.

The ^{1}H-NMR spectrum of the product that is shown in Figure 3.2 confirmed norbornene functionalization as new broad peaks at 5.9-6.1 ppm and 3-4.5 ppm were visible. SEC chromatograms showed no significant change in molecular weight dispersity and a minimal decrease in relative molecular weight of the CMC before and after the functionalization reaction (Figure 3.3). Since the chemistry is not expected to degrade the CMC, this minor change in molecular weight can be a result of a change in hydrodynamic radius. Several degrees of functionality were obtained by varying the molar ratios of norbornene amine, NHS, and EDC relative to CMC (Table 3.1). For example, increasing molar ratios of NA, EDC, and NHS to repeat units from 0.7 to 1.4, increased the functionalization percentage from 9 to 15. NorCMC with 18%

of the repeat units functionalized was used throughout these studies as this degree of functionalization provided numerous reaction points per polymer chain (56 NB groups per one CMC polymer chain on average that was sufficient for this work), while not noticeably altering its water solubility. Overall, these results demonstrated that this functionalization reaction can yield NorCMC at high yields and a sufficient degree of functionalization.

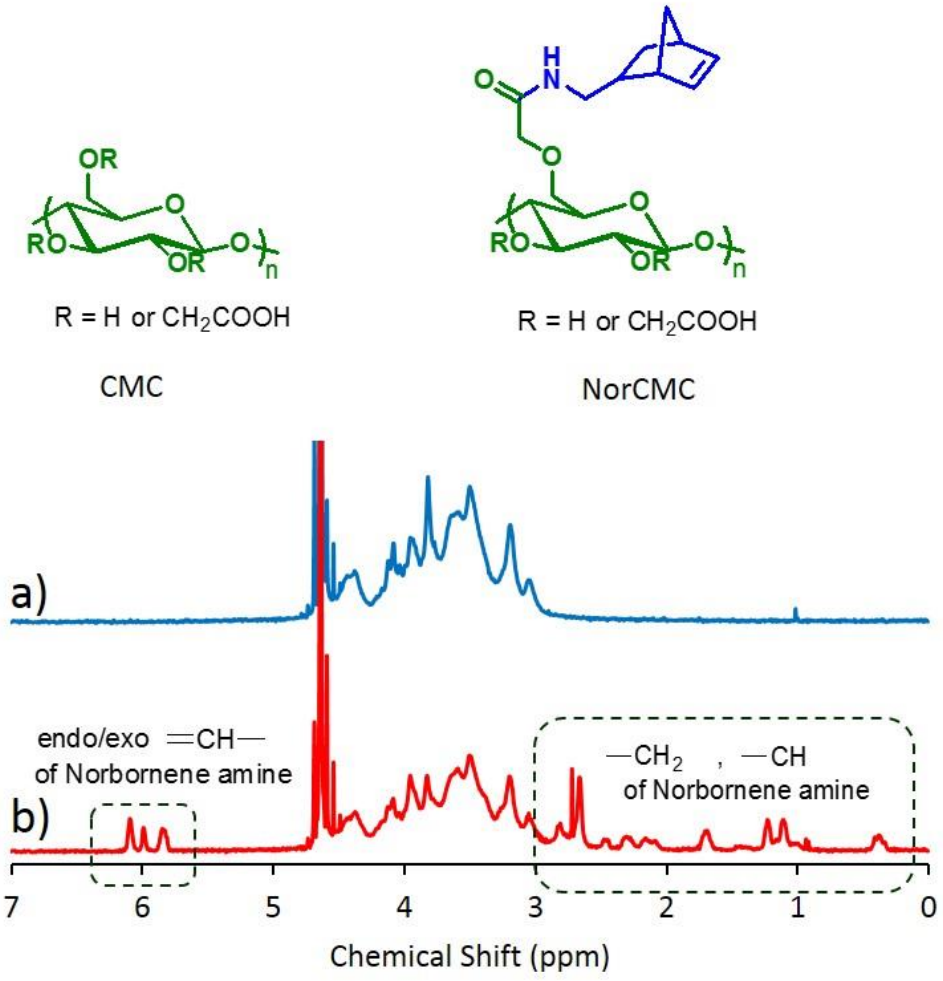

Figure 3.2. NMR spectra of CMC and NorCMC. Representative ^{1}H NMR spectra of (a) CMC and (b) NorCMC. Appearance of peaks at 6 ppm and in the range of 0.5- 3 ppm confirms that CMC was functionalized with norbornene amine.

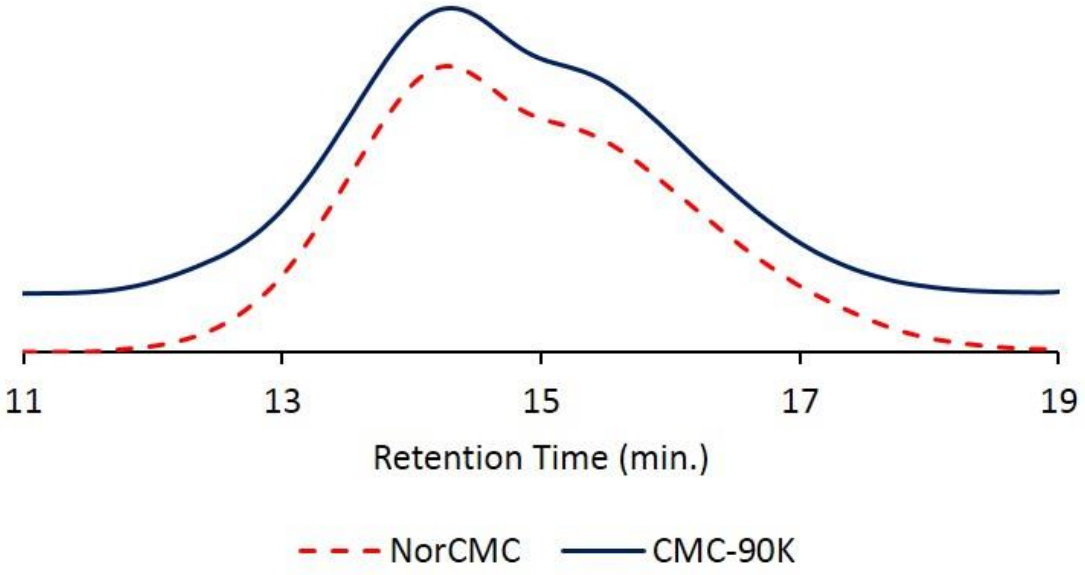

Figure 3.3. SEC elusion curves of CMC and NorCMC. SEC elugram curves for CMC-90K (solid) and NorCMC (dashed) indicating that functionalization reaction was not destructive to CMC. Đ= 3.22, M_n=42 kg/mol for CMC and Đ= 3.33, M_n=36 kg/mol for NorCMC. (Measurements were conducted against PEO standards).

Table 3.1. Functionalization parameters and degrees of functionality of CMC-90K with Norborneneamine (NA) via EDC coupling.

Sample	NaCMC	Mass NaCMC (mg)	Mole ratio to CMC RU			Mole ratio to EDC HCl			
			EDC HCl	NHS	NA	NHS	NA	Time (hr)	% funct.
1	90k	250	0.27	3.50	7.00	5.02	10.03	18	3.5
2	90k	250	0.70	0.70	0.70	1.00	1.01	18	9.0
3	90k	250	1.40	1.40	1.41	1.00	1.01	18	15.0
4	90k	4500	0.70	0.70	0.70	1.00	1.00	18	18.0

3.3.2. Fabrication of NorCMC hydrogels with tunable moduli

To fabricate NorCMC hydrogels, various amounts of NorCMC and dithiol cross-linker were mixed in phosphate buffered saline (PBS) with a UV-light sensitive radical initiator (I2959) (Figure 3.4). Irradiation of the mixture with UV-light (320-390 nm, 10 mW/cm^2) generated radicals from the I2959 to initiate the radical thiol-norbornene reaction. This particular UV wavelength and

radical initiator pair has been shown to be cytocompatible and has been used in gel formation and cell encapsulation previously.[8,9,64-67] In addition, this system enables forming testable materials with irradiation time as little as 12 s for some formulations. Since this method is light induced, cross-linking can be stopped simply by removing UV irradiation. This control is advantageous as moduli can be targeted and unreacted norbornene (NB) can be used for further functionalization or additional cross-linking. In addition to the duration of UV exposure, the mechanical properties of thiol-ene hydrogels can be tuned by varying the polymer weight percent (wt%), molar ratio of thiol to norbornene (T/NB), and cross-linker molecule.

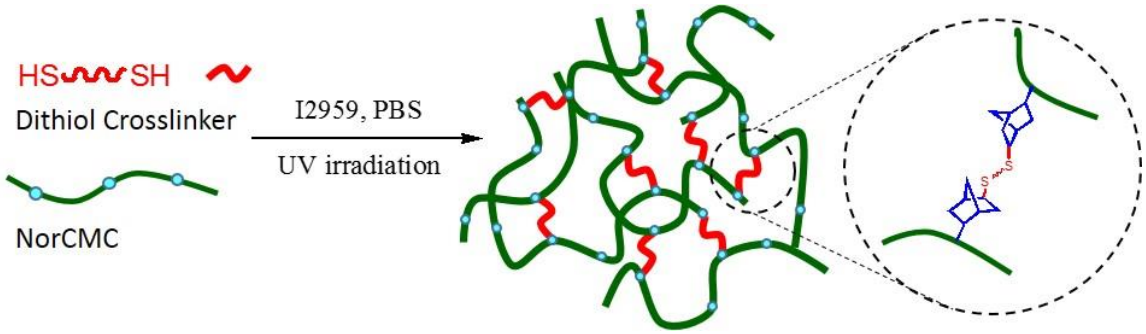

Figure 3.4. Schematic of a NorCMC hydrogel fabrication through light initiated thiol-norbornene reaction. The dithiol molecule covalently cross-links NorCMC chains.

Furthermore, the properties of cross-linker (stimuli responsiveness, enzymatic degradation, reactivity, etc.) can be imparted to the hydrogel by this cross-linking process.[62] In general, any molecule with at least two thiol groups could potentially be used to cross-link NorCMC. To investigate whether these thiol-norbornene hydrogel characteristics held true for the NorCMC hydrogels, a variety of dithiol cross-linkers with different lengths were explored (Figure 3.5).

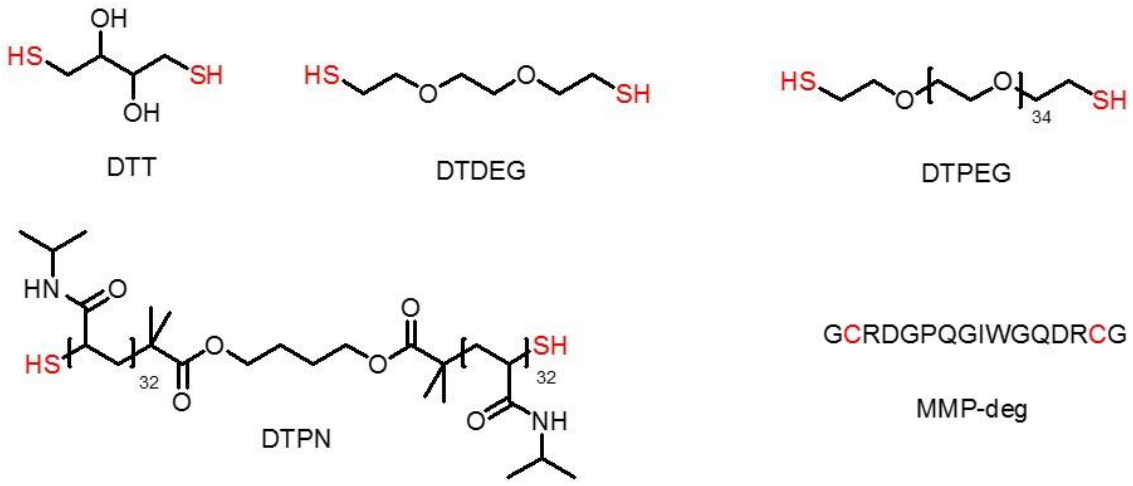

Figure 3.5. Various dithiol cross-linkers. The dithiol cross-linkers investigated to form NorCMC hydrogels. Dithiothreitol (DTT), 2,2'-(ethylenedioxy)diethanethiol (DTDEG), dithiol-terminated poly(ethylene glycol) (DTPEG), dithiol-terminated poly(N-isopropyl acrylamide) (DTPN), and a peptide with a matrix metalloproteinase (MMP) degradable sequence (MMP-deg) were used in this study to cross-link NorCMC.

The modulus of a hydrogel has an inverse relationship to the molecular weight between cross-links and as a result, controlling the formation and density of these cross-links can be used to target the stiffness of the hydrogel. To explore this behavior for NorCMC hydrogels, the UV irradiation time, polymer content, T/NB, and cross-linker type were varied one at a time while keeping all other parameters constant (Table 3.2).

Table 3.2. NorCMC hydrogels cros-linked with several dithiols at different conditions and their corresponding compression modulus.

Code	Cross-linker	Wt %[a]	T/NB[b]	Irradiation time (s)	E (kPa)[c]
NorCMC-DTT-12	DTT	4	0.5	12	16.0±5.1
NorCMC-DTT-15	DTT	4	0.5	15	26.9±4.2
NorCMC-DTT-25	DTT	4	0.5	25	32.8±4.4
NorCMC-DTT-30	DTT	4	0.5	30	30.3±3.1
NorCMC-DTT-60	DTT	4	0.5	60	36.4±8.0
NorCMC-DTT-120	DTT	4	0.5	120	42.2±5.9
NorCMC-DTT-0.1	DTT	4	0.1	60	5.3±3.1
NorCMC-DTT-0.3	DTT	4	0.3	60	12.6±3.4
NorCMC-DTT-0.7	DTT	4	0.7	60	76.9±13.4
NorCMC-DTT-1	DTT	4	1	60	103.0±14.4
NorCMC-DTT-1.2	DTT	4	1.2	60	40.3±2.4
NorCMC-DTT-1.5	DTT	4	1.5	60	32.3±2.7
NorCMC-DTT-2	DTT	2	0.5	60	11.2±3.1
NorCMC-DTT-3	DTT	3	0.5	60	20.1±1.7
NorCMC-DTT-5	DTT	5	0.5	60	66.0±6.8
NorCMC-DTT-6	DTT	6	0.5	60	89.2±15.5
NorCMC-MMP-deg	MMP-deg	4	0.5	60	7.8±1.2
NorCMC-DTDEG	DTDEG	4	0.5	60	29.0±9.8
NorCMC-DTPEG	DTPEG	4	0.5	60	9.0±4.6
NorCMC-DTPN-0.5	DTPN	4	0.5	60	4.7±1.2
NorCMC-DTPN-0.2	DTPN	4	0.2	60	1.7±0.9

[a] total polymer weight percent, [b] molar ratio of thiol to norbornene groups, and [c] compression modulus.

Using DTT as the cross-linker (T/NB=0.5 and 4 wt% polymer), stable hydrogels could be formed with a modulus of 16 kPa in just 12 s of UV irradiation as shown in Figure 3.6.a. Irradiation times less than 12 s failed to form a testable hydrogel under these conditions. Rheological study on norbornene functionalized gelatin (GelNB) hydrogel cross-linked by DTT through a light induced thiol-ene reaction done by Lin et al. showed a gel point at 12 s of irradiation which proves the fast nature of thiol-norbornene system.[59] However, in NorCMC-DTT 12 s of irradiation led to a dimensionally stable and mechanically testable hydrogel. The modulus could be tuned from 16 kPa to 32 kPa by irradiating the solutions for 25 s, demonstrating that varying the irradiation over this short window could be used to control the modulus of the hydrogels. After 25 s, the modulus appeared to plateau, suggesting that most of the DTT had reacted causing the modulus change as a function of irradiation time to become significantly slower. This observed behavior due to UV irradiation is consistent with other thiol-norbornene systems.[30]

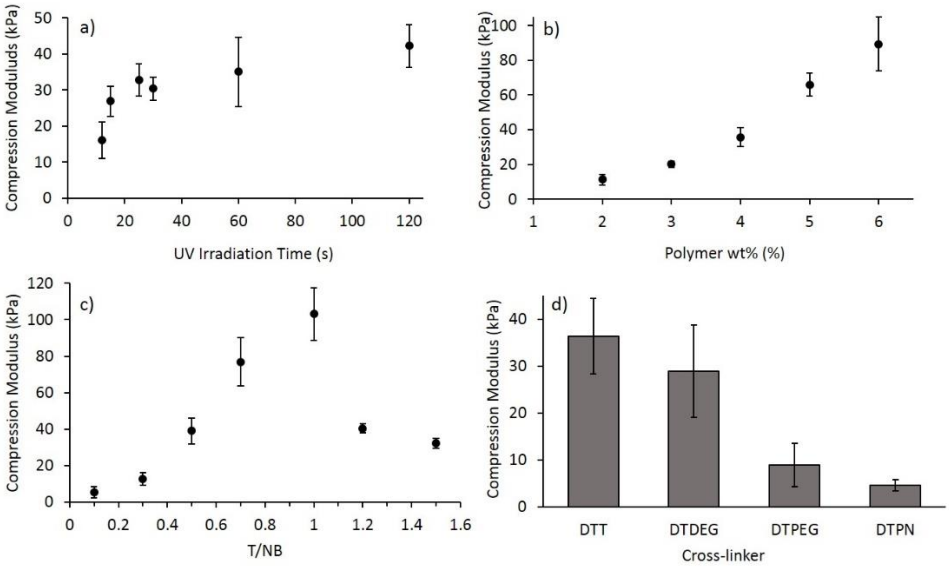

Figure 3.6. Compression modulus of NorCMC hydrogels. Compression modulus of NorCMC hydrogels as a function of (a) UV irradiation time (4 wt%, T/NB=0.5), (b) polymer weight percent (wt%) (T/NB=0.5, 60 s UV irradiation), (c) thiol to norbornene molar ratio (T/NB) (4 wt%, 60 s UV irradiation), and (d) cross-linker type (6 wt%, T/NB=0.5, 60 s UV irradiation), where the chemical

structures of the cross-linkers are given in Figure 2. Error bars represent standard deviations for measurements (n ≥9).

Figure 3.6.b shows the effect of polymer wt% on the modulus of the hydrogels where hydrogels with 2, 3, 4, 5, and 6 wt% were formed and studied (T/NB=0.5, 60 s UV irradiation, DTT cross-linker). The range of explored polymer wt% were limited to these values as stable hydrogels were not possible below 2 wt% and above 6 wt% the solution was too viscous to pipette. Increasing polymer content from 2 to 6 wt% led to an increase in compression modulus from 11 to 89 kPa. In a defined volume and when all the other parameters are kept constant, more polymer content provides more reactive sites available for cross-linking and thus a higher cross-link density. These results demonstrate that polymer wt% is another parameter that can straightforwardly be used to tune modulus and is in agreement with the results of previous study on GelNB-DTT hydrogels.[53] The most significant modulus change ranged from 5 to 103 kPa when the T/NB was varied from 0.1 to 1 (Figure 3.6.c). The more available thiols (higher T/NB) led to more cross-linking reactions and stiffer hydrogels. For T/NB ratios higher than 1, an expected modulus decrease was observed as the number of thiols exceeds the available NB groups and saturate the NB groups without forming effective cross-links.[30] This was demonstrated by calculating the concentration of cross-linker in final hydrogel volume and comparing it to the effective cross-link densities (Figure 3.7). Effective cross-link density was calculated using measured modulus and hydrogel volume after swelling and described previously in Chapter 2 Section 2.2.14. The measured moduli cover those of most soft tissues such as kidney and nucleus pulposus tissues (5-10 kPa), cardiac tissues (10-15 kPa), and muscle tissue (20-40 kPa), demonstrating that NorCMC hydrogels can mimic the stiffness of many soft tissues.[9,13,54,55]

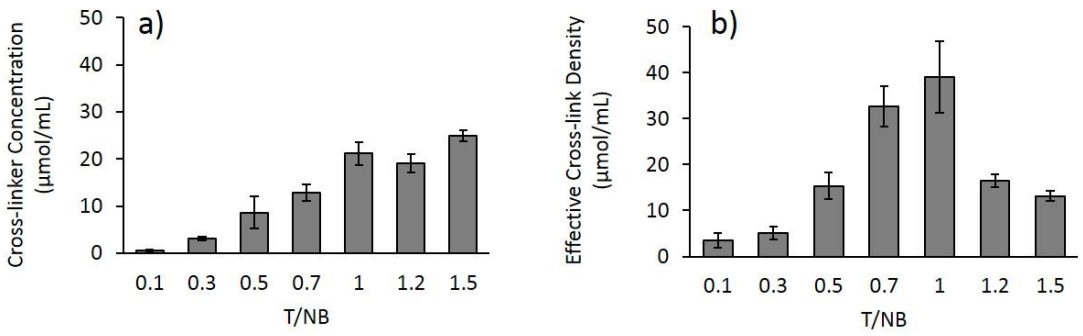

Figure 3.7. Cross-linker concentration and effective cross-link density with different T/NB. Error bars represent the tandard deviation for n≥5). a) Cross-linker density at hydrogel volumes after swelling for hydrogels with different T/NB (4 wt% total polymer, 60 s UV irradiation). b) Effective cross-link density calculated using obtained modulus values and hydrogel volumes after swelling for hydrogels with different T/NB (4 wt% total polymer, 60 s UV irradiation).

The modulus of hydrogels was also affected by the type of cross-linker used to form the hydrogel. In this study, four cross-linkers with different molecular weights (MW) were used: DTT (154 g/mol), DTDEG (182 g/mol), DTPEG (1500 g/mol), and DTPN (7000 g/mol). As shown in Figure 3.6.d, as the MW of the cross-linker increased, the compression modulus of the hydrogels decreased. By varying the cross-linkers at the same gelation conditions, moduli as high as 36.4 kPa could be achieved with DTT, while with DTPN a modulus of 4.7 kPa was obtained. In general, the stiffness of a hydrogel is inversely related to the MW between cross-links. At the same polymer content, if a cross-linker with high MW is used (DTPEG and DTPN), the MW of cross-linker adds in MW between cross-links and decreases the modulus. But the extent of modulus decrease is also dependent on the swelling of the hydrogel and concentration of cross-linker at the final hydrogel volume.it seems that a combination of different factors determines the stiffness of the material. As shown in Figure 3.8, lower cross-linker concentration in swelled hydrogel volume led to lower compression modulus and effective cross-link density.

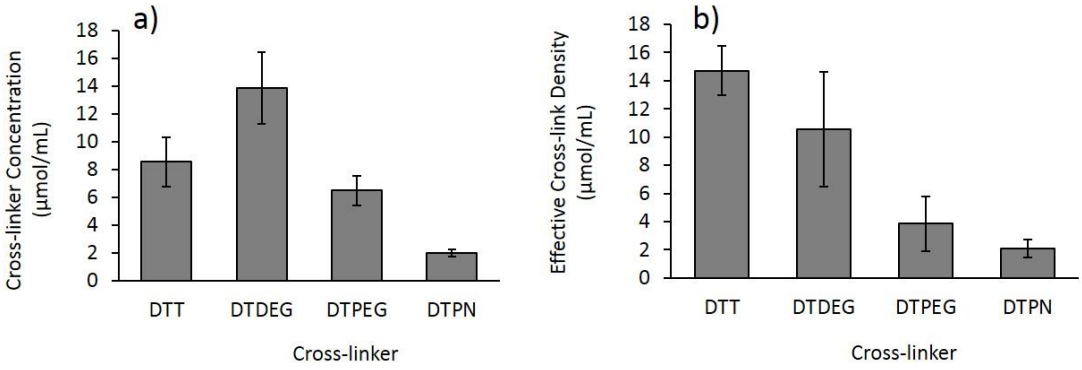

Figure 3.8. Cross-linker concentration and effective cross-link density with different cross-linkers. Error bars represent the tandard deviation for n≥5). a) Cross-linker density at hydrogel volumes after swelling for hydrogels with different cross-linkers (T/NB=0.5, 60 s UV irradiation). b) Effective cross-link density calculated using obtained modulus values and hydrogel volumes after swelling for hydrogels with different cross-linkers (T/NB=0.5, 60 s UV irradiation).

When long polymer chains were used as cross-linkers, to keep the total polymer content (4 wt%) and T/NB (0.5) constant, the NorCMC content would be less compared to when DTT and DTDEG are used. That also decreases the number of cross-links in a defined volume. Although the moles of DTT and DTDEG are the same, the cross-link density of NorCMC-DTDEG hydrogels are higher due to lower volume of hydrogel after swelling. Based on the obtained modulus and calculated cross-link densities, the stiffness of NorCMC hydrogels would be affected by several factors such as MW of the cross-linker, the extent of swelling, and the polymer content. In total, all the hydrogel fabrication parameters explored yielded moduli that spanned two orders of magnitude (2 – 103 kPa) while using the same NorCMC. This range of compression modulus is comparable with NorHA hydrogels that was reported previously.[62] This highly selectable nature of the modulus for NorCMC hydrogels can be used to target the wide range of soft tissue stiffness.

3.3.3. Fabricating thermo-responsive hydrogels

NorCMC was cross-linked with PNIPAM to create thermoresponsive hydrogels and demonstrate that stimuli response can be introduced through cross-linker selection. PNIPAM has

a lower critical solution temperature (LCST) around 32 °C above which the PNIPAM becomes insoluble in water and aggregating in the hydrated medium of a hydrogel (Figure 3.9.a).[28,97,80,133] This collapse into aggregates results in expulsion of the water content of the hydrogel.[134] Thermoresponsive NorCMC hydrogels were generated using a dithiol end-functionalized PNIPAM (DTPN, Figure 3.5) cross-linker with a M_n of 7000 g/mol (58 repeat units). This molecular weight of DTPN was chosen to ensure that the NorCMC is the major component of the hydrogel. Lower molecular weight DTPN may suffer from lower water solubility or low thermoresponsiveness at smaller T/NB. Unlike previous studies where chemical cross-linking of PNIPAM with an external cross-linker molecule have been applied, here PNIPAM itself was used as a dithiol molecule to cross-link NorCMC polymer chains to form gels that reduces the hazard of external cross-linkers. In addition, compare to physically gelled PNIPAM through temperature dependent self-assembly mechanisms, these chemically cross-linked hydrogels are stable at all temperatures. These NorCMC-PNIPAM hydrogels preserve their shape and cross-link density and only undergo reversible isotropic volume change in response to change in temperature. This method permits forming hydrogels with different thermoresponsiveness and mechanical properties without changing the length of PNIPAM or the number of functional groups on matrix (NorCMC). Moreover, this process allows to photopattern the thermoresponsiveness using a photomask that is discussed later in this paper. To demonstrate the tenability of this system, two formulations of hydrogels were synthesized with different T/NB (T/NB=0.2 and 0.5) at the same total polymer content of 6 wt% after 60 s of UV irradiation (10 mW/cm^2 and 0.05 wt% I2959). To measure the thermoresponse, the percent of hydrogel mass (water) lost upon heating relative to 4 °C (ML) was measured at 37 and 55 °C for the two formulations (Figure 3.9.b). ML values at 37 °C for T/NB of 0.2 and 0.5 were 10.8 and 39.6%, respectively, and significantly different (α= 0.05), confirming

that DTPN content can control the thermoresponse in NorCMC in a manner similar to previous work with norbornene functionalized hyaluronic acid as discussed in Chapter 2.

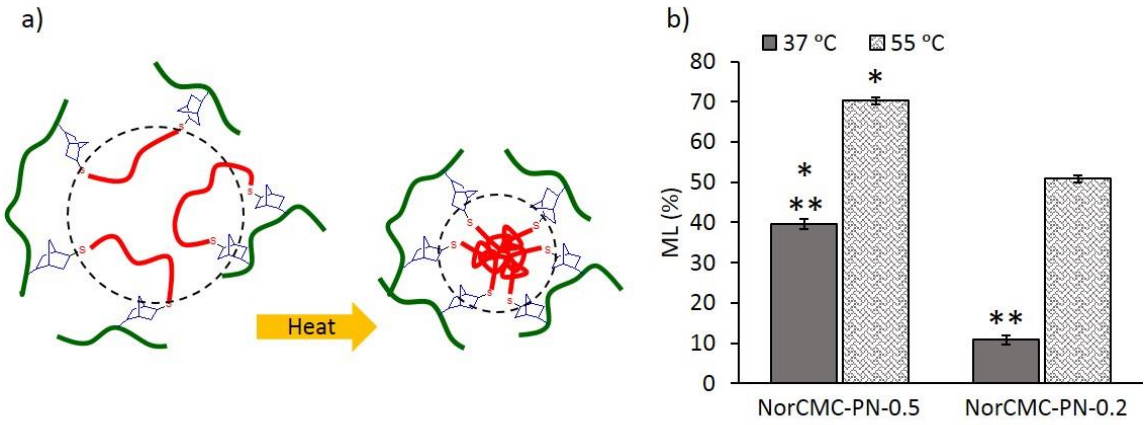

Figure 3.9. Thermoresponsivity of NorCMC/DTPN hydrogels. a) Schematic of a hydrogel cross-linked with DTPN below the LCST of PNIPAM (left) and the collapse of PNIPAM into globules at temperatures above the LCST (right), causing contraction of the hydrogel mesh. b) NorCMC/DTPN hydrogel mass loss upon heating (ML) at 37 and 55 °C for NorCMC-DTPN-0.5 (solid, T/NB=0.5, 6 wt%, 60 s) and NorCMC-DTPN-0.2 (crosshatched, T/NB=0.2, 6 wt%, 60 s) hydrogels. Error bars represent one standard deviation (n = 5). ** denotes a significant difference (α= 0.05) between values for different T/NB at the same temperature (37 °C) and * denotes a significant difference (α= 0.05) between values for the same T/NB but at different temperatures.

Previous work with hyaluronic acid hydrogels made with these DTPN cross-linkers has demonstrated that the degree of thermoresponse was a function of temperature (Chapter 2). Similar results were observed for the NorCMC/DTPN hydrogels when heated to 55 °C as indicated by significant ML increase as compared the values at 37 °C (Figure 3.9.b, marked by *). The ML as a function of temperature is likely due to the DTPN cross-linkers having a broad LCST.[135] Additionally, the thermoresponse was reversible as cooling the hydrogels back to 4 °C in PBS caused solution uptake and decreased ML (Figure 3.10). Some hysteresis was evident in this experiment, indicating that some permanent deformation or degradation may have occurred upon heating.

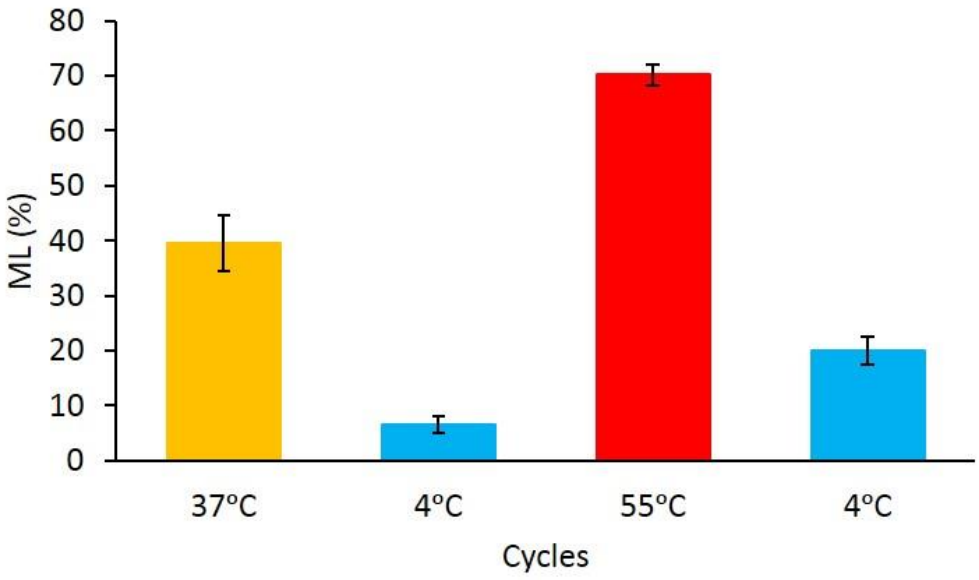

Figure 3.10. Mass loss percentage of NorCMC/DTPN hydrogels. Percent mass loss (ML) of NorCMC/DTPN (6 wt% polymer, T/NB=0.5, 60 s UV irradiation, DTPN = 7000 g/mol) hydrogels at different temperatures. Error bars represent standard deviations (n=5).

Interestingly, as shown in Figure 3.11, NorCMC/DTT hydrogels demonstrated some thermoresponse when heated, but to a significantly lesser extent as compared to the NorCMC/DTPN hydrogels, confirming that DTPN inclusion gives the significant stimuli response. The exact cause of the minor NorCMC/DTT thermoresponse is not clear, but some functionalized celluloses are known the exhibit LCST behavior so the norbornene functionality may contribute to this behavior.[136] Since stimuli response can be controlled by selecting an appropriate cross-linker, these NorCMC materials with DTPN cross-linkers could be used for drug delivery applications.[32,33,41,44]

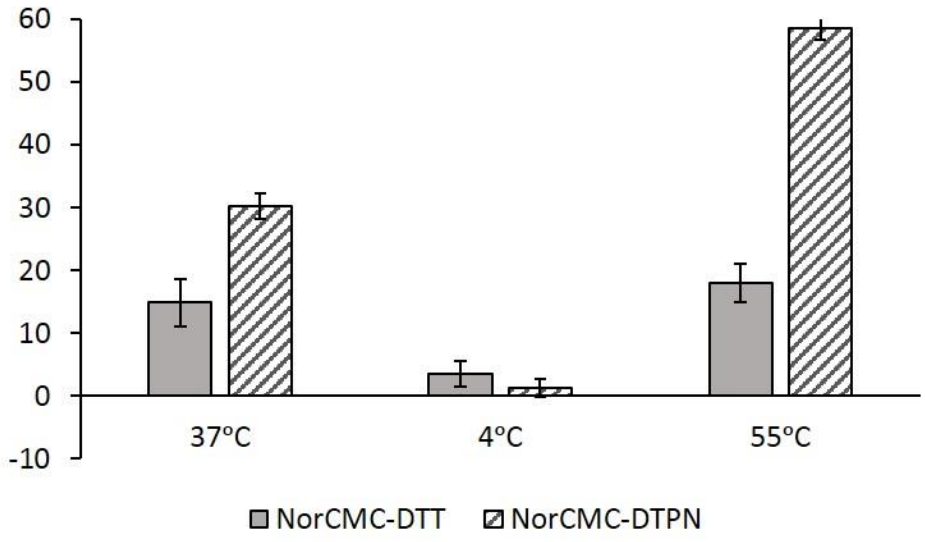

Figure 3.11. Mass loss (ML) percentage upon heat/cool cycles of NorCMC/DTT and NorCMC/DTPN hydrogels (4 wt% polymer, T/NB=0.5, 60 s UV irradiation). Error bars represent standard deviations (n≥ 4).

3.3.4. Spatiotemporal modification of hydrogels

The spatial modification of NorCMC hydrogels was investigated by photopatterning thin (2D) hydrogels with a thiol-terminated fluorescent dye. The 2D hydrogels were made by 90 s of UV irradiation on a solution of NorCMC (4 wt%), DTT cross-linker (T/NB=0.5), and I2959 (0.05 wt%) in PBS to cross-link and attach it to a thiol-coated coverslip. Since the formulation had a T/NB of 0.5, unreacted NB groups remained after gelation and were available for further functionalization with thiol-terminated rhodamine B (Figure 3.12.a). The 2D hydrogels were incubated with a solution of 1 mg/mL of this rhodamine B-peptide and 0.05 wt % radical initiator (I2959) in PBS. After 24 hours at 4 °C, the hydrogels were exposed to UV light for 60 s while covered with a photomask with alternating 200 µm stripes. Unreacted dye (rhodamine B-peptide) was washed out prior to fluorescence imaging by incubating for 24 h at 37 °C in 1 mL of PBS. Patterned red stripes in the fluorescence images (Figure 3.12.b) demonstrated that NorCMC could be photopatterned using a method similar to previous studies.[71] The widths of the stripes were measured using ImageJ

software (192 ± 8 µm for the black stripes and 202 ± 8 µm for the red stripes) and were similar to the photomask stripes (200 µm), demonstrating the precision of the photopatterning process.

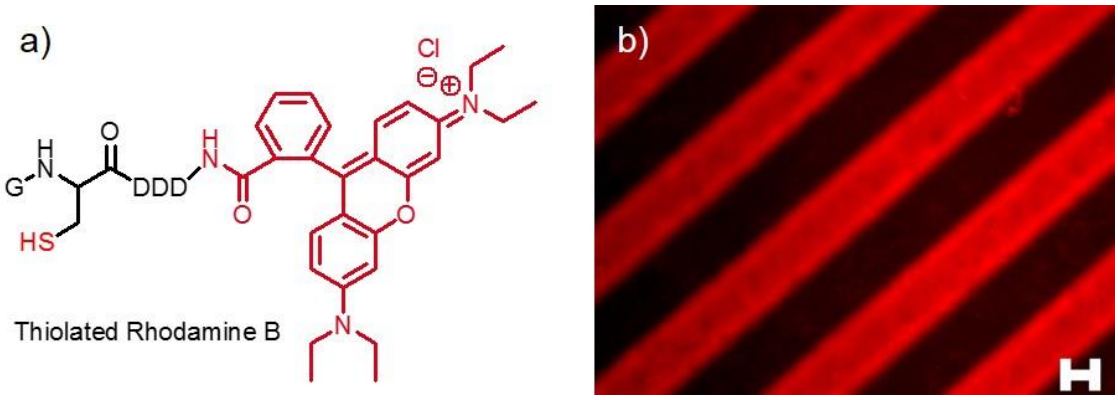

Figure 3.12. Spatiotemporal modification of 2D NorCMC hydrogels. Spatiotemporal modification of 2D NorCMC hydrogels through a light induced thiol-norbornene reaction to photopattern small molecules and additional cross-links. a) The chemical structure of the thiol-terminated rhodamine B dye (peptide with the sequence GCDDD-rhodamine B) and b) a representative fluorescence image (Zeiss.Axio Observer.Z1 microscope at 5X magnification) of a 2D NorCMC/DTT hydrogel (4 wt%, T/NB=0.5, 90 s UV irradiation) photopatterned (200 µm line photomask) with the rhodamine B peptide. Scale bars represent 100 µm.

The spatiotemporal patterning of stimuli response was investigated by patterning DTPN into a NorCMC hydrogel cross-linked with DTPEG (4 wt% polymer, T/NB=0.3, 60 s UV irradiation). A representative optical image of the 3D NorCMC/DTPEG hydrogel surface (Figure 3.13.a) demonstrates the smooth surface of the original hydrogel. Since the NorCMC/DTPEG hydrogel was synthesized with NB groups remaining, DTPN and radical initiator (8.5 mg/mL of DTPN and 0.05 wt% I2959) were introduced to it and photopatterned only in regions that were exposed to UV light through a 200 µm striped photomask. Figure 3.13.b and 3.13.c shows a representative image of the patterned hydrogels at 4 °C (below the LCST of PNIPAM). The DTPN regions appear as depressions in the hydrogel surface due to the increased level of cross-linking.

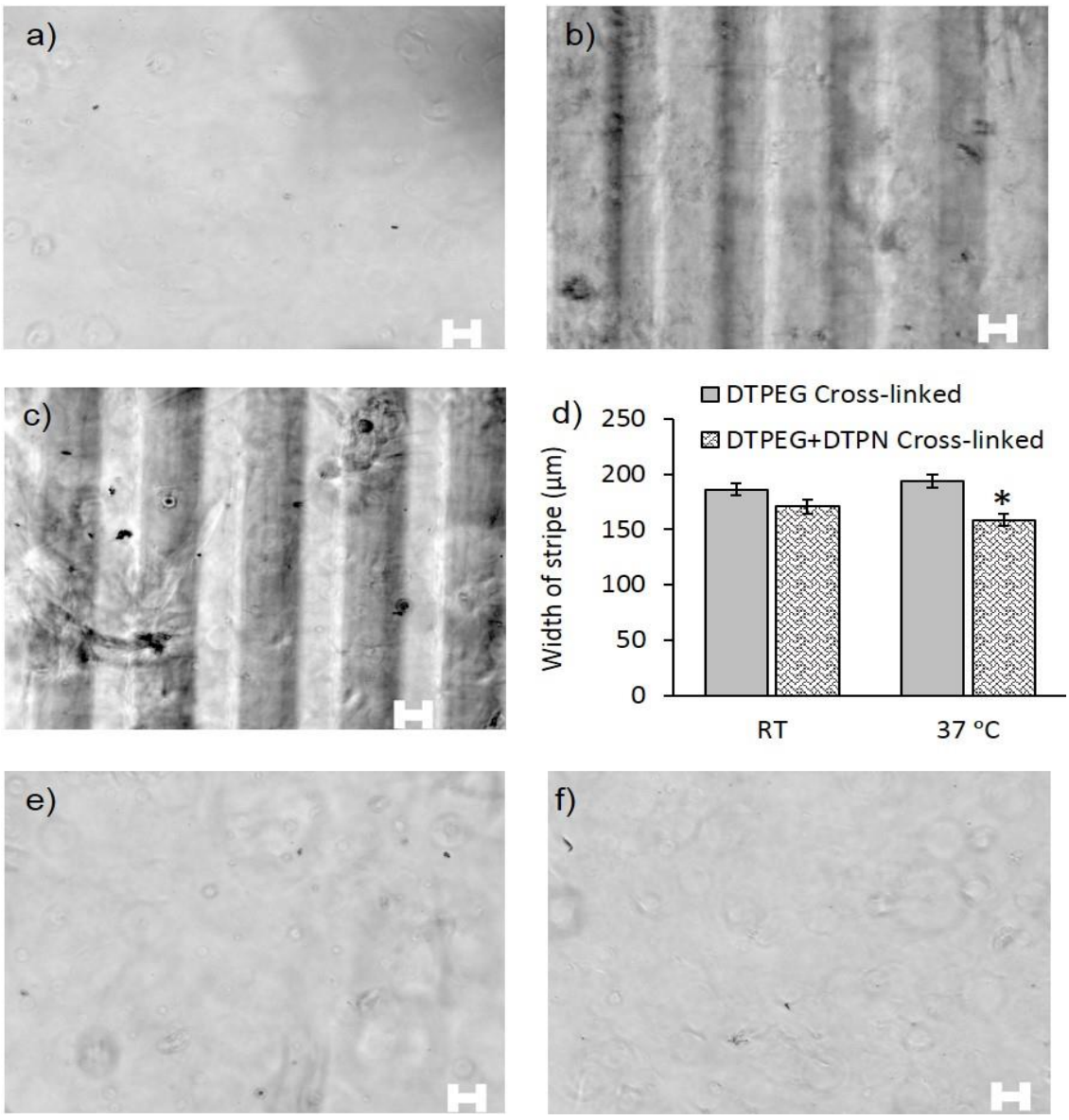

Figure 3.13. Spatiotemporal modification of 3D NorCMC hydrogels. Spatiotemporal modification of 3D NorCMC hydrogels through a light induced thiol-norbornene reaction to photopattern polymers and additional cross-links. Representative optical images (Zeiss.Axio Observer.Z1 microscope at 5X magnification) of a) an unpatterned 3D NorCMC/DTPEG hydrogel (4 wt%, T/NB=0.3, 60 s UV irradiation), b) a DTPN patterned NorCMC/DTPEG hydrogel at 4 °C, and c) a DTPN patterned NorCMC/DTPEG hydrogel at 37 °C and d) a graph that shows the difference between the width of DTPEG cross-linked regions and DTPEG/DTPN cross-linked stripes (distance between alternating stripes) measured by ImageJ software at room temperature (RT) and at 37 °C are shown. The statistically significant ($\alpha = 0.05$) decreased width of PNIPAM patterned stripe (marked by *) upon heating confirms addition of thermoresponsiveness to the hydrogel via photopatterning. Optical images (Zeiss.Axio Observer.Z1, 10X magnification) of NorCMC/DTPEG hydrogel surface. e) Surface of another initial NorCMC/DTPEG hydrogel, and f) surface of the same hydrogel after 5 minutes UV irradiation through a striped photomask with 0.05 wt% I2959 present after incubation for 24 h are shown as the control experiment. Scale bars represent 100 µm.

Measurements of the line widths (Figure 3.13.d) for the DTPEG only cross-linked regions indicate that stripe width is nearly the width of stripes of the photomask (200 μm), while DTPN cross-linked regions are significantly narrower due to the increased cross-linking and therefore reduced swelling. Upon heating above the LCST (37 °C), the DTPN cross-linked stripes significantly shrunk (Figure 3.13.c and 3.13.d) due to the phase transition of PNIPAM. As a control experiment, NorCMC/DTPEG hydrogels were incubated at 4 °C in a solution of I2959 (0.05 wt%) in PBS for 24 hours and then exposed to UV light for 5 minutes while covered with the photomask. Optical images of the resulting hydrogels do not show any patterns (Figure 3.13.e and 3.13.f), confirming that these patterns appear because of additional cross-linking with DTPN.

This thermoresponse demonstrates that stimuli response can be spatiotemporally patterned into NorCMC hydrogels, which could be used in future applications to change surface topology, direct drug delivery, and affect cell behavior. This experiment was a demonstration of the ability of the NorCMC to be photopatterned by a variety of thiol functionalized molecules including peptides, or dithiol cross-linkers including stimuli responsive polymers. Specific experiments can be designed to investigate the applications of this system in cell related studies.

3.3.5. Encapsulation of hMSC into NorCMC hydrogels

As NorCMC was introduced as a potential biomaterial, the cytocompatibility of the NorCMC hydrogels was investigated with several different cross-linkers. The viability of hMSCs encapsulated in NorCMC/DTT and NorCMC/MMP-deg hydrogels (4 wt%, T/NB=0.5, 60 s UV irradiation) was studied over 21 days. The cysteine-functionalized cell adhesion peptide GCGYGRGDSPG (RGD) was included in another set of hydrogels with the same cross-linkers to examine whether it affected the viability. Live/Dead staining of the hMSCs for all hydrogel formulations showed a high level of cytocompatibility of these materials with and without RGD

(Figure 3.14). At day 3 of cell culture, almost 100% of the hMSCs survived and after 21 days still 93% and 85% of cells were alive in NorCMC/DTT and NorCMC/MMP-deg hydrogels, respectively.

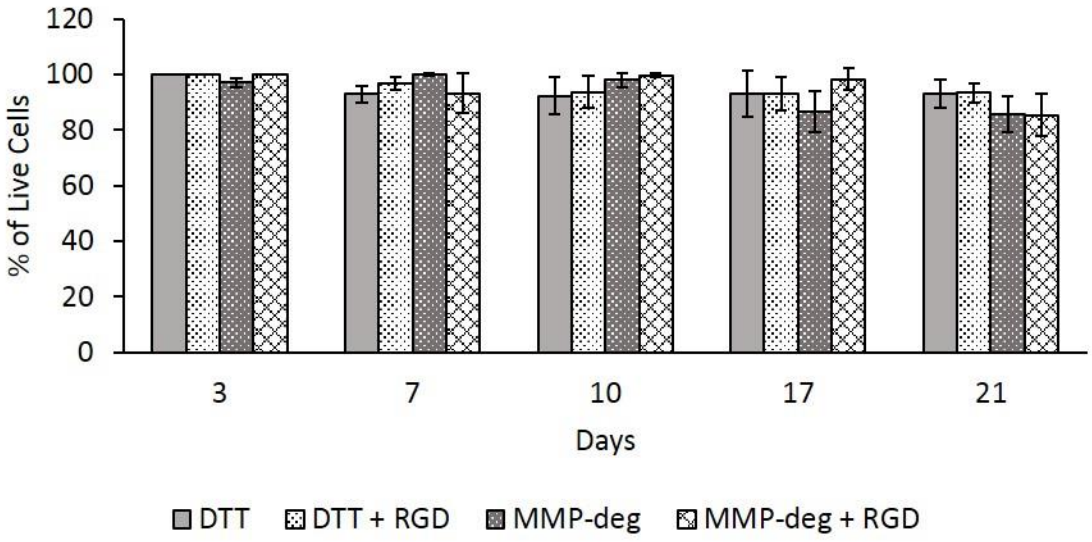

Figure 3.14. Viability of hMSCs in NorCMC/DTT and NorCMC/MMP-deg hydrogels over 21 d of incubation. All hydrogel formulations had higher than 85% viability after 21 days of culture. To generate these data, ImageJ software was used to count live (stained green) and dead (stained red) cells from fluorescence images and the percentage of live cells to total cells was reported as viability. Error bars represent standard deviations (n≥9).

In another study, NorCMC hydrogels that were cross-linked with DTPN had 73% hMSC viability at day 7 of encapsulation as shown in Figure 3.15. The lower viability in the NorCMC/DTPN hydrogels may be due to the coil collapse of the DTPN tightening the polymer network so that nutrients cannot easily reach the hMSCs. Overall, the high hMSC viabilities observed over several weeks confirm that the NorCMC matrix and encapsulation procedure are biocompatible.

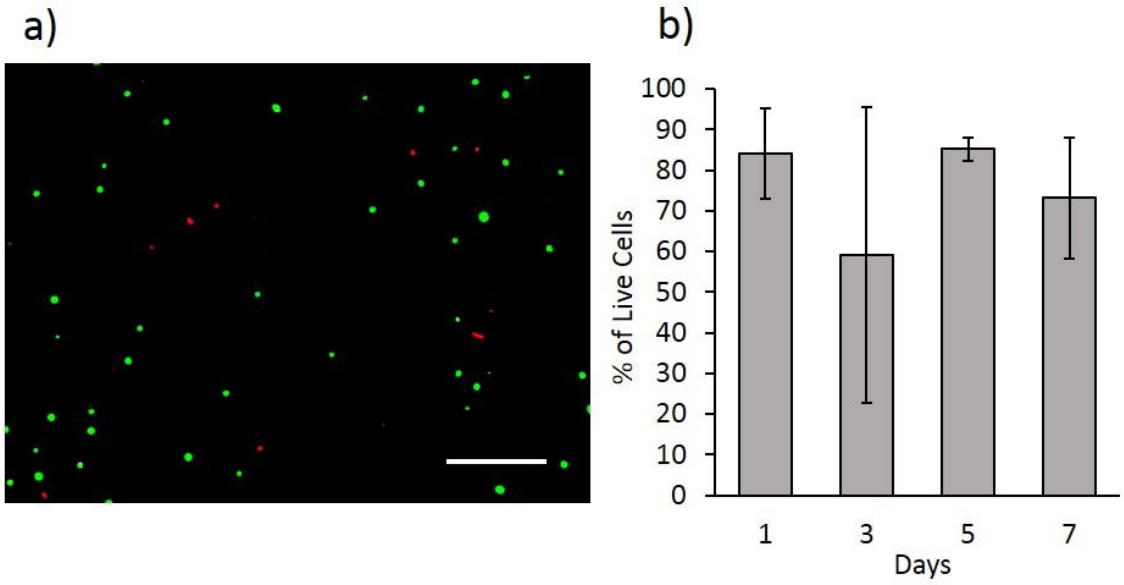

Figure 3.15. Cytotoxicity of NorCMC hydrogels cross-linked with DTPN. a) Fluorescence imaging (5x magnification) of hMSCs encapsulated in NorCMC/DTPN hydrogel (6 wt%, T/NB= 0.5, 60 sec. UV irradiation, DTPN with 64 repeat units) at day 7 (Scale bar represents 200µm). b) Live/dead cell counts at days 1, 3, 5, and 7 after encapsulation based on fluorescence images and using ImageJ software. The graph shows 85% viability at day 1 and 75% at day 7 suggesting that the DTPN cross-linker is relatively cytocompatible despite its thermoresponsivity and hydrophobicity at 37 °C. Error bars represent standard deviations (n=3).

To further demonstrate the utility of these hydrogels as extracellular matrix mimics, spreading and remodeling were investigated with hMSCs in NorCMC hydrogels cross-linked by a non-degradable (DTT) and an enzymatically degradable (MMP-deg) cross-linkers over 21 days. Fluorescence microscopy analysis of the hMSCs (Figure 3.16) indicated that the cross-linkers affected cell behavior. Aspect ratio measurements of the hMSCs at Day 3, 7, 10, 17, and 21 of encapsulation (Figure 3.17) show that hMSCs cells preserved their round shape in the non-degradable (DTT cross-linked) hydrogel as approximately 40% of the hMSCs had an aspect ratio of 1-1.2. When the MMP-deg cross-linker was used, hMSCs could cleave the peptide and remodel their environment to spread, yielding aspect ratios greater than 2 for more than 60% of the cells after 10 days and increased at days 17 and 21 with longer incubation times.[138] Although in MMP-degradable hydrogels the cell spreading changes in response to matrix moduli, but it has been

shown that in non-degradable 3D hydrogels, mMSC morphology is not affected by the matrix mechanical properties and spherical shape is preserved regardless to cell fate .[138] This suggest that for cell spreading, degradability of the matrix is essential. It must be mentioned that this fact is in contrast with findings in 2D hydrogels where cell morphology and fate is determined by the substrate stiffness.[138]

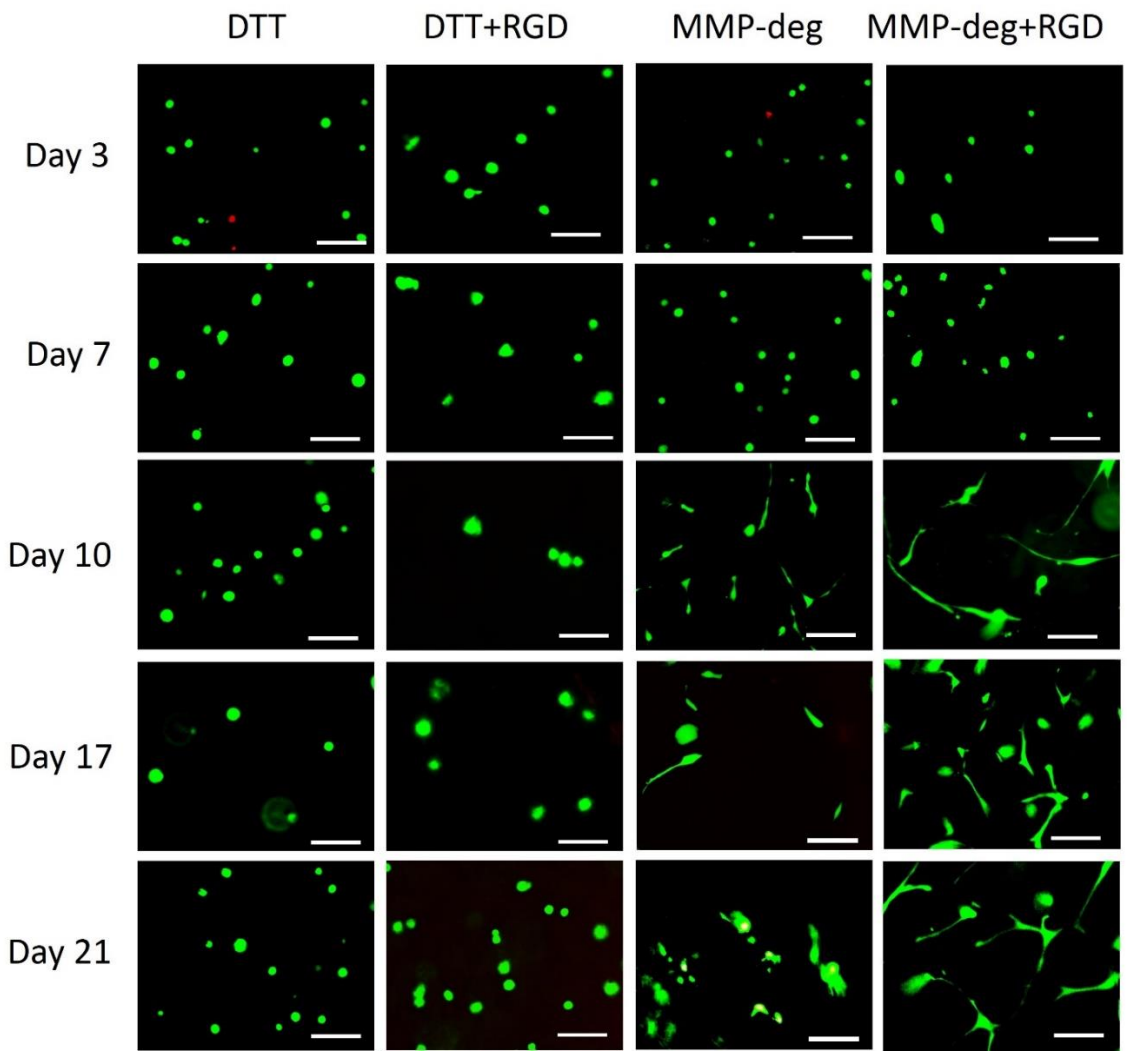

Figure 3.16. Representative fluorescence microscopy images of hMSCs encapsulated in NorCMC hydrogels cross-linked by DTT or MMP-deg and with or without RGD peptide over 21 days (Zeiss.Axio Observer.Z1, 5X magnification). The small number of cells in some pictures could be a result of uneven mixing and cell suspension in the pre-gelation solution (Scale bars represent 100µm).

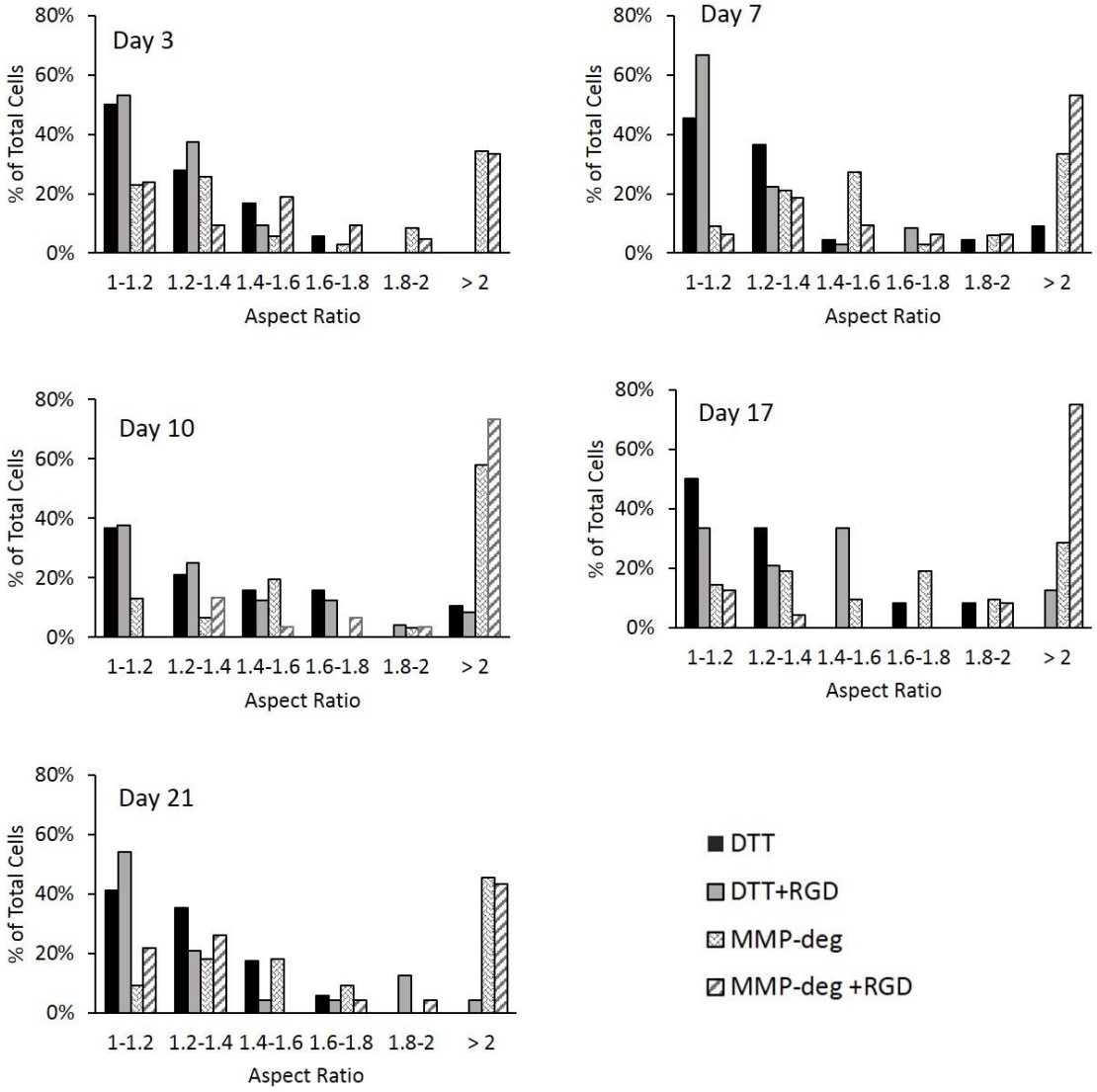

Figure 3.17. Aspect ratio histogram of hMSC Culture in 3D NorCMC Hydrogels at days 3, 7, 10, 17, and 21 of hMSC culture.

Interestingly, the average aspect ratio of the MMP-deg+RGD formulation (Figure 3.18) gave a decreasing trend after day 10, suggesting that the cell spreading and cell behavior may have begun a different phase. With the hMSCs able to remodel their microenvironment and the

demonstrated spatiotemporal control over physical and chemical properties, these NorCMC hydrogels should be viable materials for biomaterials and cell differentiation experiments.

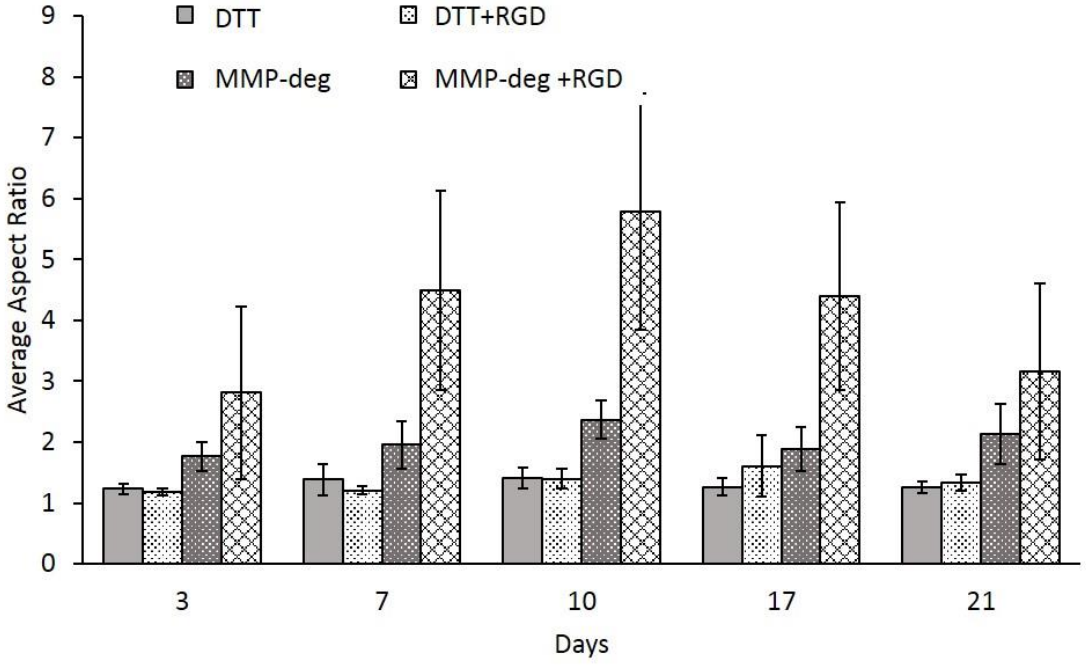

Figure 3.18. The average of aspect ratios over 3 weeks. The average of aspect ratios over 3 weeks of hMSC culture in NorCMC 3D hydrogels cross-linked with different cross-linkers with/without RGD adhesion peptide. Error bars represent standard deviations (n≥9).

Native cellular adhesion to NorCMC hydrogels without the RGD cell adhesion peptide was also investigated. In one experiment, hMSCs were cultured on 2D NorCMC/DTT hydrogels with and without RGD included in the formulation. In both formulations, fluorescence microscopy images (Figure 3.19) indicated that hMSCs adhered to the surface regardless of RGD content and no discernable difference in cell structure was observed.

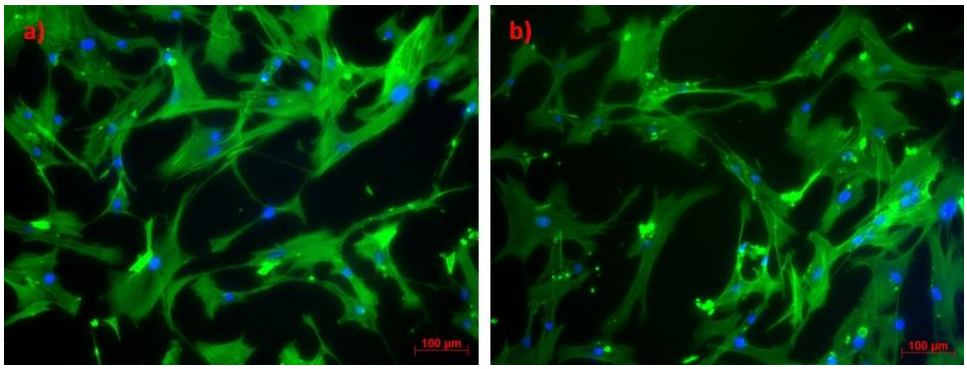

Figure 3.19. Fluorescence images (Zeiss.Axio Observer.Z1, 10X magnification) of hMSCs on the surface of 2D NorCMC/DTT hydrogels obtained at day 3 of incubation. Representative images are of a) a hydrogel that contains RGD adhesion peptide and b) a hydrogel without RGD adhesion peptide. Cell adhesion and spreading were observed on both hydrogel surfaces, suggesting that NorCMC/DTT hydrogels have cell adhesion properties in the absence of RGD.

In the 3D hydrogels, cell spreading was observed with the MMP degradable cross-linkers without RGD present (Figure 3.16) to a lesser extent as compared to the hydrogel with RGD (Figure 3.18), indicating that RGD is not necessarily required for spreading, but that RGD does help promote it. Similar observations have been reported by Mahoney and Anseth in 3D PEG-based hydrogels where a neural tissue had been grown in the hydrogel.[47] After 16 days of encapsulation, they observed fibronectin production, suggesting that in the absence of RGD, cells can produce fibronectin to adhere to their culture medium. For hMSCs to spread in 3D hydrogels, in addition to the protease degradability, cell adhesion (e.g. through an integrin-RGD binding) is also required.[59,139] In the present study, hMSCs can spread in just 3 days after encapsulation without RGD in NorCMC hydrogels suggesting that RGD-bearing proteins such as fibronectin and vitronectin may be produced by the hMSCs to promote cell adhesion; however, further experiments are needed to investigate this observation.

3.4. Conclusion

CMC was successfully functionalized with norbornene groups via an EDC coupling reaction to create NorCMC. A light induced thiol-norbornene reaction was used to cross-link NorCMC with dithiol molecules to fabricate hydrogels with highly tunable compression moduli ranging from 2 to 103 kPa. The hydrogel modulus could be controlled by varying the UV irradiation time, T/NB, polymer wt%, and cross-linker. Temperature-responsive hydrogels could be created by using DTPN as the cross-linker and this stimuli response could be spatiotemporally introduced into the hydrogel through photopatterning. Both 2D hydrogels and 3D hydrogels could be patterned with molecules through this strategy. In addition, hMSCs could be encapsulated in and on hydrogels with and without RGD adhesion peptide while retaining high cell viability. By selecting a MMP degradable cross-linker, hMSCs could remodel their microenvironment and significantly spread, further demonstrating that NorCMC as a promising versatile biomaterial for a variety of biomedical applications.

CHAPTER 4

FUNCTIONALIZATION AND CHEMICAL GELATION OF CELLULOSE NANOFIBRILS (CNF) VIA THIOL-NORBORNENE REACTION

4.1. Introduction

CNF hydrogels have been reported previously as scaffolds for tissue engineering because their fibrillar structure mimics the fibrous components of the extracellular matrix (ECM). Physically cross-linked CNF hydrogels lack stability and mechanical strength. Therefore, covalent cross-linking is need to provide the required stiffness and stability to the hydrogel. Current methods to covalently cross-link CNF suffer from either low cell viability or long gelation time. Also, these methods do not allow for spatiotemporal modification of the scaffold. Regarding these issues, CNF was functionalized with norbornene groups (nCNF) followed by thiol-norbornene cross-linking reaction to form hydrogels with controllable mechanical properties. Chemically cross-linked nCNF hydrogels were dimensionally stable in aqueous media for months without falling apart. Rheological studies on CNF hydrogels was conducted showed the shear-thinning behavior of CNF after functionalization and chemical gelation. The viability of stem cells in CNF-based hydrogels were also studied to show the potential applications of these materials in biomedical studies.

4.2. Experimental

4.2.1. Materials

Cellulose nanofibrils (CNFs) were produced at the University of Maine Process Development Center from softwood bleached kraft pulp as an aqueous dispersion with 3 wt% solid content. To determine the average diameter of cellulose fibers, diluted CNFs (0.04 wt% in deionized water) were first evaporated on a copper grid. Then uranyl acetate was used as a negative dye and images of the grid sample were collected using transmission electron microscopy (TEM) (CM10, Philips) and the Gatan microscopy software (v2.31). ImageJ software was used to measure the diameter of fibers which was determined to be 124±25 nm in average. 5-norbornene-2,3-dicarboxylic anhydride (NB) was purchased from TCI. 2-Hydroxy-4'-(2-hydroxyethoxy)-2-methylpropiophenone (I2959), 2,2'-(ethylenedioxy)diethanethiol (DEG), poly(ethylene glycol)dithiol M_n=1500 g/mol (DTPEG 1.5k), poly(ethylene glycol)dithiol M_n=3400 g/mol (DTPEG 3k), and N,N,N',N'-tetramethylethylenediamine (TEMED) were purchased from Sigma-Aldrich. Ammonium persulfate (APS) was purchased from Acros Organics. Cellulase (recombinant hydrolase enzymes) from Tricoderma Reesei was purchased from Sigma-Aldrich in aqueous solution form with $\geq$700 units/g activity and 1.10-1.30 g/mL density. All other reagent were purchase from Fisher Scientific and used without further purification.

4.2.2. Synthesis of norbornene functionalized CNF (nCNF)

In a representative synthesis, 33 g of 3 wt% CNF (6 mmol of anhydroglucose repeat units) was dispersed in 67 mL of deionized water to obtain 1 wt% CNF dispersion. To this dispersion, 19.73 g of 5-norbornene-2,3-dicarboxylic anhydride (120 mmol, 20 molar excess to anhydroglucose repeat units) was added which caused the pH to drop to 4. Sodium hydroxide (NaOH) 10 M solution was added dropwise in 10 second intervals to bring up to and keep the pH between 9.5-

10.5 throughout the reaction. The pH decrease slowed down as reaction completed and stopped after 2.5 hours. The product was washed with DI water five times via centrifugation at 7000 rpm for 15 minutes using a SORVALL RC-6 PLUS centrifuge (Thermo Electron Corporation) with a SLA-1500 rotor. The final product, norbornene functionalized CNF (nCNF), was at 2.7 wt% after the fifth wash. This synthesis was repeated varying the concentration of 5-norbornene-2,3-dicarboxylic anhydride (0.13, 0.3, 0.6, and 1.2 M) to obtain nCNF with several degrees of functionalization. Infrared (IR) Spectroscopy (PerkinElmer UATR Two, Diamond/ZnSe crystal, KBr windows, $LiTaO_3$ detector) was used to prove the presence of norbornene (NB) functional groups on CNF and obtain the relative functionalization degree. The relative functionalization degree refers to the ratio of the area under the three bands of the functional group (Figure 4.1, blue) to the area under backbone C-O stretch band (Figure 4.1, red) from the IR absorbance spectrum. The red area is constant for all nCNF samples that are made from the same CNF because it corresponds to the backbone C-O stretch. The blue area varies by changing the number of norbornene groups present on nCNF. The higher functionalization, the higher band area of functional group, and the higher ratio of bands. The nCNF dispersion was lyophilized prior to IR spectroscopy.

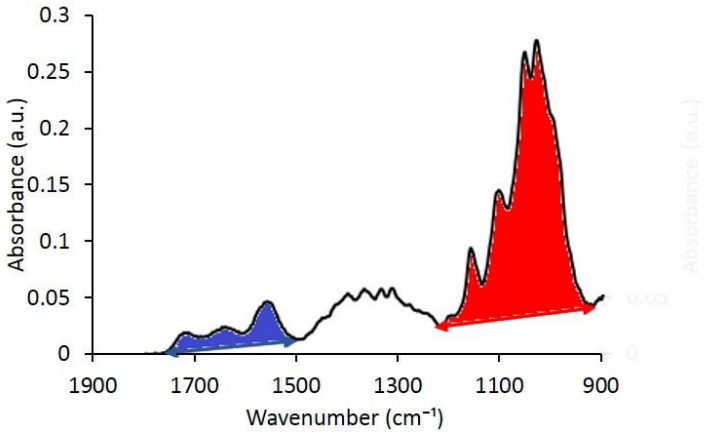

Figure 4.1. Example of an IR absorbance spectrum of nCNF. The red shaded area is the area under the C-O stretch band of the backbone and the blue shaded band area belongs to the functional group and contains C=O stretch of carboxylate, C=O stretch of ester, and C=C stretch of norbornene. The ratio of blue to red gives the relative amount of functionalization assuming that the red area is constant for all nCNF samples from the same CNF source.

4.2.3. Quantitative determination of functionalization degree of nCNF

4.2.3.1. CNF and nCNF Enzymatic Degradation

CNF or nCNF dispersion was diluted using sodium acetate/acetic acid buffered solution (pH 5) to prepare 1 mL of 1 wt% CNF or nCNF dispersion. In a representative experiment, 0.27 g of 3.7 wt% CNF was diluted in 730 µL NaOAC/HOAC buffer. To this, 10 µL of cellulase enzyme was added to the dispersion and incubated at 50 °C after vortexing for few seconds. The second dose of enzyme (10 µL) was added after 18 hours and incubated for more 2 hours. The mixture then was freeze-dried and re-dispersed in 0.65 mL of D_2O for ^{1}H-NMR spectroscopy.

^{1}H NMR spectroscopy of CNF (D_2O , 400 MHz) δ 1.73 ppm (Acetate -CH_3, Singlet, 3H), 3-4 ppm (Glucose backbone, broad), 4.46 ppm (Anomeric H (β) doublet, 1H), 5.05 ppm (Anomeric H (α) doublet, 1H)

To degrade nCNF, 0.33 g of 2.7 wt% nCNF was dispersed in 670 µL of NaOAc/HOAc buffered solution at pH 5 (to make 1 mL of 1 wt% nCNF) and incubated at 50 °C after 10 µL of enzyme was added. After 18 hours, the second dose of enzyme (10 µL) was added to the dispersion and incubated for two more hours. Degraded sample was freeze-dried and then was dissolved in 0.65 mL of D_2O for ^{1}H-NMR spectroscopy run. To degrade hydrogels, 1 mL of sodium acetate buffer was added to a 50 µL-hydrogel. The rest of the procedure was the same as mentioned above.

^{1}H NMR spectroscopy of nCNF (D_2O , 400 MHz) δ 1.17 ppm (Norbornene bridge -CH_2, Triplet, 2Hs) 1.73 ppm (Acetate -CH_3, Singlet, 3Hs), 2.90 ppm (Norbornene ester -CH, Singlet, 1H), 3-4 ppm (Glucose backbone, broad), 4.46 ppm (Anomeric H (β) doublet, 1H), 5.05 ppm (Anomeric H (α) doublet, 1H), 6.03 ppm (Norbornene double bond, singlet, 2Hs).

4.2.3.2. Calculating the degree of functionalization using ^{1}H-NMR spectroscopy

The acetate peak at 1.7 ppm was used as internal standard peak to obtain the cellulose degradation extent. From the integration of a known amount of acetate, integration for 1 mole of protons was calculated. This value was used to obtain the number of moles of anomeric protons from the overall integration of anomeric hydrogen peaks at 4.46 and 5.25 ppm (X). The initial moles of anomeric hydrogen was obtained from the known solid content in CNF or nCNF samples (Y). The degradation degree would be calculated as below:

Degradation degree= (X/Y)*100 (Equation 4.1)

The overall integration of anomeric hydrogen peaks and the integration of norbornene double bond peak at 6.03 ppm was used to calculate the degree of functionalization. The overall integration of anomeric hydrogen would be normalized for one hydrogen and norbornene double bond integration would be normalized for two hydrogen atoms. The calculation is shown below:

(Integration of H_α + Integration of H_β)/1 H = A

Integration of norbornene double bond protons/2 = B

Percentage of functionality assuming 100% degradation = (B/A) x 100 (Equation 4.2)

The calculated value from Equation 4.2 is based on the assumption that nCNF was 100% degraded. If hydrogel was not completely degraded, the calculated value from Equation 4.2 must be multiplied by degradation extent (calculated from acetate peak as described earlier) to be corrected.

Percentage of functionality = (Percentage of functionality assuming 100% degradation) x (degradation extent)

4.2.4. Chemical cross-linking of nCNF

nCNF (2.7 wt%) was centrifuged at 7000 rotations per minute (rpm) for 10 minutes to remove water (supernatant) until 4 wt% nCNF was obtained. nCNF hydrogels were formed at various molar ratios of thiol to norbornene (T/NB), cross-linker, and radical generating compounds. To prepare pre-gelelation dispersion, 4 wt% nCNF and various amount of cross-linker were mixed by vortexing for 20 minutes followed by mechanical stirring. The radical initiator 2-hydroxy-4'-(2-hydroxyethoxy)-2-methylpropiophenone (I2959) (0.05 wt %) was added and mechanically mixed with the dispersion. Then, 50 µl portions of solution were transferred by a spatula to 1 mL syringes with the top cut off. The solution was covered with coverslip (0.22 mm thickness) and irradiated with 365 nm light (Omnicure S1000 UV lamp filtered for 320-390 nm) at 10 mW/cm^2 power for 20 minutes. The hydrogels were stored in 1 mL PBS for 24 hours at 4 °C prior to subsequent testing.

For thermal gelation, to the 4 wt% nCNF/cross-linker dispersion, APS and TEMED were added. The concentration of APS and TEMED were 10 mM at the final dispersion. After vortexing and mixing with a spatula, 50 µl portions of the dispersion were transferred to the syringes with the top cut off and sealed with glass coverslips and incubated at 37 °C for 180 minutes. The hydrogels were stored in 1 mL PBS for 24 hours at 4 °C prior to subsequent testing.

4.2.5. Measure of compression modulus

A dynamic mechanical analyzer (DMA) (Q8000 Thermal Analysis) with a compression fixture was used to measure the compression moduli of the hydrogels. The hydrogels (n≥4) were subjected to a constant compression strain rate experiment at 10% strain/min up to 30% total strain. Compression modulus was defined as the slope of strain-stress curve in the limit of 10 to 20% compressive strain.

4.2.6. Rheology measurements

The maximum storage modulus of dispersions were obtained from rheological experiment using a TA Discovery HR-2 rheometer with a 40 mm aluminum cone-plate geometry with a 2° angle. CNF (4 wt%), nCNF (4 wt%), or 4 wt% nCNF/DEG dispersion with 10 mM of APS and TEMED (for thermal radical generation) with total volume of 620 µL were transferred to an aluminum pelletier plate at 37 °C. The fixture was lowered to the geometry gap (60 µm). Water droplets were placed around the geometry and covered with a plastic cup to keep the surrounding humid to assure that hydrogels are not drying during the run.

Time sweep measurements was run at 37 °C, 1 Hz oscillatory frequency, and 1% oscillatory strain for one hour. Oscillatory strain sweep (0.05% – 250%) was conducted at 37 °C and 1 Hz oscillatory frequency. Modulus recovery after shear-thinning test was done at 37 °C and a

constant oscillatory frequency (10 Hz) and alternating amplitude of oscillatory strain between 0.5% strain and 250% strain. After dispersion was transferred to the pelletier plate, time sweep at 0.5% strain was run for 5 minutes. After the initial low strain run, high strain (250% strain) was applied for 2 minutes followed by a low strain (0.5% strain) run for 2 minutes. Two more cycles of this alternating high/low strain was done.

4.2.7. Cell culture into 3D nCNF hydrogels

Passage 5 human mesenchymal stem cells (hMSCs) were expanded and grown a week to 90% confluency in DMEM cell culture media (90% low glucose DMEM containing 9% fetal bovine serum (FBS), 1% Antibiotic-Antimycotic (100x), and 5 µL fibroblast growth factor). hMSCs then were washed with sterile PBS (DPBS) twice prior to trypsinizing. Warm (37 °C) 0.05% trypsin/EDTA (3 mL) was added to the 100 mm petri dish and swirled around until all cells were covered. The dishes were incubated at 37 °C and 5% CO_2 for 5-8 minutes. Warm media (37 °C, 7 mL) was added to the dish and this suspension was transferred into a conical tube. Cells were centrifuged (5 minutes at 200 rpm), the media was removed, and cells were suspended in 1 mL of media, and centrifuged again to creat a cell pellet.

4.2.7.1. Method 1- suspending cells in dilute nCNF dispersion

Diluted nCNF (1 wt%) was added to the hMSCs in a microcentrifuge tube and cells were redispersed into the dispersion with pipetting several times. The resulted dispersion was centrifuged (at 200 rpm for overall 30 minutes) and the extra water was removed to reach 4 wt% polymer. Portions (50 µL) of this dispersion (DEG at T/NB=1, 0.05 wt% I2959, UV irradiation at 10 mW/cm^{-2}) were irradiated for 10 minutes to gel. Hydrogels were placed in a 24-well plate with 1 mL of media in each well and incubated at 37 °C and 5% CO_2 for 1 and 7 days. Every other day, media was removed and 1 mL fresh media was added.

4.2.7.2. Method 2- Seeding cells to nCNF-DEG aerogels

nCNF-DEG hydrogels (4 wt% nCNF, T/NB=1, 0.05 wt% I2959, 10 min UV irradiation at 10 mW/cm^2) were made in 50 µL molds and stored in -20 °C freezer for 24 hours. Frozen hydrogels were lyophilized for two days to remove water and prepare nCNF-DEG freeze/dried gels. hMSCs were suspended in warm DMEM (1 mL per each freeze-dried gel) at the concentration of 30000 cells/mL. Freeze-dried gels were placed in 24-well plate and 1 mL of hMSC suspension was added to each well and then were incubated at 37 ℃ and 5% for 1, 3, and 7 days prior to imaging. As a control experiment, an aerogel was soaked in 1 mL DMEM without any cells suspended.

4.2.8. Fluorescence imaging

Hydrogels (n=3 for each day) were stained for fluorescent imaging using Live/Dead viability assay (Life technologies, 0.25 µl of calcein and 1 µL of Ethidium homodimer-1 in 1 mL of sterile PBS for each hydrogel) for 40 minutes at room temperature. A ZEISS-AXIO Observer.Z1 microscope was used to take z-stack images (25 stacks) of cells inside the gels. Three gels for each day were imaged and number of cells in two stacks from each gel (stacks 13 and 21, overall 6 stacks) were counted using ImageJ software. Red dots (Nucleai DNA) and green dots (ECM) were counted to find the number of dead and live cells respectively.

4.3. Results and Discussion

4.3.1. Functionalization of CNF

The norbornene functional group was successfully added to CNF through an esterification reaction between the available hydroxyl groups on the surface of CNF and the anhydride of 5-norbornene-2,3-dicarboxylic anhydride in aqueous dispersion (Figure 4.2). Once added to the dispersion, the anhydride readily reacts with free hydroxyl groups of CNF to form the ester linkage and also a free carboxylic acid. This carboxylic acid formation accompanied by unwanted hydrolysis of anhydride by water molecules, which generates norbornene-2,3-dicarboxylic acid and contributes to a dramatic pH drop from neutral to pH 4. To adjust the pH, 10 M NaOH was added dropwise constantly for at least two hours. If too much NaOH was added at once (pH 13 or more), all the anhydrides would be hydrolyzed and therefore no reaction would take place. At the beginning of the reaction, because the concentration of anhydride is high, the esterification and hydrolysis reactions are fast and pH drops very quickly. So, NaOH should be added every 5 seconds to keep pH at the desired range. After around two hours, the reaction slowed down indicated by slower pH change. The reaction was considered complete when no more pH drop was observed over 30 minutes (around 4 hours after adding anhydride). For this reaction, molar excess of anhydride was added due to its low solubility in aqueous media and unwanted hydrolysis reaction. The reaction of CMC and norbornene-2,3-dicarboxylic anhydride was conducted at different pH ranges and the higher functionality was obtained at the range of 9.5-10.5.[140] Therefore, the same pH range (9.5-10.5) was chosen for CNF functionalization. To prevent a significant change in the volume of solution by adding NaOH, 10 M NaOH solution was used because each time only one drop of it was enough to bring the pH back to 10 very quickly.

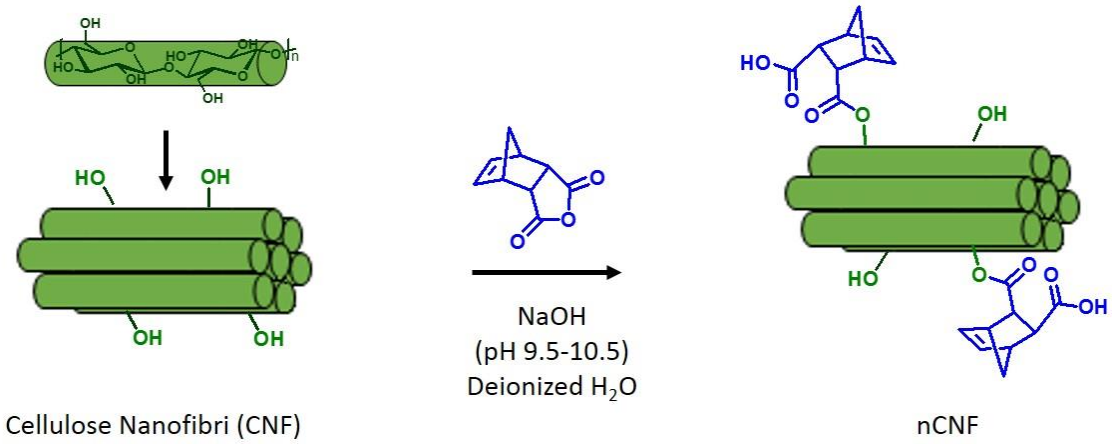

Figure 4.2-A schematic of surface functionalization of cellulose nanofibrils with 5-norbornene-2,3-dicarboxylic anhydride in aqueous media and at controlled pH.

Since nCNF is not soluble in water and the only impurity is water soluble norbornene-2,3-dicarboxylic acid from undesired hydrolysis of anhydride, purification was accomplished by five washes with deionized water using centrifugation at 7000 rpm for 15 minutes. This redisperse-centrifige-decant cycle was repeated until all the impurities were removed indicated by infrared (IR) spectroscopy. After each wash, a 1 mL sample of dispersion was collected and freeze-dried for IR spectroscopy. As shown in Figure 4.3, in IR spectrum of freeze-dried nCNF three distinguished new bands appeared at 1560, 1630, and 1720 cm^{-1} that belong to carboxylate (blue), norbornene double bond (red), and ester (green) groups respectively. The ratio of areas under the carboxylate (blue) to the ester band (green) of functional group was used to determine whether washing steps were effective. Because the trapped norbornene-2,3-dicarboxylic acid (by-product) also involves in carboxylate band area, while ester band is found in the nCNF. Each time dispersion was redispersed and washed, more norbornene-2,3-dicarboxylic acid were transferred to the supernatant and therefore, the carboxylate/ester band area decreased. When all the trapped norbornene-2,3-dicarboxylic acid were removed, the carboxylate/ester band area stayed constant after the fifth wash suggesting that five washes were enough to remove unreacted molecules. More and less washing were also tried but it appeared to be either not efficient or

extra based on (IR) spectroscopy. This purification strategy is advantageous because water is the only material used and it yields the purified product in an aqueous dispersion. Redispersion of freeze-dried nCNF in water is challenging because of the formation of irreversible hydrogen bonding known as hornification.[141,142] Therefore, obtaining nCNF in dispersion form eliminates the difficulties along with redispersing freeze-dried nCNF in water.

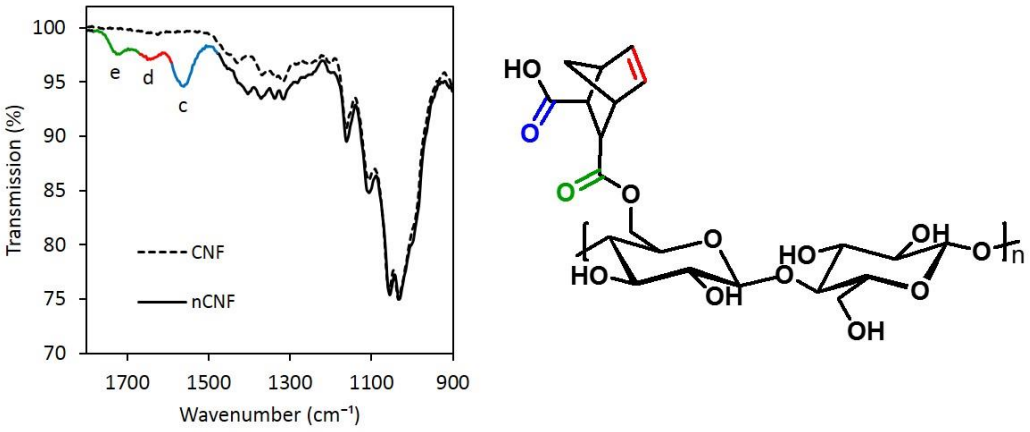

Figure 4.3. Infrared (IR) spectroscopy of CNF and nCNF-The Structure of nCNF Repeat Unit. IR Spectroscopy of CNF before (dash) and after (solid) functionalization with norbornene groups (nCNF) and the chemical structure of nCNF. Each band corresponds to functional group with the same color: green for ester (e), red for norbornene double bond (d), and blue for carboxylate(c). The spectra were normalized for the C-O stretch band of the backbone (1030 cm^{-1}).

The degree of functionality of nCNF was controlled by varying the molarity of added anhydride and changes to it could be inferred by IR spectroscopy (Figure 4.4 gray rectangular points). As shown in the graph, the functional group to the backbone band area ratio (as discussed in Section 4.2.2) increased from 3 to 10 as anhydride concentration increased from 0.13 M (2 molar excess) to 1.2 M (20 molar excess). The higher band ratio shows that the relative concentration of functional group on nCNF increased. This result suggests that the number of functional groups on CNF can be controlled by anhydride concentration. However, the error bar at 1.2 M of anhydride was very large and covers a wide range of band ratios. This could be explained if we assume that

at 1.2 M of anhydride, all the available surface hydroxyl groups were functionalized. Since the number of available surface hydroxyl groups could vary from sample to sample, different functionalization extents were obtained.

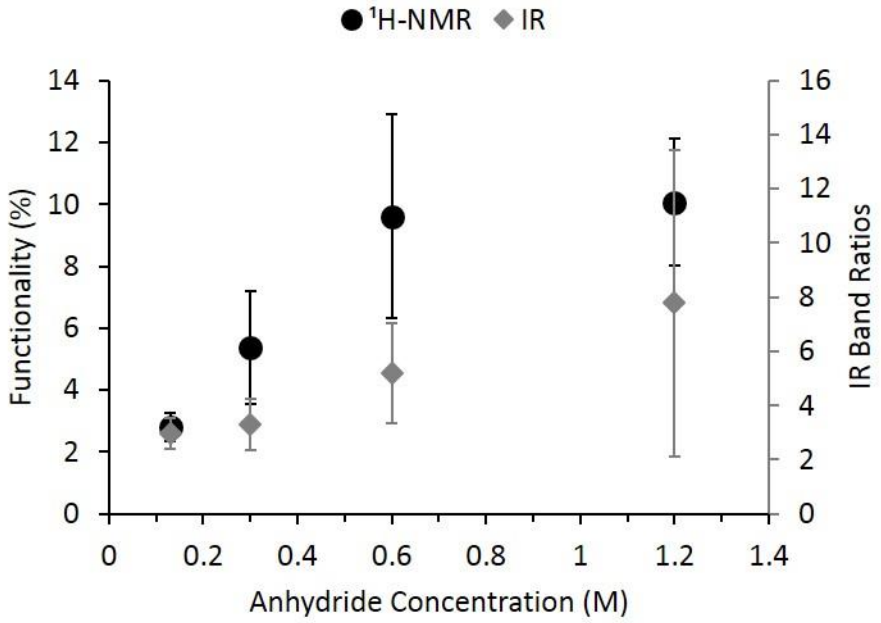

Figure 4.4. The relation between anhydride concentration and functionalization on CNF. The black circles represent the quantitative degree of functionalization obtained by ^{1}H-NMR spectroscopy and the grey rectangles represent the relative functionality based on IR band ratios. The error bars represent the standard deviation of three samples (α<0.05).

4.3.2. Quantifying the degree of functionalization

4.3.2.1. Enzymatic degradation of CNF and nCNF

The information obtained using infrared spectroscopy is relative and qualitative. Since the molar ratio of norbornene groups on the CNF backbone to cross-linker should be known to control the degree of cross-linking, the degree of functionality of nCNF must be quantitatively determined by ^{1}H NMR spectroscopy. However, CNF and nCNF are not soluble in common NMR solvents. Solid

state NMR spectroscopy of CNF also gives qualitative information.[117] To address this issue, we degraded CNF and its derivatives into water soluble sugar units using a mixture of enzymes (cellulase) that hydrolyze glycoside bonds. Enzymatic hydrolysis of CNF has been reported in several literatures using variety of enzymes. However, the characterization was limited to solubility studies, mass spectroscopy, and inverse gas chromatography while ^{1}H-NMR spectroscopy on solubilized sugar has not been reported. In this work, ^{1}H-NMR spectra of CNF and nCNF was obtained and used to determine the degree of functionalization quantitatively. For this, CNF was first degraded to water soluble segments by enzymatic treatments as shown in Figure 4.5.a. Recombinant hydrolase enzymes (Cellulase) from Ticoderma Reesei are used in this study which are mixture of enzymes with different target sites including β-glucanase units. The product of enzyme treatment would be glucose, cellobiose, and glucose oligomers as mentioned by the manufacturer. Enzymatic degradation has been reported to be most effective at pH 5 and a temperature range of 40-60°C.[143] However, above 60 °C enzymes lose their activity upon being denatured. Elevated temperature and acidic media is essential for the activity of enzymes responsible for degrading the crystalline regions. While in case of soluble single chain structures like carboxymethyl cellulose (CMC), degradation could be done at physiological temperature and pH (37°C, pH 7).[144,145] To find out the optimum time and enzyme concentration for degradation, cellulase at the various concentrations was added to 1 wt% CNF dispersions at sodium acetate buffered solution at pH 5 and incubated at 50°C. Incubation time and number of doses of enzyme were also varied and shown in Table 4.1. After degradation, samples were freeze-dried and dissolved in D_2O for ^{1}H-NMR measurements. However, samples did not completely dissolve in D_2O and contained some floating solid segments. This solid content varied based on the time period that samples were allowed to degrade as sample was almost all solid after 1h incubation, but was almost a clear solution after 20h.

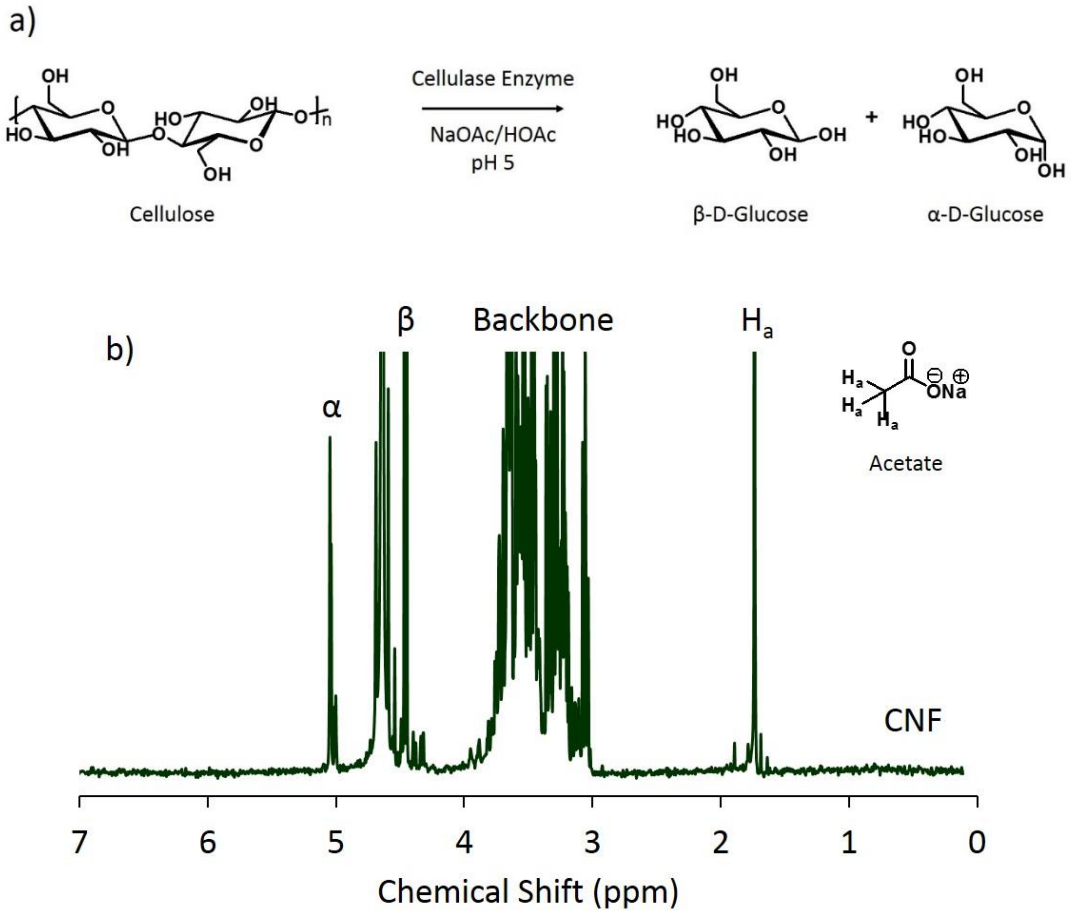

Figure 4.5- Schematic of enzymatic degradation of CNF and ^{1}H-NMR of degraded Sample. a) Schematic of enzymatic degradation of cellulose to glucose units in both anomeric forms, and b) ^{1}H-NMR spectrum of CNF after enzymatic treatments. 1 wt% CNF at NaOAc/HOAc buffered solution at pH 5 and 50 °C. Degradation was done by adding two doses of 10 µL cellulase over 20 h. Anomeric protons appeared at 4.46 and 5 ppm, backbone hydrogens at 3-4 ppm, and acetate hydrogens at 1.7 ppm.

Table 4.1. CNF enzymatic degradation to glucose units under different conditions and the resulted conversions. Data obtained from ^{1}H-NMR spectroscopy.

CNF	Buffer (pH 5) (µL)	Enzyme (µL)	Time (h) (dose1 + dose 2)	Degradation (%) (Acetate std)	Degradation (%) (Maleic std)	Comments
1 wt %	730	10	20	81		
1 wt %	730	10+10‡	18+2	86		
1 wt %	730	50	20	81		
1 wt %	730	10	5	75		
1 wt % freeze-dried	984	10	20	83		
1 wt %	730	10	1	31		80 *
1 wt %	730	10	2	44		73 *
1 wt %	730	10	3	50		
1 wt %	730	10	4	60	58	
1 wt %	730	10	5	68	71	95 *
1 wt %	730	10+10	6+14	85	90	
1 wt %	730	10+10	18+2	83		
1 wt %	730	10+10	15+22	87		

‡10+10 means that 10 µL was added (dose 1) at the beginning of the experiment and 10 µL was added (dose 2) after certain time. *after a week at room temperature in D_2O after initial ^{1}H-NMR spectroscopy, using acetate peak as standard

As shown in Figure 4.5.a, produced glucose was found in both anomeric forms (α- and β-D-glucose). As shown at Figure 4.5.b, the anomeric hydrogen appears at two chemical shifts (H_α at 5 ppm and H_β at 4.5 ppm) with slightly higher relative integration for H_β (57% to 43%). The rest of the hydrogen atoms of glucose (6 hydrogen) showed up as a multiplet at 3-4 ppm range. The peak

at 1.7 ppm (H_a, Figure 4.5.b) belongs to three hydrogen atoms of acetate which was added to the system as sodium acetate buffered solution. Since acetic acid (bp 118.1 °C) sublimed with water in the lyophilizer, only sodium acetate contributes to this peak integration. By knowing the exact amount of sodium acetate added to the degradation mixture, this acetate peak was used as internal standard to find the degree of degradation by ^{1}H-NMR spectroscopy. The overall integration of anomeric hydrogen peaks at 4.46 and 5 ppm was normalized for 1 mole of protons and then, the moles of anomeric protons in a degraded sample was obtained. The moles of anomeric hydrogen atoms, if completely degraded, was calculated from the solid content of CNF sample. The ratio of calculated moles from ^{1}H-NMR to the expected number of moles of glucose gave the degradation value. As shown in Table 4.1, the maximum degradation was achieved (≥ 85%) when two 10 µL doses of enzyme was added to 1 mL of dispersion over 20 hours at 50 °C. To further validate the results, known amount of maleic anhydride was added to the CNF NMR samples as external standard and consistent results were obtained compare to the results from acetate (Figure 4.6 and Table 4.1). Therefore, the standard method for degrading our samples was introduced as adding two 10 µL doses of enzyme to 1 mL of 1 wt% CNF (nCNF) dispersion over 20 hours at 50 °C. The same conversion was achieved when nCNF samples were treated with cellulase under the same condition (Figure 4.7).

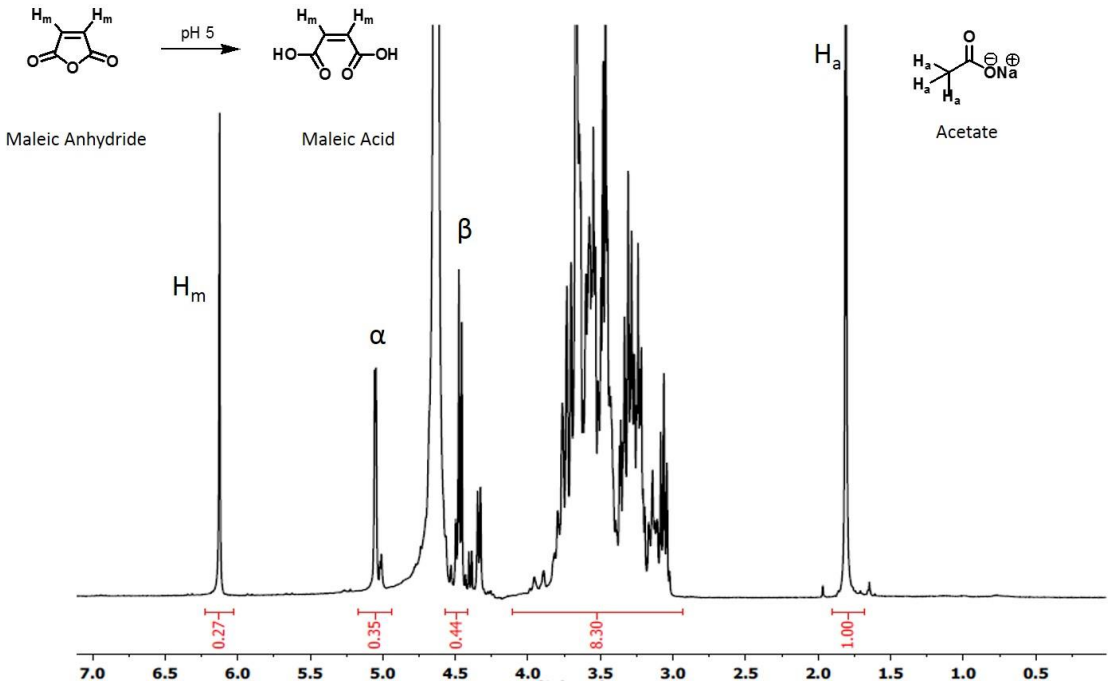

Figure 4.6. Representative ^{1}H-NMR spectrum of 1 wt% CNF degraded with 10 µL enzyme for 5 hours at 50 °C. Sodium acetate and maleic anhydride were considered as internal and external standards, respectively. CNF was degraded 68% (based on acetate peak at 1.7 ppm) and 71% (based on maleic peak at 6.2 ppm).

Interestingly, it was observed that when samples were sitting for a week in D_2O in an NMR tube at room temperature, all the solid segments disappeared and a clear solution was remained. ^{1}H-NMR spectroscopy was done on these samples again and higher degrees of degradation (up to 95%) was achieved, suggesting that the cellulase enzyme survived during freeze-drying and retains its activity. Data reported in Table 4.1 suggest that there is a fast step of degradation (68 to 75% after 5h) to degrade amorphous parts of CNF and then a slower step to break down the crystalline parts (95% after a week).[146,147]

4.3.2.2. Calculating the degree of functionality on nCNF

Using the defined standard method mentioned in Section 4.3.2.1, samples were degraded to quantitatively calculate the degree of functionality by ^{1}H-NMR spectroscopy (Figure 4.7). Enzyme breaks down the nCNF into α- and β-D-glucose units while the ester linkages between cellulose

and norbornene group is hydrolyzed under acidic condition (pH 5). The ^{1}H-NMR spectrum of degraded nCNF is compared to CNF at Figure 4.8. The presence of three new peaks at 1.17 ppm, 2.9 ppm, and 6 ppm confirms the presence of functional group on nCNF (peaks are assigned at Figure 4.8). The rest of the protons of functional group are overlapped by glucose backbone protons.

The degree of functionalization was calculated using the integration of norbornene double bond peak at 6 ppm from functional group and anomeric proton at 4.46 and 5.05 ppm of degraded backbone at Equation 4.2 (Section 4.2.3.2). The acetate peak at 1.7 ppm was also used as internal standard to determine the degradation degree (Equation 4.1). The calculated functionalization degree was corrected by multiplying by degradation percentage. Synthesized nCNF samples at different concentrations of anhydride that were previously analyzed by IR spectroscopy qualitatively in Section 4.3.1, were degraded by enzyme to determine their quantitative functionalization degree. Functionalization degree was defined as the number of functional groups per anhydroglucose repeat unit of nCNF. Results are shown in Figure 4.4 (black circle). As earlier understood from IR spectroscopy data, increasing the concentration of anhydride would increase functionality on nCNF. The functionalization degree at the 0.13, 0.3, 0.6, and 1.2 M of anhydride was determined to be 2.8%, 5.3%, 9.6%, and 10.1% respectively. From 0.13 M to 0.6 M, the functionalization degree doubled as the molarity of anhydride doubled. However, this trend was not observed from 0.6 M to 1.2 M and the degree of functionality plateaued at 0.6 M suggesting that the free hydroxyl groups on the surface of CNF were saturated when 10 molar excess of anhydride to repeat unit was added. The nCNF used throughout this study was 14% functionalized that was the highest functionality obtained in these experiments. The higher functionality leads to more cross-linking which increases the stability and modulus of resulting hydrogels.

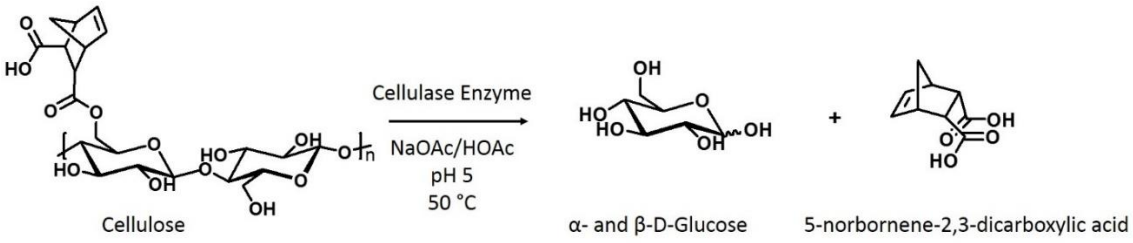

Figure 4.7. Schematic of enzymatic degradation of nCNF under acidic condition and elevated temperature. Glucose units (both anomers) produced by enzyme treatment and 5-norbornen-2,3-dicarboxylic acid is produced because of the hydrolysis of ester bond at acidic condition.

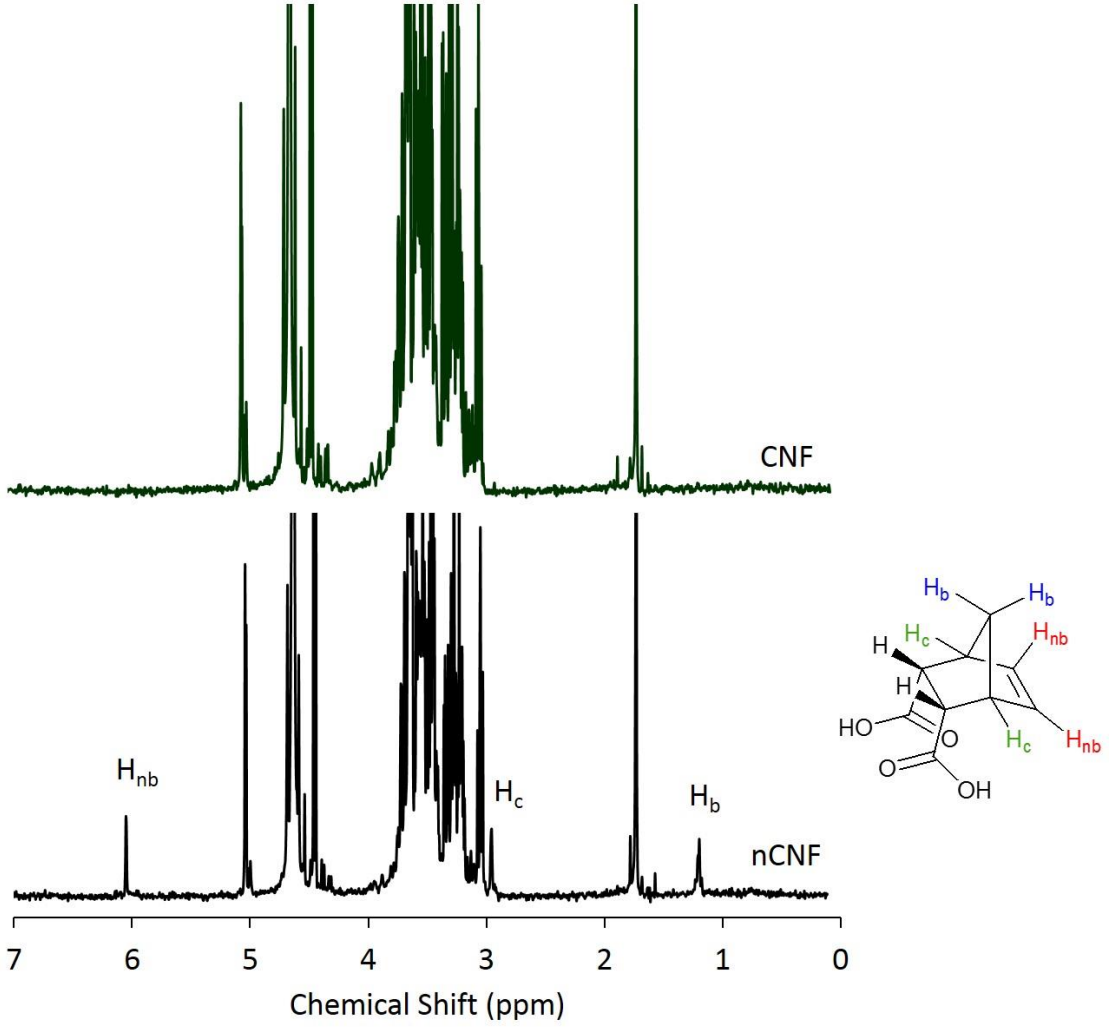

Figure 4.8. Representative ^{1}H-NMR spectra of degraded nCNF compare to CNF. ^{1}H-NMR spectra of CNF before and after functionalization (nCNF) for comparison and the structure of produced 5-norbornen-2,3-dicarboxylic acid. Three peaks related to functional group appeared in nCNF spectrum.

Methods to characterize functionality on CNF has been limited to acid-base titration for anionic functional groups, $AgNO_3$ titration for cationic functional groups, and recently quantitative solid state ^{13}C-NMR spectroscopy.[117] But to our knowledge, ^{1}H-NMR spectroscopy has never been done to characterize CNF because CNF and its derivatives are insoluble in common ^{1}H-NMR solvents. Here for the first time we discussed obtaining the degree of functionality based on the quantitative ^{1}H-NMR spectroscopy. To do this, CNF was degraded into smaller soluble segments by Cellulase enzyme and resulting sugar units were dissolved in D_2O for ^{1}H-NMR spectroscopy. We were able to calculate the extent of degradation along with the degree of functionalization. This straightforward and effective strategy opens the door to complete characterization of modified CNF.

4.3.3. Hydrogel fabrication with tunable mechanical properties

Chemically cross-linked nCNF hydrogels were made to increase the stability of CNF-based hydrogels in aqueous media using thiol-ene cross-linking reaction. nCNF (2.7 wt% dispersion) was centrifuged to remove water to obtain a 4 wt% nCNF dispersion. 2,2'-(ethylenedioxy)diethanethiol) (DEG) at various thiol to norbornene ratios (T/NB) from zero DEG to T/NB of 4.2 was added to the dispersion and mixed by vortex and mechanical stirring followed by addition of radical initiator (I2959) at 0.05 wt% and mechanical mixing. The final dispersion was transferred to 50 µL molds and sealed using glass coverslips. UV irradiation at 10 mW/cm^{-1} for 20 minutes resulted in hydrogels with different degrees of cross-linking (Figure 4.9). The cross-linking reaction occurs between the norbornene groups on the surface of different nCNF bundles and the thiol moiety of DEG.

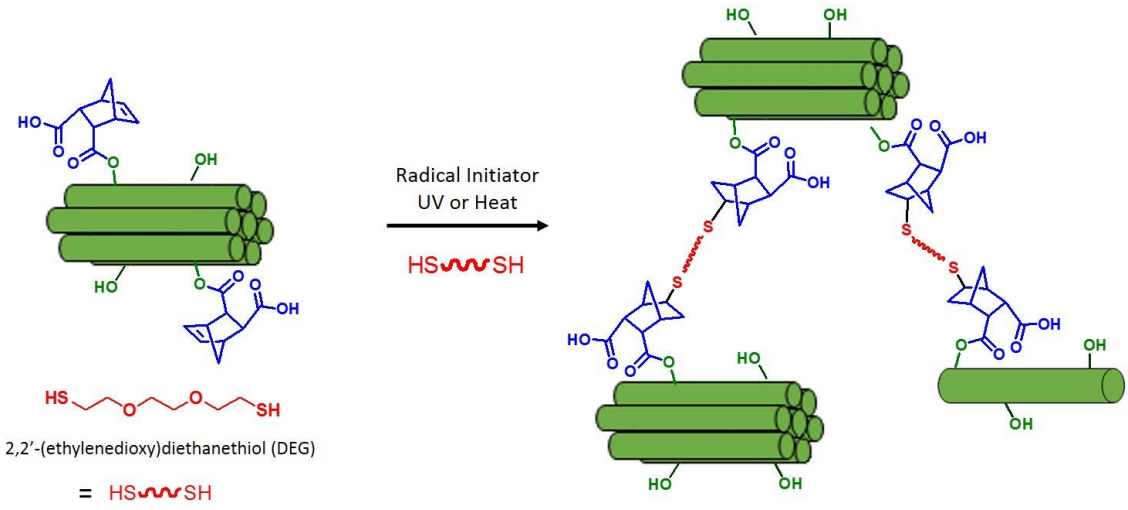

Figure 4.9. Schematic of chemical cross-linking between fibrils of nCNF via thiol-norbornene reaction to fabricate nCNF hydrogels. Hydrogen bonds between fibrils is not shown here for simplification.

To investigate whether a chemical reaction occurred, hydrogels at T/NB of 1 were made and incubated at 4 °C in PBS for 24 hours for unreacted cross-linker to diffuse out of the gel. The hydrogel was degraded by enzyme using the above procedure and the products were redissolved in D_2O for ^{1}H-NMR spectroscopy after being freeze-dried. Interestingly, as shown in Figure 4.10, the norbornene double bond peak at 6 ppm disappeared due to thiol-norbornene reaction while the peaks of the thiol-norbornene reaction product appeared at the region between 1 ppm to 3 ppm confirming that the chemical reaction between thiol and norbornene occurred. This experiment also showed that the nCNF hydrogels are degradable by enzyme.

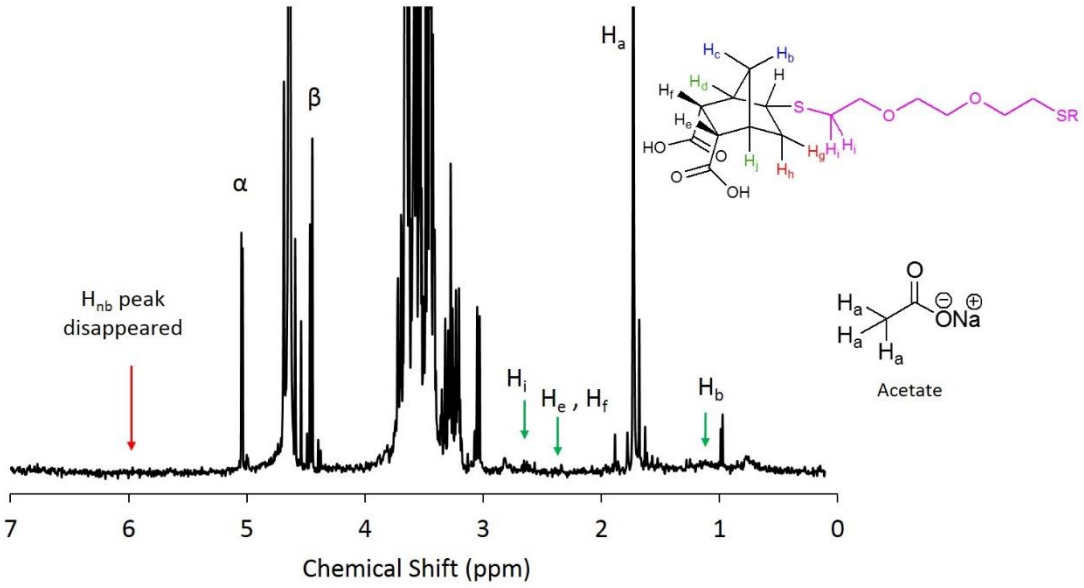

Figure 4.10. Representative ^{1}H-NMR spectrum of nCNF-DEG hydrogel (4 wt%, T/NB=1, 20 min UV irradiation) degraded with two doses of 10 µL enzyme for 20 hours at 50 °C. Sodium acetate was considered as an internal standard. The norbornene double bond peak at 6 ppm disappeared and peaks of thiol-norbornene product appeared (between 1 ppm and 3 ppm) in the spectrum.

The ability to tune the modulus of hydrogels was investigated by varying the amount of the cross-linker added. A dynamic mechanical analyzer (DMA) with a compression fixture was used to measure the compression modulus of hydrogels. Hydrogels were incubated at 4 °C in PBS for 24 hours prior to DMA measurements. The non-cross-linked hydrogels (no DEG added) failed to resist against compression stress and were mostly untestable which is common when modulus is lower than 3 kPa. As demonstrated at Figure 4.11.A, by increasing the amount of DEG, the compression modulus increases to 6 kPa at its maximum (for T/NB=1.2) and then decreases at higher thiol to norbornene ratios. Because at higher T/NB than 1, the number of thiols exceeded the number of norbornenes and saturates NB groups without forming effective cross-links. The maximum modulus was expected at T/NB=1, while it was observed at T/NB=1.2. This can be as a result of the long distance between norbornene groups on the surface of fibrils, so, cross-linking might not

occure. By adding more thiols, longer cross-linkers would form through disulfide bond formation that can form effective cross-links.

Unexpectedly, the same moduli were obtained when polymer cross-linkers with two different molecular weights were used to make hydrogels under the same conditions (Figure 4.11.B). Dithiol-polyethylene glycol (DTPEG) at M_n of 1.5 kg/mol and 3 kg/mol were used at the same range of T/NB as DEG. Theoretically, the compression modulus of a hydrogel is inversely related to the MW between cross-links.[121] Therefore, using DTPEG-1.5k as cross-linker expected to decrease the compression modulus significantly compare to where DEG is used. Such a trend was not observed with DTPEG-1.5k, also it was not observed when a higher MW cross-linker (DTPEG-3k) was used for gelation. One explanation for this result could be the fibrillar structure of nCNF. The cross-linking between fibrils was not as effective as between single polymer chains as a result of the distance between fibrils. Additionally, because of the insolubility of nCNF in water and its dispersion form, mixing could be not sufficient and thus cross-linkers were not homogenously dispersed. Additionally, because of high MW of nCNF fibrils and the long distance between cross-links, the MW between cross-links is already high, so it is not significantly changed by the difference of MW of cross-linkers.

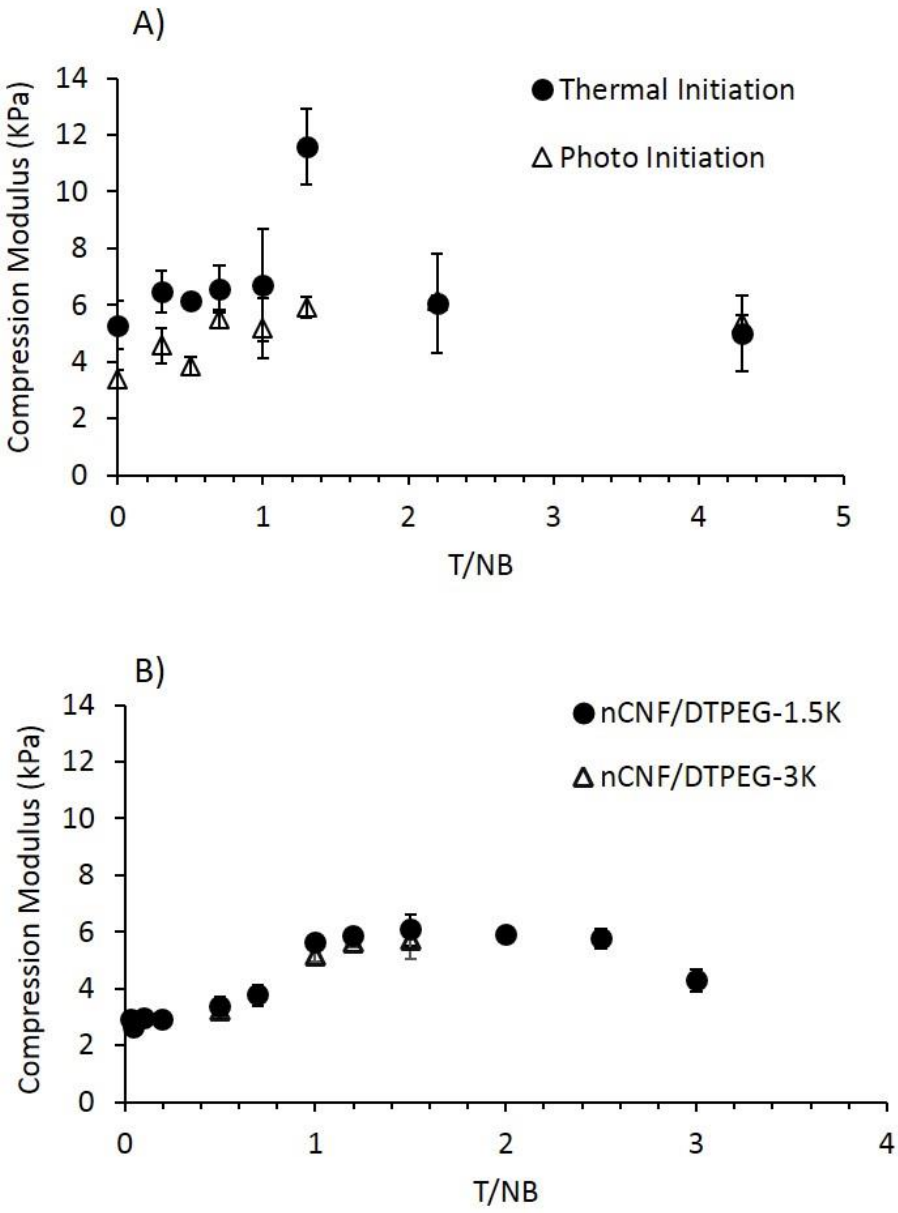

Figure 4.11. Compression modulus of nCNF hydrogels. A) Compression modulus of nCNF-DEG hydrogels at various T/NB (4 wt% nCNF, T/NB=0. 0.3, 0.5, 0.7, 1, 1.3, 2.2, 4.3) made by light initiated (triangle) and thermal initiated (round) gelation system. B) Compression modulus of nCNF-DTPEG 1.5k (round) and nCNF-DTPEG 3k (triangle) hydrogels at several T/NB (4 wt% nCNF). Error bars are standard deviations for 5 measurements.

Another probable reason for small modulus changes after cross-linking is the scattering of UV light by CNF fibrils so the power of UV light is lower than what it supposed to be. To investigate if

this data is a result of UV light scattering in the nCNF dispersion and therefore insufficient cross-linking, thermal radical initiation was explored. In this case, hydrogels with the same range of T/NB were made with 10 mM APS/TEMED by incubating at 37 °C for 3 hours. These samples were transferred to 1 mL of PBS and stored at 4 °C for 24 hours prior to mechanical testing. Compression modulus of these samples were slightly higher than UV-initiated samples. This slight increase in modulus suggests that low modulus is not related to UV-light scattering by the dispersion (Figure 4.11.A).

Rheological measurements of storage modulus of thermally gelled samples also showed that varying T/NB does not significantly change the modulus. Time sweep experiments at 1% strain and 1 Hz at 37 °C were done for 4 wt% nCNF mixed with DEG at different T/NB and 10 mM APS/TEMED. CNF and nCNF without any cross-linker also were tested. The storage modulus of 4 wt% CNF was around 14 kPa which reduced to 7 kPa upon functionalization (nCNF). The addition of norbornene groups to the surface of nanofibrils interrupts the hydrogen bonds between fibrils and therefore reduces the modulus. When DEG was added to nCNF dispersion, chemical cross-linking via the thiol-ene reaction increased the storage moduli to 13-15 kPa (for a range of T/NB) (Figure 4.12). However, the storage modulus of hydrogels at different T/NB appeared to be in a same range (13-15 kPa) that shows that varying T/NB does not influence the mechanical properties significantly.

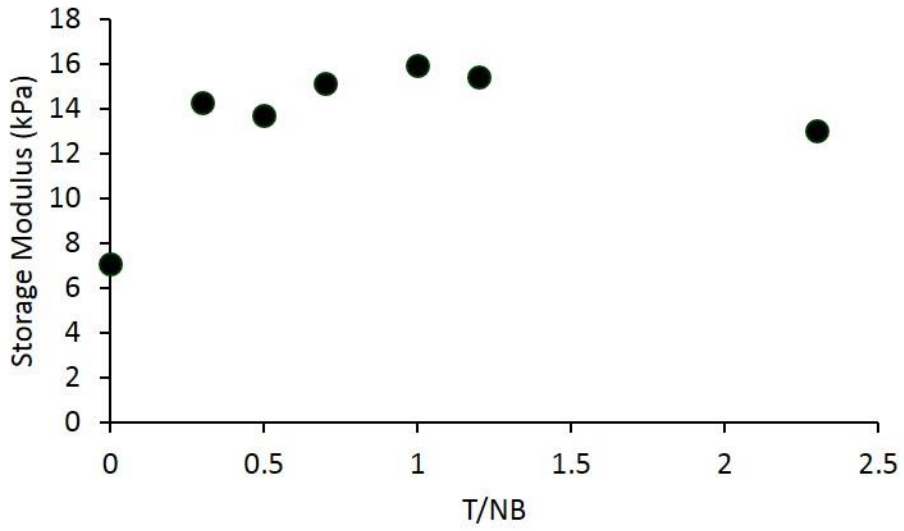

Figure 4.12. Storage modulus of nCNF hydrogels. Storage modulus of CNF and nCNF-DEG hydrogels (4 wt%, T/NB=0. 0.3, 0.5, 0.7, 1, 1.3, 2.2 and 10 mM APS/TEMED) obtained from time sweep rheological measurements at 1% strain, 1 Hz oscillatory frequency, and 37 °C using a 40 mm cone geometry.

Although varying T/NB did not provide highly tunable mechanical properties, the dimensional stability of hydrogels increased compare to non-cross-linked samples due to replacement of hydrogen bonds between fibrils with the stronger covalent bonds and resulted in materials with the same modulus as CNF but stable toward dilution in water compare to CNF. Figure 4.13 demonstrates the effect of cross-linking on the dimensional stability of hydrogels, the non-cross-linked gels broke apart after one day in PBS at 37 °C, while cross-linked samples were still stable after three weeks. It is not presented here, but these gels are kept at 4 °C until now (for a year) without breaking apart.

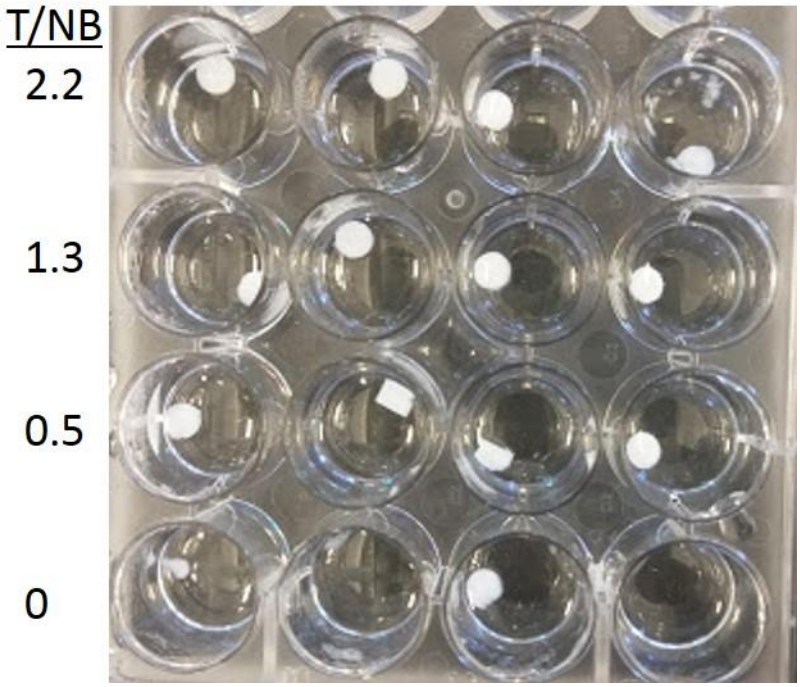

Figure 4.13. Images of nCNF-DEG hydrogels at different T/NB after 20 days in PBS at 37 °C. Cross-linked hydrogels are shown dimensional stability while non-cross-linked gels were almost broken apart completely.

Another approach to control modulus of hydrogels is by varying the nCNF content. As shown in Figure 4.14, 1 wt% decrease in nCNF content (from 4 wt% to 3 wt%) led to an order of magnitude decrease in storage modulus of hydrogels which is the consequence of a 25% reduction of cross-linkable sites (norbornene groups). The decrease of modulus as a result of lower solid content was also shown in strain sweep measurements of 3 and 4 wt% samples of CNF, nCNF, and nCNF-DEG hydrogels (Appendix, Figure C.1-C.3). The storage and loss modulus of nCNF dispersion increased two orders of magnitude with increasing concentration. This observation is in agreement with general trend that has been reported for viscoelastic dispersions.[148]

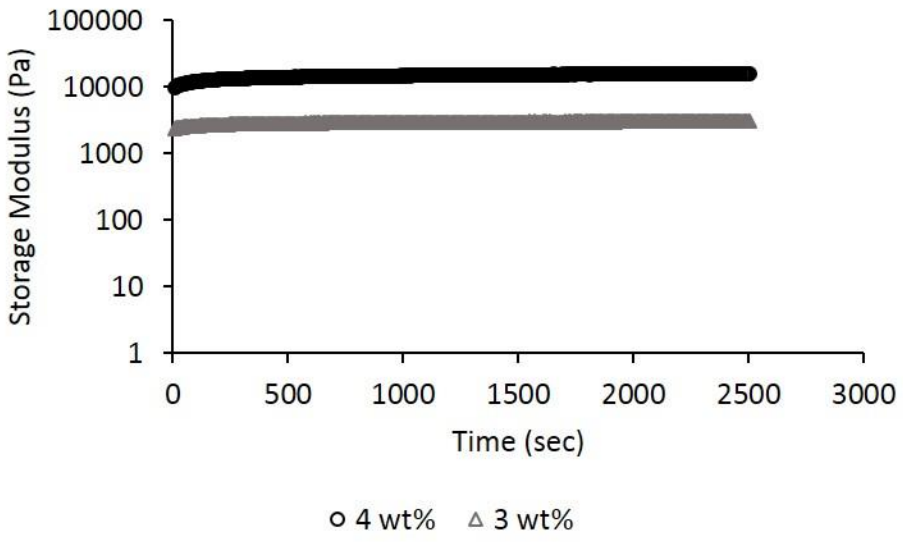

Figure 4.14. Time sweep rheological measurements of CNF dispersion at 4 wt% (Black circle) and 3 wt% (gray triangle) at 1% strain and 1 Hz angular frequency at 37 °C using a 40 mm cone geometry.

4.3.4. Shear-thinning behavior

CNF aqueous dispersion is classified as shear-thinning material.[148,149] The viscosity of a Shear-thinning material decreases when shear strain increases. This characteristic is very important for biomaterials. Materials with shear-thinning behavior have been used as injectable scaffolds for in situ cell culture and as bioink for 3D printing.[53,150] For example, Kuzmenko et al reported 3D-printed CNF-based scaffold for neural tissue engineering.[150] Neural cells successfully adhered to the scaffold and proliferated. Shear-thinning characteristic is reported in physical gels. In this study, the shear-thinning behavior and the ability to recover the mechanical properties of three samples (4 wt% CNF, nCNF, and nCNF-DEG with T/NB=1) was explored by oscillatory strain step experiments (Figure 4.15). A strain sweep was run first to determine the yield strain that was shown to be around 37% (Appendix, Figures A.4.1-A.4.3). Based on the yield strain, a lower and a higher strain than 37% were selected for modulus recovery test. Strain was altered between 0.5

and 250% every two minutes after initial 5 minutes run at lower amplitude and the storage and loss modulus was recorded. All three samples exhibit a shear-thinning character and the modulus reduced three orders of magnitude after applying higher amplitude oscillatory strain (Figure 4.15). The initial moduli of CNF (29 kPa) and nCNF (16.7 kPa) were 40% recovered (to 12 kPa for CNF and 6.6 kPa for nCNF) at lower amplitude. But this reduced modulus was fully recovered at next cycles of alternating amplitudes. This initial recovery was around 27% for nCNF-DEG hydrogel (from 25.4 kPa to 6.8 kPa) but the complete recovery at next cycles was also observed for nCNF-DEG sample.

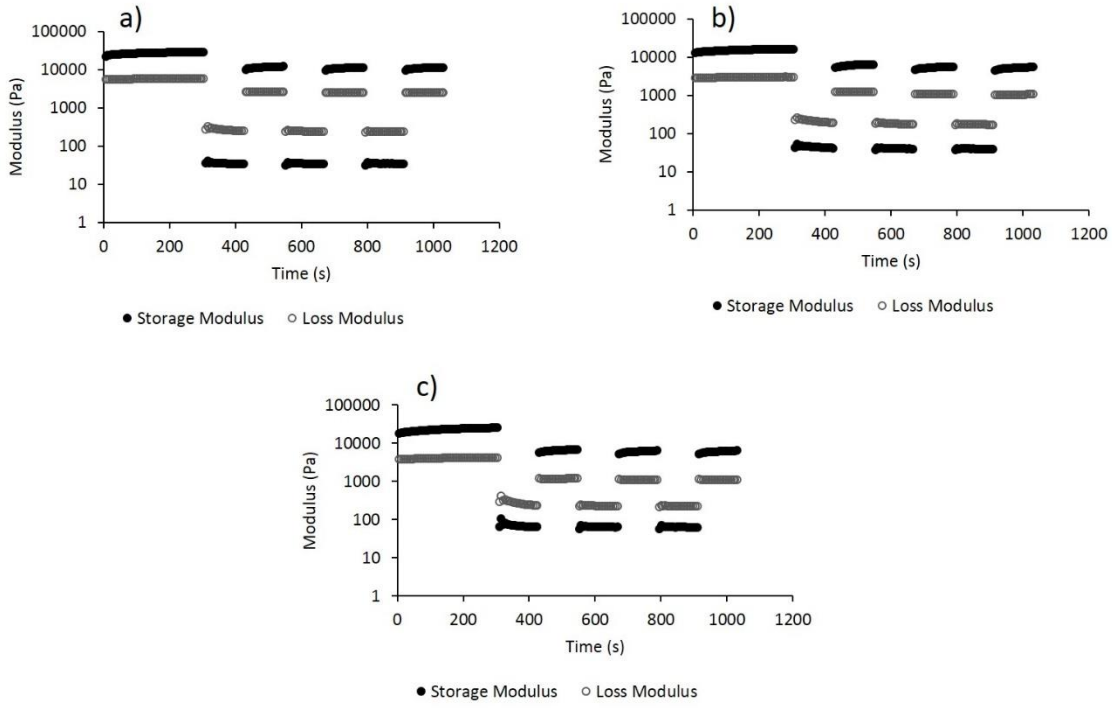

Figure 4.15. Strain step rheological measurements of CNF, nCNF, and nCNF-DEG hydrogel. Strain step rheological measurements of CNF, nCNF, and nCNF-DEG hydrogel to demonstrate the shear thinning behavior and modulus recovery. Oscillatory strain step at 10 Hz and alternating low (0.5%) and high (250%) strain for a) 4 wt% CNF, b), 4 wt% nCNF and c), 4 wt% nCNF-DEG hydrogel (T/NB=1, 10 mM APS/TEMED) is shown. Each step was 2 minutes long after an initial 5 min-long step.

In all samples, after shear was removed the recovery of modulus was quick and it took less than 20 seconds to reach to 90% of the maximum modulus. The shear thinning character and the

rapid recovery of modulus can be explained by the entanglement of fibrils. Under shear stress, nanofibrils align in line with the flow which causes a decrease in viscosity.[148] The recovery of nCNF and nCNF-DEG modulus also showed that functionalization and even thiol-norbornene cross-linking did not fully change the dynamicity of the interactions between fibrils. The initial reduction of storage modulus could be as a result of hydrogen bond formation between aligned fibrils that is broken with the initial shear.[148] When nanofibrils are aligned under high shear stress, hydrogen bonds could form between fibrils, causing fibrils to stay aligned even after shear is removed. This alignment of fibrils could decrease the resistance against strain and reduce the modulus of the dispersion. The shear thinning behavior and the recovery of mechanical properties was also observed at lower solid content (3 wt%) (Appendix, Figure A.4), confirming the viscoelastic behavior of nCNF dispersion.

4.3.5 Human mesenchymal stem cell viability in nCNF 3D hydrogels

Modified CNF has been used for tissue regeneration and exhibited acceptable cytocompatibility (references). In this study, the hMSC viability using our gelation process was explored. Dispersing cells into polymer solutions usually is done through pipetting which was not possible in this case due to high viscosity of 4 wt% nCNF. Therefore, cells were dispersed via pipetting in a diluted nCNF (1 wt%) followed by water removal through centrifugation to reach to a 4 wt% cell-containing nCNF dispersion. Radical initiator (I2959) was also added prior to cell dispersion at the 0.05 wt% concentration. DEG (T/NB=1) was added to the dispersion after centrifugation. Hydrogels with encapsulated hMSC were made by 10 minutes UV irradiation at 10 mW/cm^2 in 50 µL molds covered with coverslip and incubated at 37 °C and 5% CO_2 in cell culture media (DMEM). A shorter irradiation time (10 mins vs. 20 mins) was chosen to reduce the time that cells were out of DMEM. Encapsulated hMSCs were imaged at days 1 and 7 of encapsulation

(Figure 4.16). Cells were stained prior to imaging using Live/Dead assay with calcein to stain actin of cytoplasm of live cells (green) and ethidium homodimer-1 to stain the DNA of dead cells (red). Imaging was followed by cell count using ImageJ software and 24% and 50% cell viability was achieved for day 1 and 7 respectively (three gels for each day).

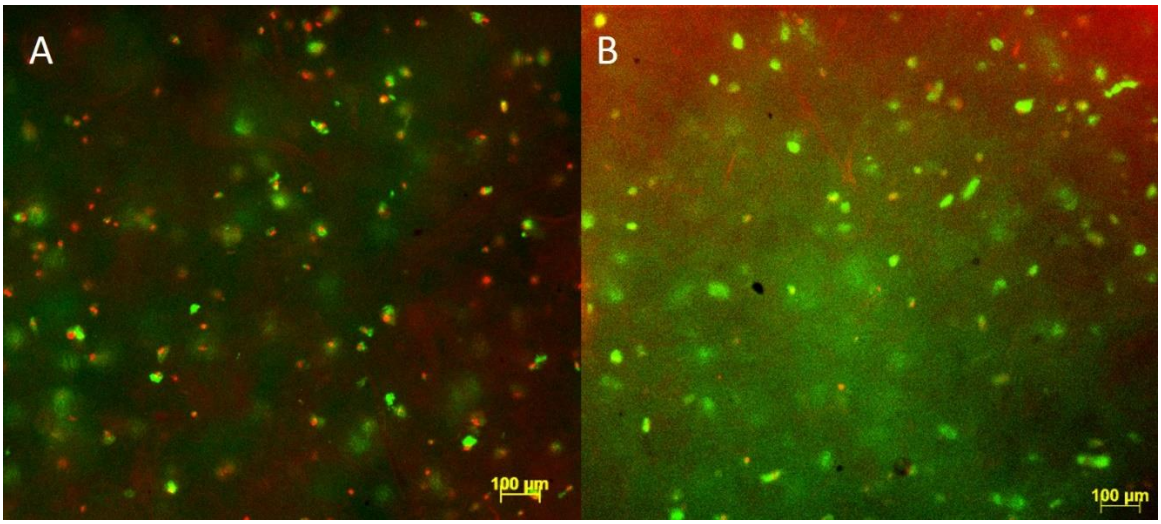

Figure 4.16. Fluorescent images of hMSC encapsulated in nCNF-DEG hydrogels (ZEISS-AXIO Observer.Z1 microscope, 5X magnification) (4 wt%, T/NB=1, 10 min UV irradiation at 10 mW/cm^2 at A) day 1 and B) day 7. Live/Dead assay was used to stain cells. Green is representing actin of live cells and red representing dead cells. The viability was determined to be 24% and 50% at day 1 and 7 of encapsulation respectively. The scale bars represent 100 µm.

Low cell viability could be the consequence of the harsh condition of mixing. Mechanical stirring after centrifigation to redisperse cells and even the long process of centrifugation could possibly burst most of the hMSCs before making hydrogels. Dead cells that were trapped in nCNF hydrogel slowly diffused out of the hydrogel over time. This slow dead cell diffusion can explain the lower viability of hMSCs at day 1 compare to day 7 where most of the dead cells were diffused out.

To resolve the difficulties of cell dispersion in nCNF, seeding hMSCs in already made nCNF-DEG hydrogels were examined. Hydrogels with 4 wt% nCNF and DEG (T/NB=1, 0.05 wt% I2959, and 20 min. UV irradiation at 10 mW/cm^{-1}) were made and stored in 1 mL of PBS overnight to let I2959

and unreacted DEG diffuse out of hydrogels. Hydrogels then were lyophilized to remove water from the system and then placed in 24-well plate. Passage 5 hMSC was dispersed in cell culture media (30000 cells/mL) and 1 mL of this dispersion was added to each gel and incubated at 37 °C and 5% CO_2 for 1,3, and 7 days. Live/Dead assay was used to stain cells which then were imaged by a fluorescent microscope (Figure 4.17.a, b, and c). Hydrogels soaked in media without cells were also imaged as control experiment (Figure 4.17.d). Interestingly, it was observed that the nCNF bundles got stained red by ethidium homodimer-1 that suggests that ethidium homidimer-1 could be adsorbed by cellulose nanofibrils (Figure 4.17.d). This phenomena was reported where other fluorescent dyes such as FITC were mixed with CNF.[151]

The morphology of re-swelled gels would be altered due to freeze-drying and would be different from hydrogels that are directly made from a dispersion. The comparison of the compression modulus of re-swelled freeze-dried gels with the modulus of initial hydrogels showed that the stiffness of gels increased after freeze-drying (Figure 4.18). The change in modulus due to freeze-drying should be considered when material is used for cell culture. Because cell behavior is affected by the mechanical properties of the matrix they are encapsulated in. The altered properties of the gels could be explained by a phenomena called ice templating. When a dispersion is freezing, formation of ice crystals pushes away the particles at the freeze front and concentrates them between ice crystals. Sublimation of ice leaves a more compact structure behind.[152] When nCNF was packed between ice crystals, irreversible hydrogen bonds between fibrils was formed through hornification. Therefore, freeze-dried gels keep their compact structure after reswelling in aqueous media. At the constant volume, more compact fibrils widen the pores between the fibrils which facilitates the diffusion of molecules and cells into and out of the gel. Therefore, live cells penetrated into the gels and adhered to the nCNF-DEG in one day after seeding as shown in Figure 4.17.a. Since dead cells could also diffuse out of the structure,

dead cells were not observed even at day 7 of seeding. Cell viability could not be calculated because the number of dead cell was unknown. However, the presence of live hMSCs after a week of seeding in an elongated form demonstrates that cells adhered to the structure successfully and could survive. Although more straight forward methods should be developed for cell encapsulation in chemically cross-linked nCNF hydrogels, these materials showed promising low cell toxicity and can be further examined for cell culture and tissue regeneration studies.

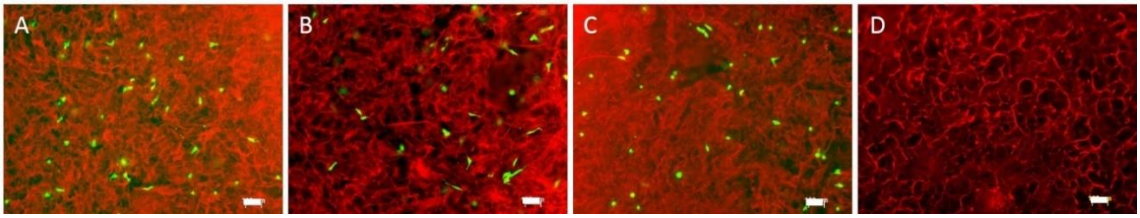

Figure 4.17. Fluorescent images of hMSC seeded in nCNF-DEG hydrogels (ZEISS-AXIO Observer.Z1 microscope, 5X magnification) (4 wt %, T/NB=1, 20 min. UV irradiation) at A) day 1, B) day 3, and C) day 7 after seeding. Live cells are stained green (Calcein, Invitrogen Live/Dead assay). D) nCNF-DEG hydrogel without cells as control experiment was stained red by ethidium homodimer-1 (Invitrogen Live/Dead assay). Scale bars are 100 µm.

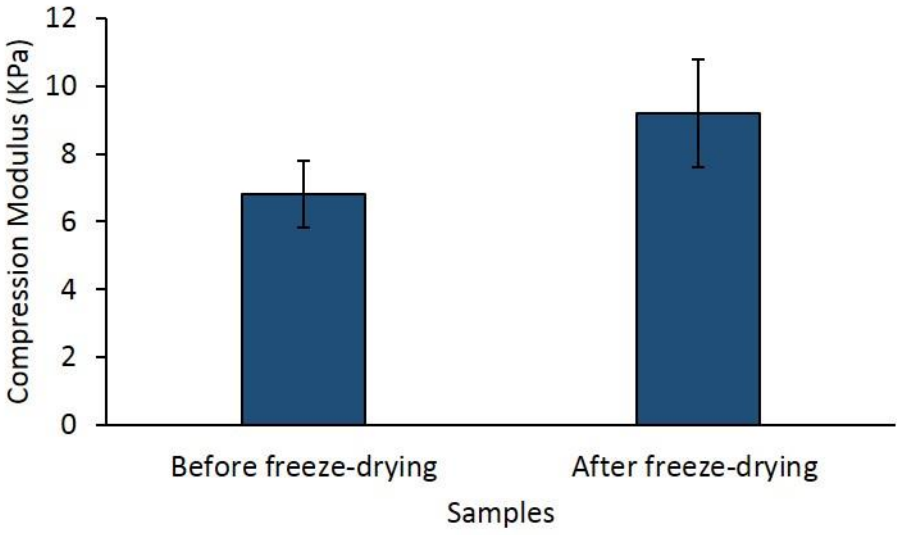

Figure 4.18. Compression modulus of freeze-dDried nCNF-DEG hydrogel before and after freeze-dring. The compression modulus of nCNF-DEG hydrogels (4 wt%, T/NB=1, 10 min UV irradiation at 10 mW/cm^2) before and after freeze-drying. Hydrogels were frozen at -20°C for 24 hours and lyophilized for two days. Error bars represent standard deviation (n≥4).

4.4. Conclusion

CNF was successfully functionalized with norbornene groups (nCNF). Esterification reaction between surface hydroxyl groups of CNF and 5-norbornene-2,3-dicarboxylic anhydride in aqueous media was completed in two hours. Purification through centrifugation produced nCNF in dispersion form which facilitated re-dispersing of material. nCNF was successfully degraded by Cellulase enzyme to soluble glucose units. Degraded samples were characterized using ^{1}H-NMR spectroscopy to obtain the quantitative degree of functionality. With our knowledge, the quantitative ^{1}H-NMR spectroscopy was done for the first time. A light and thermal-induced thiol-norbornene reaction were used to cross-link nCNF with DEGl to fabricate hydrogels with dimensional stability. The modulus of cross-linked hydrogels are higher than nCNF, but the hydrogel modulus slightly changes with changing T/NB. The same range of modulus was observed when DTPEG was used as cross-linker. Therefore, mechanical properties of nCNF hydrogels are not highly tunable. However these hydrogels showed dimensional stability in aqueous media. It was observed that nCNF and nCNF-DEG hydrogel show shear-thinning behavior. In addition, hMSCs was seeded in nCNF-DEG hydrogels and survived for 7 days showing that nCNF can be potentially used in cell culture studies.

CHAPTER 5

DEVELOPING PRACTICAL METHODS TO USE CELLULOSE-BASED HYDROGELS IN REAL APPLICATIONS

5.1. Introduction

The potential of norbornene functionalized cellulose-based hydrogels cross-linked by thiol-norbornene reaction as scaffolds in biomedical application was introduced in previous chapters. To have these systems to be applied in real applications, new methods should be developed to make stable solutions that can be stored and reused whenever it is needed. Also, this new method should be simple and straightforward so everyone can use it. Matrigel is currently used for 3D cell culture and tissue regeneration studies. But it suffers from the lack of mechanical strength that is needed for specific experiments. Therefore, chemically cross-linked cellulose-based hydrogels with controllable modulus can be a potential alternative for Matrigel. To develop our method, we are collaborating with a research group in Jackson lab in Bar harbor, Maine, to use our materials and gelation systems for explant encapsulation.

Light-initiated hydrogel formation is a fast and straightforward gelation system. But, because our collaborators did not have the light source (365 nm, 10 mW/cm^2) in their lab, thermal gelation was chosen for this study. Thermal gelation with APS/TEMED (discussed in Chapter 4) is widely used in biological studies due to its activity at physiological conditions which was needed for explant encapsulation and its low toxicity.[153,154] In our previous works, all the components (backbone polymer, cross-linker, radical initiator) were dissolved in PBS and then heated or irradiated to form gels. The pre-gelation solution would gel even at room temperature in less than 30 minutes and must be prepared fresh each time.[140] Therefore, this system should be modified in order to be stable, stored, and be easily used by other researchers. Furthermore, in our

previous works, different amount of cross-linker was added to the pre-gelation solution to control the modulus. So, it was needed to find a practical method to control mechanical properties of the hydrogels in the new system.

To address all these issues, a two-solution approach was designed. One solution contained the backbone polymer and the other solution contained the cross-linker. With this approach, norbornene functionalized cellulose and the dithiol cross-linker was mixed right before the gelation and the modulus of gels were controlled by varying the amount of dithiol-containing solution. To prevent radical generation before mixing, APS and TEMED were separately stored in either solutions. Also, both solutions were made in cell-culture media (DMEM) to provide nutrients for explants or cells while gel is forming. The two-solution method was studied in the laboratory and under sterile conditions and the application of this method in explant encapsulation was studied by our collaborators.

5.2. Experimental

5.2.1. Materials

Chemicals were purchased from either Sigma-Aldrich or Fisher Scientific and used without further purification unless otherwise noted. The compounds 5-norbornene-2,3-dicarboxylic anhydride and 5-norbornene-2-methylamine were purchased from TCI America. Ammonium persulfate (APS) was purchased from Acros Organics. Peptides were purchased from Genscript and used without further purification. NorCMC was synthesized as described in Chapter 3, Section 3.2.2. The mold used throughout this study was cut from a rubber sheet (1 mm thickness) and punched in the middle to make a hole. The volume of the hole was determined to be 11 µL by adding water from a micropipette.

5.2.2. Synthesis of Carbic Functionalized CMC (cCMC)

Targeting 30% functionalization, 5 g of NaCMC 90,000 g/mol was dissolved in 495 mL of deionized water to obtain 1 wt% NaCMC solution. NaOH 10 M was added until pH 12 was obtained. To this solution, 36.30 g of 5-norbornene-2,3-dicarboxylic anhydride (carbic anhydride, 0.22 mol, 10 molar excess to NaCMC repeat units) was added which caused the pH to drop to 8.5. More NaOH 10 M solution was added dropwise in 10 second intervals to bring up to and keep the pH between 9.5-10.5 throughout the reaction. The pH decrease slowed down after 2 hours and pH stayed at 9.4 for an hour without change indicating the completion of reaction. Another indication of the end of the reaction was disappearance of carbic anhydride as it was insoluble in water and remained as a white precipitant in the solution which was getting dissolved as it was hydrolyzed.

After the reaction, 15 g NaCl was added to improve separation. Then, the solution was added to 3 L of ice-cold acetone dropwise and over an hour for more efficient precipitation. The carbic functionalized CMC (cCMC) was separated from impurities as a white precipitant and through filtration. The precipitant was dissolved in 250 mL DI water and dialyzed for four days prior to freeze-drying. The final product was 3.4 g and the yield of the reaction was around 56%. The functionalization was confirmed and the degree of functionality was calculated to be 30% by ^{1}H-NMR spectroscopy (Figure 5.1).

^{1}H-NMR spectroscopy of cCMC (D_2O , 400 MHz) δ 1.17 ppm (Norbornene bridge -CH_2, Triplet, 2Hs) 2.90 ppm (Norbornene ester, -CH, Singlet, 1H), 3-4 ppm (Glucose backbone, broad), , 6.07 ppm (Norbornene double bond, singlet, 2Hs).

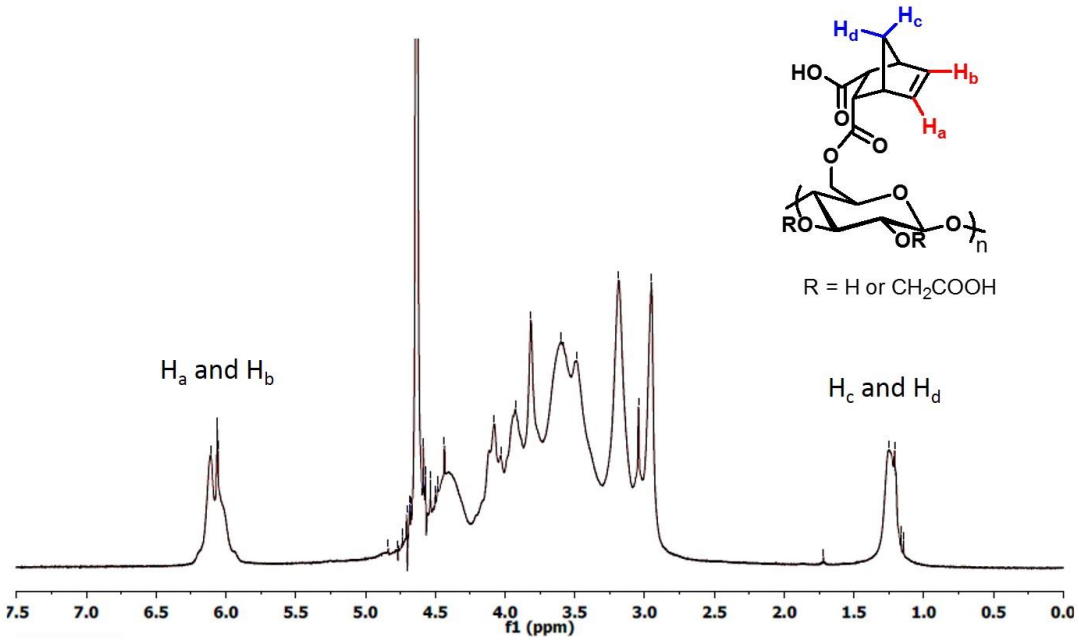

Figure 5.1. The ^{1}H-NMR spectrum of cCMC. Norbornene protons (6.07 ppm) and bridge protons (1.17 ppm) are labeled. The rest of the carbic protons and CMC backbone protons are between 2.9-4 ppm.

5.2.3. cCMC/DEG Hydrogel Formation

CT/DA Combination: For 50 µL CT solution, 0.004 g cCMC was dissolved in 47.4 µL of DMEM along with 0.5 µL of TEMED (2 M). For 50 µL DA solution, 0.4 µL DEG and 0.5 µL of APS (2 M) were dissolved in 47.4 µL of DMEM. To make hydrogels with 4 wt% cCMC, T/NB=1, and 10 mM APS/TEMED, 5.5 µL of each solution were transferred to the mold and mixed using pipette tip. The mold was sealed with coverslip and incubated at 37 °C for 20 minutes for complete gelation.

CA/DT Combination: To make hydrogels in 11 µL molds, solutions were made as cCMC/APS (CA) and Dithiol cross-linker/TEMED (DT). CA solution (500 µL) was prepared by dissolving 0.0225 g of cCMC in 474.7 µL of cell culture media (DMEM). Afterward, 2.8 µL APS (2 M) was added and mixed. For DT solution (100 µL) preparation, 4 µL of DEG and 5 µL of TEMED (2 M) were added to 91 µL of PBS and vortexed.

To have hydrogels with 4 wt% cCMC, T/NB=1, and 10 mM APS/TEMED, 10 µL of CA was added to the mold and then 1 µL of DT was added and mixed by pipette tip. The mold was sealed with coverslip and incubated at 37 °C for 20 minutes for complete gelation. The volume of DT solution added could vary to change T/NB and therefore modulus of hydrogels.

For rheology measurements, CA solution was prepared as 0.028 g of cCMC was dissolved in 598.5 µL of DMEM. APS (3.5 µL of 2 M solution in DI water) was added and vortexed right before transferring to the rheometer plate. To prepare DT, 2.8 µL of DEG and 3.5 µL of TEMED (2 M) were added to 63.8 µL PBS and vortexed. CA (630 µL) was transferred to rheometer plate first and then DT (70 µL) was added and mixed using pipette tip. This combination contains 4wt% cCMC, T/NB=1, and 10 mM APS/TEMED.

5.2.4. NorCMC/DEG Hydrogel Formation

To make hydrogels in 11 µL molds, solutions were made as NorCMC/APS (CA) and DEG/TEMED (DT). CA solution (100 µL) was prepared by dissolving 0.0045 g of NorCMC (22% functionalized) in 95 µL of DMEM. Then, 0.65 µL of APS (2 M) was added and mixed. For DT solution (100 µL) preparation, 4 µL of DEG and 5 µL of TEMED (2 M) were added to 91 µL of PBS and vortexed.

To have hydrogels with 4 wt% NorCMC, T/NB=1, and 10 mM APS/TEMED, 10 µL of CA was added to the mold and then 1 µL of DT was added and mixed by pipette tip. The mold was sealed with coverslip and incubated at 37 °C for 20 minutes for complete gelation. The volume of DT solution added could vary to change T/NB and therefore modulus of hydrogels.

For rheology measurements, CA solution (630 µL) was made by dissolving NorCMC (0.028 g) in 595 µL of DMEM followed by adding 7 µL of APS (1 M) and DT (70 µL) was prepared by dissolving 2 µL of DEG and 3,5 µL of TEMED (2 M) in 64.5 µL PBS. CA (630 µL) was transferred to rheometer plate first and then DT (70 µL) was added and mixed using pipette tip. This combination contains 4wt% NorCMC, T/NB=1, and 10 mM APS/TEMED.

5.2.5. NorCMC/MMP-deg Hydrogel Formation

In a representative experiment for hydrogel fabrication in 11 µL molds, separate CA and DT solutions were prepared and mixed in the molds. To prepare CA solution (360 µL), 0.0177 g NorCMC (22% functionalized) was dissolved in 226.8 µL DMEM. Then, 110.1 µL of RGD (GCGYGRGDSPG peptide sequence) solution (10 mg RGD/mL of DMEM,) was added and mixed. At the end, 5.4 µL of APS (1 M in DI water) was added. The DT solution (82.5 µL) was prepared by dissolving 0.015 g MMP sensitive peptide (MMP-deg) (GCRDGPQGIWGQDRCG peptide sequence) in 43 µL of PBS. TEMED (25 µL of 1 M solution in DI water) was added and vortexed to mix withDEG

and. To make a hydrogel, 9 µL of CA first was transferred to a 11 µL mold and then 2 µL of DT solution was added. Two solutions were mixed using a pipette tip to be homogenous. A glass coverslip was used to seal the mold. Molds were transferred to the incubator at 37 °C for 20 minutes for complete gelation. With this combination, the final gel would be at 4 wt% NorCMC, T/NB=1, and 10 mM APS/TEMED.

For rheology measurements, CA solution was prepared as 0.025 g of NorCMC (22% functionalized) was dissolved in 262 µL of DMEM. RGD (127 µL of 10 mg/mL solution in DMEM) and APS (3.5 µL of 2 M solution in DI water) were added and vortexed right before transferring to the rheometer plate. To prepare DT, 0.01 g of MMP-deg and 3.1 µL of TEMED (2 M) were dissolved in 197 µL of PBS and vortexed. CA was transferred to rheometer plate first and then DT was added and mixed using pipette tip. This combination contains 4wt% NorCMC, T/NB=0.5, 2 mM RGD and 10 mM APS/TEMED.

5.2.6. Rheology measurements

Maximum storage modulus of solutions were obtained from a rheological time sweep experiment (TA Discovery HR-2 rheometer) using a 40 mm aluminum cone-plate geometry with a 2° angle. CA (630 µL) and DT (70 µL) were transferred to an aluminum Pelletier plate at room temperature. The fixture was lowered to the geometry gap (60 µm). Water droplets were placed around the geometry and covered with a plastic cup to keep the surrounding humid to assure that hydrogels are not drying during the run. Time sweep measurements was run at 37 °C, 1 Hz oscillatory frequency, and 1 % oscillatory strain for 1500 seconds.

5.2.7. Sterilization of materials and equipment

The final solutions to be used for explant encapsulation must be sterilized. The preparation of solutions was done under sterile biosafety cabinet (Labconco). NorCMC, cCMC, and all the equipment used to prepare solutions for Jackson lab were sterilized by 10 minutes germicidal/sterilization UV light (254 nm) irradiation prior to use. APS solution, TEMED solution, and DEG were sterilized by passing through sterile filters filtered (Santa Cruz Biotechnology, PVDF membrane, pore size 0.22 μm) prior to use. MMP degradable peptide and RGD adhesion peptide were purchased sterile.

5.3. Results and Discussion

5.3.1. CT/DA or CA/DT combination for Hydrogel Formation

Two combinations were possible for pre-gelation solutions as cCMC could be mixed with either TEMED or APS and the cross-linker could be mixed with the other one (APS or TEMED). Both combinations were investigated to find the better approach. The third possible combination was to mix cCMC, cross-linker, and either APS or TEMED. But based on previous studies, cCMC and cross-linker gelled at room temperature even if no initiator was present (Autogelation).[140] Therefore, cCMC and cross-linker should be stored separately. All combinations used in this study are summarized in Table 5.1. Also a schematic of how to prepare and mix solutions is shown in Figure 5.2.

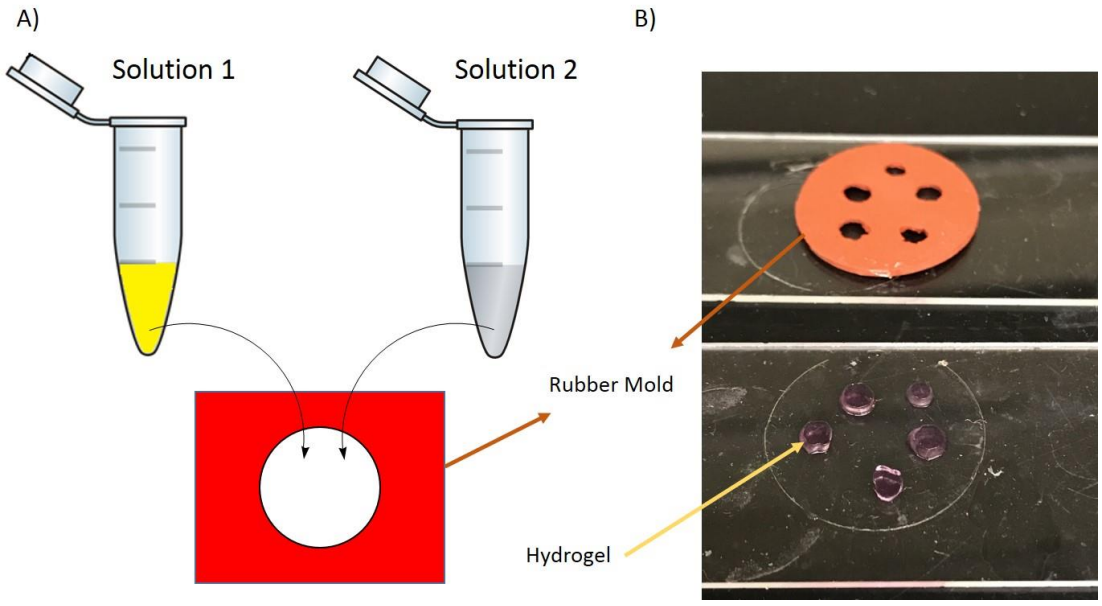

Figure 5.2. Schematic of solution preparation and gel Formation in small molds. A) Schematic of how solution A and solution B were prepared separately and mixed in the rubber mold. B) The image shows a) the 11 µL molds in a glass slide. b) Resulting hydrogels (after mold was removed) on the second glass slide that was used to seal the mold.

Table 5.1. The combinations of solution A and solution B used throughout this study are summarized.

	Components					
Exp.	Solution A	Solution B	A:B	Minimum Gel Time (min)	Stability	Freeze/Thaw
1	CT cCMC TEMED Media	DA DEG APS Media	50:50	10	DA was cloudy	DA precipitated
2	CT cCMC TEMED Media	DA DEG APS PBS	90:1	10	DA was cloudy	Longer gel time (20 min.)
3	CT NorCMC TEMED Media	DA DEG APS PBS	90:10	Not gelled	DA was cloudy	---
4	CA cCMC APS Media	DT DEG TEMED PBS	90:1	10	CA and DT clear	Two cycles of F/T Gelled at 10 min
5	CA NorCMC APS Media	DT DEG TEMED PBS	90:10	5	CA and DT clear	Three cycles of F/T Gelled at 5 min
6	CA NorCMC APS RGD Media	DT MMP-deg. TEMED PBS	80:20	5	CA and DT clear	Three cycles of F/T Gelled at 5 min

Since the targeted application of this gelation system was to encapsulate an explant, physiological conditions (37°C and pH 7.4) for gelation and cell culture media (DMEM) were essential. Moreover, showing the similar reactivity after freeze/thaw cycles was important to confirm the stability of the solutions for storage. At first, 50:50 volume ratio of two solutions in DMEM were considered. The amount of cCMC, DEG, and APS/TEMED needed for 100 µL of pre-gelation solution (4 wt% cCMC T/NB=1, 10 mL APS/TEMED) were calculated. This combination gelled after 20 minutes incubation at 37 °C. However, it was observed that after 2 hours, the solution of DEG in DMEM got cloudy and after freeze/thaw it completely precipitated. One hypothesis could be the formation of disulfide bonds between thiols of DEG and thiols of proteins presented in DMEM. Therefore, dissolving DEG into PBS was considered. But to increase the ratio of DMEM to PBS at the final pre-gelation solution, the higher CT to DA ratio (90:10 of CT:DA) was used. This mixture also gelled after 20 minutes incubation at 37 °C. After two hours of being stored, the solution of cCMC and TEMED in DMEM (CT) was clear, but a decrease in clarity of the solution was observed when DEG was mixed with APS. Even at room temperature, APS decomposes to form radicals. At the presence of these radicals, the formation of disulfide bonds between DEG molecules is probable which leads to a decrease in number of free thiols. Also, disulfide bonds between DEG molecules could form dithiols with molecular weights twice or three times (or more) higher than DEG. Less crosslink points and higher MW between cross-links lower the storage modulus of final hydrogel. Rheology measurements showed that the storage modulus decreased (50%) when solutions were at room temperature for 2 hours compare to when solutions were tested immediately after preparation (Figure 5.3). This result shows the low stability of CT/DA solutions.

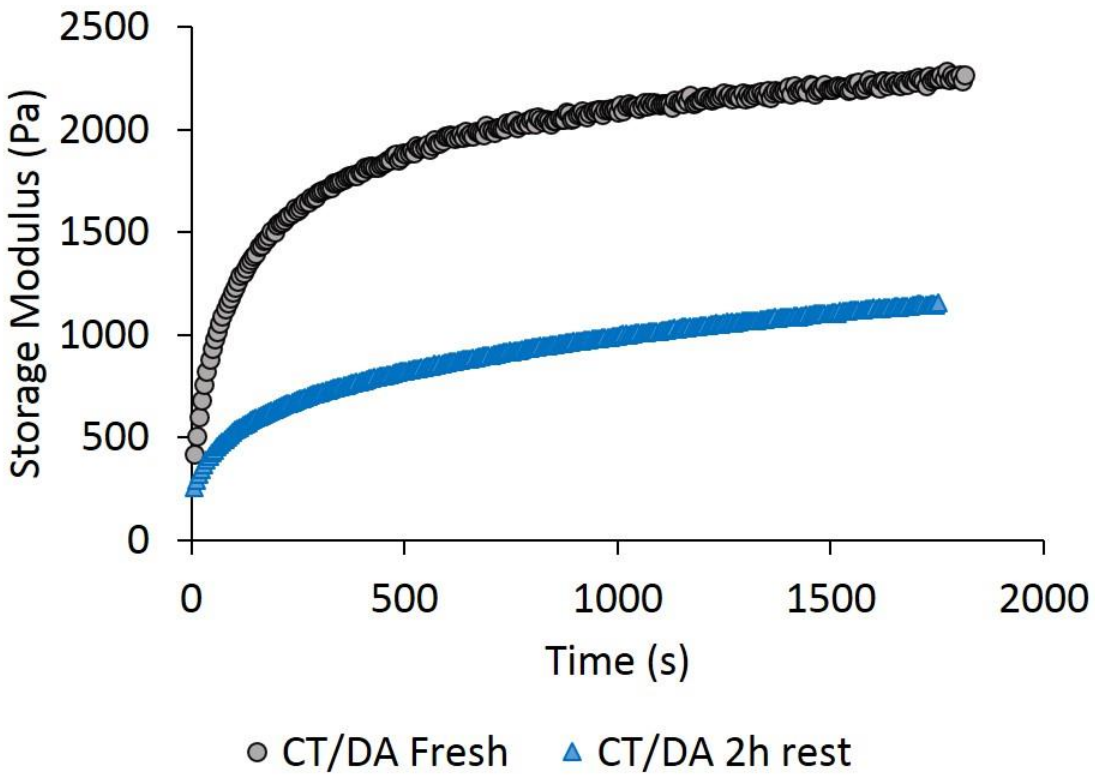

Figure 5.3. Time sweep rheology of CT/DA combination. Time sweep (1 Hz, 1 % strain, 37 °C) rheology measurements of the storage modulus of hydrogels made from mixing two solutions CT (630 µL) and DA (70 µL) when CT/DA solutions were tested as made (black circle) and after 2 hours sitting separately at RT (gray triangle). The mixed solution was at 4 wt% cCMC, T/NB=1, and 10 mM APS/TEMED.

Due to lack of stability, the combinations of DEG with TEMED and therefore cCMC with APS were investigated. Mixing these two solutions (10:1 of CA:DT) led to hydrogel formation after 20 minutes of incubation at 37 °C. CA and DT solutions were frozen at -20 °C for 24 hours and then thawed at room temperature. The gelation procedure was repeated and stiff hydrogels were obtained. This freeze/thaw cycle was repeated three times and after each cycle gels were formed indicating the stability of CA/DT solutions and the ability of being stored and reused. Autogelation (gelation without any radical initiator added) was tested for two solution systems but no gel formed. Rheology measurements of the maximum storage modulus of hydrogels made of fresh CA/DT and 2-hour-old CA/DT were compared with fresh CT/DA combination. Figure 5.4 shows that the modulus of resulting hydrogel when solutions are mixed and tested immediately after

preparation are very similar and even higher modulus was observed for hydrogels from resting solutions (opposite of what was observed for CT/DA). The modulus of CA/DT combination is more than twice of when the CT/DA was used and shows the higher stability of CA/DT compare to CT/DA. The higher storage modulus for CA/DT combination as compared to CT/DA combination confirms that CA/DT is the desired combination for this gel formation system. In a constant polymer wt%, T/NB, and initiator concentration, the higher modulus indicates that more free thiols and norbornenes were available to react. In CA solution also APS decomposes to radicals, but norbornene double bonds have a very low tendency to polymerize so the reduction of number of reactive groups is not an issue as it happened for DEG. Therefore, the CA/DT combination was used for studies.

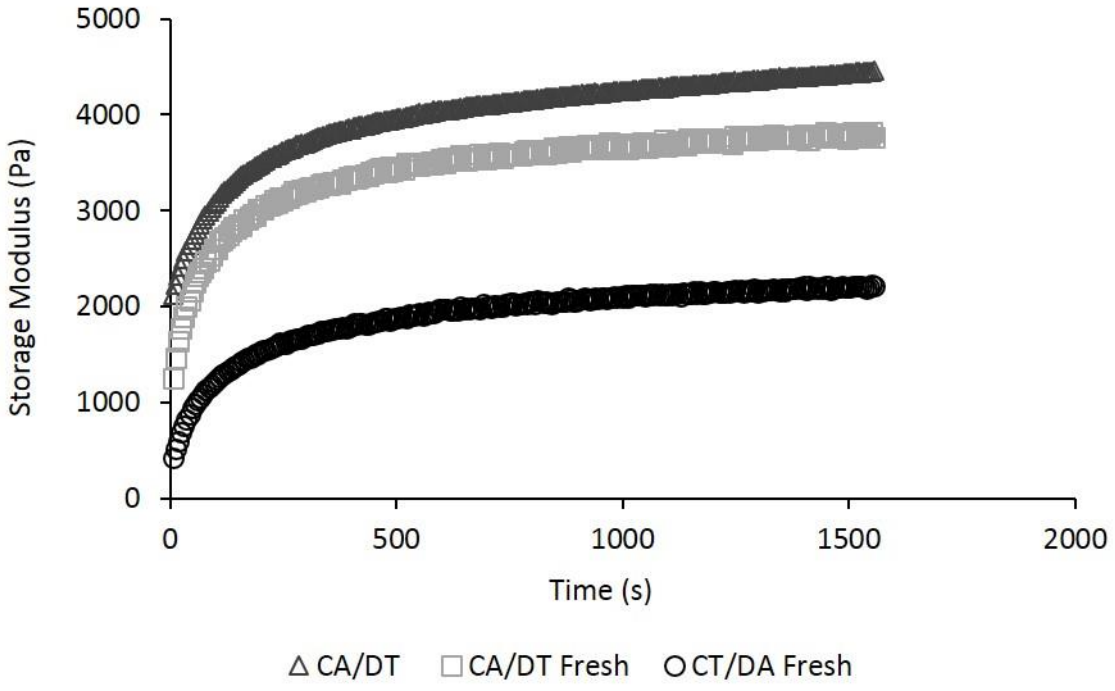

Figure 5.4. Time sweep rheology of CA/DT combination (1 Hz, 1 % strain, 37 °C). Rheology measurements of the storage modulus of hydrogels made from mixing two solutions CA (630 µL) and DT (70 µL) when CA/DT solutions were tested as made (light gray rectangle) and after 2 hours sitting separately at RT (dark gray triangle) and the freshly tested CT/DA combination (black circles) for comparison. The mixed solution was at 4 wt% cCMC, T/NB=1, and 10 mM APS/TEMED.

5.3.2. Controlling the Modulus of Hydrogels

Since the stiffness of the hydrogel has a major impact on the behavior of encapsulated cells, the control over mechanical properties of the hydrogels by changing the amount of DEG added was studied. The maximum storage modulus was measured by time sweep rheological measurements. The CA solution formulations were the same for all the samples but DT solutions were prepared varying the amount of DEG added to reach different T/NB ratios. As shown in Figure 5.5, the maximum storage modulus increased by increasing the amount of DEG added with a more remarkable jump from T/NB=0.3 to 0.5 (0.48 kPa and 2.2 kPa respectively). No gelation was obtained when T/NB was 0.1. The highest modulus was obtained was 5.1 kPa for T/NB=2. The storage modulus increased two order of magnitude when T/NB changed from 0.2 to 0.5. Also it did not decrease for T/NB higher than 1 suggesting that a portion of thiols (DEG) are consumed by disulfide bond formation with DMEM proteins. In real applications, hydrogels with desired modulus for a specific experiment can be made by simply adding different volumes of DT solutions.

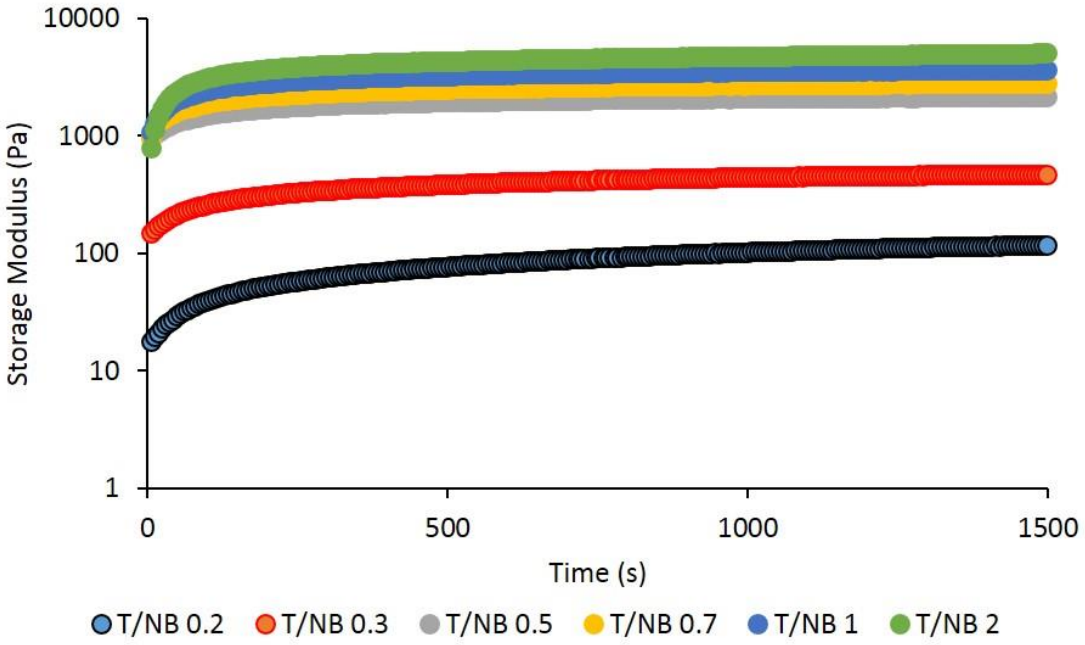

Figure 5.5. Time sweep rheology of CA/DT combination varying T/NB. Time sweep (1 Hz, 1 % strain, 37 °C) rheology measurements of the storage modulus of hydrogels made from mixing two solutions CA (630 µL in DMEM) and DT (70 µL in DMEM) when CA/DT solutions were tested as made at different T/NB. The mixed solution was at 4 wt% cCMC, and 10 mM APS/TEMED for all samples.

The increasing trend of modulus from T/NB=0.2 to 1 was expected as the number of cross-links increases. At T/NB higher than 1, the modulus is expected to decrease because the number of thiols exceeds the number of norbornenes and saturates NB groups without forming effective cross-links. Unexpectedly, the increasing trend in modulus was observed when T/NB was 2. On the other hand, compression modulus obtained for cCMC/DEG hydrogels at T/NB of 0.5 and 1 for thermally gelled samples are significantly lower compare to UV-irradiated gels.[140] UV-initiated cCMC/DEG (4 wt% cCMC, 0.05 wt% I2959, 1 minute UV irradiation at 10 mW/cm^2) gel formation in PBS at T/NB of 0.5 and 1 has been done previously, the compression moduli of 75 and 80 kPa were reported for these gels, respectively.[140] The compression modulus of cCMC/DEG hydrogels at T/NB of 1 in DMEM (4 wt% cCMC, 10 mM APS/TEMED, 20 minutes incubation at 37°C) was measured to be 7.6±2.0, which is almost an order of magnitude lower. This modulus is even lower

than the modulus of cCMC/DEG (4 wt% cCMC, T/NB=1, in PBS) hydrogels made without any radical initiation system (Autogel) which was reported to be around 30 kPa.[140] The thermally gelled cCMC/DEG hydrogels at T/NB of 0.5 in DMEM were not stiff enough to be measured by DMA. Although all these abovementioned DMA experiments were done based on one-solution gelation and cannot be directly applied for the data obtained from two-solution method, this comparison suggests that using DMEM instead of PBS has a significant negative impact on the modulus of cCMC/DEG hydrogels. One reason for this lower modulus is the formation of disulfide bonds between thiols of DEG and thiols of cysteine of proteins presented in DMEM. As a result of disulfide bond formation, the moles of available DEG would be lower than what was added. This assumption explains the higher storage modulus of cCMC/DEG hydrogels when T/NB was higher than 1 (Figure 5.5 and Table 5.1).

5.3.3. NorCMC/MMP-deg hydrogels

Since low cell viability was reported from collaborators at Jackson lab for cCMC/DEG, NorCMC was used to replace cCMC. The viability of NorCMC was previously studied in Chapter 3 and showed to be acceptable (85%) after 21 days of study. Thermal gelation and stability after freeze/thaw cycles of CA/DT system using NorCMC and DEG were tested using 11 µL molds and under the same conditions as described for cCMC/DEG hydrogels (4 wt% NorCMC, T/NB=1, 10 mM APS/TEMED, and 37 °C). The mixture gelled after 5 minutes of incubation, but they were incubated for 20 minutes to ensure the complete gelation. Solutions were frozen at -20 °C and thawed at room temperature and tested again. The NorCMC/DEG hydrogel formed again after 5 minutes of incubation at 37 °C. This freeze/thaw cycle was repeated two more times and the same gel formation was observed after each cycle. This showed that NorCMC is an appropriate polymer to replace cCMC.

The storage modulus of NorCMC/DEG hydrogels made of mixing CA/DT solutions (freshly made solutions and after freeze/thaw process) were measured from time sweep rheological experiments (1 Hz, 1% strain, and 37 °C). As shown in Figure 5.6, the modulus of resulting hydrogel when solutions are frozen and thawed are even higher than the modulus was observed for hydrogels from fresh solutions (9 kPa and 7 kPa respectively) showing the stability of NorCA/DT solutions for storing.

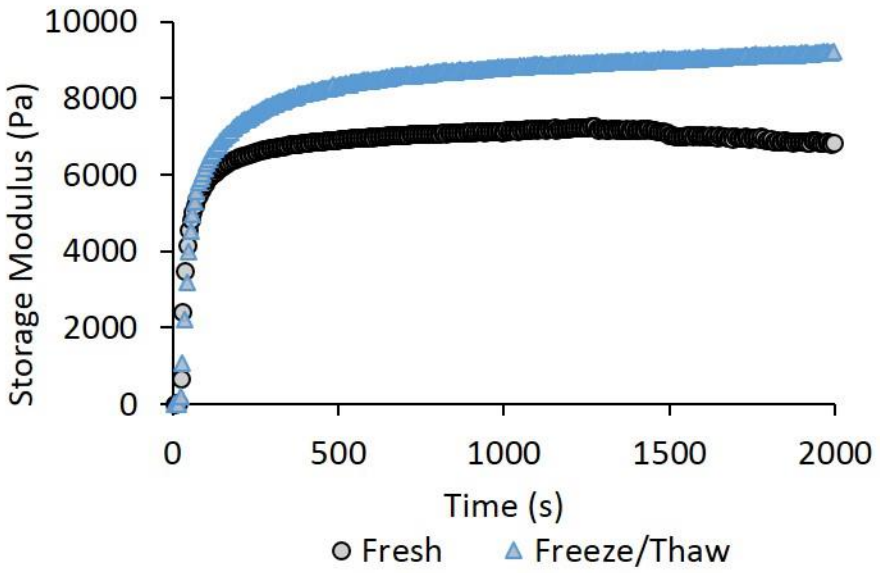

Figure 5.6. Time sweep rheology of CA/DT combination after fFreeze/thaw. Time sweep (1 Hz, 1 % strain, 37 °C) rheology measurements of the storage modulus of NorCMC/DEG hydrogels made from mixing two solutions CA (630 µL) and DT (70 µL) when CA/DT solutions were tested as made (black circles) and after being frozen (at -20°C) and thawed at RT (for 30 minutes) separately (blue triangle). The mixed solution was at 4 wt% NorCMC, T/NB=1, and 10 mM APS/TEMED.

To improve the properties of the hydrogels, other than replacing cCMC with NorCMC, we also tried to use a degradable cross-linker (MMP-deg) instead of the non-degradable DEG. Also, RGD peptide added to enhance cell adhesion to the matrix. RGD has a cysteine in its sequence and MMP-deg has two cysteine at both ends of its sequence that could react with norbornene double bond. Thermal gelation and stability of solutions after freeze/thaw was studied and same results was observed as compare to NorCMC and DEG CA/DT solutions. Again, the autogelation (gelation

when no initiator is present) after mixing solutions did not occur with these solutions. To investigate the effect of adding RGD peptide on the modulus of final hydrogels, the storage modulus of NorCMC/DEG hydrogels with RGD (4 wt%, 2 mM RGD, 10 mM APS/TEMED) and without RGD (4 wt%, 10 mM APS/TEMED) at T/NB of 0.5 and 1 was compared from rheology time sweep experiments (1 Hz, 1% strain, and 37 °C).

As shown in Figure 5.7, for both T/NB of 0.5 and 1, presence of RGD reduced the storage modulus of hydrogels. This can be explained by the competition between RGD and cross-linker to react with norbornene groups as T/NB for RGD is 0.1 in the solution. The storage modulus of NorCMC hydrogels cross-linked by MMP degradable peptide at the presence of RGD was also obtained by rheology (Figure 5.7). The storage modulus of NorCMC/MMP-deg was 1.3 kPa which is lower than the modulus of NorCMC/DEG hydrogel (3 kPa) under the same condition (4 wt% NorCMC, T/NB=0.5, 2 mM RGD, 10 mM APS/TEMED, 37°C). The modulus of hydrogel has an inverse relation with the MW between cross-links. So, because the MW of MMP-deg is higher than MW of DEG, this lower modulus for NorCMC/MMP-deg hydrogel was expected. The thiol to norbornene ratio for NorCMC/MMP-deg hydrogels was chosen to be 0.5 because MMP-deg peptide has a high molecular weight (1704.85 g/mol) and therefore higher T/NB than 0.5 leads to hydrogels in which NorCMC is no longer the major component (matrix).

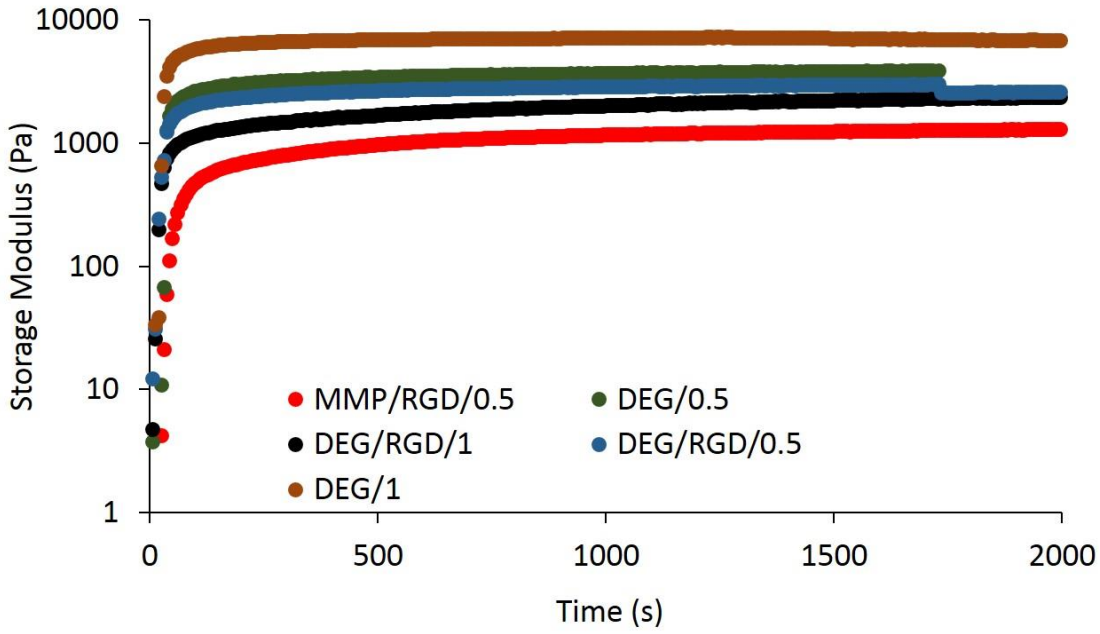

Figure 5.7. Time sweep rheology of CA/DT combination using MMP-deg cross-linke. Time sweep (1 Hz, 1 % strain, 37 °C) rheology measurements of the storage modulus of NorCMC/DEG hydrogels made from mixing two solutions CA (630 µL) and DT (70 µL) with and without RGD adhesion peptide at T/NB of 0.5 and 1. The mixed solution was at 4 wt% NorCMC, 10 mM APS/TEMED, 0 or 2 mM RGD.

5.4. Conclusion

The properties of NorCMC hydrogels and cCMC hydrogels was previously studied and it has been shown that norbornene functionalized CMC is a promising candidate for applications in cell culture scaffolds.[140] For application of these materials in actual experiments by biomedical research groups such as explant encapsulation, a product should be provided that can be shipped and stored, be stable over time, and be easy to use. For this, pre-gelation solution was divided into two separate solutions each of them contains either matrix polymer or cross-linker. NorCMC or cCMC were dissolved into DMEM as one solution and the dithiol cross-linkers (DEG or MMP-deg.) were dissolved in PBS as the second solution. Hydrogels were made successfully with two-solution approach using CA/DT combination and also it was shown that hydrogels still form after three cycles of freezing/thawing solutions. The observed gelation was supported by rheology experiments. Gelation was not observed when radical initiators were not present (Failed to autogel). This study will be continued using portable UV lamp (365 nm, 10 mW/cm^2) at the presence of UV-based radical initiator (I2959).

REFERENCES

(1) Chang, Ch., Zhang, L., Cellulose-based hydrogels: Present status and application prospects, Carbohydr. Polym. 2011, 84 (1), 40-53, DOI: 10.1016/j.carbpol.2010.12.023

(2) Akala, E.O.; Kopeckova, Kopecek, P.J., Preparation,Novel pH-sensitive hydrogels with adjustable swelling kinetics. Characterization and Controlled Release, *Biomaterials* **1998**, 19, 1037-1047, DOI:10.1016/S0142-9612(98)00023-4

(3) Li, F.; Carlsson, D.; Lohmann, C.; ,Suuronen, E.; Vascotto, S.; Kobuch, K.; Sheardown, H.; Munger, R.; Nakamura, M.; Griffith, M., Cellular and nerve regeneration within a biosynthetic extracellular matrix for corneal transplantation, *PNAS* **2003**, 100, 15346-15351, DOI:10.1073/pnas.2536767100

(4) Stile, R.A.; Healy, K.E., Thermo-responsive peptide-modified hydrogels for tissue regeneration, *Biomacromolecules* **2001**, 2, 185-194, **DOI:**10.1021/bm0000945

(5) Sannino, A., Demitri, Ch., Madaghiele, M., Biodegradable Cellulose-based Hydrogels: Design and Applications, *Materials* **2009**, *2*(2), 353-373; DOI:10.3390/ma2020353

(6) Frantz, Ch., Stewart, K. M., Weaver, V. M., The ectracellular matrix at a glance, J. of Cell Science 2010, 123, 4195-4200, DOI: 10.1242/jcs.023820

(7) Sausa, F., Netti, P. A., Ambrosio, L., A multi-functional scaffold for tissue regeneration: The need to engineer a tissue analogue, Biomaterials 2007, 28 (34), 5093-5099, DOI: 10.1016/j.biomaterials.2007.07.030

(8) Muhamad, I. I., Fen, L. S., Hui, N. H., Mustapha, N. A., Genipin-cross-linked kappa-carrageenan/carboxymethyl cellulose beads and effects on beta-carotene release, *Carbohydrate Polymers* **2011**, 83,1207, 10.1016/j.carbpol.2010.09.021

(9) Butun, F. G. Ince, H. Erdugan, N. Sahiner, One-step fabrication of biocompatible carboxymethyl cellulose polymeric particles for drug delivery systems, *Carbohydrate Polymers* **2011**, 86, 636. 10.1016/j.carbpol.2011.05.001

(10) Sakai, Y. Ogushi, K. Kawakami, Enzymatically crosslinked carboxymethylcellulose-tyramine conjugate hydrogel: cellular adhesiveness and feasibility for cell sheet technology, *Acta Biomaterialia* **2009**, 5, 554. 10.1016/j.actbio.2008.10.010

(11) Oh, E. J., Park, K., Kim, K. S., Kim, J., Yang, J.-A., Kong, J.-H., Lee, M. Y., Hoffman, A. S., Hahn, S. K., Target Specific and Long-Acting Delivery of Protein, Peptide, and Nucleotide Therapeutics Using Hyaluronic Acid Derivatives. *J of Controlled Release*, **2010**, *141, 2-12.* 10.1016/j.jconrel.2009.09.010

(12) Schante, C. E., Zuber, G., Herlin, C., Vandamme, T. F., Chemical Modifications of Hyaluronic Acid for the Synthesis of Derivatives for a Broad Range of Biomedical Applications. *Carbohydrate Polymers*, **2011**, *85, 469-489* 10.1016/j.carbpol.2011.03.019

(13) Phillips, M. A.; Gran, M. L.; Peppas, N. A.,Targeted nanodelivery of drugs and diagnostics, *Nano Today* **2010**, 5, 143-159, DOI:10.1016/j.nantod.2010.03.003

(14) Francis, R.; Baby, D. K.; Sakthi, K. D., Poly(N-isopropylacrylamide) Hydrogel: Effect of hydrophilicity on controlled release of Ibuprofen at different pH, *Journal of Applied Polymer Science* **2012**, 124, 5079-5088, DOI 10.1002/app.35644

(15) Nolan, C. M.; Serpe, M. J.; Lyon, L. A., Thermally Modulated Insulin release from microgel thin films, *Biomacromolecules* **2004**, 5, 1940-1946*,* DOI:10.1021/bm049750h

(16) Hoffmann, J.; Plotner. M.; Kuckling, D.; Fischer, W.J., Photopatterning of thermally sensitive hydrogels useful for microactuators, *Sensors and Actuators* **1999**, 77, 139-144, DOI:10.1016/S0924-4247(99)00080-1

(17) Ito, Y.; Chen, G.; Guan, Y.; Imanishi, Y., Patterned immobilization of thermoresponsive polymer, *Langmuir* **1997**, *13,* 2756-2759, **DOI:**10.1021/la961087y

(18) Sahiner, N., Jia, X., One step synthesis of hyaluronic acid-based hydrogel particles: Process, optimization and preliminary characterization. *Turk J. Chem*. **2008**, 32, 397-409

(19) Menaa, F., Menaa, A., Menaa, B., Hyaluronic acid and derivatives for tissue engineering, *J Biotechnol Biomaterial* **2011**, 1-7, DOI:10.4172/2155-952X.S3-001,

(20) Price, R. D., Berry, M. G., Navsaria, H. A., Hyaluronic acid: the scientific and clinical Evidence, *Journal of Plastic, Reconstructive & Aesthetic Surgery* **2007** 60, 1110-1119, DOI:10.1016/j.bjps.2007.03.005

(21) Camci-Unal, G., Cuttica, d., Annabi, N., Demarchi, D.,Khademhosseini, A., Synthesis and characterization of hybrid hyaluronic acid-gelatin hydrogels, *Biomacromolecules* **2013**, 14, 1085−1092, DOI:10.1021/bm3019856

(22) Wu, Sh., Xu, R., Duan, B., Jiang, P., Three-dimensional hyaluronic acid hydrogel-based models for *in vitro* human iPSC-derived NPC culture and differentiation , *J. Mater. Chem. B***,** 2017,**5**, 3870-3878 DOI:10.1039/C7TB00721C

(23) Peterson, N., Gatenholm, P., Bacterial cellulose-based materials and medical devices: current state and perspectives, Appl. Microbiol. Biotechnl. 2011, 91, 1277, DOI:10.1007/s00253-011-3432-y

(24) Lou, Y.-R., Kanninen, L., Kuisma, T., Niklander, J., Noon, L. A., Burks, D., Urtti,A., Yliperttula, M., The Use of Nanofibrillar Cellulose Hydrogel As a Flexible Three-Dimensional Model to Culture Human Pluripotent Stem Cells, *Stem Cells and development* **2014**, 23(4) DOI:10.1089/scd.2013.0314

(25) Roy, D., Semsarilar, M.,Guthria, J. T., Perrier, S., Cellulose modification by polymer grafting: a review *Chem. Soc. Rev.***, 2009**,38, 2046-2064 10.1039/B808639G

(26) Liu, J., Li, L., Cai Y., Immobilization of camptothecin with surfactant into hydrogel for controlled drug release*, European Polymer Journal* **2006**, 42, 1767-1774.

(27) Vasile, C., Bumbu G. G., Dumitriu, R. P., Staikos, G., Comparative study of the behavior of carboxymethyl cellulose-g-poly (N-isopropylacrylamide) copolymers and their equivalent physical blends*European Polymer Journal* **2004**, *40*, 1209-1215.

(28) Reza, A. T., Nicoll, S. B., Characterization of novel photocrosslinked carboxymethylcellulose hydrogels for encapsulation of nucleus pulposus cells*Acta Biomaterialia* **2010**, *6*, 179-186.

(29) Ko, I. K.**,** Kato**,** K., Iwata**,** H., A thin carboxymethyl cellulose culture substrate for the cellulase-induced harvesting of an endothelial cell sheet**,** *J. Biomater. Sci. Polymer Edn.* 2005, 16 (10), 1277-1291.

(30) E. Entcheva, H. Bien, L. Yin, C.-Y. Chung, M. Farrell, Y. Kostov, Functional cardiac cell constructs on cellulose-based scaffolding*Biomaterials* **2004**, *25*, 5753.

(31) Lin, H. A.; Gupta, M. S.; Varma, D. M.; Gilchrist, M. L.; Nicoll, S. B., Lower Crosslinking Density Enhances Functional Nucleus Pulposus-like Matrix Elaboration by Human Mesenchymal Stromal Cells in Carboxymethyl Cellulose Hydrogels, *J. Biomedical Materials Res.* **2016**, 104A, 1, 165-177, DOI: 10.1002/jbm.a.35552

(32) Gupta, M. S.; Nicoll, S. B., Functional Nucleus Pulposus-like Matrix Assembly by Human Mesenchymal Stromal Cells Is Directed by Macromer concentration in Photocrosslinked Carboxymethyl Cellulose Hydrogels, Cell Tissue Res. 2014, 358, 527-539, DOI: 10.1007/s00441-014-1962-1

(33) Gao, X.; Cao,Y.; Song,X.; Zhang, Z.; Zhuang, X.; He, C.; Chen, X., Biodegradable, pH-Responsive Carboxymethyl Cellulose/Poly(Acrylic Acid) Hydrogels for Oral Insulin Delivery, *Macromol. Biosci.* **2014**, 14, 565-575, DOI: 10.1002/mabi.201300384

(34) Akara, E.; Altınıs¸ A.; Sekib, Y., Preparation of pH- and Ionic-Strength Responsive Biodegradable Fumaric Acid Crosslinked Carboxymethyl Cellulose. *Carbohydrate Polymers* **2012**, 90, 1634-1641, DOI:10.1016/j.carbpol.2012.07.043

(35) Chang. C.; Han, K.; Zhang, L., Structure and properties of cellulose/poly(N-isopropylacrylamide) hydrogels prepared by IPN strategy. *Polym. Adv. Techol.* **2011**, 22, 1329-1334, DOI: 10.1002/pat.1616

(36) Barbucci, R.; Magnani, A.; Consumi, M., Swelling Behavior of Carboxymethylcellulose Hydrogels in Relation to Cross-Linking, pH, and Charge Density, *Macromolecules* **2000,** *33,* 7475-7480, DOI:10.1021/ma0007029

(37) Pal, K.; Banthia, A. K.; Majumdar, D. K., Preparation of Novel pH-Sensitive Hydrogels of Carboxymethyl Cellulose Acrylates: A Comparative Study, *Materials and Manufacturing Processes* **2006**, 21, 877-882, DOI: 10.1080/10426910600773464

(38) Pal, K.; Banthia, A. K.; Majumdar, D, K., Development of Carboxymethyl Cellulose Acrylate for Various Biomedical Applications, *Biomed. Mater.* 2006, 1, 85-91, DOI:10.1088/1748-6041/1/2/006

(39) Rokhade, A. P.; Agnihotri, S. A.; Patil, S. A.; Mallikarjuna, N. N.; Kulkarni, P. V.; Aminabhavi, T.M., Semi-interpenetrating Polymer Network Microspheres of Gelatin and Sodium Carboxymethyl Cellulose for Controlled Release of Ketorolac Tromethamine, *Carbohydrate Polymers* **2006**, 65243-252, DOI:10.1016/j.carbpol.2006.01.013

(40) Bajpai, A. K.; Mishra, A., Preparation and Characterization of Tetracycline-loaded Interpenetrating Polymer Networks of Carboxymethyl Cellulose and Poly(acrylic acid): Water Sorption and Drug Release Study, *Polym Int* **2005**, 54, 1347-1356, DOI: 10.1002/pi.1839

(41) Kulkarni, R. V.; Sa, B., Evaluation of pH-Sensitivity and Drug Release Characteristics of (Polyacrylamide-Grafted-Xanthan)–Carboxymethyl Cellulose-Based pHSensitive Interpenetrating Network Hydrogel Beads, *Drug Development and Industrial Pharmacy*, **2008,** 34,1406-1414, DOI: 10.1080/03639040802130079

(42) Lee, S.; Park, Y. H.; Ki, Ch. S., Fabrication of PEG-carboxymethylcellulose Hydrogelby Thiol-norbornene Photo-click Chemistry, *International Journal of Biological Macromolecules* **2016**, 83,1–8 doi.org/10.1016/j.ijbiomac.2015.11.050

(43) Kono, H., Characterization and Properties of Carboxymethyl Cellulose Hydrogels Crosslinked by Polyethylene Glycol, *Carbohydrate Polymers* **2014**, 106, 84-93, DOI:10.1016/j.carbpol.2014.02.020

(44) Ekici, S., Intelligent Poly(N-isopropylacrylamide)-Carboxymethyl Cellulose Full Interpenetrating Polymeric Networks for Protein Adsorption Studies, *J Mater. Sci.* **2011**, 46, 2843-2850, DOI 10.1007/s10853-010-5158-0

(45) Valeriani, M.; Mezzana, P.; Madonna Terracina, F.S., Carboxy-methyl-cellulose Hydrogel Mammary Implants: Our Experience, *Acta Chir. Plast*. 2002, 44, 71.

(46) Ogushi, Y.; Sakai, S.; Kawakami, K., Synthesis of Enzymatically-Gellable Carboxymethylcellulose for Biomedical Applications, *J. Biosci. Bioeng*. **2007**, 104, 30-33, DOI: 10.1263/jbb.104.30

(47) Mahoney, M. J.; Anseth, K. S., Three-dimensional Growth and Function of Neural Tissue in Degradable Polyethylene Glycol Hydrogels, *Biomaterials* **2006**, 27, 2265-2274 , DOI: 1016/j.biomaterials.2005.11.007

(48) Oksman, K., Mathew, A. P. & Sain, M. (2009). Novel bionanocomposites: Processing, Properties and potential applications. Plastics, Rubbers and Composites, 38(9–10), 396–405.

(49) Lou, Y.-R., Kanninen, L., Kuisma, T., Niklander, J., Noon, L. A., Burks, D., Urtti,A., Yliperttula, M., The Use of Nanofibrillar Cellulose Hydrogel As a Flexible Three-Dimensional Model to Culture Human Pluripotent Stem Cells, *Stem Cells and development* **2014**, 23(4) DOI:10.1089/scd.2013.0314

(50) Bhattacharya, M., Malinen, M. M., Lauren, P.,Lou, Y.-R., Kuisma, S. W., Kanninen, L., Niklander, T., Noon, J. Lille, M., Corlu, A., GuGuen-Guillouzo, Ch., Ikkala, O.,Urtti, A., Laukkanen, A., Yliperttula, M., Nanofibrillar cellulose hydrogel promotes three-dimensional liver cell culture, *Journal of Controlled Release* **2012**,164, 291298

(51) Malinen, M. M., Kanninen, L. K., Corlu, A., Isoniemi, H. M., Lou, Y.-R., Yliperttula, M., Urtti, A., Differentiation of liver progenitor cell line to functional organotypic cultures in 3D cellulose and hyaluronan-gelatin hydrogels, *Biomaterials* **2014**, 35, 5110-5121

(52) Mathew, A. P. Oksman, K., Pierron D., Harmand, M.-F., O., Fibrous cellulose nanocomposite scaffolds prepared by partial dissolution for use as ligament or tendon substitutes, *Carbohydrate Polymers* **2012**, 87, 2291- 2298

(53) Rashad, A., Mustafa, K., Heggset, E.B., Syverud, k., Cytocompatibility of Wood-Derived Cellulose Nanofibril Hydrogels with Different Surface Chemistry, *Biomacromolecules* **2017**, 18, 1238-1248, DOI: 10.1021/acs.biomac.6b01911

(54) Eyholzer, C., Borges Coura, A., Duc, F. Bourban, P. E., Tingaut, P., Zimmermann, T., Manson, J. A. E., Oksman K., Biocomposite Hydrogels with Carboxymethylated, Nanofibrillated Cellulose Powder for Replacement of the Nucleus Pulposus, *Biomacromolecules* **2011**, 12, 1419-1427, DOI:10.1021/bm101131b

(55) Cherian, B. M., Lopesleao, A., Ferreirade Suza, S., ManzineCosta, L. M., Olyveira, G. M., Kottaisamy M., Nagarajan, E. R., Thomas, S., Cellulose nanocomposites with nanofibres isolated from pineapple leaf fibers for medical applications, *Carbohydrate Polymers* **2011,** 86, 1790- 1798, DOI:10.1016/j.carbpol.2011.07.009

(56) Koo, S. P. S., Stamenovic, M. M., Prasath, A. R., Inglis, A. J., Du Perez, F., Barner-Kowllik, Ch., Camp, W. V., Junkers, T., Limitations of Radical Thiol-ene Reactions for Polymer–Polymer Conjugation, *Journal of Polymer Science: Part A: Polymer Chemistry* **2010,** 48, (815), 1699-1713

(57)) Desai, R.M.; Koshy, S.T.; Hilderbrand, S.A.; Mooney, D.J.; Joshi, N.S., Versatile click alginate hydrogels crosslinked via tetrazineenorbornene chemistry, *Biomaterials* **2015**, 50, 30-37, DOI:10.1016/j.biomaterials.2015.01.048

(58) Hoyle, C.E.; Bowman, C. N., Thiol-ene click chemistry, *Angew. Chem. Int. Ed.* **2010**, 49, 1540-1573, DOI:10.1002/anie.200903924

(59) Munoz, Z. Shih, H., Lin, Ch.-Ch., Gelatin hydrogels formed by orthogonal thiol–norbornene photochemistry for cell encapsulation, *Biomaterials Science* **2014**, *2*, 1063-1072

(60) McKinnon, D. D.; Kloxin, A.M.; Anseth, K.S., Synthetic hydrogel platform for three-dimensional culture of embryonic stem cell-derived motor neurons, *Biomater. Sci.* **2013**, 1, 460-469, DOI:10.1039/C3BM00166K

(61) McGann, C.L.; Dumm, R. E.; Jurusik, A.K.; Sidhu, I.; Kiick, K.L., Thiol-ene photocrosslinking of cytocompatible resilin-like polypeptide-PEG hydrogels, *Macromol. Biosci*. **2015**, 129-138, DOI:10.1002/mabi.201500305

(62) Gramlich, W.M.; Kim, I.L.; Burdick, J.A., Synthesis and orthogonal photopatterning of hyaluronic acid hydrogels with thiol-norbornene chemistry, *Biomaterials* **2013**, 34, 9803-9811, DOI:10.1016/j.biomaterials.2013.08.089

(63) Leach, J. B.; Bivens, K. A.; Patrick, C. W. Jr.; Schmidt, C. E., Photocrosslinked hyaluronic acid hydrogels: natural, biodegradable tissue engineering scaffolds, *Biotechnology and Bioengineering* **2003**, 82, 578-589, DOI: 10.1002/bit.10605

(64) Tsang, V.L.; Chen,A.A.; Cho, L.M.; Jadin, K.D.; Sah, R.L.; DeLong, S.; West, J.L.; Bhatia, S.N., Fabrication of 3D hepatic tissues by additive photopatterning of cellular hydrogels, *The FASEB Journal* **2007**, 21, 790-801, DOI:10.1096/fj.06-7117com

(65) Liu, V. A.; Bhatia, S. N., Three-dimensional photopatterning of hydrogels containing living cells, *Biomedical Microdevices 4* **2002**, 4, 257-266, DOI:10.1023/A:1020932105236

(66) Chan, V.; Zorlutuna,P.; Jeong, J.H.; Kong, H.; Bashir, R., Three-dimensional photopatterning of hydrogels using stereolithography for long-term cell encapsulation, *Lab Chip* **2010**, 10, 2062-2070, DOI:10.1039/C004285D

(67) Bryanta, S.J.; Cuya, J.L.; Haucha, K.D.; Ratner, B.D., Photo-patterning of porous hydrogels for tissue engineering, *Biomaterials* **2007**, 28, 2978-2986, DOI:10.1016/j.biomaterials.2006.11.033

(68) Fairbanks, B. D.; Singh, S. P.; Bowman, C. N.; Anseth, K. S., Photodegradable, photoadaptable hydrogels via radical-mediated disulfide fragmentation reaction, *Macromolecules* **2011**, 44, 2444-2450, DOI:10.1021/ma200202w

(69) Lin, F.; Yu, J.; Tang, W.; Zheng, J.; Defante, A.; Guo, K.; Wesdemiotis, C., Becker, M.L., Peptide-functionalized oxime hydrogels with tunable mechanical properties and gelation behavior, *Biomacromolecules* **2013**, 14, 3749-3758, DOI: 10.1021/bm401133r

(70) Francini, N.; Purdie, L.; Alexander, C.; Mantovani, G.; Spain, S.G., Multifunctional Poly[N-(2-hydroxypropyl)methacrylamide] copolymers via postpolymerization modification and sequential thiol-ene chemistry, *Macromolecules* **2015**, 48, 2857-2863

(71) DeForest, C. A.; Polizzotti, B. D.; Anseth, K. S., Sequential click reactions for synthesizing and patterning three-dimensional cell microenvironments, Nat Mater. 2009, 8, 659-64, DOI:10.1038/nmat2473

(72) Elliotta, J.E.; Macdonalda, M.; Niea, J.; Bowman, C.N., Structure and swelling of poly(acrylic acid) hydrogels: effect of pH, ionic strength, and dilution on the crosslinked polymer structure, *Polymer* **2004**, 45, 1503-1510, DOI:10.1016/j.polymer.2003.12.040

(73) Manavi-Tehrani, I.; Rabiee, M.; Parviz, M.; Tahriri, M.; Fahimi, Z., Investigation of biocompatible pH-sensitive PVA/PAA hydrogels, *Macromol. Symp*. **2010**, 296, 457-465, DOI:10.1002/masy.201051062

(74) Kloxin, A M.; Tibbitt, M. W.; Anseth, K.S**.,** Synthesis of photodegradable hydrogels as dynamically tunable cell culture platforms. *nature protocols* **2010**, 5, 12, 1867-1887, DOI:10.1038/nprot.2010.139

(75) Khetan, S.; Burdick, J.A.; Patterning network structure to spatially control cellular remodeling and stem cell fate within 3-dimensional hydrogels, *Biomaterials* **2010**, 31, 8228-8234, DOI:10.1016/j.*biomaterials*.2010.07.035

(76) Ibusuki, S.; Fujii, y.; Iwamoto, Y.; Matsuda, T., Tissue-Engineered Cartilage Using an Injectable and in Situ Gelable Thermoresponsive Gelatin: Fabrication and in Vitro Performance, *Tissue Engineering* **2003**, 9, 371-384, DOI:10.1089/107632703764664846

(77) Phillips, M. A.; Gran, M. L.; Peppas, N. A.,Targeted nanodelivery of drugs and diagnostics, *Nano Today* **2010**, 5, 143-159, DOI:10.1016/j.nantod.2010.03.003

(78) Francis, R.; Baby, D. K.; Sakthi, K. D., Poly(N-isopropylacrylamide) Hydrogel: Effect of hydrophilicity on controlled release of Ibuprofen at different pH, *Journal of Applied Polymer Science* **2012**, 124, 5079-5088, DOI 10.1002/app.35644

(79) Nolan, C. M.; Serpe, M. J.; Lyon, L. A., Thermally Modulated Insulin release from microgel thin films, *Biomacromolecules* **2004**, 5, 1940-1946*,* DOI:10.1021/bm049750h

(80) Hoffmann, J.; Plotner. M.; Kuckling, D.; Fischer, W.J., Photopatterning of thermally sensitive hydrogels useful for microactuators, *Sensors and Actuators* **1999**, 77, 139-144, DOI:10.1016/S0924-4247(99)00080-1

(81) Ito, Y.; Chen, G.; Guan, Y.; Imanishi, Y., Patterned immobilization of thermoresponsive polymer, *Langmuir* **1997**, *13,* 2756-2759, **DOI:**10.1021/la961087y

(82) Tsudaa, Y.; Kikuchib, A.; Yamatob, M.; Nakaoc, A.; Sakuraia, Y.; Umezua, M,; Okano, T., The use of patterned dual thermoresponsive surfaces for the collective recovery as co-cultured cell sheets, *Biomaterials* **2005**, 26, 1885-1893, DOI:10.1016/j.biomaterials.2004.06.005

(83) Geever, L.M.; Devine, D.M.; Nugent, M.J.D.; Kennedy, J.E.; Lyons, J. G.; Higginbotham, C. L., The synthesis, characterisation, phase behaviour and swelling of temperature sensitive physically crosslinked poly(1-vinyl-2-pyrrolidinone)/poly(N-isopropylacrylamide) hydrogels, *European Polymer Journal* **2006**, 42, 69-80, DOI:10.1016/j.eurpolymj.2005.09.027

(84) Miyahara, Y.; Nagaya, N.; Kataoka, M.; Yanagawa, B,; Tanaka, K.; Hao, H,; Ishino, K.; Ishida, H.; Shimizu, T.; Kangawa, K.; Sano,S.; Okano, T.; Kitamura, S.; Mori8, H., Monolayered mesenchymal cells repair scarred myocardium after myocardial infarction, *Nature Medicine* **2006**, 12, 459-465, DOI:10.1038/nm1391

(85) Nishida, K.; Yamato, M.; Hayashida, Y.; Watanabe, K.; Yamamoto, K.; Adachi, E.; Nagai, S.; Kikuchi, A.; Maeda, N.; Watanabe, H.; Okano, T.; Tano, Y.; Corneal Reconstruction with tissue-engineered cell sheets composed of autologous oral mucosal epithelium, *N. Engl. J. Med.* **2004**, 351, 1187-1196, DOI:10.1056/NEJMoa040455

(86) Yanga, J.; Yamatoa, M.; Kohnoa, C.; Nishimotob, A.; Sekinea, H.; Fukaib, F.; Okanoa, T.; Cell sheet engineering: Recreating tissues without biodegradable scaffolds, *Biomaterials* 26 **2005** 6415-6422, DOI:10.1016/j.biomaterials.2005.04.061

(87) Dang, J. M.; Leong, K. W.**,** Myogenic induction of aligned mesenchymal stem cell sheets by culture on thermally responsive electrospun nanofibers, *Adv. Mater.* **2007**, 19, 2775-2779, DOI:10.1002/adma.200602159

(89) Malachowski, J.; Hye R. K.; Breger, J.; Wang, M. O.; Fisher, J. P.; Selaru, F. M.; Gracias, D. H., Stimuli-responsive theragrippers for chemomechanical controlled release, *Angew. Chem.* **2014**, 126, 8183-8187, DOI:10.1002/ange.201311047

(90) Stile, R. A.; Healy K. E.; Poly(N-isopropylacrylamide)-based semi-interpenetrating polymer networks for tissue engineering applications. 1. effects of linear poly(acrylic acid) chains on phase behavior, *Biomacromolecules*, **2002**, 3, 591-600, DOI: 10.1021/bm0101466

(91) Magdanz, V.; Stoychev, G.; Ionov, L.; Sanchez, S.; Schmidt, O. G.; Stimuli-responsive microjets with reconfigurable shape, *Angew. Chem*. **2014**, 126, 2711-2715, DOI:10.1002/ange.201308610

(92) Stoychev, G.; Zakharchenko, S.; Turcaud, S.; Dunlop, J. W. C.; Ionov, L., Shape-programmed folding of stimuli-responsive polymer bilayers, *ACS Nano* **2012**, 6, 3925-3934, DOI:10.1021/nn300079f

(93) Stoychev, G.; Puretskiy, N.; Ionov, L., Self-folding all-polymer thermoresponsive microcapsules, *Soft Matter* **2011**, 7, 3277-3279, DOI: 10.1039/c1sm05109a

(94) Kim, J.; Nayak, S.; Lyon, L. A.; Bioresponsive hydrogel microlenses, *J. Am. Chem. Soc.* **2005**, 127, 9588-9592, DOI:10.1021/ja0519076

(95) Gutowska, A.; Bae, Y. H.; Feijen, J.; Kim, S. W., Heparin release from thermosensitive hydrogels, *Journal of Conrrolled Release* **1992**, 22, 95-104, DOI:10.1016/0168-3659(92)90194-V

(96) Sershen, S. R.; Westcott, S. L.; Halas, N. J.; West, J. L., Temperature-sensitive polymer–nanoshell composites for photothermally modulated drug delivery, *J. Biomed. Mater. Res.* 2000, 51, 293-298, DOI:10.1002/1097-4636(20000905)51:3<293::AID-JBM1>3.0.CO;2-T

(97) Pérez, P.; Gallardo, A.; Corrigan, O. I.; San-Román, J., Thermosensitivity of N-isopropylacrylamide hydrogels cross-linked with degradable crosslinker, *J. Biomater. Sci. Polymer Edn*. **2008**, 19, 769-783, DOI:10.1163/156856208784522074

(98) Hoffman, A. S.; Stayton, P. S., Bioconjugates of smart polymers and proteins: synthesis and applications, *Macromol. Symp.* **2004**, 207, 139-151, DOI: 10.1002/masy.200450314

(99) Nayak, S.; Lyon, L. A., Photoinduced Phase Transitions in Poly(*N*-isopropylacrylamide) Microgels, *Chem. Mater.* **2004,** 16, 2623-2627, DOI:10.1021/cm049650i

(100) Thayer, P. S.; Verbridge, S. S.; Dahlgren, L. A.; Kakar, S. Guelcher, S. A. Goldstein, A. S., Fiber/collagen composites for ligament tissue engineering: influence of elastic moduli of sparse aligned fibers on mesenchymal stem cells, *J. Biomed. Mater. Res. A.* **2016**, DOI:10.1002/jbm.a.35716

(101) Akhtara, R.; Sherrattc, M. J.; Cruickshankb, J. K.; Derbya, B., Characterizing the elastic properties of tissues, *Mater. Today (Kidlington)* **2014**, 96-105, DOI:10.1016/S1369-7021(11)70059-1

(102) Trappmann, B.; Chen,C. S., How cells sense extracellular matrix stiffness: a material's perspective, *Curr. Opin. Biotechnol.* **2013**, 5, 948-953, DOI:10.1016/j.copbio.2013.03.020

(103) Handorf, A. M.; Zhou, Y.; Halanski, M. A.; Li, W.-J., Tissue siffness dictates development, homeostasis, and disease progression, *Organogenesis* **2015**, 11, 1-15, DOI:10.1080/15476278.2015.1019687

(104) Guvendiren, M.; Burdick, J. A., The control of stem cell morphology and differentiation by hydrogel surface wrinkles, *Biomaterials* **2010**, 31, 6511-6518, DOI:10.1016/j.biomaterials.2010.05.037

(105) Hackelbusch, S.; Rossow, T.; Steinhilber, D.; Weitz, D. A.; Seiffert, S., Hybrid microgels with thermo-tunable elasticity for controllable cell confinement, *Adv. Healthcare Mater.* **2015**,1841-1848, DOI: 10.1002/adhm.201500359

(106) Pek, Y. S.; Wan, A. C. A.; Ying, J. Y., The effect of matrix stiffness on mesenchymal stem cell differentiation in a 3D thixotropic gel, *Biomaterials* **2010**, 31, 385-391, DOI:10.1016/j.biomaterials.2009.09.057

(107) Barnes, M. J., Przybyla, L., Weaver, V. M., Tissue mechanics regulate brain development, homeostasis and disease, *Journal of Cell Science* **2017**, 130, 71-82, DOI:10.1242/jcs.191742

(108) Kim, J.-H.; Lee, S.-B.; Kim, S.- J.; Lee, Y.-M., Rapid temperature/pH response of porous alginate-g-poly(Nisopropylacrylamide) hydrogels, *Polymer* **2002**, 43, 7549-7558, DOI:10.1016/S0032-3861(02)00675-4

(109) Giammanco, G. E.; Ostrowski, A. D., Photopatterning the Mechanical Properties of Polysaccharide-Containing Gels Using Fe3+ coordination, *Chem, Mater*., 2015, 27, 4922−4925, DOI: 10.1021/acs.chemmater.5b01727

(110) Tang, Y.; Zhang, S.; Wang, M.; Zhu, J.; Sun, T.; Jiang, G., A glucose-based diblock copolymer: synthesis, characterization and its injectable/temperature-sensitive behaviors, J. Polym. Res. **2014**, 21, 390, DOI:10.1007/s10965-014-0390-y

(111) Ohya, S.; Sonodaa, H.; Nakayamaa, Y.; Matsuda, T., The potential of poly(N-isopropylacrylamide) (PNIPAM)-grafted hyaluronan and PNIPAM-grafted gelatin in the control of post-surgical tissue adhesions, *Biomaterials* **2005**, 26, 655-659, DOI:10.1016/j.biomaterials.2004.03.002

(112) Peroglio, M.; Grad, S.; Mortisen, D.; Sprecher, C. M.; Illien-Jünger, S.; Alini, M.; Eglin, D., Injectable thermoreversible hyaluronan-based hydrogels for nucleus pulposus cell encapsulation, *Eur Spine J.* **2012**, 21, 839-849, DOI:10.1007/s00586-011-1976-2

(113) Syverud, K., Petterse, S.R., Draget, K., Chinga-Carrasco, G., Controlling the elastic modulus of cellulose nanofibril hydrogels-scaffolds with potential in tissue engineering, *Cellulose* **2015**, 22,473-481, DOI: 10.1007/s10570-014-0470-5

(114) Khin, Y. Y., Ganda, S., Stenzel, M. H., Covalent Tethering of Temperature Responsive pNIPAm onto TEMPO-Oxidized Cellulose Nanofibrils via Three-Component Passerini Reaction, *ACS Macro Lett.* **2018**, 7, 412-418, DOI: 10.1021/acsmacrolett.8b00051

(115) Dong, H., Snyder, J. F., Williams, K. S., Andzelm, J. W., Cation-Induced Hydrogels of Cellulose Nanofibrils with TunableModuli, *Biomacromolecules* **2013**, 14, 3338-3345, DOI: 10.1021/bm400993f

(116) Liu, Y., Sui, Y., Liu, C., Liu, Ch-Q., Wub, M., Lib, B., Li, Y., A physically crosslinked polydopamine/nanocellulose hydrogel as potential versatile vehicles for drug delivery and wound healing, *Carbohydrate Polymers* **2018,** 188, 27-3610.1016/j.carbpol.2018.01.093

(117) Courtenay, J. C., Ramalhete, S. M., Skuze, W. J., Soni R., Khimyak, Y. Z., Edler K.J., Scott , J.L., Unravelling cationic cellulose nanofibril hydrogel structure: NMR spectroscopy and small angle neutron scattering analyses, *Soft Matter,* **2018,** 14, 255-263, DOI: 10.1039/c7sm02113e

(118) Lai, J. T.; Filla, D.; Shea, R., Functional polymers from novel carboxy-terminated trithiocarbonates as Highly Efficient RAFT Agents, *Macromolecules*, 2002, 35, 6754-6756. DOI: 10.1021/ma020362m.

(119) Qui, X.-P.; Winnik, F. M., Synthesis of α,ω-dimercapto poly(N-isopropylacrylamides) by RAFT polymerization with a hydrophilic difunctional chain transfer agent, *Macromolecules*, 2007, 40, 872-878. DOI: 10.1021/ma062225l.

(120) Anseth, K.S.; Bowma, C. N.; Brannon-Peppas, L. Mechanical properties of hydrogels and their experimental determination, *Biomaterials* **1996**, 17, 1647-1657.

(121) Hiemenz, P. C.; Lodge, T. P. In *Polymer Chemistry*, 2nd ed. CRC Press: New York, NY, 2007; p 413.

(122) Garciá-Garciá, J. M.; Liras, M.; Quijada-Garrido, I.; Gallardo, A.; París, R., Swelling control in thermo-responsive hydrogels based on 2-(2-methoxyethoxy)ethyl methacrylate by crosslinking and copolymerization with N-isopropylacrylamide, *Polymer Journal* **2011**, 43, 887-892, DOI:10.1038/pj.2011.83

(123) Cai, T.; Yang, W. J.; Zhang, Z.; Zhu, X.; Neoh, K.-G.; Kang, E.-T., Preparation of stimuli-responsive hydrogel networks with threaded b-cyclodextrin end-capped chains via combination of controlled radical polymerization and click chemistry, *Soft Matter* **2012**, 8, 5612-5620, **DOI:**10.1039/C2SM25368B

(124) Yang, J.; Lee, J.; Kang, J.; Oh, S. J.; Ko, H.-J.; Son, J.-H.; Lee, K.; Suh, J.-S.; Huh, Y.-M.; Haam, S., Smart drug-loaded polymer gold nanoshells for systemic and localized therapy of human Eepithelial, *Adv. Mater.* **2009**, 21, 4339-4342, DOI:10.1002/adma.200900334

(125) Chen, J.; Wang, D.; Xi, J.; Au, L.; Siekkinen, A.; Warsen, A.; LI, Z.-Y.; Zhang, H.;| Xia, Y.; Li, X., Immuno gold nanocages with tailored optical properties for targeted photothermal destruction of cancer cells, *Nano Lett.* **2007**, 7, 1318-1322, DOI: 10.1021/nl070345g

(126) Raula, J.; Shan, J.; Nuopponen, M.; Niskanen, A.; Jiang, H.; Kauppinen, E. I.; Tenhu, H., Synthesis of gold nanoparticles grafted with a thermoresponsive polymer by surface-induced reversible-addition-fragmentation chain-transfer polymerization, *Langmuir* **2003,** 19*,* 3499-3504, DOI: 10.1021/la026872r

(127) Cho, E. C.; Kim, Y. D.; Cho, K., Thermally responsive poly(N-isopropylacrylamide) monolayer on gold: synthesis, surface characterization, and protein interaction/adsorption studies, *Polymer* **2004**, 45, 3195-3204, DOI:10.1016/j.polymer.2004.02.052

(128) Zhang, X.; Pint, C. L.; Lee, M. H.; Schubert, B. E.; Jamshidi, A.; Takei, K.; Ko, H.; Gillies, A.; Bardhan, R.; Urban, J. J.;Wu, M.; Fearing, R.; Javey, A., Optically- and thermally-responsive programmable materials based on carbon nanotube-hydrogel polymer composites, *Nano Lett.* **2011**, 11, 3239-3244, DOI:10.1021/nl201503e

(129) Gramlich, W.M.; Rai, R.; Holloway, J. L.; Burdick, J. A., Transdermal gelation of methacrylated macromers with near-infrared light and gold nanorods, *Nanotechnology* **2014**, 25, 014004, DOI:10.1088/0957-4484/25/1/014004

(130) Kumashiro, Y.; Matsunaga, T.; Muraoka, M.; Tanaka, N.; Itoga, K.; Kobayashi, J.; Tomiyama, Y.; Kuroda, M.; Shimizu, T.; Hashimoto, I.; Umemura, K.; Yamato, M.; Okano, T., Rate control of cell sheet recovery by incorporating hydrophilic pattern in thermoresponsive cell culture dish, *Journal of Biomedical Materials Research Part A* **2014**, 102, 2849-2856, DOI: 10.1002/jbm.a.34959

(131) Lutolf, M. P. Lauer-Fields, J. L., Schmoekel, H. G. , Metters, A. T., Weber, F. E., Fields, G. B., Hubbell, J. A., Synthetic matrix metalloproteinase-sensitive hydrogels for the conduction of tissue regeneration: Engineering cell-invasion characteristic, *PNAS* **2003**, *100* (9) *5413*.

(132) Engler, A. J. Sen, S. Sweeney, H. L., Discher, D. E., Matrix Elasticity Directs Stem Cell Lineage Specification, *Cell* **2006**, *126*, 677.

(133) Chee, C. K., Rimmer, S., Shaw, D. A., Soutar, I., Swanson, L., Manipulating the Thermoresponsive Behavior of Poly(*N*-isopropylacrylamide). On the Conformational Behavior of a Series of *N*-Isopropylacrylamide−Styrene Statistical Copolymers, *Macromolecules* **2001**, *34,* 7544.

(134) Hoffman, A. S., *MRS BULLETIN*, **September 1991**

(135) Schild, H. G., Poly(*N*-isopropylacrylamide): experiment, theory and application *Prog. Polym. Sci.,* **1992,** *17*, 163.

(136) Harsh, D. C., Gehrke, S. H, Controlling the swelling characteristics of temperature-sensitive cellulose ether hydrogels**,** *Journal of Contrtled Release* **1991,** *17*, 175-185.

(137) S. Khetan, J. S. Katz, J. A. Burdick, *Soft Matter* **2009**, *5*, 1601.

(138) Huebsch, N, Arany, P. R., Mao, A. S. Shvartsman, D. Ali, O. A., Bencherif, S. A., Rivera-Feliciano, J., Mooney, D. J., Harnessing traction-mediated manipulation of the cell/matrix interface to control stem-cell fate, *Nature Materials* **2010**, *9*, 518.

(139) Khetan, S. Guvendiren, M., Legant, W. R., Cohen, D. M., Chen, C. S., Burdick, J. A., Degradation-mediated cellular traction directsstem cell fate in covalently crosslinked three-dimensional hydrogels, *Nature Materials* **2013**, *12*, 458.

(140) McOscar, Thomas, "Renewable Hydrogels From Norbornene-Functionalized Carboxymethyl Cellulose and a Short Dithiol Crosslinked Via a Thiol-Ene Reaction" (2017). *Electronic Theses and Dissertations*. 2761., http://digitalcommons.library.umaine.edu/etd/2761

(141) Diniz, F., Castro, G., Hornification—its origin and interpretation in wood pulps, *Wood Sci Technol* **2004**, 37, 489-494, DOI 10.1007/s00226-003-0216-2

(142) Kato, K. L., Cameron, R. E., A review of the relationship between thermally-accelerated ageing of paper and horni®cation, *Cellulose* **1999**, 6, 23-40

(143 Shinner, F., Von Mersi, W**.,** Xylanase-,CM-Cellulase- And Invertase activity in soil: An improved method, *Soil boil biochem*, **1990**, 22(4)511-515

(144) Bacillus pumilus S124A carboxymethyl cellulase; a thermo stableenzyme with a wide substrate spectrum utilityNatesan Balasubramanian∗, Nelson SimõesInternational Journal of Biological Macromolecules 67 (2014) 132–139

(145) Wang, J., Hua, B., Wang, X., Cui, Z., Characteristics of cellulase in cellulose-degrading Bacterium strain *Clostridium straminisolvens* (CSK1), *African Journal of Microbiology Research* **2017**, 11(10), 414-421, DOI: 10.5897/AJMR2016.8357

(146) Mansfield, Sh., Meder, R., Cellulose hydrolysis – the role of monocomponent cellulases in crystalline cellulose degradation, *Cellulose* **2003,** 10, 159-169

(147) Mandels, M., Hontz, L., Nystrom, J., Enzymatic Hydrolysis of Waste Cellulose, *BIOTECHNOLOGY AND BIOENGINEERING* **1974**, XVI, 1471-1493

(148) Lotti, M., Gregersen, Ø. W., Moe, S., Lenes, M., Rheological studied of macrofibrillar cellulose water dispersions, *J Polym Environ* **2011**, 19, 137-145.

(149) Karppinen, A., Saarinen, T., Salmela, J., Laukkanen, A., Nuopponen, M., Seppälä, Flocculation of microfibrillated cellulose in shear flow, *Cellulose* **2012**, 19, 1807-1819.

(150) Kuzmenkoa, V., Karabuluta, E., Pernevikc, E., Enokssona, P., Gatenholma, P., Tailor-made conductive inks from cellulose nanofibrils for 3D printing of neural guidelines, *Carbohydrate Polymers* **2018**, 189, 22-30, DOI: 10.1016/j.carbpol.2018.01.097

(151) Ding, Q., Zeng, J., Wang, B., Gao, W., Chen, K., Yuan, Zh., Xu, J., Tang, D., Effect of retention rate of fluorescent cellulose nanofibrils on paper properties and structure, *Carbohydrate Polymers* **2018**, 186, 73-81

(152) Deville, S., Ice-templating, freeze casting: Beyond materials processing, *Mater. Res*., **2013**, 28 (17), DOI: 10.1557/jmr.2013.105

(153) Steinhilber, D., Seiffert, S., Heyman J, A., Paulus, F., Weitz, D. A., Haag, R., Hyperbranched polyglycerols on the nanometer and micrometer scale, *Biomaterials* **2011**, 32, 1311-1316

(154) Betz, M. W., Modi, P. C., Caccamese J. F., Coletti, D. P., Sauk, J. J., Fisher, J. P., Cyclic acetal hydrogel system for bone marrow stromal cell encapsulation and osteodifferentiation, *Journal of Biomedical Materials Research Part A,* 84 (3), 662-670, DOI: 10.1002/jbm.a.31640.

(155) Lin, N., Dufresne, A., Nanocellulose in biomedicine: Current status and future prospect, *European Polymer Journal* **2014**, 59, 302-325, DOI: 10.1016/j.eurpolymj.2014.07.025

APPENDICES

APPENDIX A: SUPPLEMENTARY FIGURES FOR CHAPTER 2

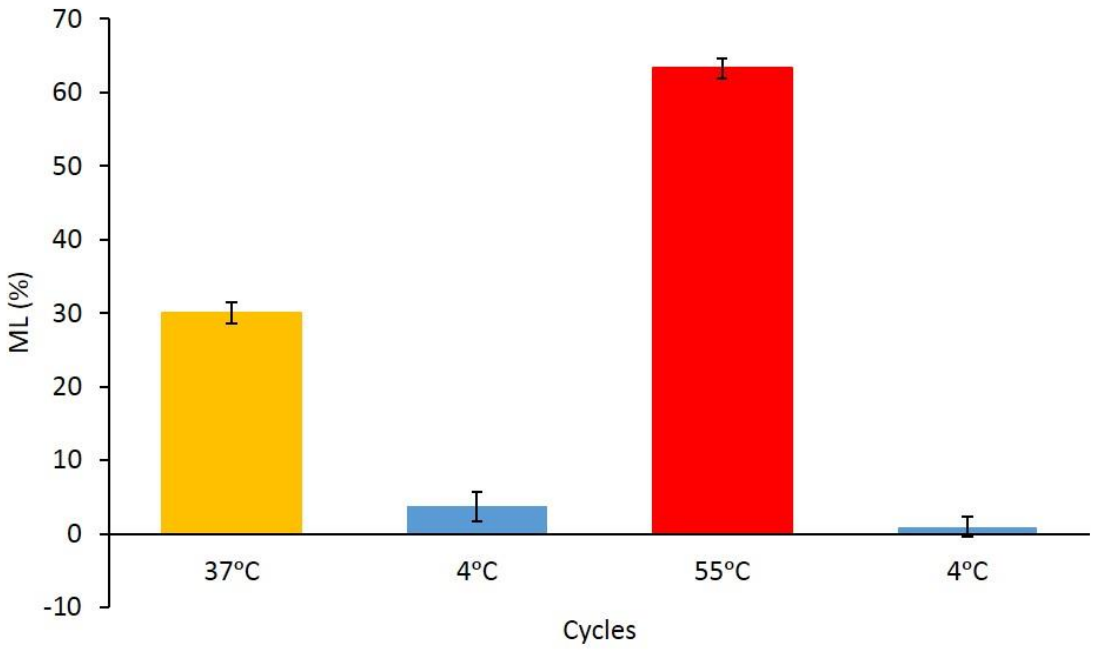

Figure A.1. Mass loss percentages of 2DTPN8-45 hydrogels (n=4) made from a solution of NorHA and DTPN8 with 2 wt% of polymer, $X_{T/N}$=0.5, and 45 s UV irradiation at 4, 38, and 55 °C cycles.

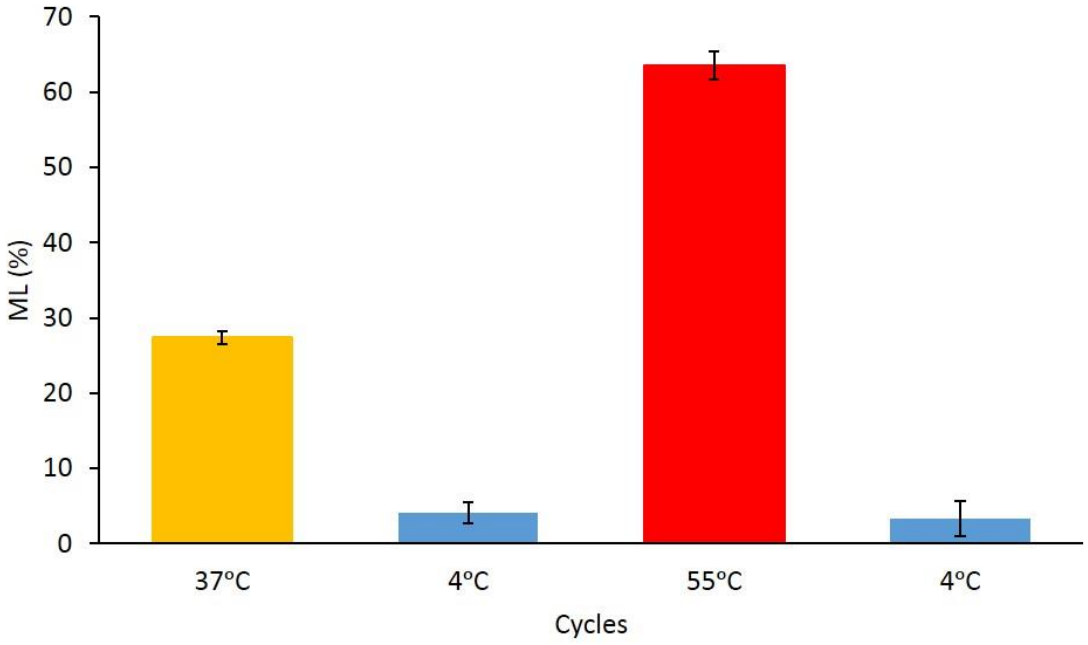

Figure A.2. Mass loss percentages of 4DTPN8-45 hydrogels (n=4) made from a solution of NorHA and DTPN8 with 4 wt% of polymer, $X_{T/N}$=0.5, and 45 s UV irradiation at 4, 38, and 55 °C cycles.

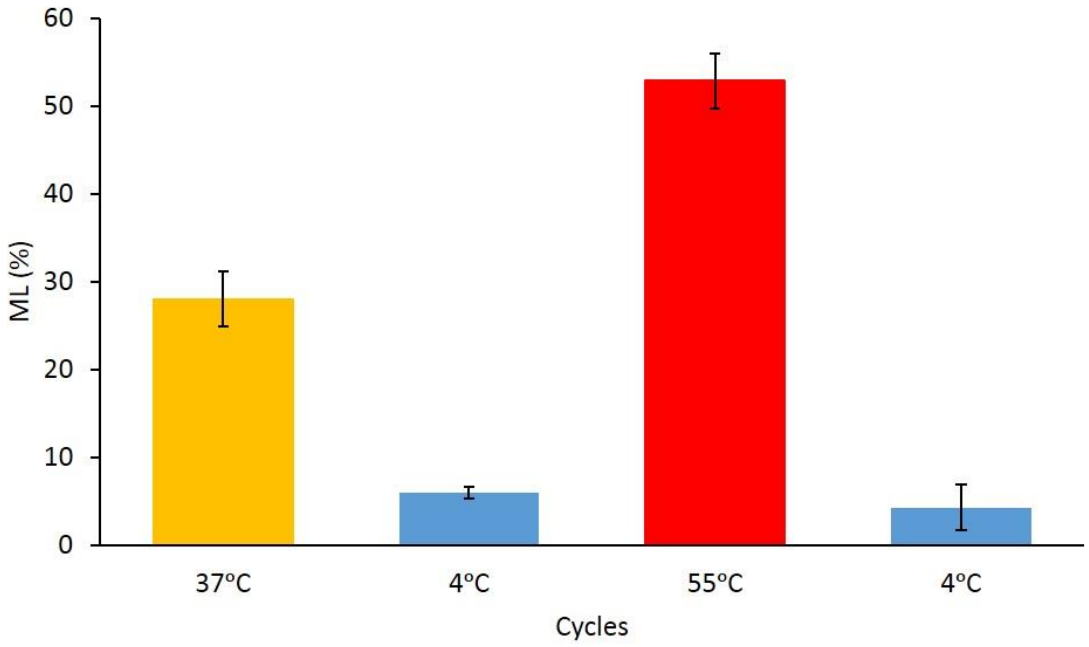

Figure A.3. Mass loss percentages of 0.5DTPN8-45 hydrogels (n=4) made from a solution of NorHA and DTPN8 with 6 wt% of polymer, $X_{T/N}$=0.5, and 45 s UV irradiation at 4, 38, and 55 °C cycles.

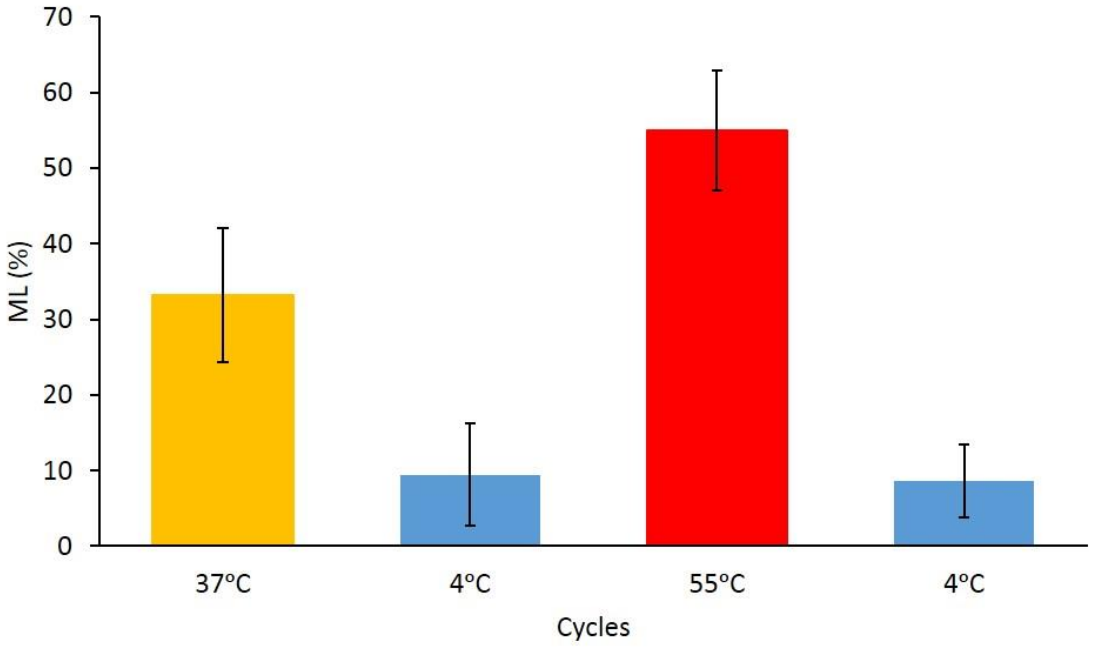

Figure A.4. Mass loss percentages of 0.7DTPN8-45 hydrogels (n=4) made from a solution of NorHA and DTPN8 with 6 wt% of polymer, $X_{T/N}$=0.7, and 45 s UV irradiation at 4, 38, and 55 °C cycles.

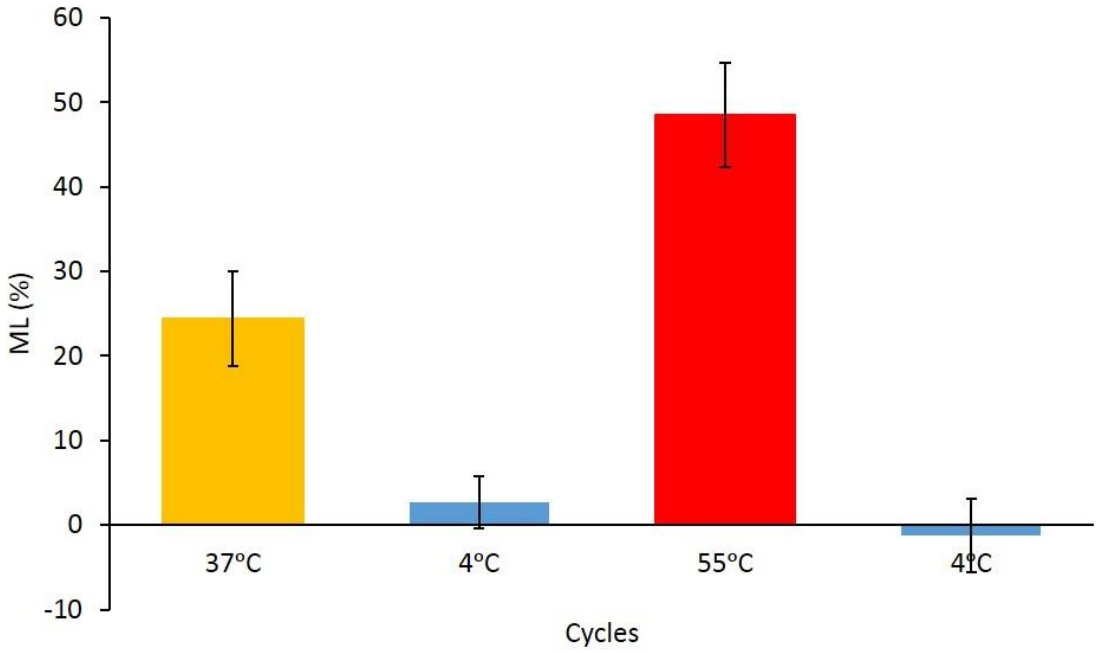

Figure A.5. Mass loss percentages of 0.3DTPN8-45 hydrogels (n=4) made from a solution of NorHA and DTPN8 with 6 wt% of polymer, $X_{T/N}$=0.3, and 45 s UV irradiation at 4, 38, and 55 °C cycles.

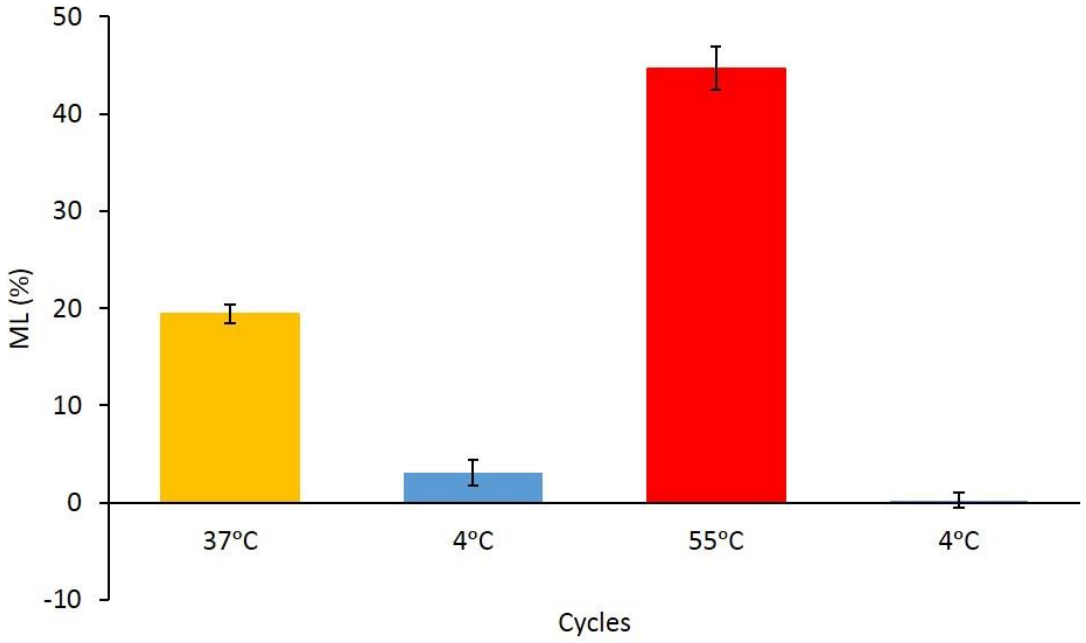

Figure A.6. Mass loss percentages of 0.5DTPN8-90 hydrogels (n=4) made from a solution of NorHA and DTPN8 with 6 wt% of polymer, $X_{T/N}$=0.5, and 90 s UV irradiation at 4, 38, and 55 °C cycles.

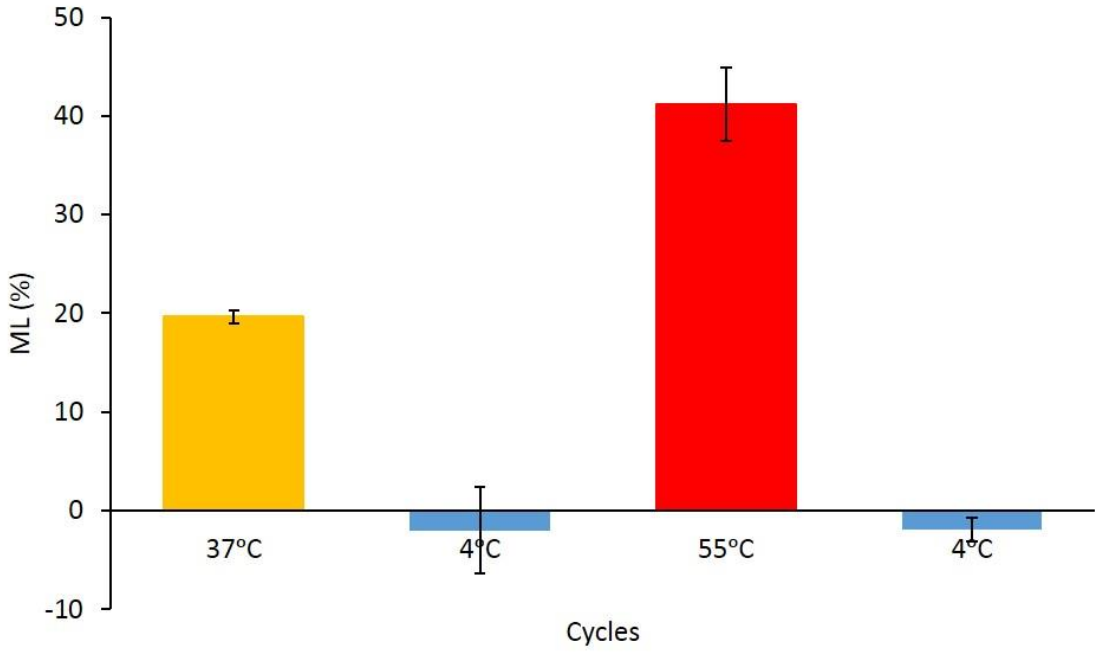

Figure A.7. Mass loss percentages of 0.5DTPN8-180 hydrogels (n=4) made from a solution of NorHA and DTPN8 with 6 wt% of polymer, $X_{T/N}$=0.5, and 180 s UV irradiation at 4, 38, and 55 °C cycles.

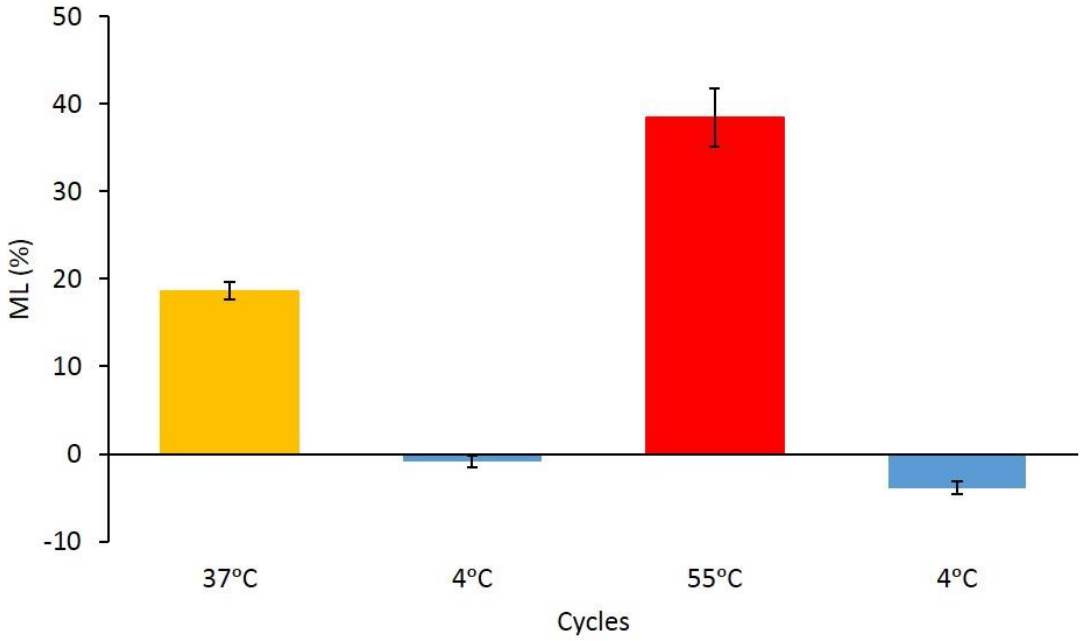

Figure A.8. Mass loss percentages of 0.3DTPN8-90 hydrogels (n=4) made from a solution of NorHA and DTPN8 with 6 wt% of polymer, $X_{T/N}$=0.3, and 90 s UV irradiation at 4, 38, and 55 °C cycles.

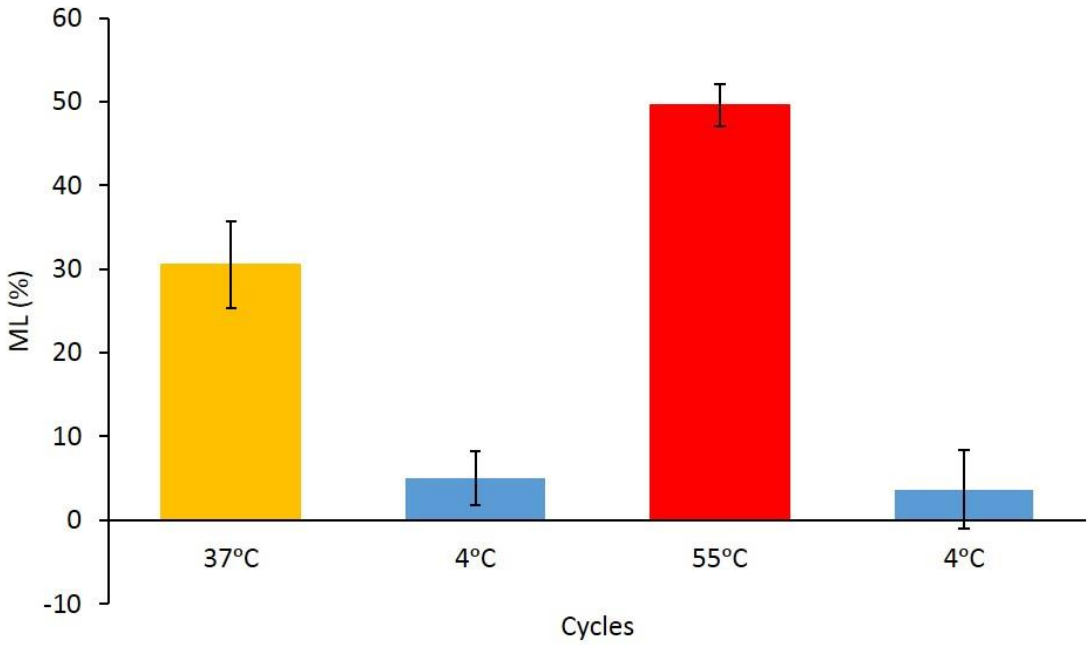

Figure A.9. Mass loss percentages of 0.7DTPN8-90 hydrogels (n=4) made from a solution of NorHA and DTPN8 with 6 wt% of polymer, $X_{T/N}$=0.7, and 90 s UV irradiation at 4, 38, and 55 °C cycles.

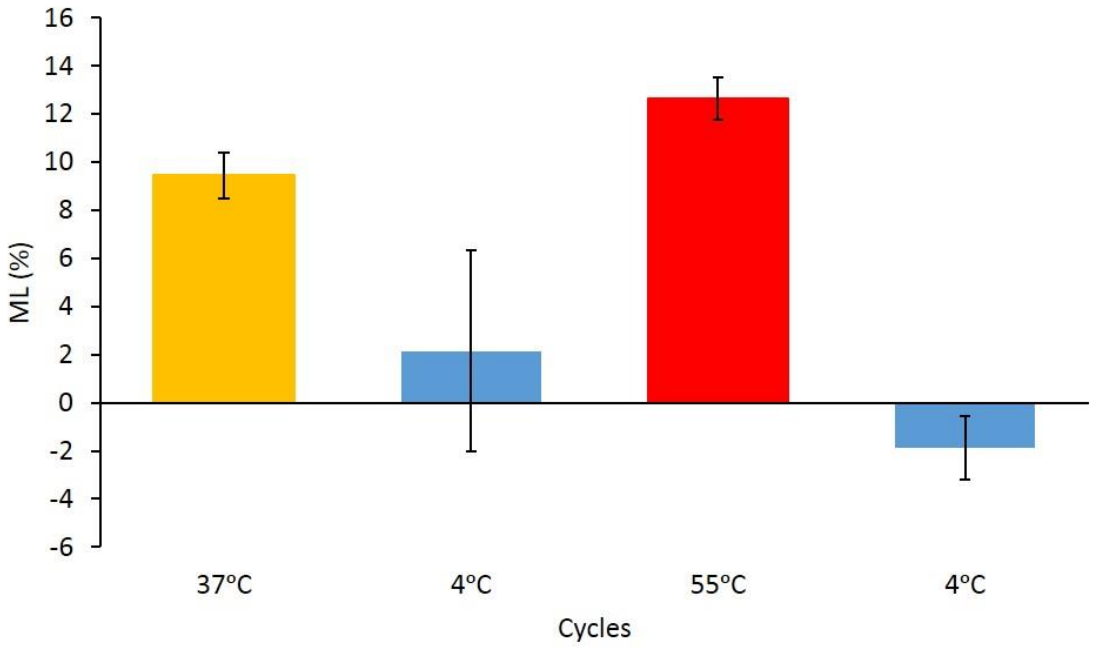

Figure A.10. Mass loss percentages of 0.5DTPN4-90 hydrogels (n=4) made from a solution of NorHA and DTPN4 with 6 wt% of polymer, $X_{T/N}$=0.5, and 90 s UV irradiation at 4, 38, and 55 °C cycles.

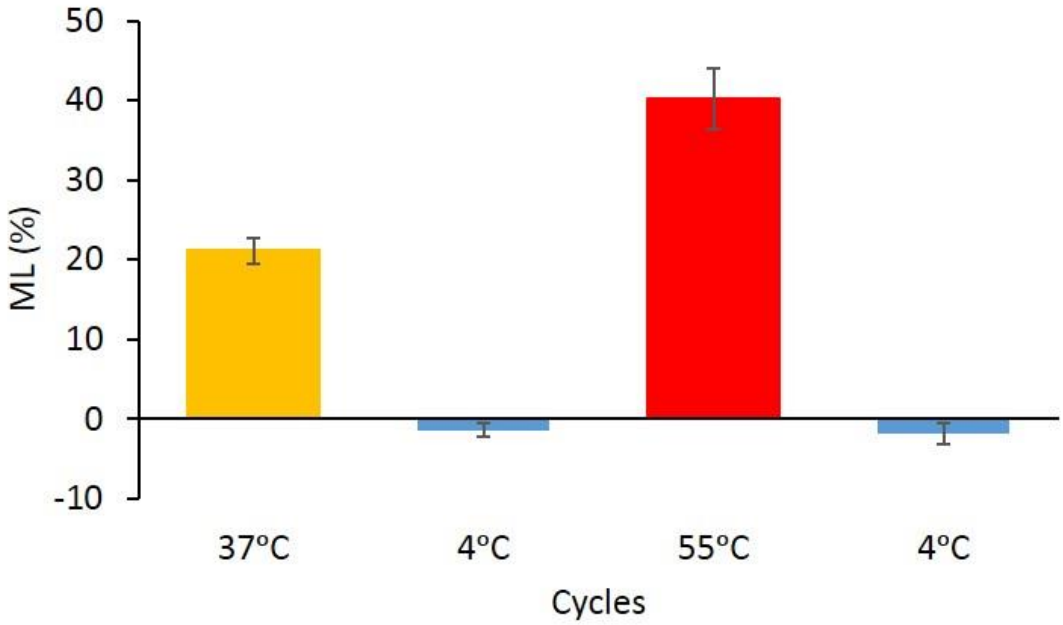

Figure A.11. Mass loss percentages of M,D-TPN8-90 hydrogels (n=4) made from a solution of NorHA and DTPN8 and MTPN8 with 6 wt% of polymer, $X_{T/N}$=0.3 for cross-linker, and 90 s UV irradiation at 4, 38, and 55 °C cycles.

APPENDIX B: SUPPLEMENTARY FIGURES FOR CHAPTER 3

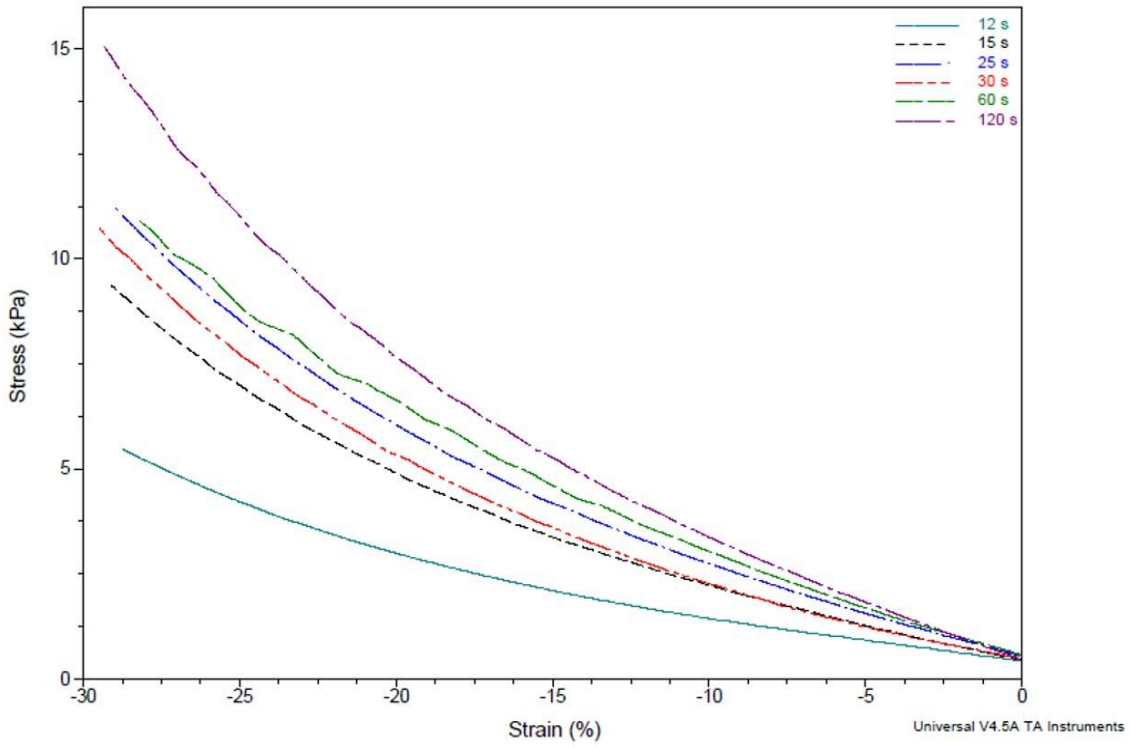

Figure B.1. Representative stress/strain curves obtained by DMA for NorCMC-DTT hydrogels made at different UV irradiation times (4 wt% polymer, T/NB=0.5). The reported values are an average of n≥9 measurements for each condition.

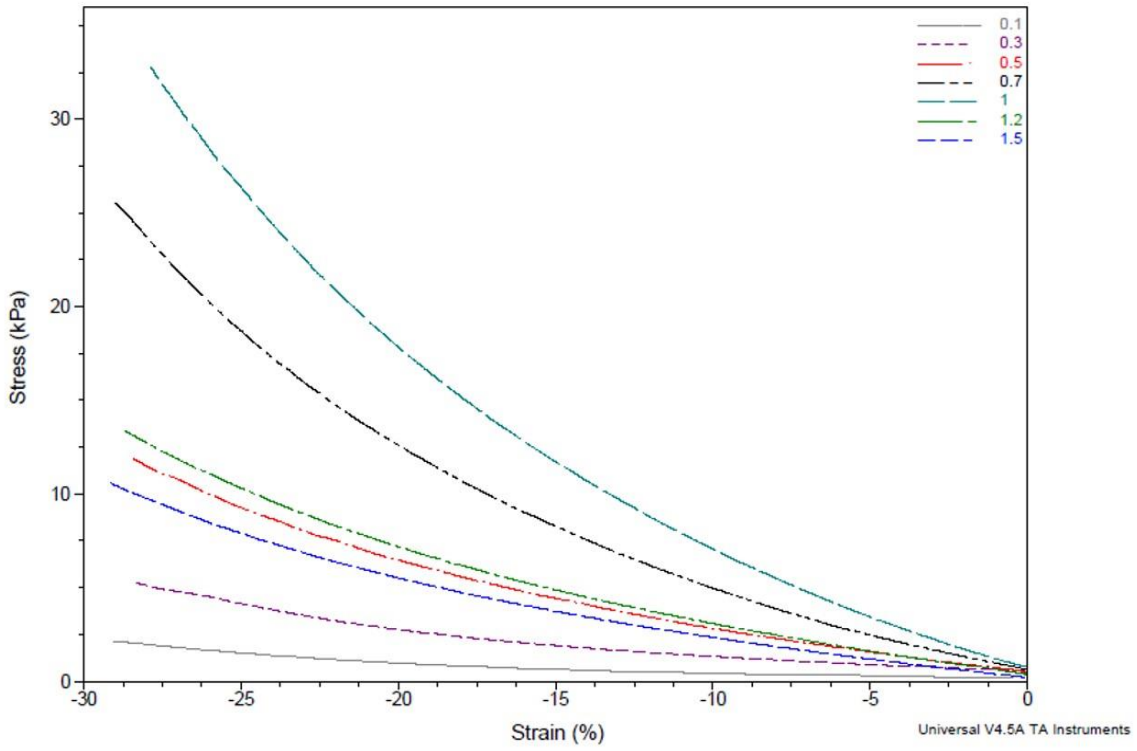

Figure B.2. Representative stress/strain curves obtained by DMA for NorCMC-DTT hydrogels made at different thiol to norbornene ratios (4 wt% polymer, 60 s UV irradiation). The reported values are an average of n≥9 measurements for each condition.

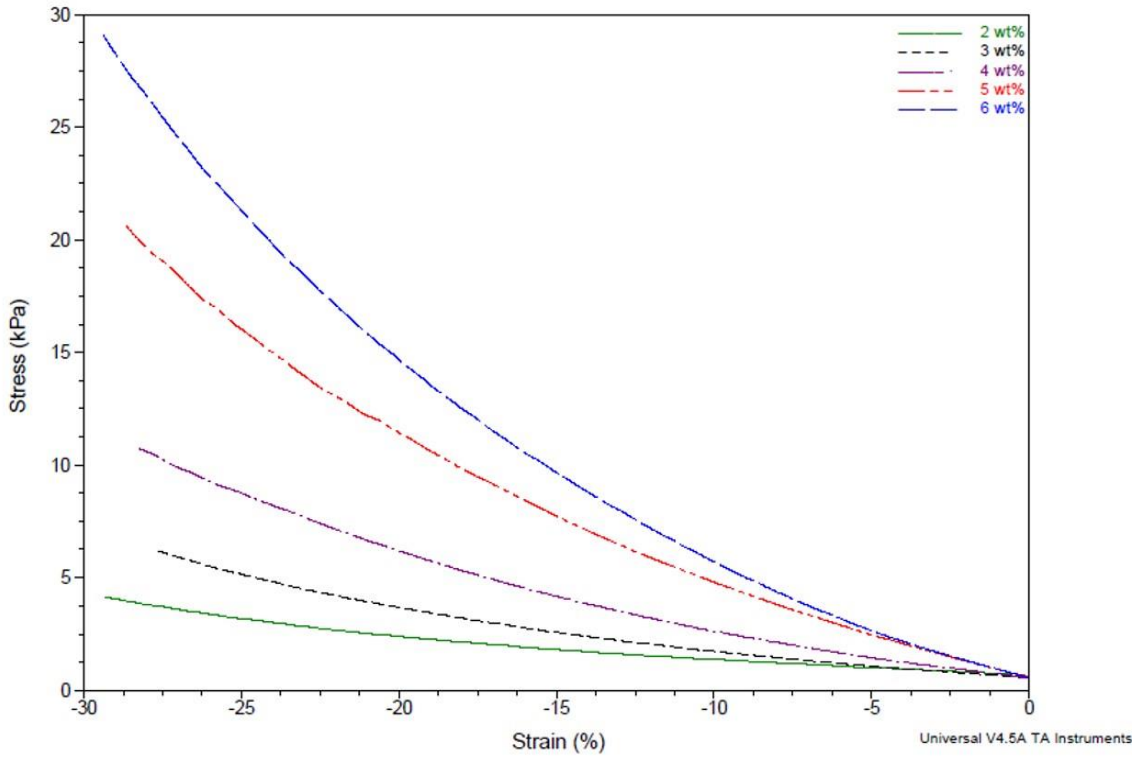

Figure B.3. Representative stress/strain curves obtained by DMA for NorCMC-DTT hydrogels made at different polymer wt% (T/NB=0.5, 60 s UV irradiation). The reported values are an average of n≥9 measurements for each condition.

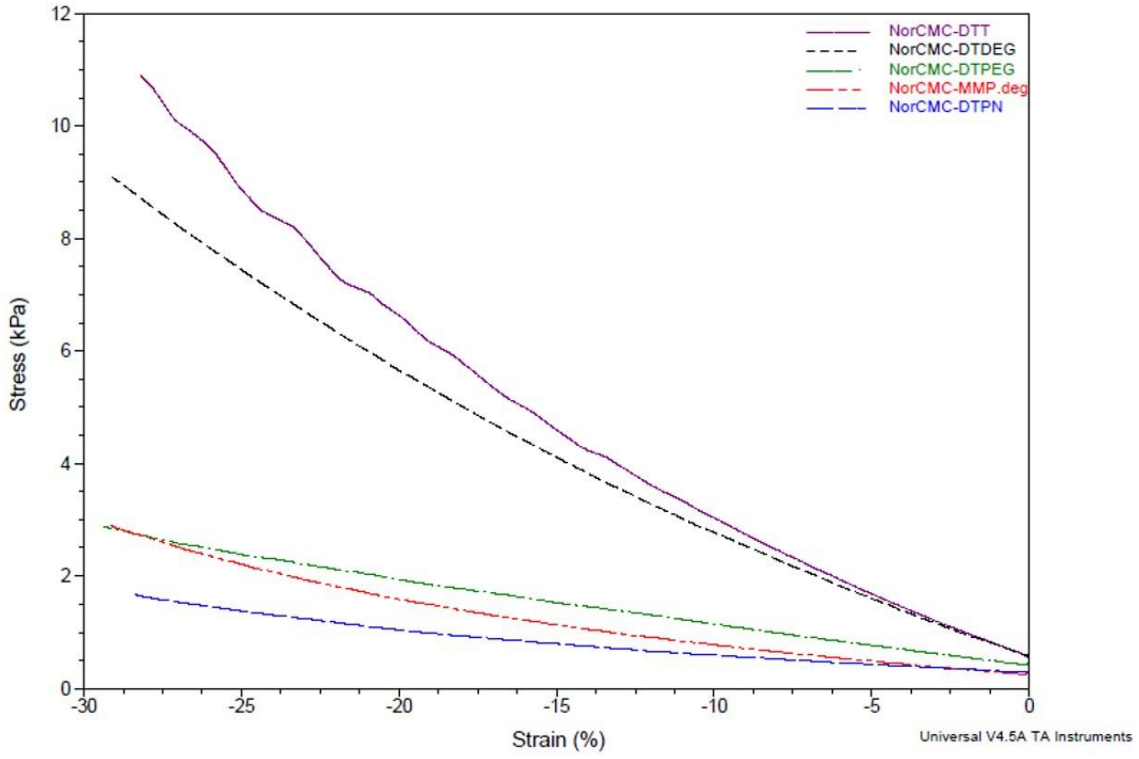

Figure B.4. Representative stress/strain curves obtained by DMA for NorCMC hydrogels cross-linked by different dithiol cross-linkers (4 wt% polymer, T/NB=0.5, 60 s UV irradiation). The reported values are an average of n≥9 measurements for each condition.

APPENDIX C: SUPPLEMENTARY FIGURES FOR CHAPTER 4

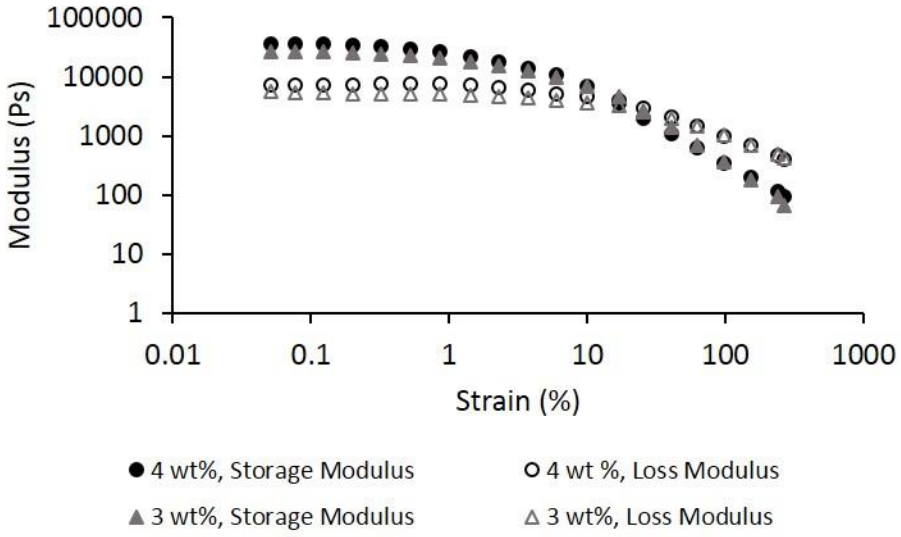

Figure C.1. Strain sweep from 0.05% to 250% at 1 Hz for CNF at 4 wt% (black circle) and 3 wt% (gray triangle).

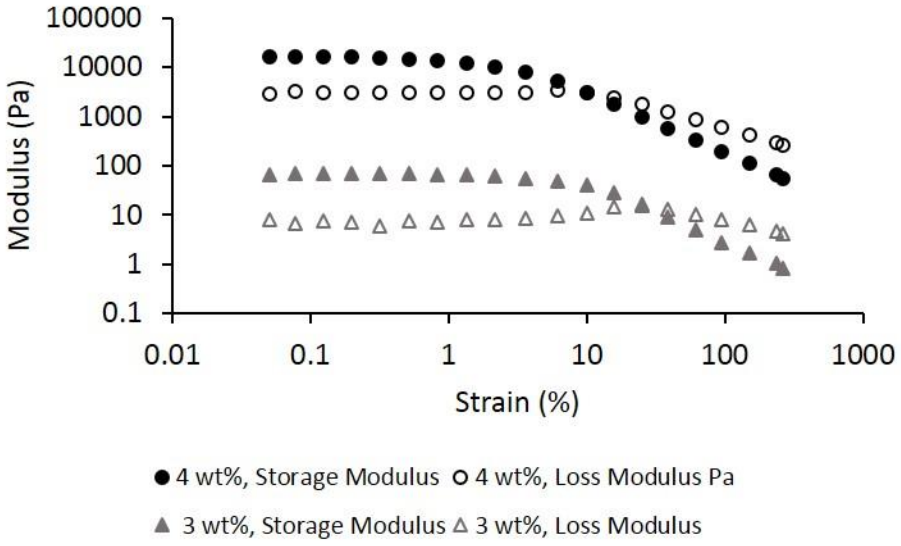

Figure C.2. Strain sweep from 0.05% to 250% at 1 Hz for nCNF at 4 wt% (black circle) and 3 wt% (gray triangle).

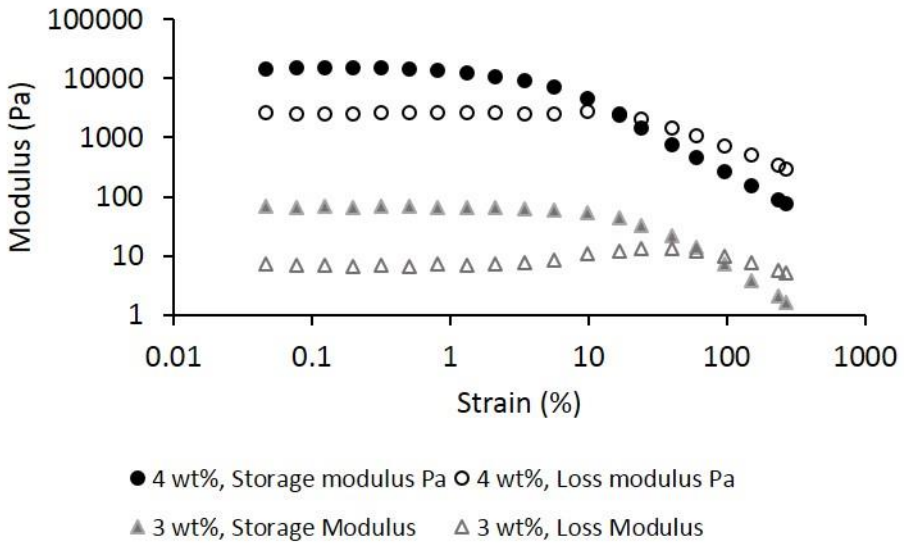

.

Figure C.3. Strain sweep from 0.05% to 250% at 1 Hz for nCNF-DEG hydrogel (10 mM APS/TEMED, 37 °C) at 4 wt% (black circle) and 3 wt% (gray triangle).

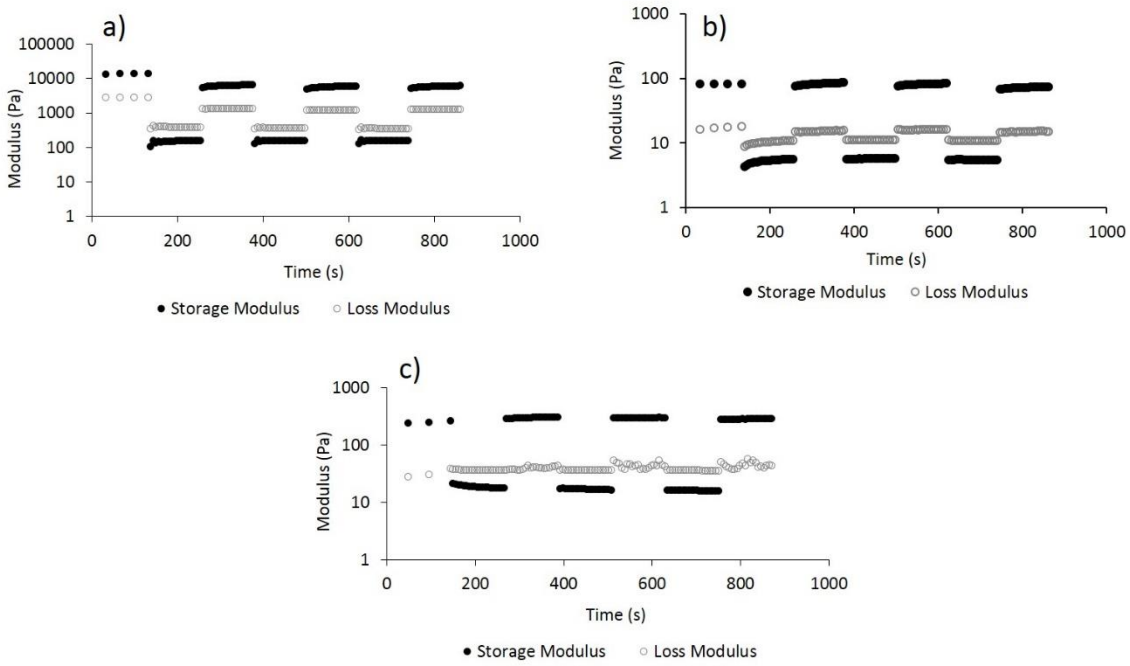

Figure C.4. Strain step rheological measurements of CNF, nCNF, and nCNF-DEG hydrogel to demonstrate the shear thinning behavior and modulus recovery. Oscillatory strain step at 10 Hz and alternating low (0.5%) and high (250%) strain for a) 3 wt% CNF, b), 3 wt% nCNF and c), 3 wt% nCNF-DEG hydrogel (T/NB=1, 10 mM APS/TEMED) is shown. Each step was 2 minutes long.

BIOGRAPHY OF THE AUTHOR

Nayereh Dadoo was born on January 29, 1983 in Tehran, Iran where he was raised and lived until she graduated from High School. Nayereh moved to Mashhad, Iran to attend a Bachelor's degree in Chemistry at the Ferdowsi University. After graduation in 2006, she moved back to Tehran to start her Master's degree in Organic Chemistry at the chemistry and chemichal engineering research center of Iran. She received her Master's degree in 2010 and then joined research institute of petroleum in Iran as a research assistant. She was not satisfied with the work so, she attended the University of Maine on August 2013 to pursue a doctorate degree in polymer chemistry. She joined Dr. Gramlich laboratory where she obtained experiences in polymer synthesis, hydrogel fabrication, and characterization. Nayereh was a teaching assistant for organic chemistry laboratory for two years. After graduation, Nayereh will join Dr. Theresa Reineke's lab at the University of Minnesota as a postdoctoral researcher. Nayereh is a candidate for the Doctor of Philosophy degree in Chemistry from the University of Maine in August 2018.